

UNIVERSITY OF WARMIA AND MAZURY IN OLSZTYN

Technical Sciences

11



PUBLISHER UWM

EDITORIAL BOARD

Leszek Mieszkalski (Editor-in-Chief) – University of Warmia and Mazury in Olsztyn,
Stefan Cenkowski – University of Manitoba, Canada, Adam Chrzanowski – University
of New Brunswick, Canada, Janusz Laskowski – University of Agriculture in Lublin,
Władimir Nikołajewicz Tilipałow – University of Technical in Kaliningrad, Russia,
Alojzy Wasilewski – University of Warmia and Mazury in Olsztyn

Executive Editor
Mariola Jezierska

The Journal is also available in electronic form.
The online edition is hosted by MetaPress (www.metapress.com)
in partnership with Versita (www.versita.com)

PL ISSN 1505-4675

© Copyright by Wydawnictwo UWM • Olsztyn 2008

Address

ul. Jana Heweliusza 14
10-718 Olsztyn-Kortowo, Poland
tel.: (48) (089) 523 36 61
fax: (48) (089) 523 34 38
e-mail: wydawca@uwm.edu.pl

Ark. wyd. 25, ark. druk. 20,25
Druk – Zakład Poligraficzny UWM w Olsztynie
zam. nr 658

Contents

Agricultural Engineering

Tarak C. Panda, P.K. Omre, B.K. Kumbhar – <i>Effect of Different Parameters on Clarification Efficiency of Mechanical Clarifier</i>	1
T.P. Singh – <i>Performance of No-till Drill for Establishment of Rice and Its Comparison with Drum Seeder and Conventional Method</i>	11
M.P. Singh, S.C. Sharma – <i>Studies on Bio-Energetics of Draught Buffalo</i>	21
S. Juściński, W. Piekarski – <i>An Analysis of Logistic Structure of Farm Tractors Inspections and Repairs in the Aspect of the Calendar of Agrotechnical Operations</i>	35
S. Juściński, W. Piekarski – <i>An Analysis of Farm Tractors Sales Results in the Aspect of the Calendar of Agrotechnical Operations</i>	47
S. Juściński, W. Piekarski – <i>An Analysis of the Territorial Range of Farm Tractors Servicing Realised as an Element of Distribution Logistics</i>	59
P. Kolber, J. Piechocki – <i>Chosen Results of Voltage Asymmetry Simulation Investigations at Rural Consumers Supplied by Low Voltage Power Line</i>	68
P. Kolber, J. Piechocki – <i>Simulation Model to Evaluate Voltage Asymmetry in a Rural Low Voltage Power Line</i>	77
J. Pawlak – <i>Method for Estimation of Efficiency of Using the Biomass for Energy</i>	87
Z. Kaliniewicz – <i>Analysis of the Efficiency of Cereal Grain and Buckwheat Nutlet Separation in a Grader with Indented Pockets</i>	95
A.J. Lipiński – <i>Obligatory Inspections of the Equipment to Plant Protection Chemicals Using – Legal Regulations, Testing Procedures and Controversies</i>	102

Civil Engineering

M. Jędrzejczak, M. Knauff – <i>The Plastic Equalization Method for Bending Moments and the Rotation Capacity of Plastic Hinges in Continuous Reinforced Concrete Beams in Light of Eurocode Requirements</i>	108
B.M. Deja – <i>Renovation of Buildings and Modernization of Built-Up Areas – a Case Study</i>	117
E. Szafranko – <i>Possible Applications of Network Methods to Optimization of Certain Aspects in the Construction Industry Management</i>	131
K. Klempka – <i>Methods of Calculating Concrete Strain Taking Into Account the Nonlinear Creep</i>	141
J. Pawłowicz, M. Zagroba – <i>The Question of Designing Modern Architecture in Conservation Areas: a Case Study of Kortowo, the Campus of the University of Warmia and Mazury in Olsztyn</i>	151

Environmental Engineering

L.M. Kaczmarek, S. Sawczyński – <i>Modelling of the Silting up Processes in Water Routes of Leba and Tolkmicko Ports</i>	161
L.M. Kaczmarek – <i>Modelling of the Silting up of Navigation Channels</i>	175
P. Bogacz, J. Kaczmarek, D. Leśniewska – <i>Influence of Air Entrapment on Flood Embankment Failure Mechanism – Model Tests</i>	188

Geodesy and Cartography

Z. Wiśniewski – <i>Split Estimation of Parameters in Functional Geodetic Models</i>	202
M. Bakula, R. Pelc-Mieczkowska, B. Chodnicka, M. Rogala, A. Tyszko – <i>Initial Results of RTK/OTF Positioning Using the Ntrip Data Teletransmission Technology</i>	213

Mechanical Sciences

M. Kučera, J. Pršan – <i>Tribologic Properties of Selected Materials</i>	228
Z.T. Kurlandzka – <i>Electromagnetic Forces in Polarizable, Magnetizable, Conducting Medium</i>	242
S. Kłysz, J. Lisiecki – <i>Selected Problems of Measurement Uncertainty – Part 1</i>	253
S. Kłysz, J. Lisiecki – <i>Selected Problems of Measurement Uncertainty – Part 2</i>	265
L. Romański – <i>Power Output of a Wind Turbine in Tubular Housing Equipped with a Diffuser</i>	277
L. Romański – <i>Operating Efficiency of a Non-Membrane Ground Heat and Mass Exchanger after 15 Years of Operation</i>	283
K. Ligier – <i>Methods of Diagnosing an ACWW 1000 Sugar Centrifuge with the Use of Vibration Processes</i>	289
T. Lipiński, A. Góral, P. Mikołajczyk, M. Cudakiewicz, A. Wach – <i>Effect of Environment-Friendly Modification of Al-12%Si Alloy on its Structure</i>	301
W. Dudda – <i>Truss Analysis in View of the Replacement of Degraded Structural Components</i>	312

Spis treści

Inżynieria rolnicza

Tarak C. Panda, P.K. Omre, B.K. Kumbhar – <i>Wpływ wybranych parametrów na efektywność mechanicznego oczyszczania soku z trzciny cukrowej</i>	1
T.P. Singh – <i>Wydajność siewu bezpośredniego ryżu w porównaniu z siewem metodą konwencjonalną i siewnikiem bębnowym</i>	11
M.P. Singh, S.C. Sharma – <i>Studia nad bioenergetyką bawotu domowego</i>	21
S. Juściński, W. Piekarski – <i>Analiza struktury logistycznej przeglądów i napraw ciągników rolniczych w aspekcie kalendarza zabiegów agrotechnicznych</i>	35
S. Juściński, W. Piekarski – <i>Analiza wyników sprzedaży ciągników rolniczych w aspekcie kalendarza zabiegów agrotechnicznych</i>	47
S. Juściński, W. Piekarski – <i>Analiza zasięgu terytorialnego obsługi serwisowej ciągników rolniczych realizowanej jako element logistyki dystrybucji</i>	59
P. Kolber, J. Piechocki – <i>Wybrane wyniki badań symulacyjnych asymetrii napięciowej u odbiorców wiejskich zasilanych z linii niskiego napięcia</i>	68
P. Kolber, J. Piechocki – <i>Symulacyjny model oceny niesymetrii napięć w wiejskiej linii niskiego napięcia</i>	77
J. Pawlak – <i>Metoda szacowania efektywności zastosowania biomasy do celów energetycznych</i>	87
Z. Kaliniewicz – <i>Analiza skuteczności separacji ziarniaków zbóż i orzeszków gryki w tryjerze z wgłębieniami kieszonkowymi</i>	95
A.J. Lipiński – <i>Obowiązkowe badania sprzętu do stosowania środków ochrony roślin – uregulowania prawne, procedury badań i kontrowersje</i>	102

Budownictwo lądowe i wodne

M. Jędrzejczak, M. Knauff – <i>Metoda plastycznego wyrównania momentów a zdolność do obrotu w przegubach plastycznych żelbetowych belek ciągłych w świetle wymagań eurokodu ...</i>	108
B.M. Deja – <i>Wybrane przykłady renowacji budynków i modernizacji obszarów zabudowanych</i>	117
E. Szafranko – <i>Możliwości zastosowania metod sieciowych w optymalizacji niektórych zagadnień z dziedziny zarządzania w budownictwie</i>	131
K. Klempka – <i>Metody obliczania odkształceń betonu z uwzględnieniem nieliniowego pękania</i>	141
J. Pawłowicz, M. Zagroba – <i>Problematyka projektowania współczesnych obiektów architektury w strefach ochrony konserwatorskiej na przykładzie kampusu Uniwersytetu Warmińsko-Mazurskiego w Olsztynie</i>	151

Inżynieria środowiska

L.M. Kaczmarek, S. Sawczyński – <i>Modelowanie zapiaszczania torów wodnych portów w Łebie i Tolkmicku</i>	161
L.M. Kaczmarek – <i>Modelowanie procesów zapiaszczania kanałów nawigacyjnych</i>	175
P. Bogacz, J. Kaczmarek, D. Leśniewska – <i>Wpływ zamykania powietrza na mechanizm zniszczenia wału przeciupowodziowego – badania modelowe</i>	188

Geodezja i kartografia

Z. Wiśniewski – <i>Rozszczepiona estymacja parametrów w funkcjonalnych modelach obserwacji geodezyjnych</i>	202
M. Bakula, R. Pelc-Mieczkowska, B. Chodnicka, M. Rogala, A. Tyszek – <i>Wstępne wyniki pozycjonowania RTK/OTF z wykorzystaniem technologii teletransmisji danych NTRIP .</i>	213

Nauki mechaniczne

M. Kučera, J. Pršan – <i>Właściwości trybologiczne wybranych materiałów</i>	228
Z.T. Kurlandzka – <i>Siły elektromagnetyczne w ośrodku z polaryzacją, magnetyzacją i przewodnością</i>	242
S. Kłysz, J. Lisiecki – <i>Wybrane zagadnienia niepewności pomiaru – cz. 1</i>	253
S. Kłysz, J. Lisiecki – <i>Wybrane zagadnienia niepewności pomiaru – cz. 2</i>	265
L. Romański – <i>Moc siłowni wiatrowej pracującej w obudowie rurowej wyposażonej w dyfuzor</i>	277
L. Romański – <i>Efekty pracy bezprzeponowego gruntowego wymiennika ciepła i masy po 15 latach eksploatacji</i>	283
K. Ligier – <i>Metoda diagnozowania wirówki cukrowniczej ACWW 1000 z wykorzystaniem procesów drganiowych</i>	289
T. Lipiński, A. Góral, P. Mikołajczyk, M. Cudakiewicz, A. Wach – <i>Ekologiczna modyfikacja stopu Al-12%Si a jego struktura</i>	301
W. Dudda – <i>Analiza konstrukcji w aspekcie wymiany degradujących się elementów</i>	312

EFFECT OF DIFFERENT PARAMETERS ON CLARIFICATION EFFICIENCY OF MECHANICAL CLARIFIER

Tarak C. Panda, P.K. Omre, B.K. Kumbhar

Department of Post Harvest Process and Food Engineering
College of Technology
G. B. Pant University of Agriculture & Technology
Pantnagar – 263 145, U S Nagar, Uttarakhand, INDIA

Key words: mechanical clarification efficiency, centrifugation, sugarcane juice.

Abstract

Effects of parameters namely, height of agitator from lid (15, 16, 17 cm.), centrifugation speed (2500, 3000, 3500 RPM) and time of centrifugation (5, 10, 15 min.) on mechanical clarification of sugarcane juice were studied. Filtration was incorporated as a pretreatment which reduced the amount of impurities in the juice. Soluble solids, total solids, sediment obtained, optical density and percent transmittance were measured and used for determining the efficacy of mechanical clarification of sugarcane juice. Full factorial design was used for selecting the levels of parameters in the experiment. Full second order polynomial and best fit equations were developed to predict various responses and to study individual, square and interactive effects of parameters on the responses. The clarification efficiency ranged between 11.3-42.2% and Optical density varied between 1.52 and 0.92 for mechanical clarification of sugarcane juice. Minimum percent transmittance was 3 and maximum was 13. Minimum sediment per 20 ml. of juice due to centrifugal force was 0.989 g. and maximum was 2.358 g. for mechanical clarification. Centrifugation time had highly significant effect on clarification efficiency followed by centrifugation speed, and height of agitator in that order. However, centrifugation speed had significant effect on optical density and percent transmittance.

WPŁYW WYBRANYCH PARAMETRÓW NA EFEKTYWNOŚĆ MECHANICZNEGO OCZYSZCZANIA SOKU Z TRZCINY CUKROWEJ

Tarak C. Panda, P.K. Omre, B.K. Kumbhar

Katedra Procesów Pożniwnych i Inżynierii Żywności
Wydział Technologii
Uniwersytet Rolniczo-Technologiczny G. B. Pant
Pantnagar – 263 145, U S Nagar, Uttarakhand, INDIE

Słowa kluczowe: efektywność klaryfikacji mechanicznej, wirowanie, sok z trzciny cukrowej.

A b s t r a k t

Badano wpływ następujących parametrów: odległość mieszadła od nakrywy (15, 16, 17 cm), szybkość wirowania (2500, 3000, 3500 RPM) i czas wirowania (5, 10, 15 min), na proces mechanicznego oczyszczania soku z trzciny cukrowej. Filtrację włączono do procesu jako obróbkę wstępną redukującą sumę zanieczyszczeń w soku. Zmierzono ciała rozpuszczalne, sumę składników stałych, otrzymany osad, gęstość optyczną oraz współczynnik przezroczystości i oceniono skuteczność mechanicznej klaryfikacji soku z trzciny cukrowej. Do doboru parametrów eksperymentu zastosowano metodę pełnego planowania czynnikowego. Dopasowane do wyników wielomiany drugiego stopnia i równania pierwszego stopnia opracowano do oceny procesu mechanicznej klaryfikacji oraz zbadania indywidualnego, łącznego i krzyżowego wpływu na nią różnych parametrów eksperymentu. Efektywność oczyszczania mieściła się w zakresie: 11.3-42.2%, a gęstość optyczna w zakresie 1.52-0.92. Minimalny współczynnik przezroczystości był równy 3, maksymalny równy 13. Minimalny osad na 20 ml soku w zależności od siły wirowania wyniósł 0.989 g, natomiast maksymalny 2.358 g. Na efektywność klaryfikacji najbardziej wpływał czas wirowania, bardziej niż szybkość wirowania, która znacząco wpływała na gęstość optyczną i współczynnik przezroczystości. Najmniej znaczący wpływ na mierzone parametry soku miała wysokość mieszadła.

Introduction

Sugarcane (*Saccharum officinarum*), is an integral component of agriculture in our country, as an agro-industrial crop. Total production of sugarcane in 2005-06 was nearly 266.88 million tones that was higher by 15% vis-à-vis the production of 2004-05 (INDIA 2006). The sugar industry is the second largest agro-based industry in India, involving nearly 50 million farmers, their dependents and a large mass of agricultural laborers in sugarcane cultivation, harvesting and ancillary activities, constituting 7.5% of the rural population (JAIN 2004).

Both white sugar and jaggery production involves extraction of juice and its clarification. The clarification of juice depends on the composition of juice that affects the quality of sugar and jaggery. Besides sugars, it contains suspended impurities in the form of coarse particles and colloids. Soil particles, wax, fat, protein, gum, pectin, tannins, and coloring matters are extracted from the cane during juice extraction and they remain in colloid form (RAO 1984).

In general term clarification means the extraction or separation of desired material and discarding the rest in a particular system either by means of chemical treatment or by mechanical operation. At times both may be applied for ultimate degree of separation requirement. In the instant proposition the cane juice which is a colloidal suspension of inorganic and organic non-sugars along with dissolved impurities needs dual operation followed by thickening, crystallization and centrifugation for the manufacture of sugar.

Clarification of sugarcane juice can be classified into two categories such as chemical clarification and mechanical clarification. Commonly vegetative clarificants are used in boiling pan. Some chemicals such as hydros (sodium

hydro-sulphite), lime (calcium oxide), sodium bicarbonate, sodium carbonate, super phosphate and alum have been used in combination with the vegetative clarificants. A good flocculant should increase the settling rate of insoluble solids, decrease the mud volume, produce good clarity of clarified juice with the least turbidity and should produce good filterability of mud, with good clarity of filtrate.

Several of these have been already marketed under various trade names like Sedipur TF2, Mafloc – 985, Magnafloc LT 22, Magafloc LT 22 SP, Betz 1420, Midland PCS/ 3016, C5 Eugel Series, Biosugar (Seta Products) and ABC clarifiers. Most of them are polyacrylamide based compounds, while some are basically ion exchange resins.

Chemical clarificants adversely affect the health of human beings since traces of chemicals remain in the final product (ANJAL, TAGARE 1972). All these chemicals (except lime) brighten colour of jaggery initially, but the colour of the jaggery becomes dull during storage. So alternative methods of clarification such as centrifugation is being explored to alleviate the use of chemical clarificants (VISHAL 2003, TARAK 2006).

Centrifugation is one of the established unit operations in the sugar industry. Although the designing aspect as based on density difference has been utilized most successfully in separation of sugar crystals from massecuite and various trials were conducted by KIRBY et al. (1990) at the initial stage of sugar manufacture, its application has not yet been systematically applied.

Materials and Methods

The process of clarification is shown schematically in Figure 2. Juice was extracted from the sugarcane (Variety Co.66) using three roller crusher. It was filtered using a strainer to remove baggasse and then fed into centrifugal clarifier. Process variables were height of agitator, speed of agitator and time of centrifugation and their levels are reported in Table 1. Full factorial design was used for experimentation.

Table 1
Variables and their levels

Variables	Levels
Height of agitator (X_1), cm	15, 16, 17
Agitator speed (X_2), rpm	2500, 3000, 3500
Time of centrifugation (X_3), min	5, 10, 15

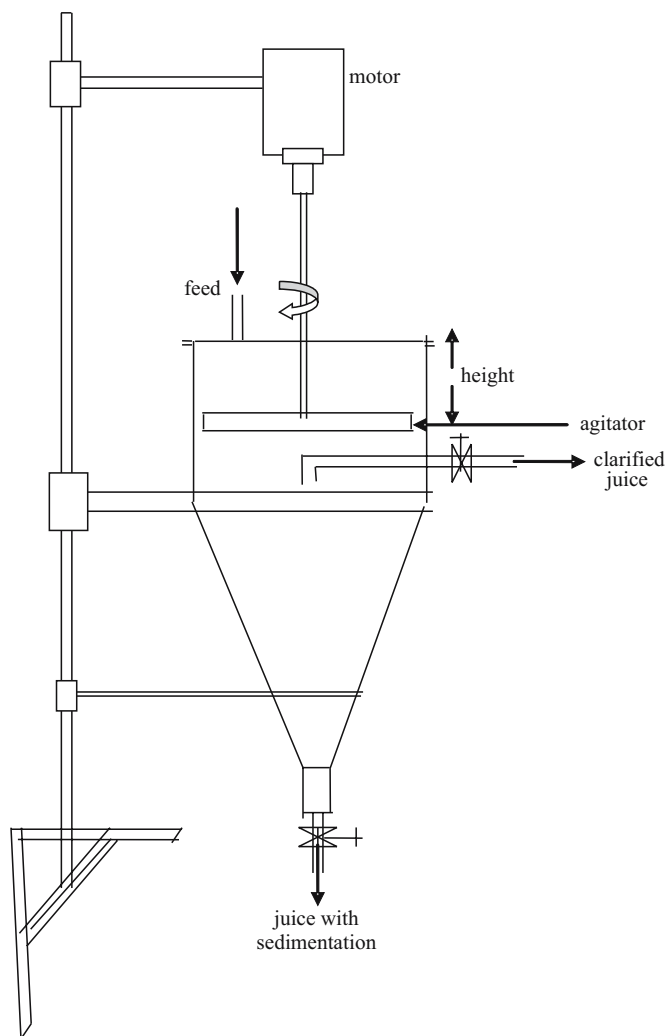


Fig. 1. Schematic diagram of the clarifier

The brix content, optical density (OD), percentage transmittance (%T), sediment obtained per 20 ml juice and solid content of the raw juice were measured. The brix content was measured by a hand refractometer. The OD and %T were measured by the colorimeter. For sediment obtained, 20 ml of juice was taken in a test tube and kept for 45 min for sedimentation. The clear juice from top of test tube was separated and the remaining sedimented juice was weighed. The OD was used as a measure for the degree of clarity of the juice. The OD of both raw and clarified juice was measured in a colorimeter at 540 nm and it was considered as the color of the sample.

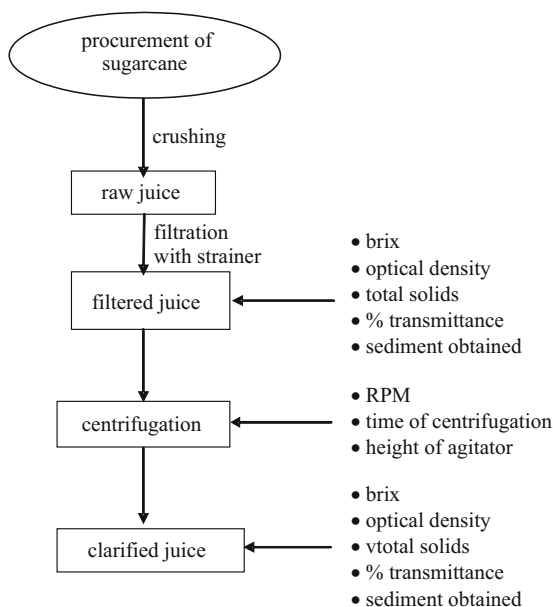


Fig. 2. Flowchart for mechanical clarification of sugarcane juice

The juice was fed to the clarifier. The height of agitator and its rpm were adjusted as per the design. The clarifier was operated for different centrifugation times as per the design. The clear juice was present on the upper part of clarifier. Juice samples were collected for the measurement of optical density, brix content, total solids and sediment.

Calculation for clarification efficiency

Amount of different types of solids in the juice were estimated using following relationships:

$$\text{Total Solids} = \text{Soluble Solids} + \text{Non-Soluble Solids}$$

$$\text{Brix} = \text{Total Soluble Solids}$$

$$\text{Insoluble Solids} = \text{Total Solids} - \text{Brix}$$

$$\text{Soluble Solids other than Sucrose} = \text{Brix} - \text{Sucrose Content}$$

Objective of centrifugal clarification was to remove only the insoluble solids.

Hence, the separation efficiency ($\hat{\eta}$) was defined as:

$$\dot{\eta} = \frac{S_r - S_c}{S_r} \cdot 100,$$

where:

$\dot{\eta}$ – separation efficiency, %,

S_r – insoluble solids in raw juice, g,

S_c – insoluble solids in clarified juice, g.

Results and Discussion

The clarification efficiency (η_i) varied from 11.3 to 42.2% by mechanical clarification which suggested that the clarification efficiency is affected due to height of agitator, agitator speed and time of centrifugation. The lowest clarification efficiency was 11.3% after 5 min at 2500 rpm and the highest was 42.2% after 15 min at 17 cm and 3500 rpm. Here agitator speed accounts for centrifugal force that increases the clarification efficiency of sugarcane juice.

Table 2

ANOVA for clarification efficiency, η_i

SOURCE	DF	SEQ SS	MS	F
Regression	9	1840.5		
Error	17	20.6	204.50	
Total	26	1861.2	1.21	168.04*

Significant at * 1% level

Clarification efficiency data were fitted into second order mathematical model using regression analysis and ANOVA is presented in Table 2. The coefficient of determination was 98.8%, suggesting the model could account 98.8% data. Therefore, the second order model was adequate in describing clarification efficiency. However it was observed that all the terms in the model were not significant. Therefore, best fit regression was carried out for clarification efficiency and the following best fit equation was obtained as:

$$\begin{aligned} \eta_i = & 65.41111 - 17.1111 X_1 + 0.005744 X_2 + 3.35 X_3 + 0.766667 X_1^2 \\ & - 0.10733 X_3^2 \end{aligned} \quad (1)$$

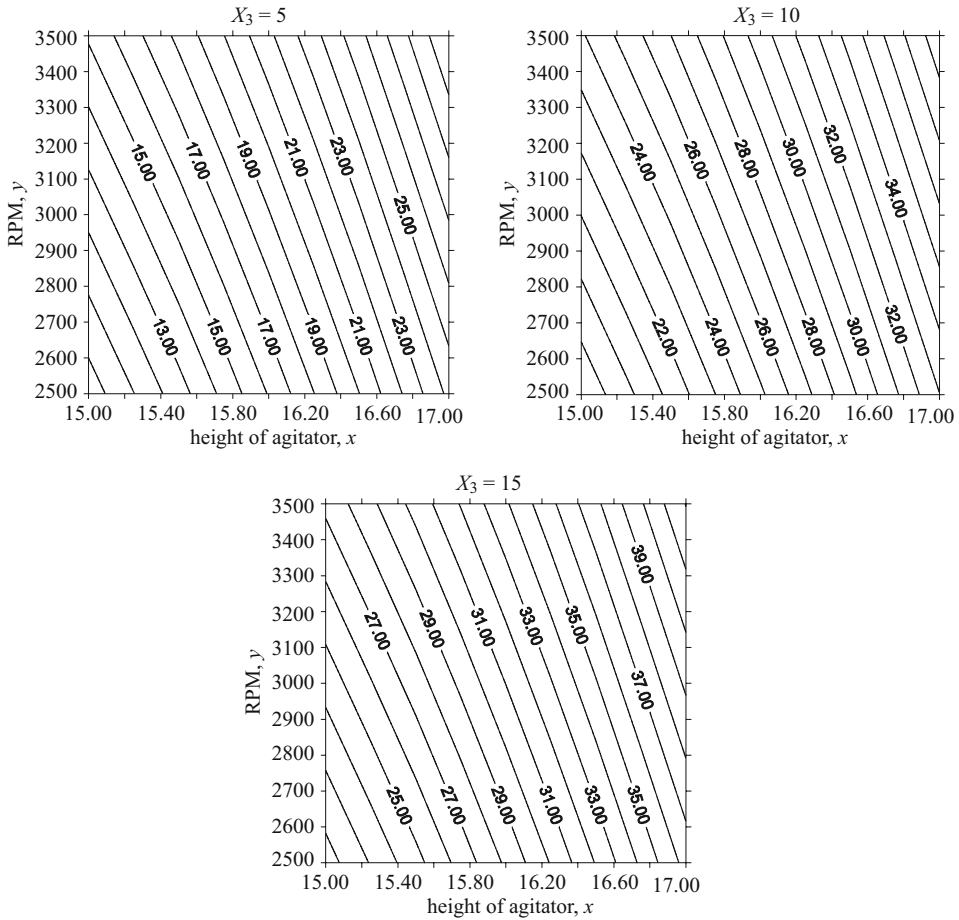
$(R^2 = 0.988)$

The model indicates that the interactive effect of the variables was insignificant. Moreover, the effect of speed was insignificant at quadratic levels.

Table 3

Contour equations for varying X_3 for clarification efficiency

X_3	Contour equations
5	$\eta_i = 79.485 - 17.11 X_1 + 0.0057 X_2 + 0.766 X_1^2$
10	$\eta_i = 88.21 - 17.11 X_1 + 0.0057 X_2 + 0.766 X_1^2$
15	$\eta_i = 91.585 - 17.11 X_1 + 0.0057 X_2 + 0.766 X_1^2$

Fig. 3. Contour plots for clarification efficiency (η_s) with respect to height of agitator and centrifugation speed

The contours are shown in Figure 3 for various combinations of time of centrifugation. It is clear from the figures that the clarification efficiency was minimum at low levels of height of agitator and centrifugation speed. It

increased with increase in their levels and was maximum at high levels of height and centrifugation speed. This is as expected since increased height of agitator enhances more juice towards centrifugal force while increased centrifugation speed imparts more centrifugal force for separation of particles

The optical density (OD_i) varied from 1.63 to 0.92 for mechanical clarification, suggesting that the optical density decreased due to centrifugal force. The highest optical density was 1.63 before clarification and the lowest optical density was 0.92 after 15 min at 17 cm and 3500 rpm.

ANOVA for optical density, OD_i

Table 4

SOURCE	DF	SEQ SS	MS	F
Regression	9	1.67	0.186	90.95*
Error	26	0.06	0.002	
Total	35	1.74		

Significant at * 1% level

Optical density data were fitted into second order mathematical model using regression analysis and ANOVA is presented in Table 4. The coefficient of determination was 96.38%, suggesting the model has the ability to account 96.38% data. Therefore, the second order model was adequate in describing optical density. However it was observed that all the terms in the model were not significant. Therefore, best fit regression was carried out for clarification efficiency and the following best fit equation was obtained as:

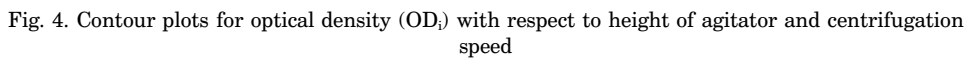
$$OD_i = 1.7475 - 0.0031 X_1 - 2.6E-05 X_2 + 0.1285 X_3 + 0.0011 X_3^2 - 0.0099 X_1 X_3 + 7.1E-06 X_2 X_3 \quad (R^2 = 0.963) \quad (2)$$

The model indicates that the interactive effect of height of agitator and speed of agitator were insignificant. Moreover the effect of height of agitator and speed of agitator individually were insignificant at quadratic levels.

Contour equations for varying X_3 for optical density (OD_i)

Table 5

X_3	Contour equations
5	$OD = 2.414 - 0.052 X_1 - 0.000061 X_2$
10	$OD = 3.137 - 0.102 X_1 - 0.000097 X_2$
15	$OD = 3.914 - 0.15167 X_1 - 0.000132 X_2$



Conclusions

It may be concluded from above presentation that the centrifugal clarification has an edge over chemical methods with proven advantages. If the speed of agitator will be made more and proper design of agitator can be done for the above clarifier then better clarification efficiency can be achieved.

It has been observed on the basis of practical and theoretical approach that in case of cane juice clarification the mechanical means have an edge over chemical process for its better control without affecting the system. However these approaches need detailed study. The proposed alternative for this purpose is the centrifugation of cane juice in which the past work lacks the systematic approach and improvement as compared to that in the case of centrifugation of massecuite. In the present paper a critical analysis of cane juice centrifugation as carried out by above clarifier has been studied.

References

- ANJAL S.T., TAGARE A.G. 1972. *Grading of Kolhapur gur*. Proc. 38th Annual Convention, Sugar Technologists; Association, India, Kanpur. G105-G113.
- INDIA 2006. pg-60.
- KIRBY L.K., GREIG C.R., ALTERTON P.G., WHITE E.T., MURRY C.R. 1990. *The performance of a new design of continuous centrifugal*. Sugarcane Technoogy, pp. 232-244.
- RAO P.J.M. 1984. *Administration in the Indian Sugar Industry*. Sugar Technol., 52(9): 19.
- PANDA T.C. 2006. *Performance evaluation of sugarcane juice clarifier*. M. Tech. Thesis, G.B. Pant University of Agriculture and Technology, Pantnagar, Uttaranchal, India.
- VISHAL K. 2003. *Studies on centrifugal clarification sugarcane juice*. M. Tech. Thesis, G.B. Pant University of Agriculture and Technology, Pantnagar, Uttaranchal, India.

Accepted for print 19.09.2009 r.

PERFORMANCE OF NO-TILL DRILL FOR ESTABLISHMENT OF RICE AND ITS COMPARISON WITH DRUM SEEDER AND CONVENTIONAL METHOD

T.P. Singh

Department of Farm Machinery and Power Engineering
College of Technology
G.B. Pant University of Agriculture & Technology
Pantnagar – 263 145, U S Nagar, Uttarakhand, INDIA

Key words: rice seeding methods, rice production economic analysis, no-till drill.

Abstract

In Tarai region of state of Uttaranchal, mainly contractual laborers are engaged for accomplishing rice transplanting, which is very tedious and labor intensive operation. Also they do not maintain required plant population resulting in poor yield. Shortage of agricultural laborers during the peak transplanting season is often faced by the farmers due to which timely transplanting is jeopardized again contributing to lower field. Direct seeding of dry or pre-germinated rice through suitable machineries could be a solution to this problem. This will not only reduce labor and production cost but also increases turn-around time for the subsequent crop. Considering the above facts, an experiment was laid down during 2001 and 2002 to evaluate the performance of Pantangar zero-till ferti-seed drill (T_1) for establishment of rice and the result was compared with manually operated rice seeder (T_2) and conventional method of transplanting (T_3). The experimental results indicate higher plant population with no-till drill as compared to rice seeder and transplanting method. The grain yield was recorded maximum for T_1 followed by T_2 and T_3 . The economic analysis shows lower cost of production and higher benefit-cost ratio in order. Based on the result, no-till drilling and drum seeding could be recommended to the farmers in labor scarcity area for establishment of rice.

WYDAJNOŚĆ SIEWU BEZPOŚREDNIEGO RYŻU W PORÓWNIANIU Z SIEWEM METODĄ KONWENCJONALNĄ I SIEWNIKIEM BĘBNOWYM

T.P. Singh

Katedra Maszyn Rolniczych i Energetyki Przemysłowej
Wydział Technologii
Uniwersytet Rolniczo-Technologiczny G. B. Pant
Pantnagar – 263 145, U S Nagar, Uttarakhand, INDIE

Słowa kluczowe: metody siewu ryżu, ekonomiczna analiza produkcji ryżu, siew bezpośredni.

A b s t r a k t

W regionie Tarai stanu Uttaranchal pracownicy kontraktowi są zatrudniani głównie do przesadzania ryżu, operacji bardzo żmudnej i pracochłonnej. Liczba pracowników nie jest wystarczająca do utrzymywania odpowiedniej wielkości zasiewów, powoduje to niezachowanie właściwych terminów przesadzania i niski plon. Siew bezpośredni suchego lub kielkowego ryżu przeznaczonymi do tego maszynami może być rozwiązaniem tego problemu. Stosowanie go zmniejsza zapotrzebowanie na pracowników i koszt produkcji, daje więcej czasu na kolejną uprawę. Biorąc to pod uwagę, w latach 2001 i 2002 przeprowadzono eksperyment, by sprawdzić wydajność siewnika bezpośredniego „Pantangar” (T_1) w uprawie ryżu i porównać rezultaty z wynikami siewu siewnikiem ręcznie sterowanym (T_2) i konwencjonalną metodą przesadzania (T_3). Wyniki wskazują na to, że wyższy plon jest osiągany po siewie siewnikiem bezpośrednim niż dwoma pozostałymi metodami. Maksimum plonu osiągnięto dla T_1 , a potem kolejno dla T_2 i T_3 . Analiza ekonomiczna wykazuje niższy koszt produkcji oraz lepszy bilans zysków i kosztów. Na tej podstawie można powiedzieć, że dla rolników borykających się z brakiem rąk do pracy w uprawie ryżu jest zalecany siew bezpośredni lub siewnikami bębnowymi.

Introduction

Rice is the staple food of more than 70 percent of the world's population. The rice belt is distributed geographically over a wide range of conditions between 45°N to 40°S latitudes. However 90 percent of total area under rice is situated in the wet tropical South and South East Asia. China is believed to be the origin of rice. Among the rice growing countries, India has the largest area under rice in the world, accounting for about 31 percent of the total area under rice cultivation producing about 80 million tons of rice annually.

Broadly there are three methods of growing rice. Firstly, direct seeding either manually or with traditional drills in well-prepared seedbed. A smooth, level seedbed is necessary to ensure that seeds are not planted at depths greater than 10 to 15 mm. Sowing is considered at the correct depth when five to ten percent of the seed is visible on the surface after sowing. The benefit of drilling the seed is that fertilizer can be applied at the same time as the seed. Also manual weeding is much easier in machine-drilled crops than in broadcasted crops.

The second method is to sow pre-soaked sprouted seed (soaked for twenty four hours and incubated for forty-eight hours), at 80 to 100 kg/ha, with the help of rice seeder in puddle soil. It has been reported that this method reduces labor hours by 69 percent (183 to 57 h/ha) and production cost by 59 percent that is mainly due to reduced labor requirement in seedling raising and seeding operations. However, weeding and water management efforts in the paddy field increases. The advantage is that direct-seeded crop matures seven to ten days earlier than the transplanted rice as the seedlings are not subjected to stress such as being pulled from the soil and reestablishing fine rootlets. This provides more turn-a-round time available for the next crop. However, it has

disadvantages also like the seeds are exposed to birds, rats, and snails. There is greater crop-weed competition being of similar age and plants tend to lodge more because of less root anchorage.

The third and most widely adopted method of growing rice is transplanting method. It is preferred over other two methods with the reason that this method gives better yield and there is less weed infestation. In the Tarai region of Uttaranchal, hired/contractual labourers mainly accomplish transplanting of rice. This method is very tedious and labour intensive operation. Approximately, more than 25 percent of the total working hours for rice production are spent for the process of transplanting and raising nursery (KHAN et al. 1989). The average plant population of manually transplanted rice has been reported much less than the required one (KHAN et al. 1979).

Often the farmers face the problem of shortage of labours during the peak transplanting season due to which timely rice transplanting is jeopardized. It has been reported that delay in transplanting by one and two months has a yield reduction of about 25 to 70 percent, respectively (RAO, PRADHAN 1973). Due to late transplanting the turn-around time available for the next crop is very small which again affects the yield of the subsequent crop.

Considering the above facts and advantages of direct sowing an experiment was conducted to evaluate the performance of Pantnagar zero-till ferti-seed drill and drum seeder for establishment of direct seeded rice (dry and pre-germinated) and its comparison with traditional method of transplanting as well as economics.

Materials and Method

Pantnagar no-till ferti-seed drill

Pantnagar no-till Ferti-Seed Drill with inverted-T type furrow opener, generally used for direct seeding of wheat in no-till condition, was used for sowing dry rice seed in well prepared seedbed. This ferti-seed drill can be used in well prepared soil as well without any modification. Precaution should be taken to adjust the seeding depth while sowing in friable soil. The position of leaf provided in seed metering device should be adjusted to lower most position for seeding rice.

Rice seeder

A manually operated 8-row rice seeder was used for sowing the pre-germinated rice seed in puddled bed. The machine has four cylindrical hollow

drums with peripheral opening at both the ends to give eight rows with a line spacing of 200 mm. Two lug wheels are fitted to support the weight of the seeder as well as to rotate the circular drum. A handle is provided to drag the machine in the field. A furrow opener under each perforated line of the drum is provided to open a shallow furrow for placement of seed into the puddle soil. The total weight of the machine is about 15 kg. The technical detail of the rice seeder is given in Table 1.

Table 1

Technical specifications of manually operated rice drum seeder

Particulars	Dimensions
Number of drum	4
Length of drum, mm	275
Diameter of drum, mm	145
Diameter of hole, mm	8.6
Number of holes	36
Number of rows	8
Row spacing, mm	200
Size of opening in drum, mm	115 x 85
Shape of the opening	rectangular
Length of handle, mm	900
Material of handle	GI Pipe
Diameter of pipe for handle, mm	21
Diameter of drive wheel, mm	390

Calibration of drill and rice seeder

Before actual sowing operation, the Pantnagar zero-till ferti-seed drill was calibrated for correct seed rate by keeping the leaf position in the seed metering device at the lower most position to facilitate the free flow of rice seed without breakage. The calibration of the drill was done as per the standard test procedure. However, there was no provision to adjust the seed rate in case of rice drum seeder. The seed rate was kept at 60 kg/ha for dry and pre-germinated rice seeding whereas it was 40 kg/ha for transplanting.

Experimental field

The field investigation was carried out for growing rice, by all the three methods, at Crop Research Center of the university continuously in the same field for two years. The texture of the soil is silty – clay ~ loam (sand 8.8%, silt

61.4% and clay 29.7%). The average bulk density of the soil is 1.44 g/cc with organic matter content as 3.4%. The hydraulic conductivity of soil is 0.648 mm/h. The previous crop sown was wheat.

Field preparation

The field was prepared using two operations of rotavator for direct seeding of rice. The depth of operation was kept shallow (about 10 cm). The seeding operation was performed with the help of Pantnagar no-till ferti-seed drill.

For seeding pre-germinated rice, the field was prepared again by using two operations of rotavator and then it was flooded with irrigation water. The shallow, weed free and leveled puddled bed was created by using peg type puddler. After puddling operation, the sprouted seed was sown with the help of drum seeder after allowing 24 hours sedimentation period.

In conventional method of transplanting, the puddled bed was prepared in similar way as it was done for pre-germinated rice. The transplanting was performed by manual labour on contract basis.

After sowing/transplanting operation, all the cultural practices in respect of weeding, chemical application, fertilizer application and plant protection etc was done similar in all the plots as per the agronomical requirement.

Treatments

The treatments for this experiment were as under:

T₁ – Direct seeding of dry rice – By zero-till ferti-seed drill

T₂ – Direct sowing of sprouted rice – By manually operated rice seeder, and

T₃ – Rice transplanting – By conventional method – control

The number of replication was kept three with total nine experiments. The plot size was kept 30 x 6 m.

Results and Discussion

The various machine and crop parameters noted during the experimentation period have been discussed as under:

Calibration result of seed drill

The calibration test was performed in the laboratory for Pantnagar zero-till ferti-seed drill for sowing dry rice at a seed rate of 60 kg/ha and the results have been presented in Table 2. It is clear from the table that the drill could deliver 61.30 kg/ha of seed at an exposure length of 7.64 mm. The seed rate was kept slightly higher (about 2 percent) than the desired rate of 60 kg/ha to accommodate positive slip. The visible grain damage was also determined and the same was found as 3.16 percent which was well within the acceptable range. The co-efficient of variation was found as 8.40.

Table 2
Calibration result of Pantnagar no-till ferti-seed drill for rice

Replication	Exposure length (mm)	Weight of seed dropped (g)	Seed rate (kg/ha)	Visible gram damage (%)	Coefficient of variation
1.	7.64	272	63.29	2.38	9.30
2.	7.64	263	61.20	3.80	9.79
3.	7.64	264	61.21	3.80	7.41
4.	7.64	258	60.27	2.71	7.99
5	7.64	260	60.51	3.11	7.51
Average	7.64	263.4	61.30	3.16	8.40

Performance of Pantnagar zero-till drill and drum seeder

The performance of Pantnagar zero-till ferti-seed drill and rice drum seeder was determined in actual field condition and the results so obtained have been presented in Table 3. The actual speed of operation was found about

Table 3
Performance results of Pantnagar no-till ferti-seed drill and manually operated rice drum seeder

Parameter	Pantnagar no-till ferti-seed- drill	Manually operated rice drum seeder
Crop	rice	rice
Soil condition	friable	puddled
Speed of operation, km/h	5.18	1.50
Field capacity, ha/h	0.50	0.13
Field efficiency, %	80	62
Cost of machine, Rs	12600 (USD 280)	2500 (USD 55.56)
Cost of operation, Rs/ha	500 (USD11.11)	300 (USD 6.67)
Labor requirement, man- h/ha	4-6	15-20

5.18 km/h for Pantnagar no-till ferti-seed drill where as it was 1.50 m/h for manually operated rice drum seeder. The data indicates that an area of about 0.50 and 0.13 ha/h could be covered with the no-till ferti-seed drill and drum seeder with observed field efficiency of 80 and 62 percent, respectively. The cost of operation was found higher, Rs 500/- per ha, for seed drill compared to Rs 300/- per ha for rice drum seeder. However, no difficulty was encountered in sowing dry and pre-germinated rice with both the equipment. The Pantnagar zero-till ferti-seed drill required no modification for sowing dry rice.

Crop yield and its attributing parameters

Number of tillers per meter

The number of tillers per meter length was recorded at the time of maturity of the crop and the pooled data for both (First and second) years have been presented in Table 4. The data shows higher number of tillers (340) per square meter for treatment T_1 where as it was only 318 and 279 for drum seeded and transplanted rice. The higher number of tillers in case of drilled rice (T_1) may be due to the reason that in case of drilling continuous dropping of grain takes place instead of hill sowing. Incase of drum seeding (T_2) the seeds do not drop individually in line but the grain drops in hills at uneven spacing. The reason for lowest number of tillers in case of manual transplanting (T_3) may be due to the fact that the contractual labour does not plant the nursery at required spacing and they want to cover more area within the available time. This indicates that the higher plant population could be maintained with no-till drill as compared to rice sown by drum seeder and transplanting method.

Table 4
Crop performance (average of two years pooled data)

Treatments	Number of tillers/sq (m)	Plant height (cm)	Panicle length (cm)	Grain yield t/ha (d.b.)	Straw-grain ratio
Drilling of dry rice (T_1)	340	108.10	29.40	7.82	1.78
Drum seeding of sprouted rice (T_2)	318	102.30	29.20	7.28	1.77
Manual transplanting (T_3) – Control	279	100.10	21.60	5.97	1.65
CD	3.799760	1.181826	0.06445955	0.1260482	0.03462295
CV	0.5389316	0.5058353	0.1095463	0.6515567	0.8848665

Plant height

The plant height was also measured at the time of crop maturity and it was found higher in T₁ (108.10 cm) over T₂ (102.30 cm) and T₃ (100.10 cm) respectively. The reason of lower plant height in case of treatment T₃ may be that plant takes more time to recover itself after being uprooted for transplanting.

Panicle length

The panicle length of the crop measured at the time of harvest has been presented in Table 4. It was found as 29.40 cm in T₁, 29.20 cm in T₂ and 21.60 cm in treatment T₃. This indicates that the panicle length do not vary much in case of treatment T₁ and T₂ however it was found less in transplanted rice which may be due to the reason explained earlier.

Grain yield and straw-grain ratio

The grain yield and straw-grain ratio was determined and has been presented in Table 4. The data shows maximum grain yield (7.82 t/ha) for the rice sown by zero-till drill (T₁) followed by 7.28 t/ha with drum seeder (T₂) and 5.97 t/ha in transplanted rice. The reason for higher yield in case of treatments T₁ and T₂ may be due to higher number of tillers, height of crop and panicle length as compared to transplanted rice (T₃). The straw-grain ratio was also found higher, 1.78 and 1.77, for treatments T₁ and T₂, respectively as compared to transplanted rice (T₃) as 1.65.

Economics of direct seeded rice

The economics of establishing rice crop by all the three methods as discussed earlier was determined and has been presented in Table 5. The cost of production was found lower in case of drilled rice (T₁) as Rs. 10020.00 (USD 222.67) per ha followed by Rs. 11424.50 (USD 253.88) in pre-germinated rice sown by drum seeder (T₂). The highest cost of production of Rs. 12587.50 (USD 279.72) per ha was found for transplanted rice. The specific cost of production also followed the similar trend. The benefit-cost ratio was found higher (3.99) for direct seeded rice (T₁) as compared to 3.07 for sprouted rice (T₂) and 2.00 for transplanted rice (T₃). This indicates that the direct seeded

rice is more beneficial to the farmers as compared to other two methods of establishing rice.

Economics of direct seeded rice

Table 5

Parameters	Rice establishing method		
	drilled rice by no-till drill	drum seeded rice	manually transplanted rice
Field condition	friable	puddled	puddled
Seed rate, kg/ha	60	60	40
Equipment used	no-till drill	manually operated drum seeder	manually
Grain yield, t/ha	7.82	7.28	5.97
Straw yield, t/ha	13.92	12.89	9.85
Total cost of production, Rs/ha	10020 (USD 222.67)	11424.50 (USD 253.88)	12587.50 (USD 279.72)
Total output, Rs/ha	49970 (USD 1110.44)	46485 (USD 1033)	37760 (USD 839.11)
Net saving, Rs/ha	39950 (USD 887.78)	35060.5 (USD 779.12)	25172.5 (USD 559.39)
Benefit-cost ratio	3.99	3.07	2.00
Specific cost of production, Rs/kg	1.28	1.57	2.11

Cost of grain = Rs 5.50 per kg and cost of straw = Rs 0.50 per kg was taken for determining the costs, 1 USD = 45 INR

Conclusions

Based on the experimental results following conclusions can be drawn.

The sowing of dry rice is feasible with Pantnagar no-till drill without any modification in its metering device. The visible mechanical grain damage was found only 3.16 percent.

The field capacity of the drill and manually operated drum seeder was found as 0.53 and 0.13 ha/h with an observed field efficiency of 80 and 62 percent respectively.

The plant population was found higher in dry seeded drilled rice followed by pre-germinated rice sown by drum seeder and transplanted rice. The yield was also found to follow the similar pattern.

The cultivation of direct and sprouted seeded rice was found to be economical over conventional method of transplanting rice.

References

- Annual report of NATP project on “Mechanization of rice-wheat cropping system for increasing the productivity” Pantnagar centre. 2001-02. GBPUA T, Pantnagar
- RAO M.V., PRADHAN S.N. 1973. *Cultivation Practices*. Rice Production Manual. ICAR, 71-95.
- KHAN A.U., KHAN A.S., CHAUDHRY A.D., CHAUDHRY, F.M. 1979. *Modification and testing for Korean paddy transplanter*. AMA, 10 (1): 79-85.
- KHAN A.S., MAJID A., AHMAD S.I. 1989. *Direct sowing: An alternative to paddy transplanting*. AMA, 20(4): 31-35.

Accepted for print 19.09.2008 r.

STUDIES ON BIO-ENERGETICS OF DRAUGHT BUFFALO

M.P. Singh, S.C. Sharma

Department of Farm Machinery and Power Engineering
College of Technology
G. B. Pant University of Agriculture & Technology
Pantnagar – 263 145, U S Nagar, Uttarakhand, INDIA

Key words: respiration rate, pulse rate, rectal temperature, humidity, temperature, speed, inclination of treadmill, draught and fatigue score.

Abstract

The effects of environment and work conditions on fatigue of draught buffalo have been studied under controlled condition using an animal treadmill. The physiological, hematological, biochemical, skin temperature, cardiovascular, and muscle strain responses along with distress symptoms of test draught he-buffaloes when exerting a draught of 0, 10 and 14% body weight at 1.5 and 2.0 km/h speed with 0, 5 and 10° inclination of treadmill at two temperatures (22 and 42°C) and two levels of humidity (45 and 90%) were studied for four effective hours or time till test draught he-buffalo reached a state of fatigue. Model developed with multiple linear regression technique which showed best fit for physiological, hematological, biochemical, mineral variables, skin temperature, cardiovascular, muscle strain parameters and duration of exercise.

STUDIA NAD BIOENERGETYKĄ BAWOŁU DOMOWEGO

M.P. Singh, S.C. Sharma

Katedra Maszyn Rolniczych i Energetyki Przemysłowej
Wydział Technologii
Uniwersytet Rolniczo-Technologiczny G. B. Pant
Pantnagar – 263 145, U S Nagar, Uttarakhand, INDIE

Słowa kluczowe: częstość oddechowa, tętno, temperatura odbytnicza, wilgotność, temperatura, szybkość, nachylenie kieratu, wysiłkowe próby oddechowe.

Abstrakt

Badano wpływ środowiska i warunków pracy na wyniki prób wysiłkowych bawołu domowego w kontrolowanych warunkach podczas pracy w kieracie. Bawoły chodziły z prędkością 1,5 i 2,0 km/h,

z obciążeniem równym: 0, 10 i 14% masy ciała, w kieracie nachylonym pod kątami: 0, 5 i 10°, w warunkach: temperatura 22 i 42°C, wilgotność powietrza 45 i 90%. Wyniki: fizjologiczne, hematologiczne, biochemiczne, sercowo-naczyniowe, temperaturę skóry i napięcie mięśni oraz objawy zaburzeń, zebrano podczas czterech godzin efektywnego testu trwającego do zmęczenia bawołu. Technika wielokrotnej regresji liniowej opracowano model parametrów opisujących otrzymane wyniki i pozwalających na dobór właściwego czasu trwania wysiłku.

Introduction

Animal traction has a long history in agricultural production. It is an appropriate, affordable and sustainable technology requiring very low external inputs. It has played and still playing an important role in meeting the power requirements of farming system in the country. The draught buffalo are in continuous stress during tillage operations especially in summer season and extreme winter and rainy seasons. The success of large-scale utilization of the draught animal power depends upon the scientific investigation undertaken to optimize animal power utilization. The physiological parameter of animals reflects the stress of work imposed on draught animals. Increase in respiration rate and rectal temperature after exercise has been reported by various researchers, MUKHERJEE et al. (1961), SINGH et al. (1968), DEVADATTAM, MAURYA (1978), UPADHYAY, MADAN (1985). Pulse rate also increases after work (THAKUR et al. 1989, AGGARWAL, UPADHYAY 1998)

The change in physiological parameters with the exercise often leads to fatigue in the field. This may give some reliable data on physiological responses while performing the exercise on animal treadmill at different speeds, draughts and treadmill inclination in various seasons. It was therefore, felt necessary to conduct extensive studies on physiological responses of draught buffalo taking these parameters in to account while performing the intense treadmill exercise under controlled condition. The experiment was conducted in department of Farm Machinery and Power Engineering, College of Technology, G.B. Pant University of Agriculture and Technology, Pantnagar. The site is situated at 29°N latitude, 79.3°E longitude and 283.8 m above the mean sea level and lies in a narrow belt to the south foothills of Shivalik range of Himalayas known as *Tarai* region. The experiments with the treadmill in controlled conditions at two speeds (1.5 and 2.0 km/h), three inclinations of treadmill (0, 5 and 10°), three draughts (0, 10 and 14% of body weight), two temperatures (22 and 42°C) and two levels of humidity (45 and 90%) were conducted for determining work efficiency without undue fatigue. The experiments were carried out under controlled environmental conditions with two replications for four effective hours in morning and evening or up to the period the test draught he-buffalo reached a state of fatigue.

Materials and methods

Male Murrah buffaloes of body weight 440 ± 5 kg were selected for the present investigation. A treadmill was used to control the speed and inclinations. The draught animals were trained for 15-20 days to walk on treadmill before recording the observations. The maximum and minimum temperatures and humidity were taken as 22 and 42°C and 45 and 90% respectively during the experiment.

The treadmill consisted of a conveyor belt on which the draught buffaloes were made to stand during the experiment. The length of the conveyor belt is 7500 mm with 1000 mm width and 10 mm thickness and was run by an electric motor (7.5 kW). With the rearward movement of the conveyor belt the draught buffaloes make forward movements in order to maintain its position on the belt. The draught buffalo was harnessed with Pant adjustable single animal collar harness and loaded with the help of hanging loads on a pan attached at rear of buffalo. During experiment, the physiological parameters were recorded on hourly basis. Each treatment was replicated twice.

During the course of investigation respiration rate and pulse rate was recorded using two channel Student Physiograph with the help of respiration belt and pulse transducers. The respiration belt transducer was placed around the chest of draught buffaloes and pulse transducer was placed on the middle coccygeal artery (about 100 mm below the level of anus) of the draught buffalo with the help of bandage provided with the sensors. The above transducers are connected with physiograph by means of wire, which senses signals of the respiration rate and pulse rate separately and transfer it to the physiograph with the help of strain gauge and pulse respiration coupler. The draught buffalo was not to be disturbed by any means prior to recording of data. The pointer attached with the physiograph marks the respiration rate and pulse rate of the draught buffalo on graph paper separately. Rectal temperature reflects core body temperature of the animals. The rectal temperature of draught buffalo was recorded at rectal mucous membrane. The rectal temperature was recorded with the help of digital thermometer.

On the basis of data obtained from the present investigation fatigue score card for test draught he-buffalo was developed. The values recorded for respiration rate, heart rate and rectal temperature before the start of the experiment and after 4th h of exercise or till fatigue. The difference of the initial and final values of the respiration rate, heart rate and rectal temperature were divided in to five equal parts, after that fatigue points were assigned as 1, 2, 3, 4 and 5 on the basis of increment in the values of above parameters from initial hour of working. Other visual parameter such as frothing, leg un-coordination and tongue protrusion were taken in to consideration as suggested by UPAD-

HYAY, MADAN (1985). It was assumed that maximum fatigue point up to 30 during severe work load for test draught he-buffalo could be achieved. A critical fatigue point (15) was decided on the basis of 50% of maximum fatigue points achievable by test draught he buffalo (Table 1).

Table 1
Developed Fatigue score card for working buffalo

Parameters	Score card					Total points
	1	2	3	4	5	
Respiration rate, (blows/min)	R_0+37	R_0+74	R_0+111	R_0+148	R_0+185	5
Heart rate, (beats/min)	H_0+17	H_0+34	H_0+51	H_0+68	H_0+85	5
Rectal temperature, °C	$T_0+1.40$	$T_0+2.80$	$T_0+4.20$	$T_0+5.60$	$T_0+7.00$	5
Frothing	first appearance	dribbling of saliva starting	continuous dribbling	appearance of forth on upper lip	full mouth frothing	5
Leg uncordination	strides uneven	occasional dragging of feet	movement of leg uncoordinated and frequent dragging of feet	no coordination in fore and hind legs	unable to move because of uncordination	5
Tongue protrusion	mouth closed	occasional opening of mouth	frequent appearance of tongue	continuous protrusion of tongue	tongue fully out	5

R_0 , H_0 and T_0 represent initial respiration rate, heart rate and rectal temperature respectively

Note – when the total score is 15 the working buffalo is under fatigue

Results and discussion

The mean values of respiration rate (blows/min) of draught buffaloes during exercise on animal treadmill under controlled environmental conditions at two speeds, three inclinations of treadmill, three draughts, two temperatures and two level of humidity have been depicted in Table 2. The variation in respiration rate with duration of exercise has been presented in Figure 1. It can be seen from the data that respiration rate increased with increase in speed, inclination of treadmill, draught at both the levels of temperature (22°C and 42°C) and humidity (45% and 90%). It is also clear from the Table 2 that at 90% humidity level the rate of respiration was higher in comparison to 45% humidity at both the temperatures in draught buffaloes for different combinations of speeds, inclination of treadmill and draughts. Higher respiration rate was found at 2.0 km/h speed, 10° inclination of treadmill and 14% draught for 22°C temperature and 90% humidity, while at 42°C tempera-

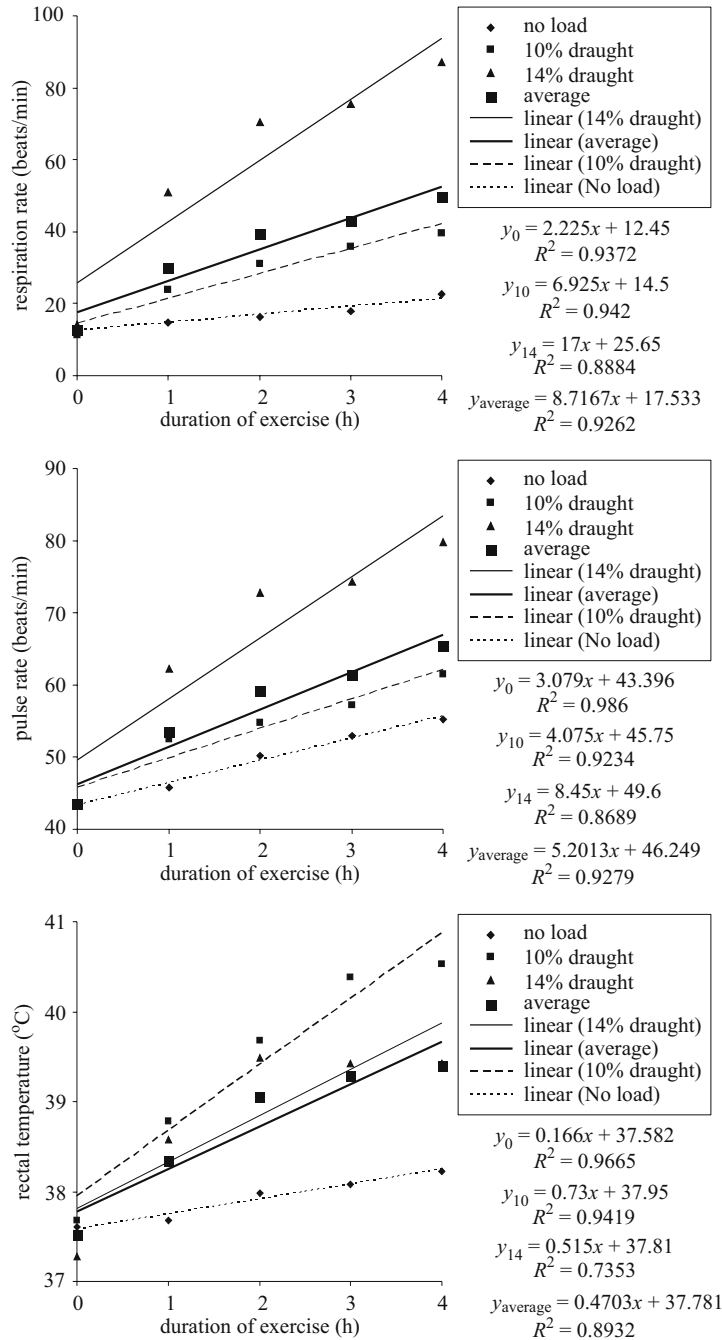


Fig. 1. Typical relationship of physiological parameters and duration of exercise

Table 2

Typical values of respiration rate (blows/min) Pulse rate (beats/min) and rectal temperature (°C) of test draught he buffalo on treadmill exercise under controlled condition at three draughts, two speeds, three inclination of treadmill, two humidity and two temperatures

Respiration rate, blows/min												
Temperature, °C = 22												
Speed, km/h	inclination of treadmill, degree	draught,* (%)	humidity, % = 45					humidity, % = 90				
			duration of exercise, h					duration of exercise, h				
			0	1	2	3	4	0	1	2	3	4
1.5	0	0	16.25	16.75	17.75	19.00	22.00	12.50	16.00	17.50	18.25	21.75
				3.08	9.23	16.92	35.38		28.00	40.00	46.00	74.00
2.0	10	14	17.00	158.00	#			16.00	156.00	#		
				829.41					875.00			
Temperature, °C = 42												
1.5	0	0	21.50	94.00	111.50	129.00	133.75	25.75	44.00	66.25	79.25	100.25
				337.21	418.60	500.00	522.09		70.87	157.28	207.77	289.32
2.0	5	14	62.50	169.00	#			46.75	166.00	196.00	#	
				170.40					255.08	319.25		
Pulse rate, beats/min												
Temperature, °C = 22												
1.5	0	0	42.00	49.75	50.25	55.50	56.25	48.00	48.75	51.00	53.00	58.00
				18.45	19.64	32.14	33.93		1.56	6.25	10.42	20.83
2.0	10	14	48.00	87.00	#			39.00	90.00	#		
				81.25					130.77			
Temperature, °C = 42												
1.5	0	0	45.75	51.00	53.25	56.75	59.75	40.50	55.25	58.75	61.25	65.50
				11.48	16.39	24.04	30.60		36.42	45.06	51.23	61.73
2.0	5	14	50.25	66.75	#			46.50	69.00	73.00	#	
				32.84					48.39	56.99		
Rectal temperature, °C												
Temperature, °C = 22												
1.5	0	0	37.26	37.80	37.83	37.90	37.95	37.14	37.40	37.24	37.43	37.68
				1.45	1.53	1.72	1.85		0.70	0.27	0.78	1.45
2.0	10	14	36.78	40.83	#			37.13	39.73	#		
				11.01					7.00			
Temperature, °C = 42												
1.5	0	0	38.16	39.14	39.62	40.28	40.67	37.06	37.84	38.34	38.55	39.11
				2.57	3.83	5.56	6.58		2.10	3.45	4.02	5.53
2.0	5	14	37.88	40.98	#			37.37	41.68	43.83	#	
				8.18					11.53	17.29		

P.C. – percentage change

* – draught equivalent to percentage of body weight

– test draught he buffalo did not exercise due to fatigue

ture the increase in respiration rate was also recorded higher for 90% humidity with different combinations of speeds, inclination of treadmill and draughts. For 42°C temperature and 90% humidity, higher respiration rate was observed for 2.0 km/h speed, 5° inclination of treadmill and 14% draught. In general the figures reveal that the respiration rate of test draught he-buffaloes increases with increase in draughts. This result was in agreement with the findings of THAKUR et al. (1987), who reported an increase of approximately 100 to 570% in respiration rate from its resting level for Male Murrah buffalo pulling 30 to 120 kg draught in rotary mode of operation. Similar results were also observed by AGGARWAL, UPADHYAY (1998).

The increase in respiration rate with duration of exercise is mainly due to the effect that the muscles of the draught buffalo involved in draught work, produce more amount of carbon dioxide and lactic acid. The oxidative process due to increased carbon dioxide is triggered to remove excess lactic acid produced by muscles. Subsequently the requirement of oxygen is increased and to overcome oxygen debt, respiratory center is stimulated by increased level of carbon dioxide. This causes increase in respiration rate through increased respiratory frequency. The percentage increase in respiration rate was more pronounced during first two hour of exercise on treadmill at different combinations of speeds, inclination of treadmill and draughts (Tab. 2). This was mainly due to the fact that the draught buffalo attained the steady state after about 2h of exercise. However, no distinct steady state in respiration rate of draught buffalo could be obtained as the main avenue of heat loss in draught buffalo is through mouth. The draught buffalo frequently open the mouth and increase respiration to compensate the thermal loads. These results are consistent with the findings of AGGARWAL, UPADHYAY (1997) who reported an increase in respiration rate by 145.83% from its resting level after 1h exercise on treadmill in hot humid conditions.

The respiration rate values were statistically analyzed using four factorial completely randomized design (CRD). The ANOVA for respiration rate shows that speed, inclination of treadmill and draught were significant at 1% level of significance. The interaction terms (Speed x Draughts, Inclination of treadmill x Draughts) was also significant at 5% and 1% level of significance for 22°C temperature but no definite trend in ANOVA could be obtained from the data at 42°C. Only draught and interaction term (Speed x Inclination of treadmill x Draught) was found significant at 5% level of significance which may be due to changing environmental load and physiological parameters of the draught buffalo.

The mean values of pulse rate (beats/min) of draught buffaloes recorded during experiment have been shown in Table 2. The variation in pulse rate with duration of exercise has been presented in Figure 1. It is clear from the

data that pulse rate increased with increase in speed, inclination of treadmill, draught at both the levels of temperature (22°C and 42°C) and humidity (45% and 90%). It is also clear from the Table 1 that at 90% humidity the pulse rate was higher in comparison to 45% humidity at both the temperatures in draught buffaloes for different combinations of speeds, inclination of treadmill and draughts. Higher pulse rate was found at 2.0 km/h speed, 10° inclination of treadmill and 14% draught for 22°C temperature and 90% humidity, while at 42°C temperature the increase in pulse rate was also recorded higher for 90% humidity with different combinations of speeds, inclination of treadmill and draughts. In general the figures reveal that the pulse rate of draught buffaloes increases with increase in draughts.

The result revealed that increase in pulse rate was more prominent during 42°C than 22°C. This was mainly due to environmental conditions; especially air temperature which has more pronounced effect on pulse rate of draught buffaloes. Similar results were observed by AGGARWAL, UPADHYAY (1997). From, this discussion, it is clear that the pulse rate increased from its resting level more at higher draught at both speeds (1.5, and 2.0 km/h) at 22°C and 42°C. This was mainly due to fact that the effect of draught is more pertinent on pulse rate of draught buffalo. Thus with increase in draught, the draught buffalo are subjected to greater physiological strain.

The mean values of rectal temperature have been presented in Table 2. The variation in rectal temperature with duration of exercise has been presented in Figure 1. It is clear from Table 2 that rectal temperature increased with increase in speed, inclination of treadmill, draughts at both the levels of temperature (22°C and 42°C) and humidity (45% and 90%). It is also clear from the Table 2 that at 90% humidity the rectal temperature was higher in comparison to 45% humidity at both the temperatures in draught buffaloes for different combinations of speeds, inclination of treadmill and draughts. Higher rectal temperature was found at 2.0 km/h speed, 10° inclination of treadmill and 14% draught for 22°C temperature and 90% humidity, while at 42°C temperature the increase in rectal temperature was also recorded higher for 90% humidity with different combinations of speeds, inclination of treadmill and draughts. In general the figures reveal that the rectal temperature of draught buffaloes increases with increase in draughts. Similar trends were observed by SARMA (1994), AGGARWAL, UPADHYAY (1998).

Just like other physiological parameters, the rectal temperature of draught buffalo increased with the exercise on treadmill for different combinations of speeds, inclination of treadmill and draughts. With the progress of exercise, the demand of oxygen to liberate energy from stored food by oxidation is increased, but the respiratory system is not able to cope up with the increased demand of oxygen resulting into anaerobic respiration rate to supplement

additional requirement of energy. In turn, anaerobic respiration results into lactic acid formation (a by-product) which accumulates in muscles causing its stiffness. This accumulated lactic acid is removed by oxidative process later on, liberating heat, resulting into increase in body temperature. The draught animals are homoeothermic like human beings. The environment surrounding of animal at any particular instant influences the amount of heat exchanged between it and that of environment, consequently it influences the physiological adjustments, and the animals must make to maintain a body heat balance. These adjustments cause a thermal stress on the animals. Due to these thermal stresses, the sweat glands get activated producing sweat and the evaporation of sweat causing cooling of skin (KACHRU et al. 1987). Draught buffaloes specifically have limitations over bullocks in terms of lower number of sweat glands (1.83 to 4.32 per mm² of skin) as compared to bullocks (13 to 16 per mm² of skin) thus; the buffalo cool slower by sweating. Moreover, colour of skin, its thickness and accumulation of fat layers under the skin which serves as an insulating media also affects the cooling process (COCKRALL 1974, THAKUR et al. 1987).

A comparative study of variation in rectal temperature at all speeds revealed that increase in rectal temperature was minimum at 1.5 km/h speed at 22°C temperature as well as at 42°C, followed by 2.0 km/h speed during 22°C and 42°C temperature respectively. The minimum increase in rectal temperature at 1.5 km/h was mainly due to the fact that the working speed of treadmill was less as compared to 2.0 km/h speed. The draught buffalo did not feel any stress and the rectal temperature along with other physiological parameters were well within the permissible range at a slow speed of 1.5 km/h compared to other higher speeds. In general, increase in rectal temperature was more at 14% draught during exercise on treadmill. This was mainly due to the fact that the effect of draught is more effective on rectal temperature of draught buffalo. A comparison of data of rectal temperature at 22°C and at 42°C indicated higher values of rectal temperature during 42°C which was mainly due to poor heat dissipation characteristics of draught buffalo in summer season.

The rectal temperature was statistically analyzed using four factorial completely randomized design (CRD) for different combinations of speeds, inclination of treadmill, draughts and combination of temperature and humidity. The ANOVA for rectal temperature shows that speed, inclination of treadmill and draught were significant at 1% level of significance and interaction term (Inclination of treadmill x Draughts) was significant at 1% level of significance for 22°C temperature but no definite trend in ANOVA could be obtained from the data at 42°C which may be due to changing environmental load and physiological parameters of the animal. Other parameters and their interactions show non-significant effect on rectal temperature.

The variation in fatigue scores of test draught he buffalo during exercise on treadmill under controlled environmental condition at two speeds, three inclinations of treadmill, three draughts and two level of temperature and humidity has been studied. The combinations of speed, inclination of treadmill, draughts and temperature and humidity causes fatigue to test draught he buffalo. The fatigue score card has been developed (Tab. 1) in the present investigation was used for fatigue analysis. During experiment, the fatigue of test draught he buffalo increased with the duration of exercise and the increase was more pronounced at higher speed, inclination of treadmill and draught for both the combinations of temperature and humidity. This is mainly due to the fact that the effect of draught is more prominent on all the physiological responses and on visual parameters of test draught he buffalo.

Summary and conclusion

The performance of test draught he-buffalo on animal treadmill at two speeds (1.5 and 2.0 km/h), three inclinations of treadmill (0, 5 and 10°), three draughts (0, 10 and 14% of body weight), two temperatures (22 and 42°C) and two levels of humidity (45 and 90%) were evaluated for determining work efficiency without undue fatigue. The experiments were carried out on animal treadmill under controlled environmental conditions with two replications for four effective hours in morning and evening or upto the test draught he-buffalo reached a state of fatigue. The respiration rate, pulse rate and rectal temperature increased with combinations of speeds, inclinations of treadmill and draughts. The physiological responses such as respiration rate, pulse rate and rectal temperature were more prominent during 42°C temperature and 90% humidity. The respiration rate of test draught he-buffalo was found to be more sensitive to increase during exercise on treadmill at different level of speeds, inclination of treadmill and draughts, therefore it can be considered as good indices of physiological response for quantifying fatigue. The percentage increase in pulse rate of test draught he-buffalo with duration of exercise and increasing speeds, inclination of treadmill and draughts were of minor nature and thus, pulse rate is not a good indicator of heat stress. The percentage increase in rectal temperature of test draught he-buffaloes with increasing speeds, inclination of treadmill, draughts and duration of exercise was more sensitive and thus can be considered as a good indicator of physiological load for the comparative study.

Fatigue score card prepared for test draught he-buffaloes showed the best performance upto 14% draught at 1.5 km/h speed followed by 2.0 km/h speed (upto 10% draught) for 0 and 5° inclination of treadmill during 22°C tempera-

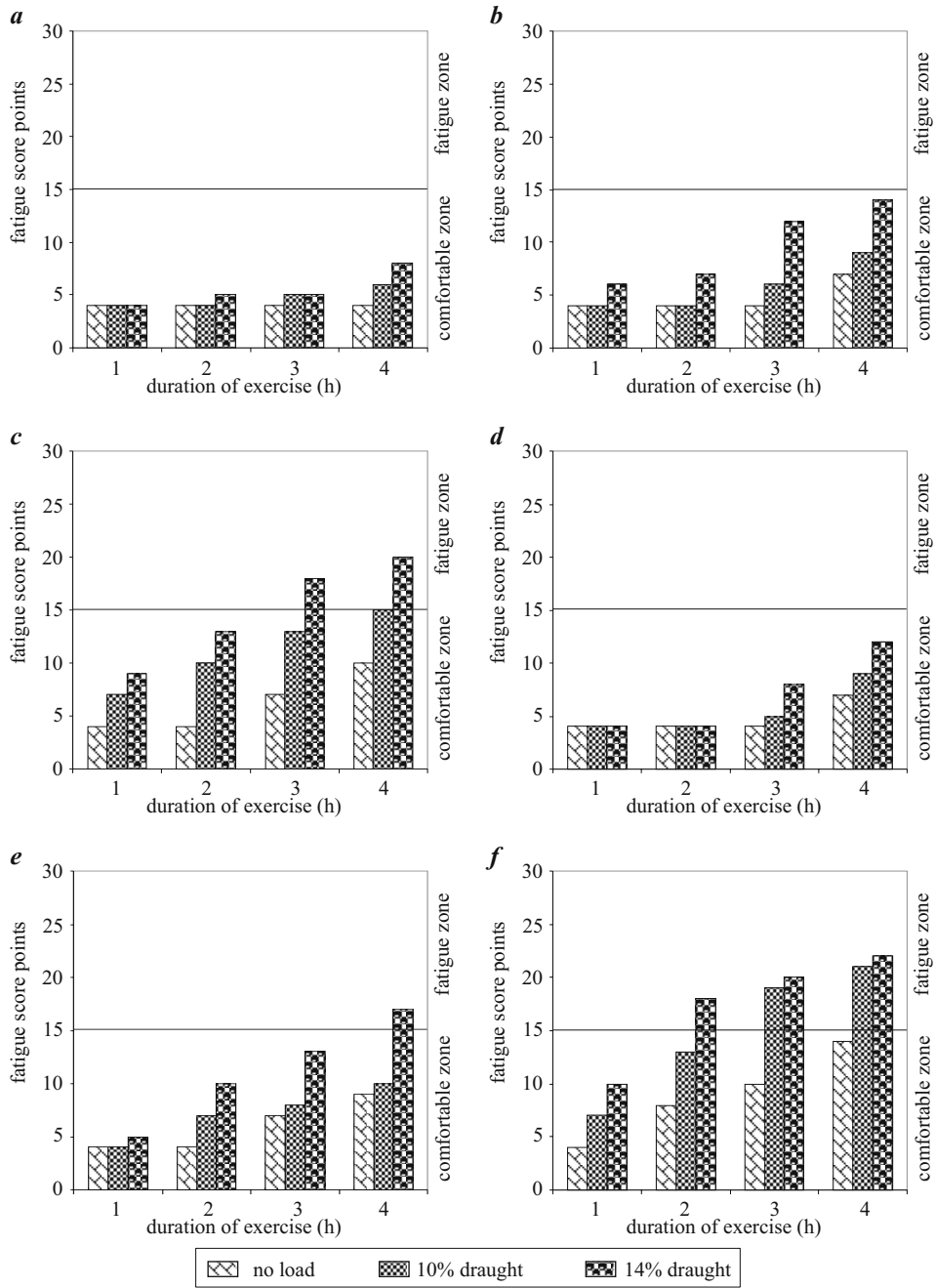


Fig. 2. Relationships between fatigue score points and duration of exercise at different draughts and test conditions

ture and 45% humidity upto 4th hour of exercise. At 22°C temperature and 90% humidity the best performance was shown at 14% draught for 0° inclination of treadmill 10% draught for 5° inclination of treadmill and 0% draught for 10° inclination of treadmill at 1.5 km/h speed while at 2.0 km/h speed the best performance was shown at 0% draught for 0, 5 and 10° inclination of treadmill. During 42°C temperature and 45% humidity the best performance was shown only for 0% draught at 1.5 km/h speed with 0° inclination of treadmill.

On the basis of above findings and relationships shown in Figure 2, it is concluded that out of two speeds (1.5 and 2.0 km/h), the 1.5 km/h speed showed the best performance (at 14% draught) for 0 and 5° inclination of treadmill followed by 2.0 km/h speed at 14 and 10% draughts respectively for 0 and 5° inclination of treadmill during 22°C temperature and 45% humidity. At 10° inclination of treadmill the test draught he-buffalo reached a state of fatigue beyond 1h at 1.5 and 2.0 km/h speed at 14% draught. During 22°C temperature and 90% humidity the best performance was shown at 14% draught for 0° inclination of treadmill, 10% draught for 5° inclination of treadmill and 0% draught for 10° inclination of treadmill at 1.5 km/h speed beyond which the test draught he-buffalo reached the state of fatigue so this draught (14%) level could only be recommended only for very short duration of exercise.

The Hematological parameter such as hemoglobin, packed cell volume, total erythrocyte count, total leukocyte and chloride concentration show irregular but declining trend while potassium and sodium concentration shows irregular but increasing trend where mean corpuscular concentration shows variable but increasing trend during treadmill exercise. These results and relationships are presented in Table 3 and Figure 3.

Table 3
Hematological parameter (gm%) of test draught he-buffalo on treadmill exercise under controlled condition at three draughts, two speeds, three inclination of treadmill, two humidity and two temperatures

Parameters	Speed, 1.5 km/h				Speed, 2 km/h			
	humidity, % = 45		humidity, % = 90		humidity, % = 45		humidity, % = 90	
	temperature		temperature		temperature		temperature	
	22°C	42°C	22°C	42°C	22°C	42°C	22°C	42°C
Hemoglobin	8.23	19.27	8.99	15.84	4.34	17.14	12.54	15.23
Packed Cell volume	13.44	25.55	15.76	18.50	22.85	24.48	11.40	29.12
Total Erythrocyte count	12.98	19.30	10.85	17.90	8.51	11.80	12.31	5.76
Total Leukocyte	16.11	27.95	22.85	29.34	19.84	35.82	23.08	24.70
Potassium concentration	1.11	4.97	2.21	3.32	4.70	3.04	5.52	7.74
Sodium concentration	3.60	5.82	4.11	9.08	10.62	10.96	13.19	13.02

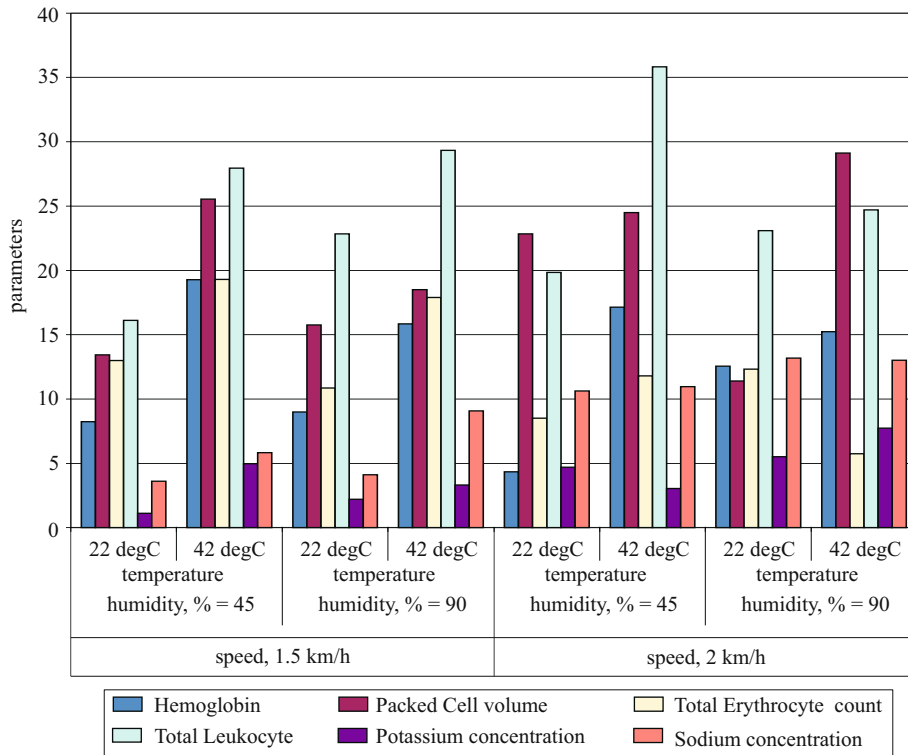


Fig. 3. Relationship between Hematological parameter (gm%) and three draughts, two speeds, three inclination of treadmill, two humidity and two temperatures of test draught he-buffalo on treadmill exercise under controlled condition

References

- AGGARWAL A., UPADHYAY R.C. 1998. *Studies on evaporative heat losses from skin and pulmonary surfaces in male buffaloes exposed to solar radiations*. Buffalo J., 2: 179-187.
- AGGARWAL A., UPADHYAY R.C. 1994. *Effect of different speeds and gradients upon some of the physiological parameters in cross bred males*. Int. J. Anim. Sci., 9: 65-68.
- AGGARWAL A., UPADHYAY R.C. 1997. *Exercise induced changes in cutaneous and pulmonary water loss in buffaloes*. Indian J. Anim. Sci., 67 (5): 433-437.
- AGGARWAL A., UPADHYAY R.C. 1998. *Effect of treadmill exercise and solar exposure on sweating and pulmonary function in crossbred (Sahiwal x Holstein) cattle*. Indian J. Anim. Prod. Mgmt., 14 (3): 175-178.
- AGGARWAL A., UPADHYAY R.C. 1998. *The effect of treadmill exercise on some physiological reactions and blood acid-base equilibrium in male buffaloes*. Indian J. Anim. Prod. Mgmt., 14 (3): 181-182.
- COCKRALL W.R. 1974. *The husbandry and health of the domestic buffalo*. FAO, Rome, pp. 99-102.
- KACHRU R.P., BARGALE P.C., SRIVASTAVA P.K. 1987. *Effect of thermal environment on draught animal*. Proceedings of the National Seminar on Status of Animal Energy Utilization, CIAE, Bhopal Jan., 24-25: 41-49.
- SHARMA S. 1996. *Studies on draught capacity of he-buffaloes under different work rest cycles and modes of operation*. Thesis M. Tech. (Agril. Engg), G. B. P. U. A. & T. Pantnagar.

- THAKUR T.C., SINGH M.P., SINGH B. 1987. *An investigation on physiological responses of buffaloes at different work rest cycles in rotary mode of operation*. Proceedings of the National Seminar on Status of Animal Energy Utilization, CIAE, Bhopal Jan., 24-25: 92-116.
- THAKUR T.C., SINGH M.P., VASTSA D.K. 1989. *Assessment of draught capacity of he-buffaloes during different work rest schedule under rotary mode of working*. Annual Report on U. A. E., Pantnagar centre, pp. 53-73.
- UPADHYAY R.C., MADAN M.L. 1985. *Draught performance of Haryana and crossbred bullocks in different seasons*. Indian J. Anim. Sci., 55(1): 50-54.

Accepted for print 19.09.2008 r.

AN ANALYSIS OF LOGISTIC STRUCTURE OF FARM TRACTORS INSPECTIONS AND REPAIRS IN THE ASPECT OF THE CALENDAR OF AGROTECHNICAL OPERATIONS

Sławomir Juściński, Wiesław Piekarski

Department of Power Engineering and Vehicles
University of Life Sciences in Lublin

Key words: logistics, logistic services, farm tractors inspections and repairs.

A b s t r a c t

In the present article we have discussed the logistic management of services and the characteristic features of these services which constitute logistic products. We have presented the results of a research along with an analysis concerning such services as pre-sale inspections, guarantee inspections and repairs, post-guarantee repairs of farm tractors. The research was carried out at the Service Department of an authorized dealer of farm tractors and machines. The cycle of the research included the years 2003-2005. The time schedules of inspections and repairs have been analyzed in the aspect of the calendar of agrotechnical operations recommended for cultivation in Poland.

ANALIZA STRUKTURY LOGISTYCZNEJ PRZEGŁADÓW I NAPRAW CIĄGNIKÓW ROLNICZYCH W ASPEKcie KALENDARZA ZABIEGÓW AGROTECHNICZNYCH

Sławomir Juściński, Wiesław Piekarski

Katedra Energetyki i Pojazdów
Uniwersytet Przyrodniczy w Lublinie

Słowa kluczowe: logistyka, usługi logistyczne, przeglądy i naprawy ciągników rolniczych.

A b s t r a k t

W artykule przedstawiono zarządzanie logistyczne usługami i cechy charakterystyczne usług będących produktem logistycznym. Zaprezentowano wyniki badań i ich analizę dla usług: przeglądów przed sprzedażą, przeglądów gwarancyjnych, napraw gwarancyjnych i napraw pogwarancyjnych ciągników rolniczych. Badania zrealizowano w dziale serwisu autoryzowanego dystrybutora ciągników i maszyn rolniczych. Cykl badań obejmował lata 2003-2005. Wyniki badań opracowano statystycznie, wyznaczając wartość indeksów sezonowych. Rozkłady czasowe przeglądów i napraw analizowano w aspekcie kalendarza zabiegów agrotechnicznych zalecanego dla upraw w Polsce.

Introduction

The distribution of industrial products and purchaser service constitutes the organizational elements of one logistic chain. The recent years have shown that technical and technological advancement stimulates a continuous growth of customer's demands concerning the branch of industrial products. Farm tractors and machines users require from trade service companies' punctual and infallible realization of technical inspections as well as guarantee and post-guarantee repairs within the service. An important aspect that should be taken into account in the logistic management of the Service Department is the seasonality of farm vehicles and machines' use, which is a consequence of the realization of field works according to the calendar of agrotechnical operations.

Research problem

Plenty of actions in the field of distribution, which are optimized by logistic management, are targeted at achieving the level of customer service perceived as a very important element of a company's activity. The system of purchaser service should function smoothly and, at the same time, effectively in terms of generated costs. The service during the process of product use is supposed to meet the purchaser's expectations since it is the factor, which determines customers' loyalty to the brand and distributor on the long run. It should be mentioned that a company, being responsible for the product, contacts the purchaser a number of times during the whole process of exploitation. The cycles of guarantee and post-guarantee services are present throughout the whole use of the tractor (DWILIŃSKI 2006, *Teoria i praktyka...* 2004).

The goal of this paper was to provide a thorough analysis of the generic and quantitative structure of the orders realized by the authorized Service Department. Within the period of three years the following services were investigated: pre-sale inspections (P0), guarantee inspections (P1-P4), guarantee repairs (NG), post-guarantee repairs (NP) of farm tractors.

Logistic management of services

A service is a logistic product that constitutes a set of a customer's wishes and expectations. Logistic management of services is the process of planning and performing services, which includes the analysis of capabilities, needs and ways of rendering the services offered throughout the whole logistic chain, i.e. from the producer to the purchaser (CHRISTOPHER, PECK 2005, COYLE et al.

1996, *Logistyka dystrybucji*. 2005). In the recent years a dynamic growth of the service sector has been observed. Logistic management of services is a complex process due to some specific features of a service as such (CIESIELSKI 2006, KEMPNY 2001),

- lack of a possibility of storing services,
- necessity of maintaining the readiness to render services in fluctuating demand,
- high fixed costs,
- intangibility and transitoriness,
- lack of the possibility for the purchaser of judging the quality of the service before buying,
- simultaneity of production and consumption of services
- diversity of places and duration of services
- image and competence of a contractor are seen as a base of market advantage

Market requirements comprise a functional efficiency of machines, including original spare parts supply and assistance in maintaining operation efficiency and technical consultancy. Guarantee and post-guarantee services combined with the distribution are elements in the system of the quality of farm tractors and agricultural machines (PIEKARSKI 1997).

An analysis of inspection and repairs services of farm tractors in the years 2003-2005

The spot of the research was the Service Department of a commercial-servicing enterprise that runs an authorized distribution of farm tractors and machines, i.e. DEERE & COMPANY concern and ZETOR and PRONAR factories. The company has worked since the late 80s of the 20th century in the agricultural service sector on the area of the Lublin province.

Service structure in 2003

In the analysed period, the Service Department offered in general 534 services of inspections and repairs of farm tractors. The structure of the kind of the services offered is presented in a form of a pie chart (Fig. 1). Inspections and guarantee repairs were dominating in that period.

The level of the services offered is presented in a form of a histogram (Fig. 2). The analysis of inspections before the sale of the tractors confirmed maxima in March and April as well as in June and July and at the end of the year and in December. Furthermore, there was a clear relation between

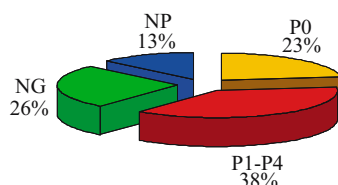


Fig. 1. The structure of the kind of inspection and repairs services of farm tractors in 2003
Source: Own study.

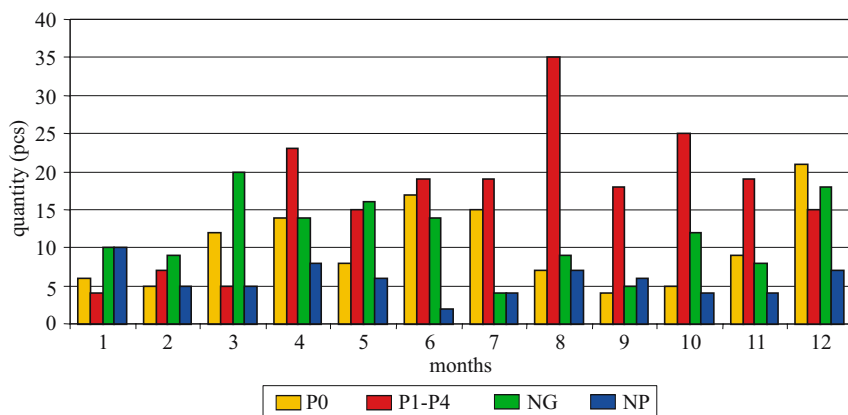


Fig. 2. The schedule of the quantity of inspection and repairs services of farm tractors in 2003
Source: Own study.

demand for technical inspections (P0) and periods of an increase in tractor sales. In a three-month presentation, there is clear demand for services in the second quarter (31.7%) and in the fourth quarter of the year (28.5%). On the other hand, the minimal number of services was realized in the first quarter and the level of the services was 18.7% for the whole year.

It results from the research that the most guarantee inspections (P1-P-4) were done in April, August and October. Moreover, there was a regularity of demand for the inspection service of a farm tractor after a defined number of moto-hours while agrotechnical operations. Maxima of the number of services coincided with the schedule of spring farm works, harvest and autumn operations (*Agrotechnika roślin uprawnych* 2005, *Agrotechnologia* 1999). In the periodical perspective, the highest level of inspections (P1-P4) was observed in the third quarter (35.3%). Demand for inspections (P1-P4) in the second and fourth quarters was at comparable levels: 28% and 28.9%. The first three months of the year had fewer services made in comparison to the summer period by 350%.

Guarantee repairs (NG) characterised with a close level of services in the first (28.1%), second (31.7%) and fourth (27.3%) quarters of 2003. But the third quarter had a fewer number of repairs (NG) to the twice lower level in comparison to other periods. Maxima of services offered appeared in March and December. The periods refer to periods of main maintenance work just before spring farm works and just after agricultural operations.

An analysis of post-guarantee repairs services (NP) has shown that the most services were offered in the first quarter and they were at the level of 29.4% of the annual number of contracts. Throughout the other analysed three-month periods, there was even demand for the services: the second quarter – 23.5%, third quarter – 25% and the fourth quarter – 22%. Generally, it resulted from the realization of the planned repairs of farm vehicles before the main season of agrotechnical operations. A high level of new farm tractors, characterizing with a low level of moto-hours, had a crucial influence on the schedule of contracts (NP).

It is worth noticing that the level of the whole package of services offered by the Service Department reached the lowest value in the first quarter of 2003. In the subsequent quarters, there was an increase by 60%, 35% and 50% in relation to the beginning of the year. Maxima of the services offered were in April, August and December. Such a time structure coincided with the periods of the biggest demand for agrotechnical operations in agriculture (*Agrotechnika roślin uprawnych* 2005, *Agrotechnologia* 1999).

Service structure in 2004

In the analysed period, the Service Department offered in general 786 services of technical inspections and repairs of farm tractors. The structure of the kind of services offered in 2004 is presented in a form of a pie chart (Fig. 3).

The level of the realised services of inspections and repairs of farm tractors in 2004 is presented in a form of a histogram (Fig. 4). The analysis of the number of the inspections made before sale (P0) has shown their highest level

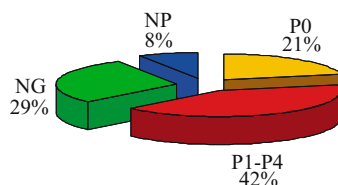


Fig. 3. The structure of the kind of services of technical inspections and repairs of farm tractors offered in 2004

Source: Own study.

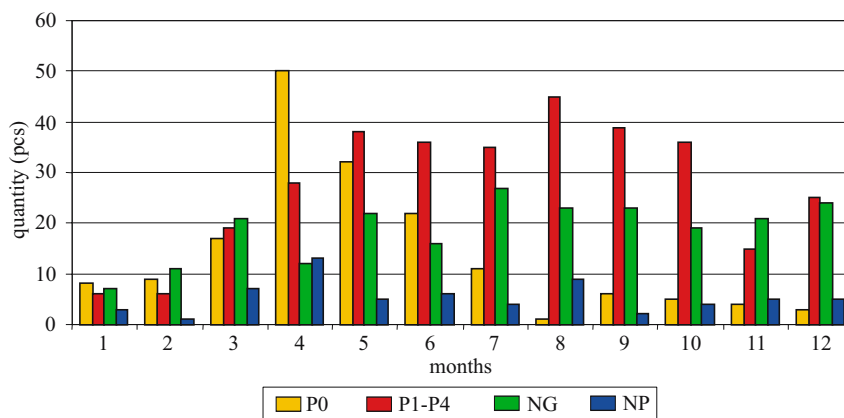


Fig. 4. The distribution of the quantity of inspections and repairs of farm tractors offered in 2004
Source: Own study.

in the second quarter of the year – 61.9% of their general number. The first half year closed with the realization of 82.1% of technical inspections throughout the entire year. The structure of the services offered by the Service Department is a precise reproduction of a dynamic increase in the sale of farm tractors in connection with the Polish access to the European Union. The second half of 2004 was a drastic decrease in inspections: in the third quarter to 10.7% and in the fourth one to 7.2%.

In the scale of the investigated year the largest number of guarantee inspections (P1-P4) were carried out in the second quarter (31.1%) and the third one (36.3%). Moreover, a high demand on guarantee inspections could be observed in October. A balanced very high level of services of this kind within seven subsequent months was a result of the number of new tractors that had been sold at the beginning of 2004. During the first four months 79% of the annual turnover was realized. After the exploitation of new tractors during agrotechnical operations in the spring and summer, they required guarantee inspections, together with the vehicles already used on the local market.

The lowest number of services rendered within guarantee repairs (NG) was observed during the first quarter of the year (17.3%), and the minimum in the scale of the year was recorded in January. This has confirmed that the level of the performed orders and agrotechnical operations within the investigated period are interrelated. The maximum demand on services (NG) occurred in the third quarter of 2004, reaching the level nearly two times higher than the minimum. The distribution of the services in the summer overlapped with a number of works connected with harvesting grain and post-harvest agrotechnical operations. What is more, the temporary increase in the number of

repairs took place in May, i.e. after the end of spring field works, as well as in December, after closing the annual calendar of agrotechnical works.

The analysis of the structure of post-guarantee repairs (NP) has confirmed that their level was minimal in the first three months (17.2%) and over a double growth of the number of these services in the second quarter (37.5%). The maximum demand on the services occurred in April, i.e. in the period of intensified agrotechnical operations. The second half of the year showed a balanced level of orders, with the temporary maximum in August during the harvest.

For the whole range of service orders, the smallest number of realized services was recorded in January and February, while in the first quarter the demand reached 14.6% per annum. A dynamic growth of demand on the services took place in March, and the maximum level was observed in April and May, which was the result of the accumulation of agrotechnical operations performed in these months. The following four months presented a balanced high level of orders due to the intensification of field works. Half of the last quarter has shown an evident decrease in the number of orders. In a three-month presentation, the second and the third quarter were dominant (35.6% and 28.6% respectively).

Service structure in 2005

In the investigated period 719 inspections and service repairs were carried out. The structure of services by category in 2005 is presented in the circular diagram (Fig. 5).

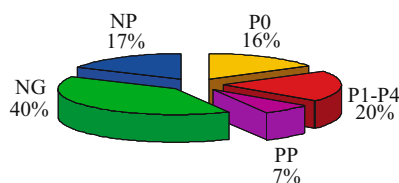


Fig. 5. The structure of the types of the inspections and repairs carried out in 2005
Source: Own study.

The distribution of the number of the rendered services, i.e. inspections and farm machines' repairs in 2005 is provided in the histogram (Fig. 6). The analysis of the level of pre-sale inspections (P0) has shown that their value was lowest in the first quarter of the year (17.4%) in relation to the annual level, with an evident minimum in January. The monthly values of inspections (P0)

reached the maximum in April, May July and November. The number of services (P0) rendered within three-month periods showed a tendency for dominance in the second (31.3%) and third quarter (26.1%), while in the last one the value was considerably lower (17.2%). The scope of the services was comparable in the first and fourth quarter of 2005. The distribution of inspections is analogous to the level of tractor sales in the investigated period.

The largest number of guarantee inspections (P1-P4) were carried out in the second quarter (29.4%) and the third one (28.7%). Temporary maxima occurred in March, April, May and September. An increased number of guarantee inspections coincided with preparing and carrying out spring agrotechnical operations and the harvest in the summer. It should be pointed out that the beginning, the middle and the end of the year was a period of the lowest number of guarantee inspections. The first quarter ended on the level of 19.6% per annum, and in the fourth quarter 22.3% were realized.

It should be mentioned that in 2005 post-guarantee inspections (PP) started being conducted due to the period of time that had passed from the beginning of service activity. Services of this type showed a similar distribution of their realization in the quarterly arrangement as guarantee inspections, and reached 22.9%, 33.3%, 25%, and 18.8% respectively.

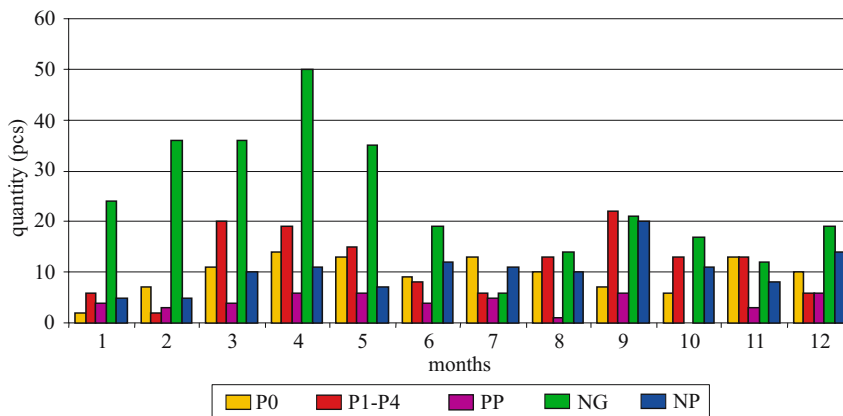


Fig. 6. The distribution of farm tractor inspections and repairs offered in 2005
Source: Own study.

Guarantee repairs (NG) reached the highest level in the first quarter (33.2%) and the second one (36%). The number of orders rendered within this period exceeded the level of repairs in the second half of the year over two times, where the number of services amounted to 14.2% in the third quarter

and 16.6% in the fourth quarter. A distinctly high demand on the services from the beginning of the year held for a few months, with a temporary maximum in April. This period coincided with the time of preparing tractors to the yearly season of agrotechnical operations and performing a number of spring field works.

The distribution of post-guarantee repairs (NP) showed the highest demand on the services in the third quarter of the year (33.1%), with the monthly maximum in September. The temporary increase in the number of repairs took place at the end of each quarter. The minimum level of services per annum fell on January and February, when the first quarter reached the number of orders of 16.2%. A balanced level of the number of repairs was recorded in the second and the fourth quarter (24.2% and 26.6% respectively).

The minimum level of the full range of services occurred in January. The first quarter was characterized by an increase in the number of realized orders, and their maximum was reached in April. June, July and August displayed a lowered demand on services at the level of 50% of the highest value in the spring. After a temporary growth in September, the number of inspections and repairs was again reduced by 30%. An increase in demand coincided with spring field works and the harvest. In a three-month presentation a dominant number of orders fell on the second quarter and amounted to 31.7% of the annual turnover. 24.3% of the services were performed in the first quarter, 23% in the second, and 21% in the last quarter per annum.

The statistical analysis of service of farm tractors

Seasonal fluctuations caused by the cyclic turn of seasons are a characteristic feature of plant production in farming. Moreover, they are the reason of the excessive growth of costs resulting from the irregularity of market processes. They may cause both not full use of companies' potential and overburdening sales and service departments in particular periods of the year.

The services, combined in the form of monthly observations, have been analyzed with regard to temporal dependence on the calendar of agrotechnical operations, which are carried out in a cyclic fashion throughout the year. The investigated processes have been studied with the use of the multiplicative model of the components of time series (ACZEL 2002).

$$Y_t = T_t \cdot S_t \cdot C_t \cdot I_t \quad (1)$$

where:

Y_t – value of the series

T_t – trend of a series
 S_t – seasonal variations
 C_t – cyclic variations
 I_t – rregular variations

Moving average based on 12 monthly observations was used to construct seasonal indices. Those indices mirror quantitative seasonal effects in the time series of the quantity of performed services. In the graphical analysis of the influence of seasonal variations on the variables distribution the term of reference level (average level) was introduced. The reference level for seasonanl indices eqals 100% in all months.

Orders of service of farm tractors in the years 2003-2005

The analysis included 2039 orders of servicing and repairs of farm tractors. The value of the seasonal indices for examined services expressed in percentage is presented in Figure 7. The fact that in the examined period the beginning of the year was characterised by the lowered need for servicing should be stressed. In January the number of the carried out orders was lower than the reference level by 48.3%. As a result of seasonal variations during the following six months of the examined period, the number of carried out orders exceeded the average level. Spring months were the time of intensive agrotechnical operations. That is why they generated incerased need for servicing and repairs of farm tractors. The need for servicing exceeded in March the reference level by 16.1%, in April by 60.0% and in May by 35.3%.

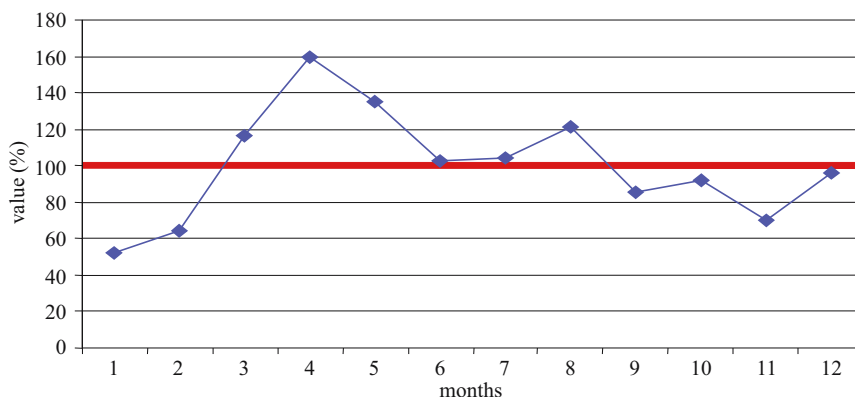


Fig. 7. Seasonal indices for servicing and repairs of farm tractors in the years 2003-2005
 Source: Own study.

In the next two months the number of carried out orders was close to the average level. As a result of seasonal variations the level of the servicing and repairs in August exceeded the average monthly demand by 21.4%. In the period from September to December seasonal indices demonstrated reduction of need for the services and values lower than the reference level.

Summary

The key term in the logistic strategy of the commercial service company is providing the client with the expected service. Realization of such programme should enable the company to obtain maximum income with the low level of incurred costs. The task of developing standards of servicing before selling, servicing and guarantee and post guarantee repairs of farm tractors is complicated. Such strategy may be based on subjective feelings of logistics managers, information coming from bookmaking or researches on the needs of strategic group of purchasers. In the field of servicing the knowledge of time layout of and structure of the orders reported by the users of farm vehicles over the year is most important.

The research concerning the structure of orders of servicing and repairs of farm tractors made by the *Servicing Department* in the years 2003-2005 confirmed the occurrence of the following unique features:

- dependence of the level of service before the sale (PO) on the number of sold new tractors. The number of guarantee inspections (P1 – P4) was dependent on the intensity of field operations recommended in the agricultural calendar. The higher number of of guarantee repairs (NG) could be noticed in the first half of the year and it was caused by preparation of farm tractors to the year-long season of agrotechnical operations. Also the relation of post guarantee repairs (NP) with the peak of agrotechnical operations was observed. The service of post guarantee inspections is fully payable and that is why, in most cases, they concerned removing failure, which had random character;

- the analysis of values of seasonal indices in the years 2003-2005 confirmed the dependence of the level of demand for the servicing and repairs of farm tractors on the intensity of field operations realised in accordance with the calendar of agrotechnical operations. The acquired number of the orders generated by farms in individual months proved that the highest number of orders was realised in the time of highest intensity of the field operations.

References

- ACZEL A.D. 2002. *Complete Business Statistics*. 4th ed. Richard D. Irwin/McGraw-Hill, Boston.
- Agrotechnika roślin uprawnych*. 2005. Red. S. Karczmarczyk. Wydawnictwo Akademii Rolniczej, Szczecin.
- Agrotechnologia*. 1999. Red. J. Banasiak. Wydawnictwo Naukowe PWN, Warszawa – Wrocław.
- CHRISTOPHER M., PECK H. 2005. *Logistyka marketingowa*. Polskie Wydawnictwo Ekonomiczne, Warszawa.
- CIESIELSKI M. 2006. *Logistyka w biznesie*. Wydawnictwo Akademii Ekonomicznej, Warszawa.
- COYLE J.J., BARDI E.J., LANGLEY C.J. 1996. *The Management of Business Logistics*. West Publishing Company, New York.
- DWILIŃSKI L. 2006. *Zarys logistyki przedsiębiorstwa*. Oficyna Wydawnicza Politechniki Warszawskiej, Warszawa.
- KEMPNY D. 2001. *Logistyczna obsługa klienta*. Polskie Wydawnictwo Ekonomiczne, Warszawa.
- Logistyka dystrybucji – specyfika, tendencje rozwojowe, dobre praktyki*. 2005. Red. K. Rutkowski. Wydawnictwo Szkoły Głównej Handlowej, Warszawa.
- PIEKARSKI W. 1997. *Analiza oddziaływania agregatów ciągnikowych na środowisko przyrodnicze*. Rozprawa habilitacyjna. Wydawnictwo Akademii Rolniczej, Lublin.
- Teoria i praktyka modelowania systemów logistycznych*. 2004. Red. I.K. Hejduk, Wydawnictwo Politechniki Koszalińskiej, Koszalin.

Accepted for print 6.05.2008 r.

AN ANALYSIS OF FARM TRACTORS SALES RESULTS IN THE ASPECT OF THE CALENDAR OF AGROTECHNICAL OPERATIONS

Sławomir Juściński, Wiesław Piekarski

Department of Power Engineering and Vehicles
University of Life Sciences in Lublin

Key words: logistics, distribution systems, farm tractors sales.

A b s t r a c t

The article presents problems of logistics of agricultural vehicles distribution. Obtained results of the research on the value and quantity levels of farm tractors sales have been presented. The research was carried out at the Commercial Department of an authorised distributor of farm tractors and agricultural vehicles. The research cycle included the years 2003-2005. The results of the research have been drawn up statistically by indicating the value of seasonal indices. The sales time schedules have been analysed in the aspect of the calendar of agrotechnical procedures.

ANALIZA WYNIKÓW SPRZEDAŻY CIĄGNIKÓW ROLNICZYCH W ASPEKCIE KALENDARZA ZABIEGÓW AGROTECHNICZNYCH

Sławomir Juściński, Wiesław Piekarski

Katedra Energetyki i Pojazdów
Uniwersytet Przyrodniczy w Lublinie

Słowa kluczowe: logistyka, systemy dystrybucji, sprzedaż ciągników rolniczych.

A b s t r a k t

W artykule przedstawiono zagadnienia logistyki dystrybucji pojazdów rolniczych. Zaprezentowano uzyskane wyniki badań poziomu ilościowego i wartościowego sprzedaży ciągników rolniczych. Badania zrealizowano w dziale handlowym autoryzowanego dystrybutora ciągników i maszyn rolniczych. Cykl badań obejmował lata 2003-2005. Wyniki badań opracowano statystycznie, wyznaczając wartość indeksów sezonowych. Rozkłady czasowe sprzedaży poddano analizie w aspekcie kalendarza zabiegów agrotechnicznych.

Introduction

The domestic market of farm tractors and agricultural vehicles, due to the globalisation of distribution, is an area of very strong competition of individual economic subjects. Vehicle producers' logistic strategies pay particular attention to the expansion and recruitment of new markets. Poland, as a member of the European Union, is carrying profound restructuring of rural areas along with the investment of financial means in technical equipment of villages. The change of the production technology triggers modernisation of machines, which results in bigger demand for farm tractors and machines. A rich offer of vehicles in a wide scope of functional capacity of engines and additional equipment along with comparable prices cause that promotion and marketing activities are comprehensively supported by logistics.

Research problem

The basic issue carried out by the sector of logistics in a planned amount of product sales is a selection of distribution channels of appropriate special structure and transport capacity. Organisation of physical distribution on a selected market area should lead to a realisation of customer service at an expected level. Control and corrective actions of the system have an objective to obtain a competitive offer that will ensure an advantage over companies supporting a given market sector. A superior objective of logistic strategy is to ensure the lowest costs for the entire sale chain (CHRISTOPHER, PECK 2005, *Usługi logistyczne*. 2004, *Rynek usług logistycznych*. 2005).

A crucial problem that should be taken into consideration in distribution management is the change ability of demand throughout a calendar year. Disproportion on the level of sales, which is a result of demand seasonally, negatively affects the supply process and may be the cause of a disruption in prompt realisation of orders (COYLE et al. 2002, *Logistyka dystrybucji*. 2005, STOCK, LAMBERT 2001).

The object of the research was the Commercial Department of an authorised distributor of agricultural vehicles. The quantity and value schedule of farm tractor sales was observed during three years of the research. The demand analysis was carried out in the aspect of the calendar of agrotechnical procedures.

Distribution logistics of agricultural vehicles

Companies that sell products and their servicing support constitute the basic model among the companies distributing farm tractors and machines. Benefits that arise from merging logistic subsystems of the distributor with organisational structure of the company stimulate expansion of extensive logistic networks (KEMPNY 2001, *Teoria i praktyka modelowania...* 2004).

Business entities connected with servicing agriculture over the long period of time and having strong position in the market and professional servicing, function as junction points linking logistic systems of a few producers of technical goods. Authorised sale and servicing of farm vehicles and machines of different make by one distributor may be realised under condition that there is no conflict of interest. Such solution functions in the examined company. It sells parallel JOHN DEERE and ZETOR farm vehicles in the area of lubelskie province. An authorised sales representative may also sell at the same time technical goods of various manufacturers, co-operating as a part of one concern. The concern SAME DEUTZ FAHR GROUP may be given as an example of such a solution. The commercial offers of the companies complement each other with vehicles of the Same, Deutz Fahr and Lamborghini makes.

In the situation when two tractors that have the same power units and similar prices are confronted, producers renegotiate with companies the terms of commercial contracts in order to sign new agreements that would guarantee exclusivity for sales of the products of one make. The conflict of interests results from a fight in the market for a potentially the same customer. The mentioned problem occurred during carrying out this research and concerned the tractors sold by the company ZETOR POLSKA and concern SDFG.

The sales of farm tractors in the commercial department in years 2003-2005

During the three-year period of research the services realised by the Commercial Department of the company that is an authorised distributor of the farm tractors and machines of over 20 producers were observed. The sales in the sector of vehicles included the makes: JOHN DEERE, ZETOR, SAME DEUTZ FAHR GROUP and PRONAR MTZ. The commercial Service Company was launched in the 80's of the twentieth century in the area of agricultural service. The sales for the leading JOHN DEERE make covered administrative area of lubelskie province. The products of the rest of the producers were distributed locally.

The sales of farm tractors in year 2003

In the analysed period 128 tractors were sold. The range of the bought goods covered products of five producers. The graphical presentation of the sales of farm tractors in separate months of the year 2003 is presented in a histogram (Fig. 1).

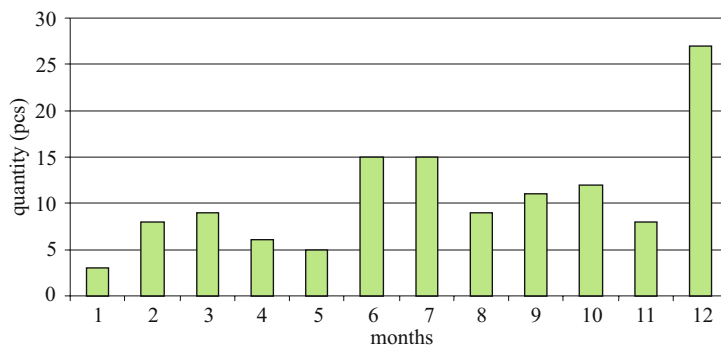


Fig. 1. The graphical presentation of the quantity of the sold farm tractors in the year 2003
Source: Own study.

The analysis of the quarterly sales was characterised by a growing tendency over the whole year. The level of the sales in the subsequent quarters increased respectively by 30%, 35% and 34%. Throughout the three-quarters regularity was observed, consisting in the fact that the highest turnover was reached in the last month of the investigated period. The lowest demand was observed in January and May. A temporary maximum of demand was recorded in June and July, while the highest level of sales was in December. Throughout the last month of the year 21% of the overall number of tractors were purchased. A rapid increase in sales was due to the subsidies from the EU within the SAPARD programme.

The value of tractors sale in the investigated year is presented in the form of a histogram (Fig. 2).

The analysis of the value of sold tractors confirms that there are relations observed throughout all the quarters with regard to demand. An increased value of turnover in relation to the number of sold tractors occurred in April, June, October and December, the latter being due to the fact that the most expensive models of tractors were purchased then.

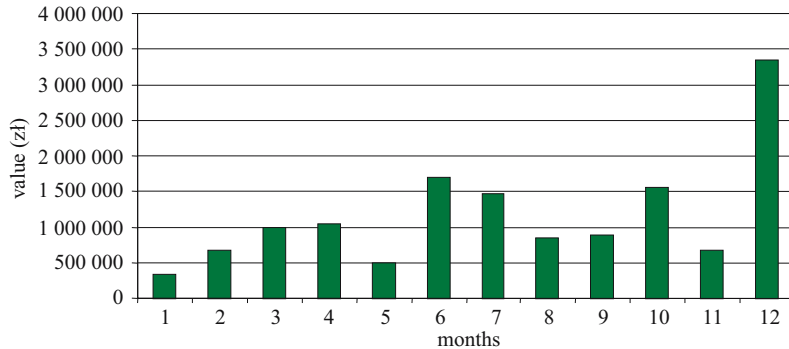


Fig. 2. The graphical presentation of the value of farm tractors sales in 2003

Source: Own study.

Farm tractors sale in 2004

In the investigated year 171 farm tractors were sold in general. The full assortment of the purchased vehicles included the tractors of five producers. The distribution of sales in the subsequent months is presented in the histogram (Fig. 3).

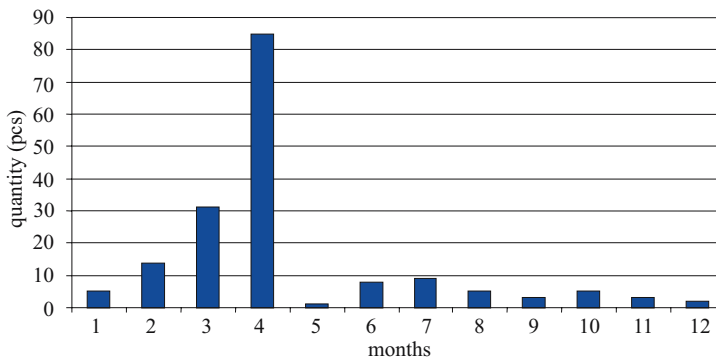


Fig. 3. The graphical representation of the quantity of farm tractors sales in 2004

Source: Own study.

In the first three months of 2004 there was observed a dynamic growth in the sales, while the maximum level of demand was recorded in April. Within one month 50% of the overall number of tractors sold in the investigated period were purchased. In the first four months 79% of the annual turnover was realised. The dynamics and structure of sales underwent a complete break-

down in the subsequent months. From May to the end of year it oscillated round the level of a few items per month. In the periodical presentation, a tendency pertaining to the three subsequent quarters was confirmed, consisting in the fact that the highest level of sales was reached in the first month of the analysed range. The opposite held true only for the first quarter.

The value of tractors sale in 2004 is presented in the histogram (Fig. 4). The distribution of the tractors sales value confirms the discussed phenomena concerning the quantitative analysis. The structure of demand on models of tractors at different price rates and of various producers was regular throughout the year. Quantitative and value characterisations of the sales in 2004 are similar.

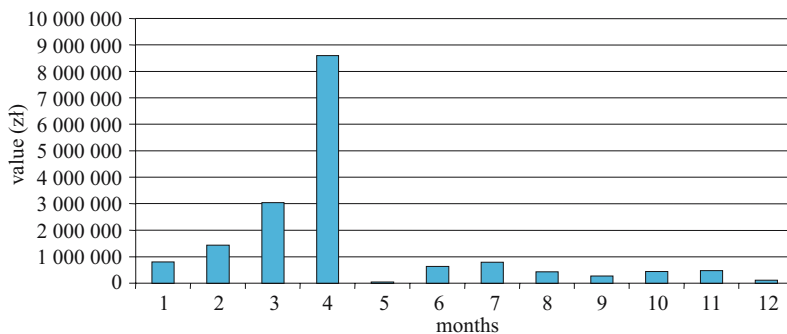


Fig. 4. The graphical presentation of the value of farm tractors sales in 2004

Source: Own study.

The structure of the presented histograms accurately reflects the phenomena that took place on the domestic market of tractors and farm machines. The dynamics and the level of demand were the result of closing the accession period for Poland and entering the EU on 1st May 2004. In accordance with EU laws, the VAT rate on farm machines and equipment rose from 0% to 22%.

Farm machines sales in 2005

In the investigated period 105 farm tractors were sold in general. The sales offer included the products of four companies. The distribution of farm tractors sales in particular months is presented in the histogram (Fig. 5). The analysis of the sales in the quarterly presentation showed an increase in the quantity throughout the year. The first and the second quarter ended in an

equal level of sales, while the third and the fourth quarter the growth was 13% and 27% respectively. What was characteristic was a very low demand in the first month of the year. There also occurred two three-month periods of a balanced level of tractors sale.

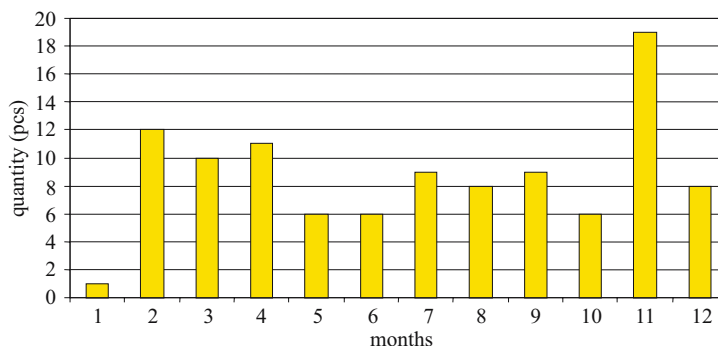


Fig. 5. The graphical presentation of the quantity of farm tractors sales in 2005
Source: Own study.

An increased demand took place in the period of performing agrotechnical procedures in the spring, as well as in the summer when the harvest was gathered. November was the month of the highest level of the purchased tractors, when their quantity exceeded the average sells level over two times. The distribution of the value of tractors sale in 2005 is presented in the histogram (Fig. 6).

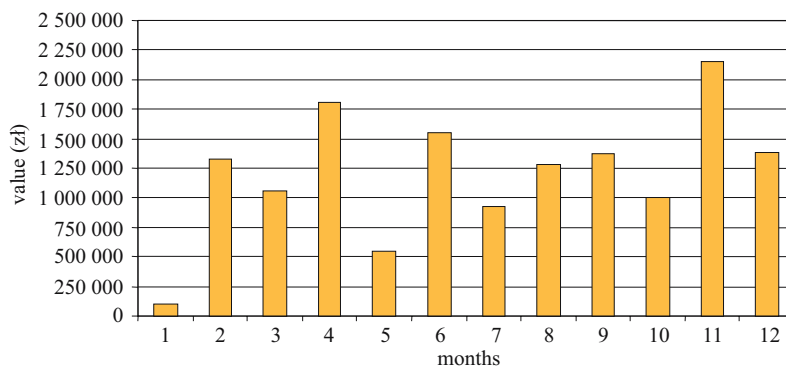


Fig. 6. The graphical presentation of the value of farm tractors sales in 2005
Source: Own study.

Temporary maxim occurred in April, June and November. A high value of turnover in April and June resulted from a large proportion of the most expensive models in the monthly sales structure. A characteristic feature of the investigated period was a very low value of the sales in January and a rapid drop of the value of turnover in May.

A comparative characterisation of farm tractors sales in the years 2003-2005

In the analysed period 404 farm machines were sold in general. The highest level of demand was in 2004, as a reaction of the market to the radical and disadvantageous change of sales conditions. The distribution of the sold tractors is presented in the histogram (Fig. 7).

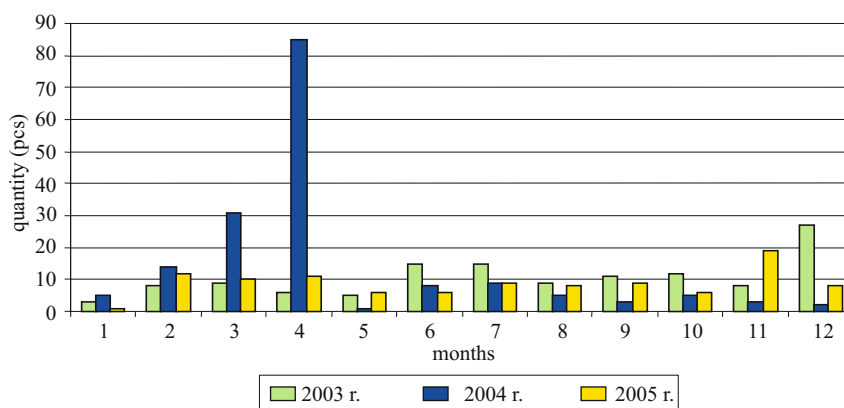


Fig. 7. The graphical presentation of the quantity of farm tractors sales in the years 2003-2005
Source: Own study.

A comparison of the quantitative and value structure in three subsequent years confirmed the similarities, in spite of different market conditions for farm tractors sale. In January a very low level of turnover was due to the winter, when field works are not performed. The season of spring field works results in a rapid growth of demand on farm tractors. What was characteristic was an abrupt decrease of the level of sales in May. A higher demand took place before the harvesting time than during the harvest of crops. An increase in the level of sales occurred at the end of the year as well.

The quantitative structure of tractors sale is presented in the histogram (Fig. 8).

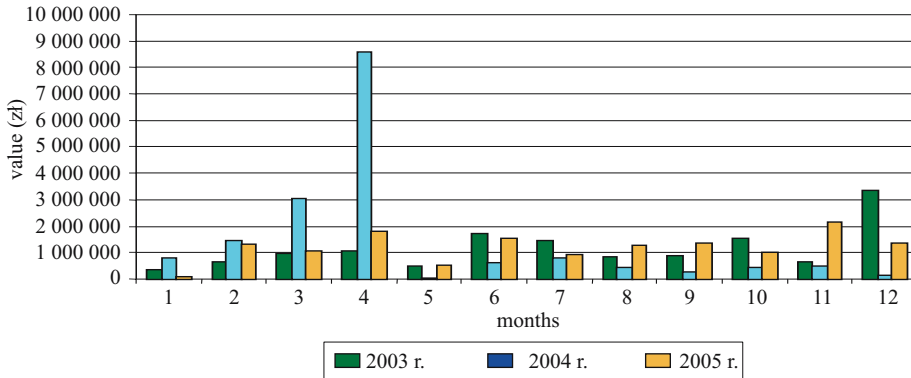


Fig. 8. The graphical presentation of the value of farm tractors sales in 2003-2005
Source: Own study.

Due to the conflict of interest between the products of ZETOR and SDFG, after two years of equal sales the products of SDFG were withdrawn from the offer of the company at the beginning of 2005. The tractors made by PRONAR MTZ constituted a supplement to the market offer, which included the models at lower price rates. They constituted a few per cent of the investigated market. The quantitative superiority of the tractors produced by an American concern DEERE & COMPANY over the ones from a Czech company ZETOR may be interpreted as a tendency of the market to favour the products, which have rich equipment offer and are at higher price rates.

A statistical analysis of farm tractors sales in the years 2003-2005

An analysis of farm tractors sales in the investigated period has demonstrated that they were of periodic nature and were prone to seasonal changes. In order to analyse this phenomenon in the aspect of the calendar of agrotechnical procedures, for each time series the quantities and values of the sold tractors, i.e. the seasonal indices, were specified. The analysis has been carried out according to the multiplicative model of the components of time series. The multiplicative model can be expressed by means of an equation (ACZEL 2002, PUŁASKA-TURYNA 2005):

$$Y_t = T_t \cdot S_t \cdot C_t \cdot I_t \quad (1)$$

where:

Y_t – value of the series

T_t – trend of a series

S_t – seasonal variation

C_t – cyclic variation

I_t – irregular variation

The value of seasonal indices has been calculated on the basis of moving average for 12 monthly observations. The calculated indices show seasonal effects in the time series for the quantity and value of the sold tractors. When analysing the influence of the seasonal variation on the distribution of the quantity and value of the sold assortment, the notion of (average) level value has been employed, which for seasonal indices in particular months amounted to 100%.

A statistical analysis of the quantity of sold farm tractors

The value of seasonal indices for the quantity of farm tractors sold in years 2003-2004 is presented in the graph (Fig. 9).

At the beginning of the year, when the field agrotechnical procedures were performed, farm tractors sale was lower than the reference level by 77.7%. Due to seasonal variations in the three following months, the level of the sales exceeded the average level: in February by 38.9%, in March by 68.2% and in April by 238.6%. The spring months are the period of particularly intensive agrotechnical procedures and, at the same time, of high demand for driving power source and towing power, that is for tractors.

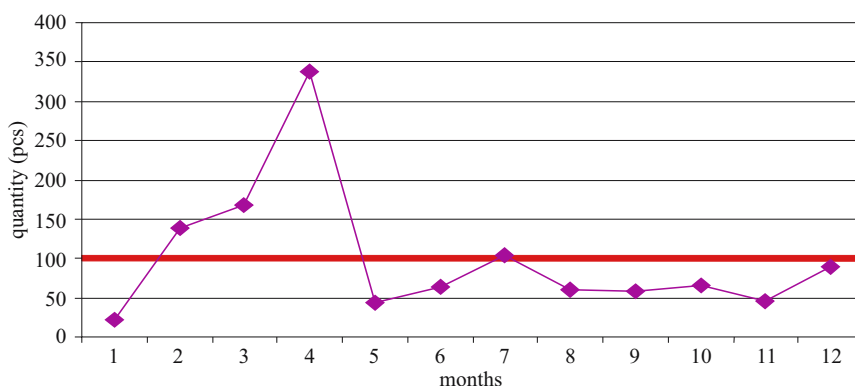


Fig. 9. Seasonal indices for the quantity of sold farm tractors in the years 2003-2005
Source: Own study.

The calendar of agrotechnical procedures includes in this period sowing of spring cereals, planting bulb and root plants and sowing spring oleaginous plants (*Agrotechnika roślin uprawnych* 2005, *Agrotechnologia* 1999). It should be stressed that two subsequent months show considerable decrease in demand. So, in May it was lower than the average by 56.2% and in June by 36.8%. In July the sales increased and the sales exceeded the average level by 4.6%. This temporary maximum is connected in the calendar of agricultural operations with the beginning of gathering crops. The level of demand from August to November, due to seasonal variations constituted 50% of the reference level. The end of the year was the time, when the demand increased, but it was still below the average.

A statistical analysis of the value of sold farm tractors

The value of seasonal indices for the value of farm tractors sold in years 2003-2004 is presented in the graph (Fig. 10).

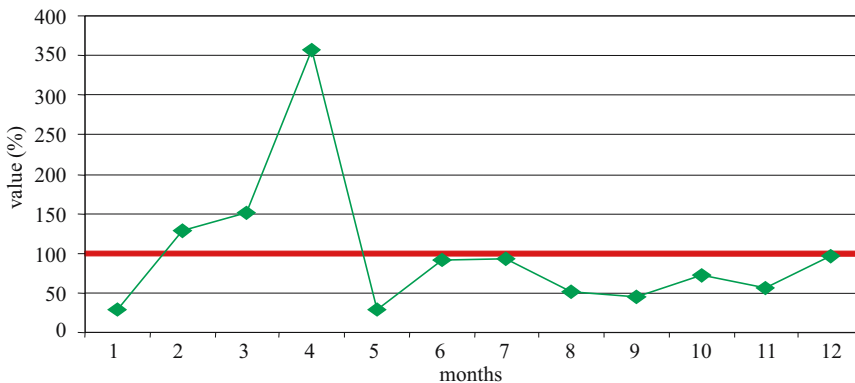


Fig. 10. Seasonal indices for the value of sold farm tractors in the years 2003-2005
Source: Own study.

General characteristic of the line in the graph confirmed all the features of the values of tractors sales described in the commentary on the indices for the quantity of the bought vehicles. The significant decrease of the demand took place in January and May, when there was no field labour included in the calendar of agrotechnical procedures. The spring months confirmed higher level of the sales, and June and July reached the reference level. The long-lasting reduction in sales during second half of the year ended in December.

Summary

The purchaser's satisfaction from complex customer service and then, from prompt supply of the bought tractors run by the Commercial Department of the dealer company, is a basic condition of building long-term co-operation. The loyal purchaser is not prone to jump at an offer of competing companies during the whole process of using technical products.

The effective selective distribution of farm tractors and machinery requires thorough knowledge of agricultural market. The sudden increase and the high level of demand for farm tractors over short period of time generate a number of logistic objectives. A successful customer service is then the result of implementing the solutions based on logistic systems that function in a net of distribution inside and outside the commercial Service Company.

The value of the seasonal indices in the investigated period of years 2003-2005 indicates that there is a relationship between the level of sales and the calendar of agrotechnical procedures. The level of demand provided farm households with new tractors, especially during the spring months. This allowed using them fully, as the source of energy during the whole season in a given calendar year. The purchase at the beginning of the period had also a significant economical aspect for the farm households. Investment in these kind of fixed assets allowed benefiting from current use of tractors. The purchasers bought more tractors before the harvest time than during intensive field labour. Another distinct increase of the level of sales took place by the end of the year and was connected to investments into fixed assets coming from the income from the current activities of farm households.

References

- ACZEL A.D. 2002. *Complete Business Statistics*, 4th ed. Richard D. Irwin/McGraw-Hill, Boston.
- Agrotechnika roślin uprawnych*. 2005. Red. S. Karczmarczyk, Wydawnictwo Akademii Rolniczej, Szczecin.
- Agrotechnologia*. 1999. Red. J. Banasiak, Wydawnictwo Naukowe PWN, Warszawa – Wrocław.
- CHRISTOPHER M., PECK H. 2005. *Logistyka marketingowa*. Polskie Wydawnictwo Ekonomiczne, Warszawa.
- COYLE J.J., BARDI E.J., LANGLEY C.J. 2002. *Zarządzanie logistyczne*. Polskie Wydawnictwo Ekonomiczne, Warszawa.
- KEMPNY D. 2001. *Logistyczna obsługa klienta*. Polskie Wydawnictwo Ekonomiczne, Warszawa.
- Logistyka dystrybucji – specyfika, tendencje rozwojowe, dobre praktyki*. 2005. Red. K. Rutkowski. Wydawnictwo Szkoły Głównej Handlowej, Warszawa.
- Usługi logistyczne*. 2004. Red. W. Rydzkowski. Wydawnictwo Instytutu Logistyki i Magazynowania, Poznań.
- PULASKA-TURYNA B. 2005. *Statystyka dla ekonomistów*. Wydawnictwo Difin, Warszawa.
- Rynek usług logistycznych*. 2005. Red. M. Cisielski, Wydawnictwo Difin, Warszawa.
- STOCK J.R., LAMBERT D.M. 2001. *Strategic Logistic Management*. Mc Graw – Hill/Irwin, New York.
- Teoria i praktyka modelowania systemów logistycznych*. 2004. Red. I.K. Hejduk. Wydawnictwo Politechniki Koszalińskiej, Koszalin.

AN ANALYSIS OF THE TERRITORIAL RANGE OF FARM TRACTORS SERVICING REALISED AS AN ELEMENT OF DISTRIBUTION LOGISTICS

Sławomir Juściński, Wiesław Piekarski

Department of Power Engineering and Vehicles
University of Life Sciences in Lublin

Key words: logistics, logistics systems, servicing distribution.

A b s t r a c t

The research on farm tractors inspections and repairs considering the territorial scope of the carried out orders is presented. The structure of the orders for service for four radiuses of distance that were investigated in the years 2003-2005 is demonstrated. The function of logistics concerning service teams interventions in commercial Services Company is explained. The solutions that provide the expected level of service and, at the same time, cost minimisation are presented. The article demonstrates the analysis of servicing structure and schedule of the number of farm tractor inspections and repairs for individual radiuses, of distance in the aspect of the calendar of agrotechnical operations.

ANALIZA ZASIĘGU TERYTORIALNEGO OBSŁUGI SERWISOWEJ CIĄGNIKÓW ROLNICZYCH REALIZOWANEJ JAKO ELEMENT LOGISTYKI DYSTRYBUCJI

Sławomir Juściński, Wiesław Piekarski

Katedra Energetyki i Pojazdów
Uniwersytet Przyrodniczy w Lublinie

Słowa kluczowe: logistyka, systemy logistyczne, dystrybucja usług serwisowych.

A b s t r a k t

Zaprezentowano badania usług przeglądów i napraw ciągników rolniczych w aspekcie zasięgu terytorialnego wykonanych zleceń. Przedstawiono strukturę zleceń serwisowych dla czterech promieni odległości, które badano w latach 2003-2005. Wyjaśniono funkcje logistyki w przedsiębiorstwie handlowo-usługowym w zakresie organizacji wyjazdów zespołów serwisowych. Przedstawiono rozwiązania, które zapewniają oczekiwany poziom obsługi klienta i jednocześnie minimalizację kosztów. Zaprezentowano analizę struktury obsługi serwisowej oraz rozkład liczby usług przeglądów i napraw ciągników rolniczych dla poszczególnych promieni odległości w aspekcie kalendarza zabiegów agrotechnicznych.

Introduction

Distribution management of farm tractors is based on business entities. The necessity to provide guarantee and postguarantee service results in the fact those very often-commercial services companies constitute the logistic network of the sales. *The Service Department*, which is responsible for carrying out the extensive orders as a part of inspections and repairs of technical means, plays an important role in maintaining the state of technical and exploitation of farm tractors. Farm tractors are the main source of driving and towing power (PIEKARSKI 1997, SKROBACKI et al. 2006). Meeting the requirements of customer service forces the authorised dealers to incur capital expenditure for the created company infrastructure (COYLE et al. 1996, CHRISTOPHER et al. 2005, CIESIELSKI 2006).

Research problem

Selective sales network created by leading producers extorts the division of home market into commercial zones. It creates a barrier to enter the market for the other companies in the same line of business. The areas serviced by individual dealers should be dependent, first of all, on the absorption capacity for new farm vehicles. What is more, it is necessary to build up appropriately high population of tractors of a given make. Providing functional efficiency will be the basis for effective activity of both, *the Service Department* and spare parts wholesalers (RUTKOWSKI 2005, PFOHL 2001). The object of the research was the authorised service of the distributor of farm vehicles that carries out guarantee and postguarantee inspections and repairs. The analysis concerning territorial layout of the carried out repair services for four radiuses of distances: $r = 0$ km, $0 \text{ km} < r < 50 \text{ km}$, $50 \text{ km} < r < 100 \text{ km}$ and $r > 100 \text{ km}$ was conducted.

The structure of the orders carried out by service teams

The reduction of the level of logistic costs in services provided by a service station may be stimulated by controlling the structure of service teams' trips. It is possible to maintain the optimal level of customer service and, at the same time, to reduce the route of travel, as shown in the diagram (Fig. 1).

The basic model of service consists of trips of a team of mechanics individually to each of the received reports. Employing such a system in the period of intensive field works may lead to a quick exhaustion of the potential

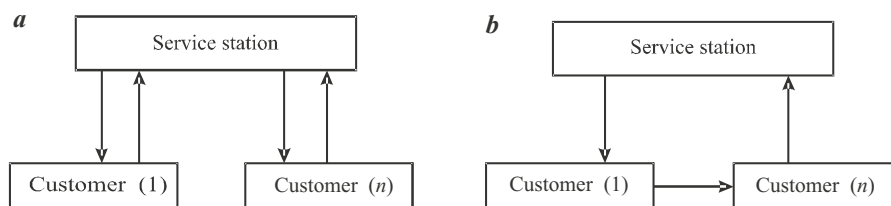


Fig. 1. The structure of service teams' trips in order to carry out repairs: a) individual trips, b) joint trips

Source: Own study.

of service teams that a company hires. This often leads to an accumulation of the works undertaken and a prolongation of the time that is needed for the realisation of the service. The lack of help from the authorised dealer negatively influences the co-operation between the purchaser and the seller after the transaction (KEMPNY 2001).

Moreover, the cyclical prolongation of the time needed for repair or for the arrival of the service team lowers the customer's loyalty and perpetuates a negative image of the brand on the market. The system aiming at increasing the coefficient of the use of working time attempts to join the service of several customers within one trip.

The realisation of this model is put into practice when:

- the scope of the service orders allows for short visits at the successive principals,
- a visit's aim is to diagnose and verify the scope of the repair,
- a visit serves the purpose of submitting some spare parts and operation materials,
- the destinations are within the same area.

In the case of joint trips it is possible to use the graph theory in service logistics. A commercial traveller is then employed and his task is to find the shortest route, which begins and ends at the service station, under the assumption that each principal is visited only once.

The problem of joining and matching the routes is connected with planning the level of the costs related to the service station activity, as well as with general distribution expenses. The trips should be planned according both to the time that is required for the realisation of the orders, and to the time needed in order to get to particular points on the route. The functioning of the system is distorted when the theoretical timing principles become negatively verified in relation to the real conditions. The issue constitutes an organisational challenge to the *Service Department*, especially during the period of intensive field works recommended in the calendar of agricultural operations.

An analysis of inspections and repairs of farm tractors in the service department carried out in the years 2003-2005

During a three-year period the services rendered by the Service Department of a company which is an authorised dealer of tractors such as JOHN DEERE and ZETOR were investigated. The object of the research was a trade-service company that conducts business activity in the sector of agricultural services. The JOHN DEERE concern was a market-leading brand with regard to the quantity of the vehicles sold by the dealer in the years 2003-2005. During this period creating a high population of these vehicles on the local market has begun through selective distribution. Due to the above, servicing was carried out in relation to a large number of tractors in working order with a short period of exploitation.

The territorial scope (radius) of the orders carried out in 2003

In the investigated period *the Service Department* rendered 534 services concerning inspections and repairs of farm machines. The territorial distribution of the services has been presented in the circular graph (Fig. 2).

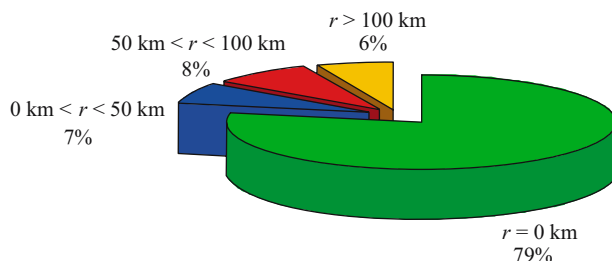


Fig. 2. The territorial structure of the services rendered within inspections and repairs of farm machines in 2003

Source: Own study.

Stationary workshop repairs ($r = 0 \text{ km}$) in the researched period constituted 79% of the realised orders. Such a division stems from the fact that the full package of guarantee inspections (services for the tractors in working order) represented the value of 61%. Moreover, in the case of the DEERE and COMPANY concern the orders included the vehicles with a short exploitation period. The services for the remaining distance ranges oscillated around a few percent.

The quantitative distribution of the orders for particular distances are shown in the histogram (Fig. 3). During the period in question an evident

dominance of workshop repairs ($r = 0$ km) was observed throughout the whole year, while the temporary maxima took place in the following months: April, June, August, October and December.

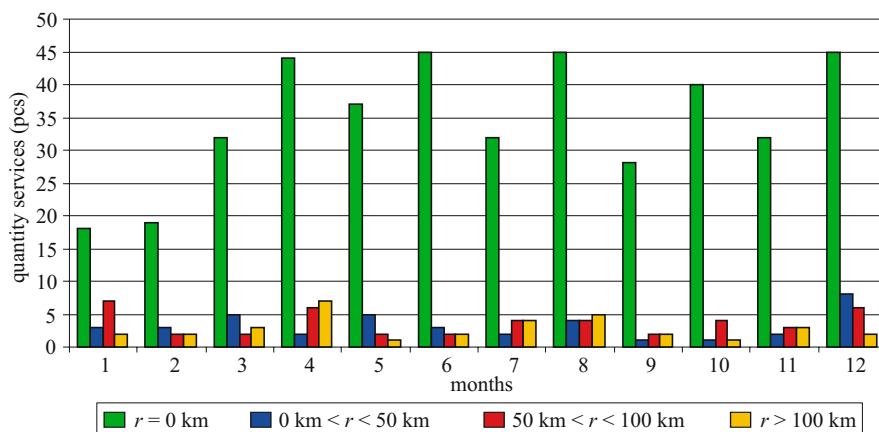


Fig. 3. The distribution of the quantity of inspections and repairs of farm tractors in 2003 for particular distances of their realisation

Source: Own study.

The territorial scope (radius) of the orders carried out in 2004

In the investigated period *the Service Department* carried out 786 services that constituted inspections and repairs of farm tractors. The territorial structure of the orders is presented in the circular graph (Fig. 4).

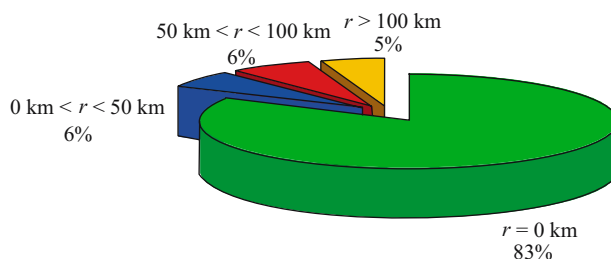


Fig. 4. The territorial structure of services that constitute inspections and repairs of farm tractors in the year 2004

Source: Own study.

Stationary workshop repairs in 2004 amounted to 83% of the orders carried out. The structure of services concerning the remaining ranges of distance from the company's headquarters was on a balanced level of a few percent. Such a structure resulted from, above all, the number of inspections carried

out with regard to the tractors in working order. In the researched period they constituted 63% of the overall number of orders. The accession of Poland to the EU, which took place on 1st May 2004, together with the increase of the VAT rate on farm machines and equipment from 0 to 22%, caused a very high level of demand in this sector.

The distribution of the orders for particular distances is presented in the histogram (Fig. 5). The workshop repairs ($r = 0$ km) reached the highest level in April and May. The period from June to October was characterised by balanced and high demand for services. Traditionally, at the beginning of the year and in November there is low demand for servicing.

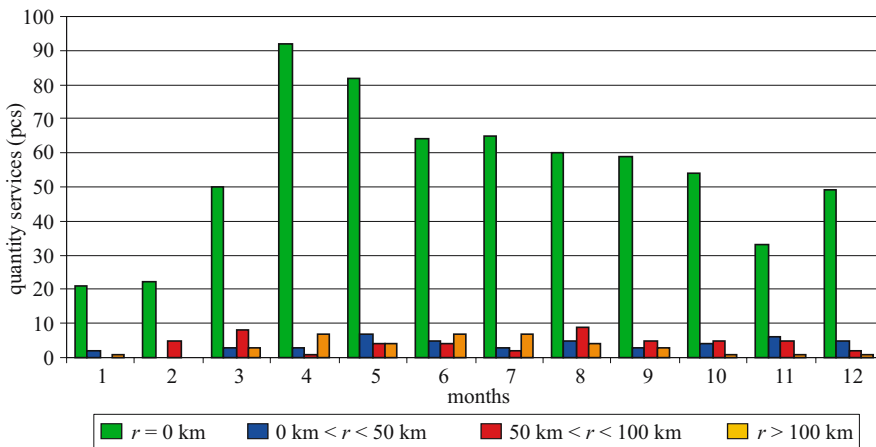


Fig. 5. The distribution of quantity of inspections and repairs of farm tractors in 2004 for the individual distances of their completion

Source: Own study.

Territorial scope (radius) of the orders carried out in 2005

Over the investigated year *the Service Department* carried out in total 719 services by inspections and repairs of farm tractors. The territorial structure of the servicing orders in the aspect, of the distance from the headquarters of the company is presented in the circular graph (Fig. 6).

Stationary workshop repairs in the investigated year 2005 constituted 60% of the carried out orders. The level of their completion resulted from the fact that all the inspections in the analysed period constituted 43% of all the orders. The structure of the servicing operations carried out in the place of residence of the employers demonstrated that the number of orders coming from the distances of $50 \text{ km} < r < 100 \text{ km}$ is twice as high as the number of orders from

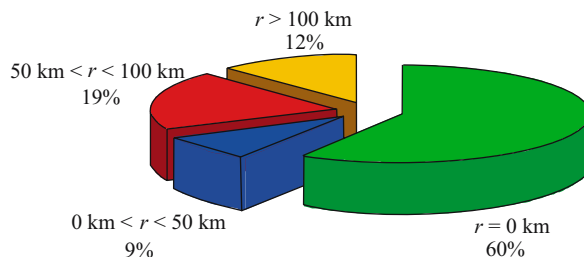


Fig. 6. The territorial structure of inspections and repairs of farm tractors carried out in 2005
Source: Own study.

shorter distances. The level of 12% of the services in the distance of over 100 km proves wide territorial scope of the examined company on the domestic market of servicing.

The distribution of orders for inspections and repairs of farm tractors in 2005 for individual distances of their completion is presented in the histogram (Fig. 7).

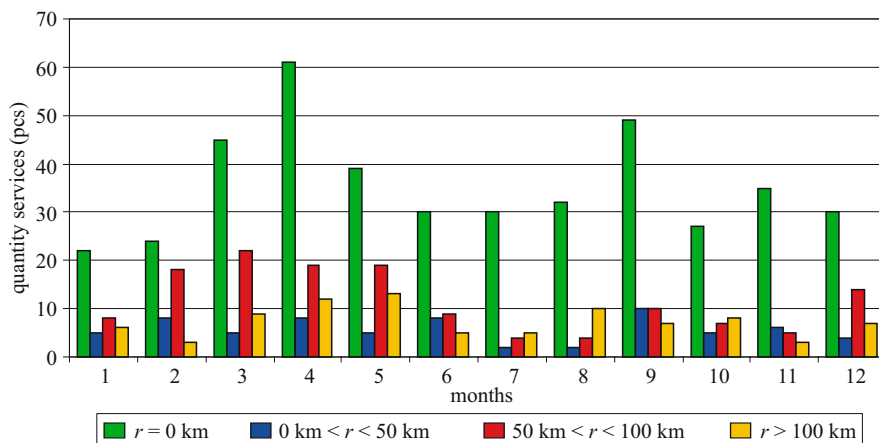


Fig. 7. The distribution of inspections and repairs of farm tractors in 2005 for individual distances of their completion
Source: Own study.

Workshop services ($r = 0 \text{ km}$) constituted the dominating group of orders which were realised by the *Service Department*. However, their level was lower by over 20% in comparison with the years 2003 and 2004. The works carried out in the service station reached the local maxima in: March, April, May and September, so in the periods when the demand for agrotechnical operations is higher. The second area in respect of the quantity, was the group of orders

coming from the distances of $50 \text{ km} < r < 100 \text{ km}$. The services rendered by service teams at the place of residence of the employers dominated especially the first and second quarters of the year. Such a phenomenon took place in all the three scopes of distances. It confirmed the relation between the demand for inspections and repairs of farm tractors and the process of preparation and realisation of the field labours in separate periods of the year 2005. The number of orders was highest in April and September, i.e. in the time of higher demand for agrotechnical operations (KARCZMARCZYK 2005, BANASIAK 1999).

Summary

Servicing of farm tractors and machines constitutes an important element of distribution logistics. From high technological and structural level of modern farm vehicles stems the necessity to provide professional servicing. The inspections and repairs should be carried out irrespective of territorial distribution and the length of the radius of the trip of service team, in the time that takes into account the specific needs of the market. The reaction speed, delivery time of a given service and successful performances are most often mentioned clients' requirements.

The analysis of the results of the research allows to formulate a thesis that there is a relation between the quantity of orders for individual radiuses and the change of satisfaction of the market with products of a given brand in subsequent years. Moreover, a statistic increase in the age of the tractors is crucial in the scope of services offered. There was a decrease in stationary services ($r = 0 \text{ km}$) connected, first of all, with technical inspections, and there was a steep increase in realised orders which required trips of repair teams. Such a tendency concerned all three radiuses: $0 \text{ km} < r < 50 \text{ km}$, $50 \text{ km} < r < 100 \text{ km}$ and $r > 100 \text{ km}$ in the analysed period.

References

- Agrotechnika roślin uprawnych*. 2005. Red. S. Karczmarczyk. Wyd. Akademii Rolniczej w Szczecinie, Szczecin.
- Agrotechnologia*. 1999. Red. J. Banasiak. Wydawnictwo Naukowe PWN, Warszawa – Wrocław.
- CHRISTOPHER M., PECK H. 2005. *Logistyka marketingowa*. Polskie Wydawnictwo Ekonomiczne, Warszawa.
- CIESIELSKI M. 2006. *Logistyka w biznesie*. Akademia Ekonomiczna, Warszawa.
- COYLE J.J., BARDI E.J., LANGLEY C.J. 1996. *The Management of Business Logistics*. West Publishing Company, New York.
- KEMPNY D. 2001. *Logistyczna obsługa klienta*. Polskie Wydawnictwo Ekonomiczne, Warszawa.
- Logistyka dystrybucji – Specyfika, Tendencje rozwojowe, Dobre praktyki*. 2005. Red. K. Rutkowski. Szkoła Główna Handlowa, Warszawa.

-
- PFOHL H.Ch. 2001. *Systemy logistyczne – Podstawy organizacji i zarządzania*. Instytut Logistyki i Magazynowania, Poznań.
- PIEKARSKI W. 1997. *Analiza oddziaływania agregatów ciągnikowych na środowisko przyrodnicze*. Rozprawa habilitacyjna, Akademia Rolnicza, Lublin.
- SKROBACKI A., EKIELSKI A. 2006. *Pojazdy i ciągniki rolnicze*. Wyd. Wieś Jutra, Warszawa.

Accepted for print 25.08.2008 r.

CHOSEN RESULTS OF VOLTAGE ASYMMETRY SIMULATION INVESTIGATIONS AT RURAL CONSUMERS SUPPLIED BY LOW VOLTAGE POWER LINE

Piotr Kolber¹, Janusz Piechocki²

¹ Department of Machine Maintenance
University of Technology and Life Sciences in Bydgoszcz

² Department of Electric and Power Engineering
University of Warmia and Mazury in Olsztyn

Key words: load asymmetry, simulation program, voltage asymmetry.

Abstract

A simulation program facilitating to determine values of the chosen parameters characterizing electric energy quality (δU – voltage deviation, α_{U2} – voltage asymmetry coefficient) supplied to the rural consumers has been built on the basis of the elaborated model of a low voltage power line (LV). The simulation program representing a computerised realization of the model has been written in Turbo Pascal language. This paper presents chosen investigation results regarding, among other things, influence of the cable cross-sections on the voltage asymmetry in a low voltage power line.

WYBRANE WYNIKI BADAŃ SYMULACYJNYCH ASYMETRII NAPIĘCIOWEJ U ODBIORCÓW WIEJSKICH ZASILANYCH Z LINII NISKIEGO NAPIĘCIA

Piotr Kolber¹, Janusz Piechocki²

¹ Katedra Eksploatacji Maszyn
Uniwersytet Technologiczno-Przyrodniczy w Bydgoszczy

² Katedra Elektrotechniki i Energetyki
Uniwersytet Warmińsko-Mazurski w Olsztynie

Słowa kluczowe: asymetria obciążeń, program symulacyjny, niesymetria napięć.

Abstract

Na podstawie opracowanego modelu linii niskiego napięcia (nN), zbudowano program symulacyjny umożliwiający wyznaczanie wartości wybranych parametrów charakteryzujących jakość energii elektrycznej (δU – odchylenie napięcia, α_{U2} – współczynnik asymetrii napięciowej) dostarczanej odbiorcom wiejskim. Program symulacyjny, będący komputerową realizacją modelu, napisano w języku Turbo Pascal. W artykule przedstawiono wybrane wyniki badań dotyczące m.in. wpływu przekrojów przewodów na asymetrię napięciową w linii niskiego napięcia.

Introduction

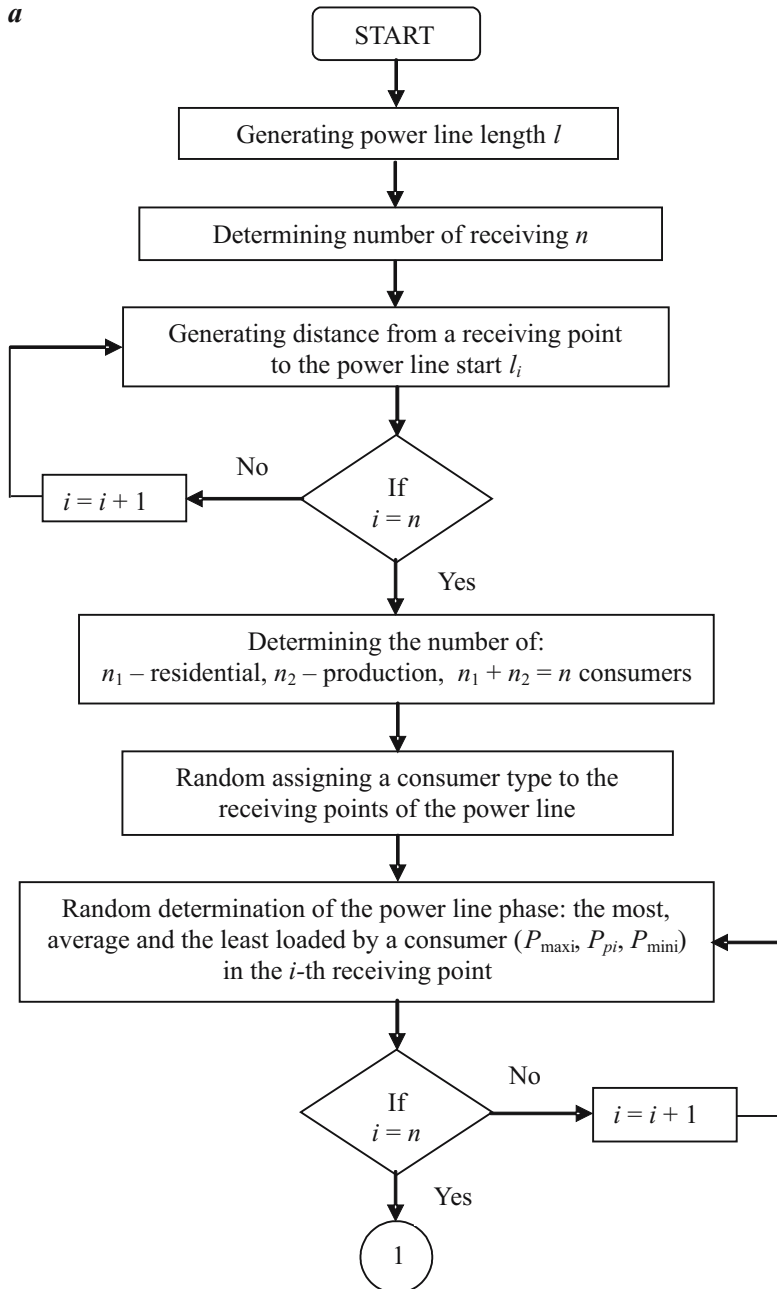
It may be stated that the values of the voltage drops, and subsequently levels and asymmetry of voltages in a LV power line are affected by the parameters of the power line being a transmission element that means its length, arrangement of the cables, cross-sections of the cables, distribution of the receiving points and the very consumers by the value of the consumed power and the asymmetry of phase loads. Because of a great number of the factors being crucial for the level and voltage asymmetry in a power line and due to the difficulties related to realization of complex investigations regarding the consumers' loads, as well as their expensiveness, a simulation model to determine values of the chosen quality parameters of electric energy has been elaborated. It facilitates to determine the values of voltage drops and deviations as well as of voltage asymmetry with various methods of distribution of the consumers along the power line, various values of the power consumed by the consumers and various levels of phase load asymmetry.

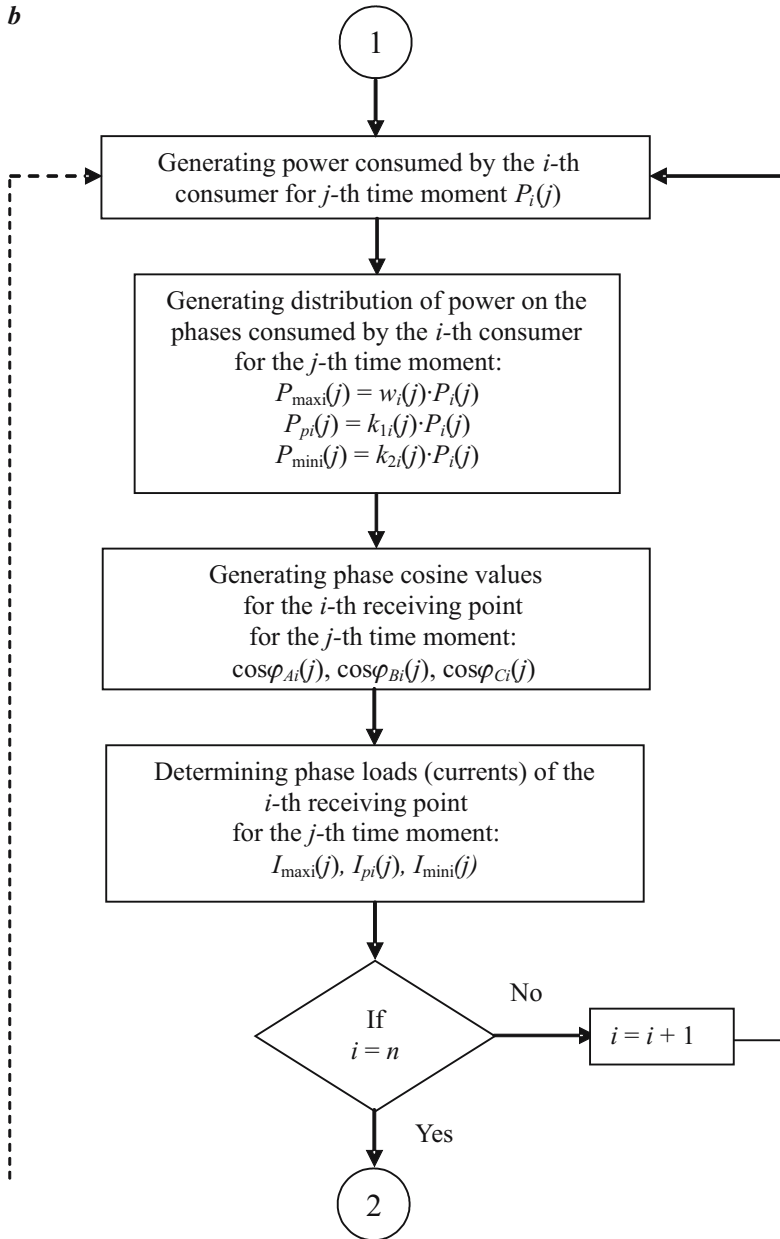
A simulation program, presented as a flowchart in Figure 1 has been elaborated on the basis of the model built to determine chosen parameters characterizing electric energy quality supplied to the consumers fed by a three-phase, four-cable low voltage power line (KOLBER 2006).

Simulation program to determine values of chosen parameters characterizing electric energy quality

The simulation program, presented below on the flowcharts, may be used to determine the values of the voltage drops and deviations as well as voltage asymmetry coefficients. This paper presents analysis of excess percentage of the admissible value of the voltage asymmetry coefficient α_{U_2} , taken from a week time, for various variants of cable cross-sections applied and various variants regarding the type of the consumers connected to. The algorithms to generate random numbers used to perform the simulation were taken from the work (ZIELIŃSKI 1979), while the probability distributions were taken from the work (HELLWIG 1993).

The standardised requirements (Polish Standard PE 50160 1998) regarding the voltage asymmetry coefficient refer to its admissible value ($\alpha_{U_{2dop}}=2\%$) and admissible excess percentage of this value over a week time, which for this parameter is equal to 5%.

a



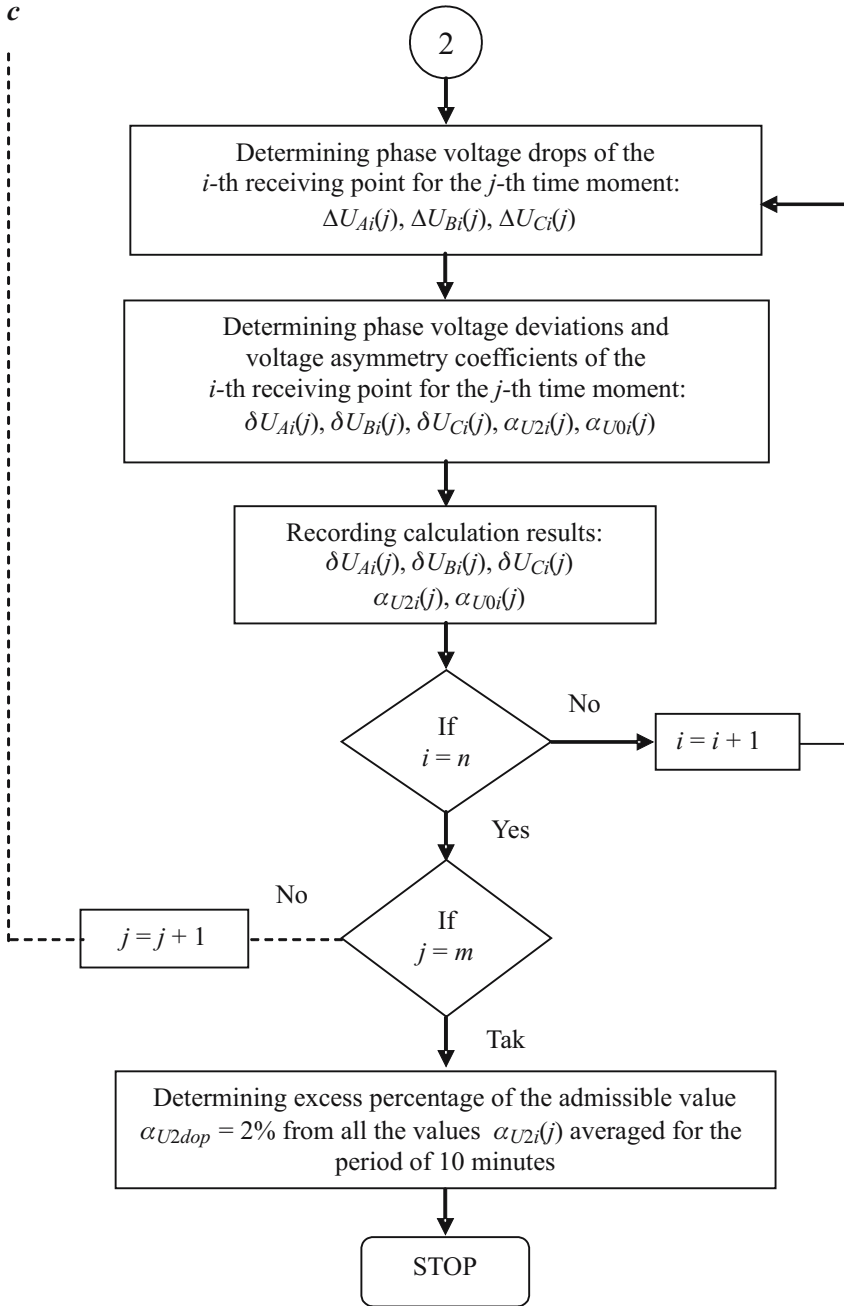


Fig. 1. Flowchart of the simulation program to determine values of the parameters characterizing electric energy quality

Chosen results of the simulation investigations

As a result of the simulation carried out a power line of length $l = 1048$ m supplying 15 consumers distributed at the following distances from the power line start has been generated:

$l_1 = 82$ m, $l_2 = 92$ m, $l_3 = 105$ m, $l_4 = 284$ m, $l_5 = 296$ m, $l_6 = 301$ m, $l_7 = 312$ m, $l_8 = 368$ m, $l_9 = 495$ m, $l_{10} = 589$ m, $l_{11} = 663$ m, $l_{12} = 750$ m, $l_{13} = 795$ m, $l_{14} = 841$ m, $l_{15} = 1048$ m.

The calculations were performed for the following variants regarding the type of the consumers connected to:

- a) 0 residential consumers, 15 production consumers,
- b) 5 residential consumers, 10 production consumers,
- c) 10 residential consumers, 5 production consumers.

They referred also to the variants of the applied cross-sections of the cables used in a low voltage power line:

- a) phase cables cross-section $s = 35$ mm²;
neutral cable cross-section $s_n = 35$ mm²,
- b) phase cables cross-section $s = 35$ mm²;
neutral cable cross-section $s_n = 50$ mm²,
- c) phase cables cross-section $s = 50$ mm²;
neutral cable cross-section $s_n = 50$ mm²,
- d) phase cables cross-section $s = 50$ mm²;
neutral cable cross-section $s_n = 70$ mm²,
- e) phase cables cross-section $s = 70$ mm²;
neutral cable cross-section $s_n = 70$ mm².

The obtained values of the asymmetry coefficient α_{U2} for the performed simulations are presented in the Figures: 2, 3, 4, 5, 6 and in the Table 1.

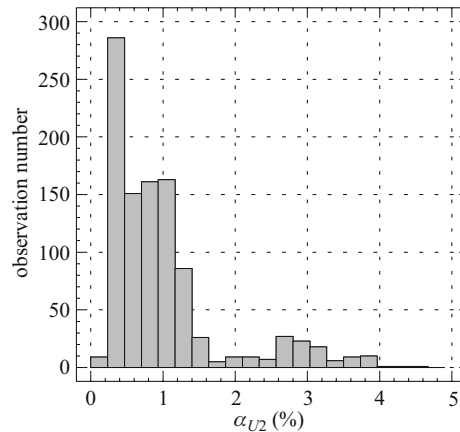
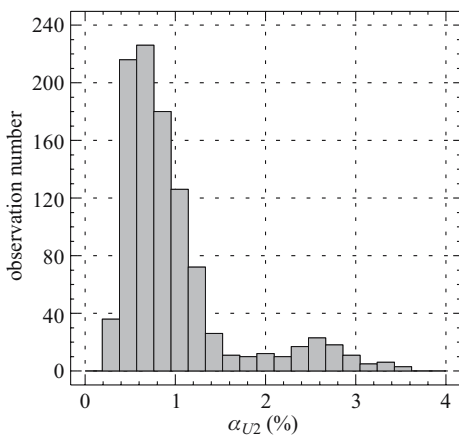


Fig. 2. Histogram of the voltage asymmetry coefficient values obtained as a simulation result for the following parameters:

- phase cables cross-section – 35 mm²,
- neutral cable cross-section – 35 mm²,
- number of residential consumers – 0



Rys. 3. Histogram of the voltage asymmetry coefficient values obtained as a simulation result for the following parameters:
 – phase cables cross-section – 35 mm²,
 – neutral cable cross-section – 35 mm²,
 – number of residential consumers – 5

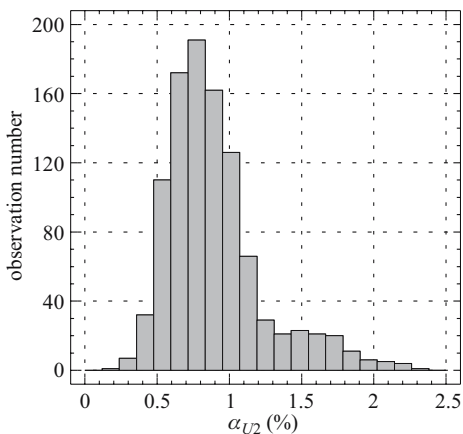


Fig. 4. Histogram of the voltage asymmetry coefficient values obtained as a simulation result for the following parameters:
 – phase cables cross-section – 35 mm²,
 – neutral cable cross-section – 35 mm²,
 – number of residential consumers – 10

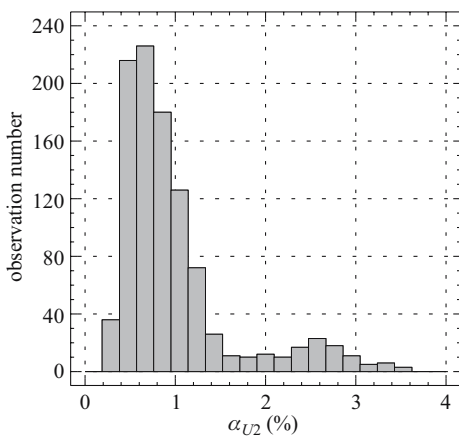


Fig. 5. Histogram of the voltage asymmetry coefficient values obtained as a simulation result for the following parameters:
 – phase cables cross-section – 35 mm²,
 – neutral cable cross-section – 50 mm²,
 – number of residential consumers – 5

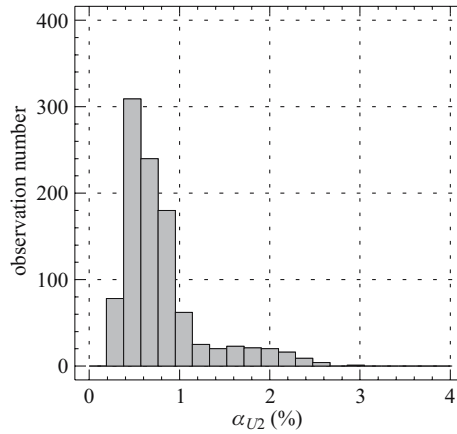


Fig. 6. Histogram of the voltage asymmetry coefficient values obtained as a simulation result for the following parameters:

- phase cable cross-section – 50 mm²,
- neutral cable cross-section – 50 mm²,
- number of residential consumers – 5

Table 1

Chosen results of the simulation investigations

Cable cross-sections:		Excess percentage value of the admissible value of the coefficient α_{U2}		
phase	neutral			
70	70	2.09	0.49	0.00
50	70	9.72	2.97	0.00
50	50	10.32	3.97	0.20
35	50	11.71	9.82	0.99
35	35	12.10	10.02	1.09
Number of residential consumers		0	5	10

Summary

On the basis of the results obtained from the simulation investigations it may be stated that the risk to exceed admissible values of the electric energy parameters caused by the load asymmetry is the greater, the greater is consumption of the power in a power line. According to the terms specified by the standard PE 50160 no excess of admissible values of the coefficient α_{U2} was observed for the prevailing number of the residential consumers (10 compared to the total number of the consumers – 15). It is caused by lower consumption of power by this type of consumers. The highest excess percentage of the parameter admissible value, in this case, was 1.09% of the weekly results

compared to the admissible 5%. In case of greater number of the production consumers (5 residential consumers) the greatest excess percentage of the parameter admissible value was 10.02%. While for the line supplying exclusively production consumers it was 12.1%.

By analysing methods to ease load asymmetry effects by increasing the cable cross-section it may be stated that increasing only cross-section of a neutral cable slightly improves the voltage asymmetry coefficient value α_{U2} . A radical improvement of the analysed parameter value was achieved by increasing cross-sections of the phase cables and the neutral one.

References

- HELLWIG Z. 1993. *Elementy rachunku prawdopodobieństwa i statystyki matematycznej*. PWN, Warszawa.
- KOLBER P. 2006. *Wpływ wybranych czynników na nierównomierność obciążeń wiejskich sieci niskiego napięcia*. Uniwersytet Warmińsko-Mazurski, Olsztyn (rozprawa doktorska).
- PN-EN 50160. *Parametry napięcia zasilającego w publicznych sieciach rozdzielczych*. 1998.
- ZIELIŃSKI R. 1979. *Generatory liczb losowych*. WNT, Warszawa.

Accepted for print 28.09.2008 r.

SIMULATION MODEL TO EVALUATE VOLTAGE ASYMMETRY IN A RURAL LOW VOLTAGE POWER LINE

Piotr Kolber¹, Janusz Piechocki²

¹ Department of Machine Maintenance
University of Technology and Life Sciences in Bydgoszcz

² Department of Electric and Power Engineering
University of Warmia and Mazury in Olsztyn

Key words: loads asymmetry, simulation model, voltage asymmetry.

A b s t r a c t

This paper presents a simulation model to evaluate phase voltage unbalance in rural local low voltage power lines. The voltage asymmetry has been evaluated by the voltage asymmetry coefficient value α_{U2} , being one of the essential parameters characterizing quality of electric energy supplied from a low voltage power line to the consumers.

SYMULACYJNY MODEL OCENY NIESYMETRII NAPIĘĆ W WIEJSKIEJ LINII NISKIEGO NAPIĘCIA

Kolber Piotr¹, Piechocki Janusz²

¹ Katedra Eksploatacji Maszyn
Uniwersytet Technologiczno-Przyrodniczy w Bydgoszczy

² Katedra Elektrotechniki i Energetyki
Uniwersytet Warmińsko-Mazurski w Olsztynie

S ł o w a k l u c z o w e: asymetria obciążeń, model symulacyjny, niesymetria napięć.

A b s t r a k t

W artykule przedstawiono symulacyjny model oceny niezrównoważenia napięć fazowych w terenowych wiejskich liniach niskiego napięcia. Niesymetria napięć była oceniana przez wartość współczynnika asymetrii napięciowej α_{U2} , który jest jednym z podstawowych parametrów charakteryzujących jakość energii elektrycznej dostarczanej do odbiorców z linii niskiego napięcia.

Introduction

The current and voltage asymmetry in three-phase power networks is mostly caused by asymmetrical loads and asymmetrical transmission devices. Work of a three-phase power supply system is called asymmetrical or symmetrical, when the working conditions of a single or of all phases are not equal. Short-term and long-term asymmetrical operational types of work occur in three-phase systems. A short-term asymmetry is usually caused by breakdown processes. They are mostly asymmetrical short-circuits and switching off one of the phases within a cycle of automatic reswitching. Long-term asymmetry in an industrial system may occur when connecting asymmetrical loads to a power network, when asymmetrical elements occur or when a transmission system works asymmetrically.

Asymmetrical states of work occur particularly in rural low voltage distribution networks. Such states result from the phase loads asymmetry, caused by unequal distribution of power on individual phases of single-phase receivers and random nature of connecting receivers to a power line.

The loads asymmetry in rural low voltage networks is an important problem, what was proven by the results obtained from investigating the current asymmetry and unbalance coefficients, the values of which reached significant figures (KOWALSKI et al. 1983, NIEBRZYDOWSKI 1992). If the loads asymmetry investigations are performed, they are being carried out in transformer stations, that means at the power line start, thus simplifying their realization and reducing the costs. Because of the fact that measuring currents and voltages (particularly at the end of a LV power line) is ineffective, the analysis of the loads asymmetry and its consequences based on simulation methods is of special importance.

Investigation object

The investigation object is a low voltage power line (LV) supplying energy to rural consumers. The model of the LV power line under analysis is shown in Figure 1. A model of II type power line characterized by zero values of the transverse parameters of a substitutive diagram (power line unitary conductance $G_o = 0$, power line unitary susceptance $B_o = 0$) has been adopted for the analysis purposes. The considered type of four-cable airborne power line, with flat arrangement of cables is characteristic for rural areas. It is also the most popular and the most disadvantageous due to power lines reciprocal impedance in terms of the loads asymmetry, and thus quality of the energy supplied to its consumers.

In order to determine the loads asymmetry and the voltage conditions occurring in low voltage power lines related to it, operational investigations have been performed in a real object. Both temporary and 24-hour registering measurements of voltages and loads (currents and powers) at the start of the power line (in a transformer station 15/0,4 kV with LV rails) were performed within the framework of the investigations.

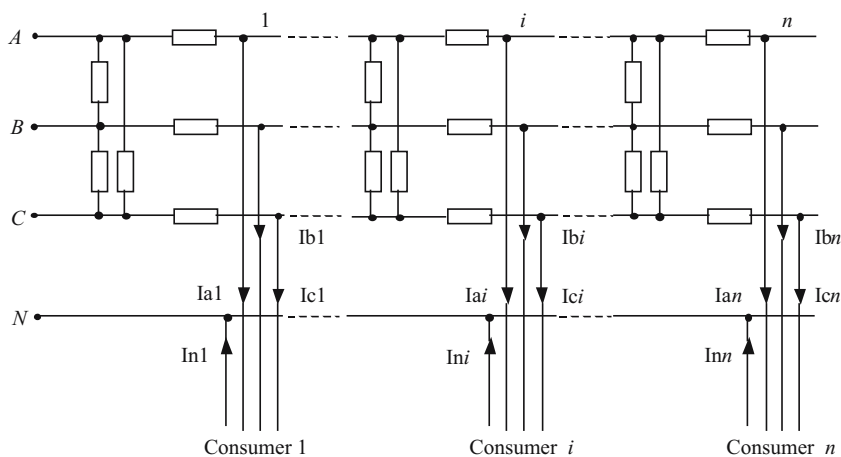


Fig. 1. Low voltage power line model

Probabilistic model to determine chosen parameters characterizing electric energy quality

The purpose to evaluate asymmetry in a low voltage power line is realization of more expensive, time consuming investigations in a real power line at each consumers' place at the same time. For that reason a simulation model was built to facilitate determination of the voltage drop and deviation values and voltage asymmetry with, among other things, various variants of distribution of consumers along the power line, various values of power consumed by the consumers and various levels of phase loads asymmetry.

The model input data are related to:

- length of the power line l ;
- number of consumers n ,
- distance from the receiving points to the power line start l_i ;
- cross-sections of: phase s , neutral s_n cables;

- distance between the cables: b_{AN} , b_{BN} , b_{CN} , b_{AB} , b_{BC} , b_{CA} ;
- value of power consumed by the consumers P_i .

A topology was specified for the power line, it means that on the basis of single-time generated: length of the power line l out of the Weibull distribution with the parameters $p = 2$, $\lambda = 0.8$, corresponding to the circuits data collected from the territory of Poland (GAWLAK 1992), given number of receiving points n their distribution along the power line l_i was generated on the basis of triangle distribution with the density function $f = 2(b-y)/(b-a)^2$ ($a = 80$ m, $b = l$) (HELLWIG 1993). Adopting triangle distribution was caused by the fact that greater number of consumers is usually situated close to a MV/LV transformer station and their number gets lower as the distance gets longer.

The temporary loads for 24-hour work were generated out of an empiric distribution. In each generation point (time moment) an average value and standard load deviation were taken out of the normal distribution based on 14 full days of 24-hour work at a consumer's place. An exemplary average 24-hour graph of loads in an agricultural holding is presented in the Figure 2.

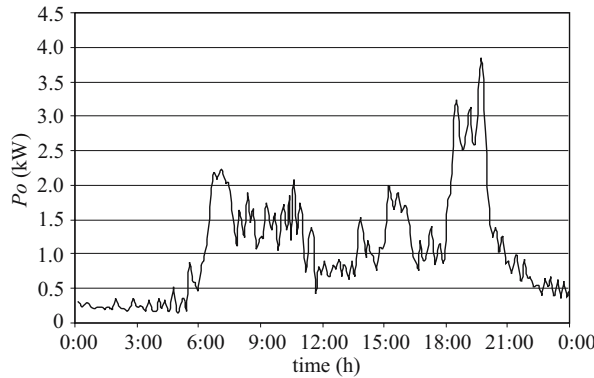


Fig. 2. Average 24-hour graph of the loads in an agricultural holding (14 days)

The value of power consumed by a consumer at the given time moment is a sum of the power value in particular phases. In each group of values of three phase powers the following may be distinguished: $P_{\max i}$ – power of the most loaded phase, P_{pi} – power of the intermediately loaded phase, $P_{\min i}$ – power of the least loaded phase. Subsequently, power in the i -th receiving point of the power line may be presented with the following relationship:

$$P_i = P_{\max i} + P_{pi} + P_{\min i} \quad (1)$$

On the basis of the said powers it is possible to determine coefficients being a measure of the consumer's phase loads unbalance (KUJSZCZYK 1991):

– intermediate load coefficient

$$k_{1i} = \frac{P_{pi}}{P_{\max i}} \approx \frac{I_{pi}}{I_{\max i}} \quad (2)$$

– minimal load coefficient

$$k_{2i} = \frac{P_{\min i}}{P_{\max i}} \approx \frac{I_{\min i}}{I_{\max i}} \quad (3)$$

where:

$I_{\max i}$, $I_{\min i}$, I_{pi} – load of the maximally, minimally and intermediately loaded phase in the i -th terminal.

In order to provide more comprehensive evaluation of the phase loads unbalance, a maximal load coefficient, described with the following relationship (KOLBER, PIECHOCKI 2005), was introduced apart from the aforementioned coefficients:

$$w_i = \frac{P_{\max i}}{P_i} \quad (4)$$

It describes the share of power consumed by the most loaded phase in relation to total power consumed at a receiving point. It may be stated that this coefficient describes to what extent the most loaded phase is a dominant phase when compared to the remaining ones in terms of the consumed power.

Between the above coefficients there is the following relationship:

$$k_{1i} + k_{2i} = \frac{1}{w_i} - 1 \quad (5)$$

Division of power into the phases was realized by generating load asymmetry coefficients values w_i , k_{1i} , the distributions of which are presented by histograms (Fig. 3 and Fig. 4).

In case of symmetrical load, these coefficients take the following values: $k_{1i} = 1$, k_{2i} , $w_i = 1/3$, however in case of an extreme asymmetry, when the total

power is consumed by one of the phases, their values are as follows: $k_{1i} = 0$, $k_{2i} = 0$, $w_i = 1$.

The admissible ranges of the respective coefficient values are described with the relationships:

$$\frac{1}{3} \leq w_i \leq 1 \quad (6)$$

$$k_{1i} \geq k_{2i} \quad (7)$$

for $w_i \in <1/3; 1/2>$

$$\frac{\frac{1}{w_i} - 1}{2} \leq k_{1i} \leq 1 \quad (8)$$

$$\frac{1}{w_i} - 2 \leq k_{2i} \leq \frac{\frac{1}{w_i} - 1}{2} \quad (9)$$

for $w_i \in <1/2; 1>$

$$\frac{\frac{1}{w_i} - 1}{2} \leq k_{1i} \leq \frac{1}{w_i} - 1 \quad (10)$$

$$0 \leq k_{2i} \leq \frac{\frac{1}{w_i} - 1}{2} \quad (11)$$

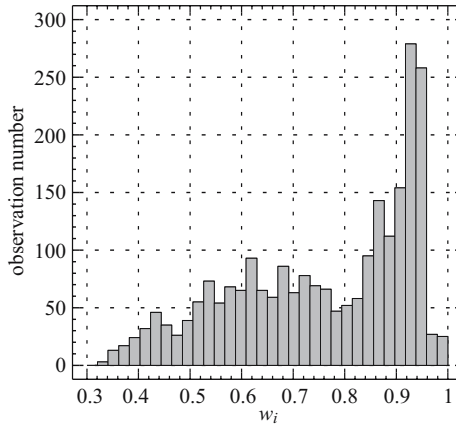


Fig. 3. Histogram of the maximal load coefficient value w_i

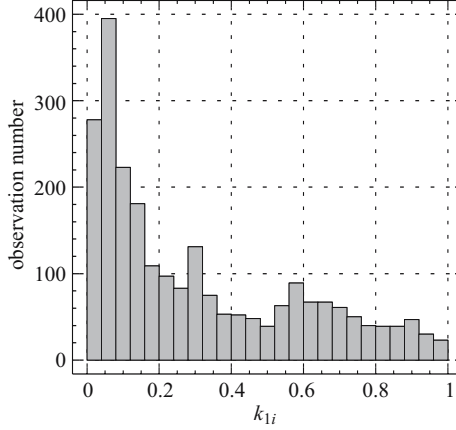


Fig. 4. Histogram of the intermediate load coefficient value k_{1i}

The value of the coefficient k_{2i} was determined on the basis of the relationship (5) after transforming it.

Some measurements were carried out in a MV/LV station for the power coefficient $\cos\varphi$. On this basis beta distribution was adopted for this parameter and conformity was verified by means of a test of empirical data conformity with theoretical distribution.

Randomisation of assigning the consumer's phase loads to the power line phases was carried out by means of a pseudorandom number generator with a uniform distribution.

The phase powers and power phase coefficients \cos were basis to determine the phase currents in individual receiving points, and thus the values of the phase voltages and voltage asymmetry coefficient.

$$\alpha_{U_{2i}} = \frac{U_{2i}}{U_{1i}} \cdot 100\% \quad (12)$$

where:

U_{2i} , U_{1i} – symmetrical components of phase voltages with opposite and consistent sequence in the i -th terminal

$$U_1 = \frac{1}{3} \sqrt{U_A^2 + U_B^2 + U_C^2 - 2U_A U_B \cos(\alpha + \frac{\pi}{3}) - 2U_B U_C \cos(\beta + \frac{\pi}{3}) - 2U_C U_A \cos(\alpha + \beta - \frac{\pi}{3})}$$

$$U_2 = \frac{1}{3} \sqrt{U_A^2 + U_B^2 + U_C^2 - 2U_A U_B \cos(\alpha - \frac{\pi}{3}) - 2U_B U_C \cos(\beta - \frac{\pi}{3}) - 2U_C U_A \cos(\alpha + \beta + \frac{\pi}{3})} \quad (13)$$

$$\alpha = \arccos \frac{U_A^2 + U_B^2 + U_{AB}^2}{2U_A U_B} \quad \beta = \arccos \frac{U_B^2 + U_C^2 + U_{BC}^2}{2U_B U_C} \quad (14)$$

$U_A, U_B, U_C, U_{AB}, U_{BC}, U_{CA}$ – values of phase and cable voltages.

According to PN-EN 50160 1998 the values of the above electric energy parameter should not exceed the admissible value:

$$\alpha_{U2i} \leq 2\% \quad (15)$$

The standardised requirements regarding the voltage asymmetry coefficient value do not describe only its admissible level but also the admissible percentage of the value excesses $\alpha_{U2} = 2\%$ within a week time. Therefore, the temporary values of the coefficient for the generated values of the phase loads in respective receiving points were determined several times per each 10 minutes of all entire days of a week in the simulation model.

The temporary values were averaged for the period of 10 minutes. On the basis of the averaged values of the parameters, their distributions were achieved and it was possible to determine the percentage of admissible value excess, as well as this excess level within a week time.

Verifying the model adequacy

In order to study the voltage conditions in a local low voltage network, and particularly voltage asymmetry, at the energy consumption places, the phase voltage measurements were carried out at those consumers who were equipped with three-phase terminals and who consumed energy supplied by the end-point section of a LV power line. At all 74 consumers under investigation, apart from the voltage measurements with the loads resulting from the normal use of the receivers in the given time of the day, the measurements were also performed after connecting an additional single-phase 1 kW and than 2 kW receiver to a randomly selected phase.

The average value of the asymmetry coefficient was tending to grow. In case of the measurements with the existing load at the consumer's place, the average value of the asymmetry coefficient was 1.29% with the standard deviation of 1.17%, and with the additional single-phase load of 1 kW power – 1.40%. With the additional single-phase load of 2 kW power, the average value of the asymmetry coefficient was 1.79%. In 19.8% of the agricultural holdings

(consumers) the asymmetry coefficient was exceeded even with the load existing at that time. After connecting a 1 kW receiver to a randomly selected phase, the number of consumers with exceeded asymmetry coefficient went up to 21.6%, and after connecting a 2 kW receiver to the same phase 2 – as much as to 31%. It should be taken into account that connecting extra single-phase receivers caused improved asymmetry at some consumers' places, however this state was deteriorated in greater number of cases.

As a result of the simulation performed for a power line with the length of $l = 1048$ m supplying energy to 15 consumers (the average number of receiving points for the rural power networks is 13) the percentage of excesses of admissible value of the coefficient $\alpha_{U2} = 2\%$ was determined out of the temporary values averaged for 10 minutes taken from a week time. In case of supplying energy to 10 production consumers and 5 residential ones the percentage of excesses of the parameter admissible value was 10.02% (Fig. 5), however the excess percentage was increased to 12.1% when supplying exclusively production consumers (increase in the power consumption in the power line).

Basing on the investigations performed in a real object and on the research carried out by means of the simulation model it may be stated that the increase in the power consumption leads to increased number of excesses of the admissible value of the voltage asymmetry coefficient. Greater percentage of the parameter excesses for the operational investigations in a local power network results from the fact that these investigations were performed in a given time of a day (peak hours), when the power consumption was the greatest, whilst the simulation investigations referred to 24-hour periods out of an entire week. However it does not change the fact that the parameter value change tendency is similar.

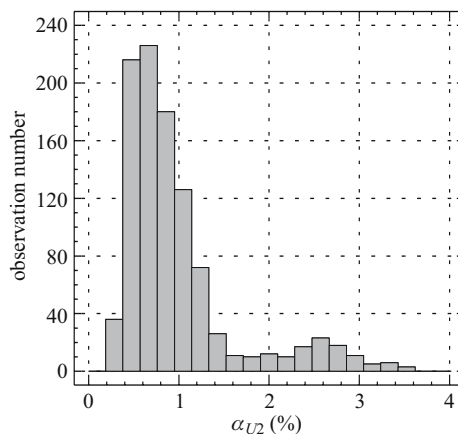


Fig. 5. Histogram of the voltage asymmetry coefficient values obtained as a simulation result for the following parameters:

- phase cables cross-section – 35 mm^2 ,
- neutral cable cross-section – 35 mm^2 ,
- number of residential consumers – 5

Summary

By analysing the investigation results in terms of the voltage asymmetry in rural low voltage networks it should be stated that the admissible value of the voltage asymmetry coefficient ($\alpha_{U_2} = 2\%$), being one of the main parameters characterizing quality of energy supplied to the consumers, is frequently exceeded in a low voltage power line. Subsequently, it may be concluded that after putting into operation new single-phase receivers improving technological processes in agricultural holdings and used in households, it should be taken into account that the number of the excesses of the admissible value of the voltage asymmetry coefficient is going to increase with the existing condition of the rural low voltage networks. Evaluation of the load asymmetry and the related voltage asymmetry in real rural low voltage networks is difficult and expensive, as it requires to perform simultaneous measurements of the loads and voltages at all the consumers' places. The analysis of the investigation results of the voltage asymmetry at the rural consumers' places and those achieved by means of the simulation model let us state that it may be used to evaluate quality of the supply voltage substituting expensive and time consuming measurements in real premises. On the basis of the investigations performed by means of the simulation model it is possible to evaluate risk of exceeding admissible value of the parameter α_{U_2} of the energy transmitted in the LV power lines.

References

- GAWLAK A. 1992. *Stan wiejskich linii niskiego napięcia w Polsce w 1991 r.* Energetyka, 10.
- HELLWIG Z. 1993. *Elementy rachunku prawdopodobieństwa i statystyki matematycznej.* PWN, Warszawa.
- KOLBER P., PIECHOCKI J. 2005. *Analiza wpływu niesymetrii obciążeń odbiorców wiejskich na jakość energii w linii niskiego napięcia.* Inżynieria Rolnicza, 6(66).
- KOWALSKI Z., MRÓZ I., RADIOWSKI M. 1983. *Skutki techniczne i gospodarcze asymetrii obciążeń w sieciach wiejskich na przykładzie wybranego obszaru sieciowego.* Praca I15/0181/16/83.
- KUJSZCZYK Sz. 1991. *Elektroenergetyczne sieci rozdzielcze.* Tom 2. PWN, Warszawa.
- NIEBRZYDOWSKI J. 1992. *Estimation of asymmetry distribution and current imbalance coefficients the rural power networks by the method of central moments of distribution.* Zeszyty Naukowe Politechniki Białostockiej Technical Sciences, 83(11).
- PN-EN 50160. *Parametry napięcia zasilającego w publicznych sieciach rozdzielczych,* 1998.

Accepted for print 28.09.2008 r.

METHOD FOR ESTIMATION OF EFFICIENCY OF USING THE BIOMASS FOR ENERGY

Jan Pawlak

Chair of Electric and Power Engineering
University of Warmia and Mazury in Olsztyn

Key words: bioenergy, costs, efficiency, calculation, method, model, environment.

A b s t r a c t

The method for estimation of the economic and energetic efficiency of the implementation of renewable energy sources has been elaborated. The main focus was laid on biomass as a source of energy. The method and relevant model is applied during the realisation of the interdisciplinary project "Modelling of biomass utilisation for energy purpose". Use of biomass for energy, as the renewable energy source is to be a way to protect the environment. Therefore economic analyses have to take into consideration also environment costs. Research to be undertaken within above mentioned project will provide data enabling rational choice of kind and technology of production of energy crop the most convenient from economic and ecological points of view. The choice has to include in reckoning local conditions, effecting both the yield and quality of product.

METODA SZACOWANIA EFEKTYWNOŚCI ZASTOSOWANIA BIOMASY DO CELÓW ENERGETYCZNYCH

Jan Pawlak

Katedra Elektrotechniki i Energetyki
Uniwersytet Warmińsko-Mazurski w Olsztynie

Key words: bioenergia, koszty, efektywność, kalkulacja, metoda, model, środowisko naturalne.

A b s t r a k t

Opracowano metodę oceny ekonomicznej i energetycznej efektywności zastosowania odnawialnych źródeł energii, ze szczególnym uwzględnieniem biomasy. Metoda ta oraz odpowiedni model są stosowane podczas realizacji interdyscyplinarnego projektu „Modelowanie wykorzystania biomasy do celów energetycznych”. Wykorzystanie biomasy jako odnawialnego źródła energii ma sprzyjać ochronie środowiska, dlatego analiza ekonomiczna musi uwzględniać koszty natury ekologicznej. Badania, które mają być prowadzone w ramach wspomnianego projektu, dostarczą danych umożliwiających racjonalny, z ekonomicznego i ekologicznego punktu widzenia, wybór rodzaju technologii produkcji roślin energetycznych. Wybór powinien uwzględniać warunki miejscowe, mające wpływ na plon i jakość produktu.

Introduction

The increases in the cost of fossil fuels as a result of the strong energy demand of the fast industrially growing Asian countries and the ongoing evolution of agriculture in Western countries, are leading to a more specific focus linked to energy issues in the rural areas (RIVA 2006). One has also not to forget the perspective of depletion of non-renewable energy resources as well as the environment aspects of the growing energy use. Therefore, this century could see a significant switch from a fossil fuel to renewable energy sources. According to BEST (2006) such a situation will cause that in this century the development of bioenergy based economy, with agriculture and forestry as the leading sources of biomass for biofuels can be expected.

The proposed solutions must be ecologically sustainable, environmentally acceptable for public and the delivered unitary costs need to be lower than for fossil fuels (SIMS 2003). On that score, results of researches carried out in different countries are not always univocal. According analyses of the Flemish Institute for Technological Research – VITO (Belgium) the biodiesel, as compared to the diesel oil, causes lower emission of greenhouse gases but is more harmful from the point of view of other environmental impacts (NOCKER et al. 1998, NOCKER et al. 2000, SPIRINCX et al. 2000). Its burning causes acidification of the atmosphere, eutrophication, formation of photochemical oxidants, as well as radioactive and non-radioactive wastes. As a result, the biodiesel is about two times more harmful for the environment than the diesel oil (NOCKER et al. 1998). Instead, according to German studies (PUPPEN 2002) the only negative impact of biodiesel, as compared to the diesel oil, would be the deterioration of the ozonosphere.

The above divergences show that continuation of researches is necessary. The diversity of potential energy sources as well as local conditions and technologies to be applied create a large field to studies and analyses.

The purpose of this paper is an attempt to present the method for estimation of the economic and energetic efficiency of the implementation of biomass for energy purposes.

The biomass is closely connected with agriculture and in Poland it is now the main renewable energy source. Besides, dedicated woody and herbaceous crops for energy were shown to provide soil and water quality benefits. They ensure the decreasing of runoff, sediment losses and nutrient transport compared with traditional agricultural crop production (TOLBERT 2002).

The method for evaluation the economic and energetic efficiency of renewable energy sources

The model method will be applied to evaluate different forms of the production and use the energy from biomass. The data necessary to build the model are collected on farms engaged in production of crops for energy. For all operations connected with production of particular energy crops the following data are registered:

- [1] the name of the operation,
- [2] the date of execution,
- [3] time of work, hours,
- [4] hectares of field works,
- [5] number of engaged persons, power units and machines,
- [6] inputs of energy carriers, according their kinds, volumes and prices,
- [7] inputs of a sowing material (seeds, seedlings or quicksets), amounts and prices,
- [8] inputs of fertilisers: kind of fertiliser, amount and price,
- [9] inputs of pesticides: kind of the chemical, amount and price,
- [10] other inputs: specification, amount and price,
- [11] harvested product: kind, amount, and market price.

Data listed in points [1]-[6] are registered for all operations, the other – only for convenient works (for instant point [9] for plant protection and [11] for harvest. The above data produce the base for calculation production costs (Fig. 1). Cost of labour is a result of multiplication of number of workers, time

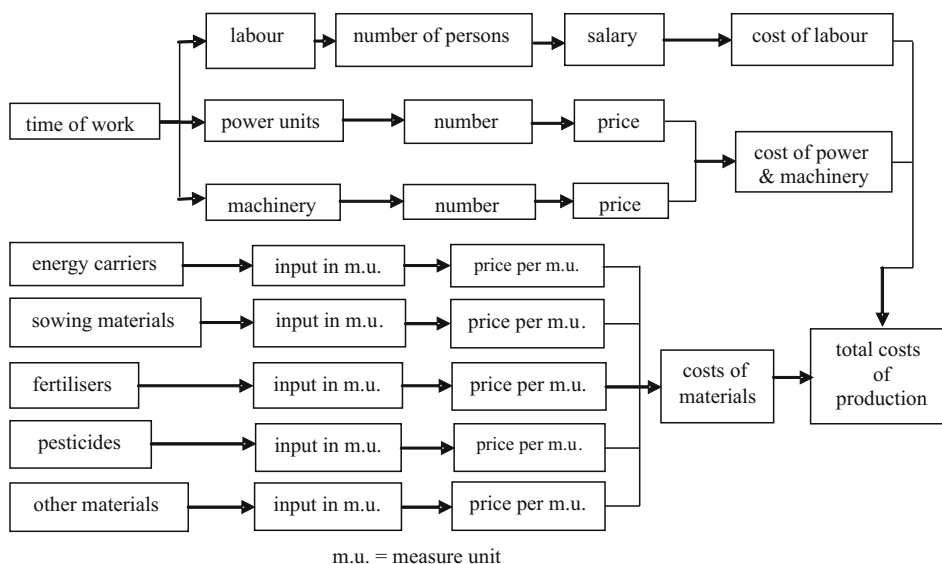


Fig. 1. Scheme of production costs of energy crop

of work and salary (including all taxes and allowances) per unit of time. Cost of power (tractors, engines and so on) and machinery includes here depreciation, storage and conservation, insurance (if it refers), repair and maintenance. Cost of energy is calculated separately, like other material inputs: (seeds, seedlings or quicksets, fertilisers, pesticides, etc.). The amount of material used in relevant units of measure is multiplied by price per unit of measure.

The same data can be used to calculate the direct and indirect energy inputs (Fig. 2). In this case the monetary units are replaced by relevant energy equivalents (MJ) per unit of measure. In a case of tractors and implements the mass of these stuff has been taken as a unit of measure. In a case of fertilisers and other chemicals the units of measure are kilograms of net ingredient (for instance kg of N in nitrogen fertilisers or kg of P_2O_5 in a case of phosphorous fertilisers). In a case of seeding material this are unitary direct and indirect energy inputs per unit of measure of seeds, seedlings or quicksets.

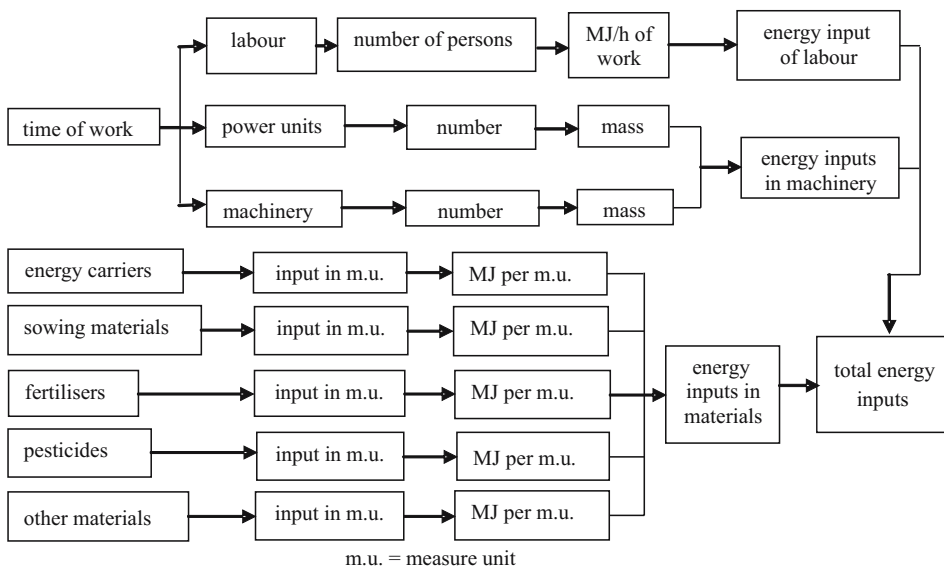


Fig. 2. Scheme of direct and indirect energy inputs for production of energy crop

Total amounts of production costs as well as direct and indirect energy inputs together with market value of produced energy crop and its calorific value create the base of model for evaluation of the economic and energetic efficiency of the bioenergy production (Fig. 3).

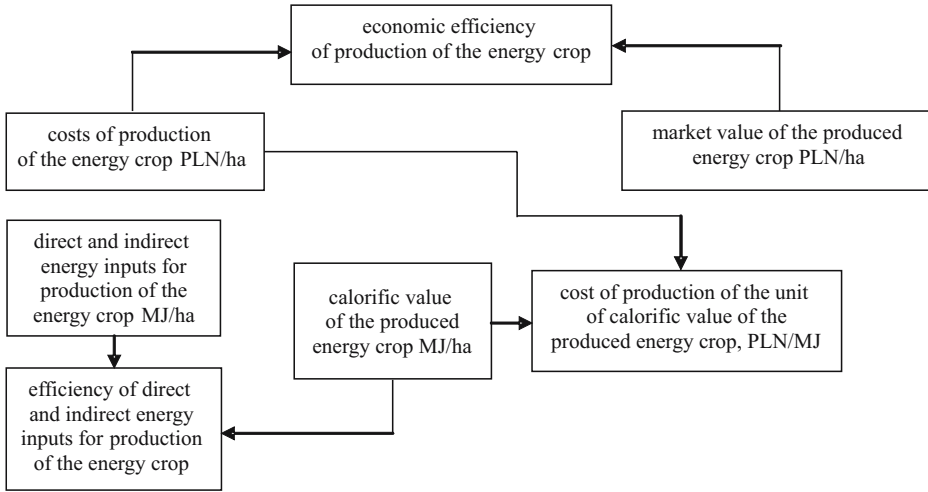


Fig. 3. Scheme of the model for evaluation the economic and energy efficiency of production of energy crops

The economic efficiency of production of i -th energy crop can be calculated using the following formula:

$$E_{ci} = \frac{P_{ci}}{N_{ci}} \quad (1)$$

Where:

E_{ci} – efficiency of production of i -th energy crop;

P_{ci} – market value of produced i -th energy crop, PLN ha⁻¹;

N_{ci} – costs of production of i -th energy crop, PLN ha⁻¹.

For comparative purposes, the cost of production of the unit of the calorific value of i -th energy crop should be determined:

$$C_{ci} = \frac{Q_{ci}}{N_{ci}} \text{ (PLN MJ}^{-1}\text{)} \quad (2)$$

Where:

C_{ci} – the cost of production of the unit of the calorific value of i -th energy crop, PLN MJ⁻¹;

Q_{ci} – calorific value of produced energy crop, MJ ha⁻¹.

The knowledge of the cost of production per unit of the calorific value of the energy crop makes it possible to compare different renewable energy sources and different technologies of their production. It can also serve as a meter to evaluate a purposefulness of the use of renewable energy source instead of a fossil energy carrier.

The use of renewable energy source is justifiable under condition that its calorific value is higher than direct and indirect energy inputs for its production. The purposefulness of use of a biofuel is the bigger; the higher is the efficiency of direct and indirect energy inputs for its production. To calculate this efficiency, the following equation can be applied:

$$En_{ci} = \frac{Q_{ci}}{Ie_{ci}} \quad (3)$$

Where:

- En_{ci} – the efficiency of direct and indirect energy inputs for production of i -th energy crop;
- Ie_{ci} – direct and indirect energy inputs for production of i -th energy crop.

An attempt to verify the proposed method

Before implementation of the discussed method, which will be applied during works within the economic section of the interdisciplinary project “Modelling of biomass utilisation for energy purpose”, realised in the frame of EOG Financial Mechanism and Norwegian Financial Mechanism (NMF) by the Consortium Agreement called “Virtual Institute of Sustainable Development” (VISA), its verification basing on data from available literature is purposeful. A comparative analysis of the efficiency of direct and indirect energy inputs for Biodiesel oil production according to kind of the crop and applied technology. The results of earlier research carried out in Poland (PODKÓWKA 2004) and in the USA (PIMENTEL, PATZEK 2005) will be used as input data. The rape (yield 25 dt ha⁻¹) produced under Polish conditions and soybean (yield 26.7 dt ha⁻¹) produced under American conditions were taken as the raw material for biofuel production. Two variants of the technology of extraction of oil and estrification were considered: the one used in Poland (A) and the other used in the USA (B). The results of calculation show that there are differences in the process efficiency and that the effect of applied technology is in this case more strongly pronounced than the one of the kind of crop being used as the source of row material. In all cases the efficiency, calculated using the formula (3) was below 1 if the by-products are not taken into account

(Tab. 1). According to technology applied 14 to 37 percent more energy is required to produce 1000 kg of Biodiesel oil than the product can deliver. However, in a case of using by-products (straw in the case of rape) for energy purposes, the energy efficiency growth up to 1.36-1.60.

Table 1

Inputs and effects of biodiesel production depending on kind of crop and the applied technology

Specification	GJ per 1000 kg of Biodiesel			
Energetic plant	Rape		Soybean	
Variant of technology	A	B	A	B
Energy inputs per:				
production of biomass	28.8	28.8	27.8	27.87
extraction of oil and estrification	22.9	15.1	22.9	15.17
total	51.7	43.9	50.7	42.9
Received product (Biodiesel oil)	37.7	37.7	37.7	37.7
Energy efficiency	0.73	0.86	0.74	0.88

Source: author's calculation basing on PODKÓWKA (2004), PIMENTEL and PATZEK (2005)

Above example of application shows that proposed method can be used for evaluation of different crops as a raw material for bioenergy production as well as different technology variants. There is a need to collect more input data, specific for different local conditions.

Research programmes carried out in the frames of the interdisciplinary project by 6 institutes will provide data on yields, calorific values of different energy crops, volumes and kinds of emissions etc. under different habitat and applied technology. Thanks of it more holistic analysis of economic and energy efficiency will be possible, taking into account environment costs. This is important not only because of divergences between results of different research results. Also knowledge of influence of different factors, such as kind of soil and climate, technology and scale of production on efficiency of production of biomass for energy is necessary. Research by DENISIUK and PIECHOCKI (2005) show that the chemical composition of straw of the same species of cereals produced in Denmark and in Poland is not the same. Consequently, also characteristic of straw as a fuel differs according to the place of production. The knowledge of interrelations between different factors will help to make a choice of the most convenient energy crop with regard to economic and environment criteria.

Conclusion

According to technology applied 14 to 37 percent more energy is required to produce an unit of mass of Biodiesel oil than the product can deliver.

Exemplary analysis shown the usability of the proposed method for evaluation of efficiency of biomass production for energy. Its results show that the choice of suitable technology can improve the efficiency of embodied energy inputs for Biodiesel production.

The diversity of both natural conditions and other factors having an effect on economic and energy efficiency of production of different energy crops cause that continuation of research in this field is necessary. Use of biomass for energy, as the renewable energy source is to be a way to protect the environment. However, results of researches of effect of biofuels on environment, carried out in different countries, are not always univocal. Therefore, economic analyses have to take into consideration also environment costs.

Research to be undertaken within the interdisciplinary project "Modelling of biomass utilisation for energy purpose" should provide data enabling rational choice of kind and technology of production of energy crop the most convenient from economic and ecological points of view. The choice has to include in reckoning local conditions, effecting both the yield and quality of product. That is why results from different habitats are needed.

References

- BEST G. 2006. *Alternative Energy Crops for Agricultural Machinery Biofuels – Focus on Biodiesel*. Agricultural Engineering International: the CIGR Ejournal. Invited Overview, 13(VIII).
- DENISIUK W.H., PIECHOCKI J. 2005. *Techniczne i ekologiczne aspekty wykorzystania słomy na cele grzewcze*. Wydawnictwo Uniwersytetu Warmińsko-Mazurskiego w Olsztynie.
- NOCKER L. DE, SPIRINCKX C., PANIS L. 2000. *Comparison of externalities of the biodiesel fuel chains for passenger transport in Belgium*. VITO, Flemish Institute for Technological Research, pp. 1-3.
- NOCKER L. DE, SPIRINCKX C., TORFS R. 1998. *Comparison of LCA and external cost analysis for biodiesel and diesel*. VITO, Flemish Institute for Technological Research, pp. 1-10.
- PODKÓWKA W. 2004. *Kierunki wykorzystania rzepaku*. W: *Biopaliwo gliceryna pasza z rzepaku*. Wydawnictwo Uczelniane Akademii Techniczno-Rolniczej w Bydgoszczy, ss. 36-41.
- PUPPEN D. 2002. *Environmental evaluation of biofuels*. Periodica Polytechnica Ser. Soc. Man. Sci., 10(1): 95-116.
- RIVA G. 2006. *Utilisation of Biofuels on Farm*. Agricultural Engineering International: the CIGR Ejournal. Invited Overview, 15(VIII).
- SIMS R.E.H. 2003. *Climate Change Solutions from Biomass, Bioenergy and Biomaterials*. CIGR Ejournal. Invited Overview, 11(V).
- SPIRINCKX C., NOCKER L. DE, PANIS L.I. 2000. *Comparative externality analysis and life cycle assessment of biodiesel and fossil Diesel fuel*. 1st World Conference on Biomass for Energy and Industry, Sevilla. Proceedings, 1: 171-173.
- TOLBERT V.R. 2002. *Environmental sustainability of dedicated bioenergy feedstocks: summary of research results*. 12th European Conference on Biomass for Energy, Industry and Climate Protection, Amsterdam. Proceedings, 1: 148-151.

Accepted for print 29.02.2008 r.

ANALYSIS OF THE EFFICIENCY OF CEREAL GRAIN AND BUCKWHEAT NUTLET SEPARATION IN A GRADER WITH INDENTED POCKETS

Zdzisław Kaliniewicz

Department of Heavy Duty Machines and Separation Processes
University of Warmia and Mazury in Olsztyn

Key words: buckwheat, cereal grain, indicators of separation efficiency.

A b s t r a c t

This study describes the impact of indented pocket depth, the factor of static load of the cylinder with mixture and the setting angle of the working edge of the trough on buckwheat nutlet yield, the efficiency of cereal (wheat, rye, barley and oat) grain removal and the efficiency of mixture separation. The highest cleaning efficiency was reported in respect of indented pockets with a depth of 2.4 mm, the factor of static load of the cylinder with mixture of 0.2 and the setting angle of the working edge of the trough of 30°. At the above grader parameters, buckwheat nutlet yield, cereal grain removal and mixture separation efficiency reached 0.95, 0.83 and 0.78 respectively.

ANALIZA SKUTECZNOŚCI SEPARACJI ZIARNIAKÓW ZBÓŻ I ORZESZKÓW GRYKI W TRYJERZE Z WGLĘBIENIAMI KIESZONKOWYMI

Zdzisław Kaliniewicz

Katedra Maszyn Roboczych i Procesów Separacji
Uniwersytet Warmińsko-Mazurski w Olsztynie

Słowa kluczowe: gryka, ziarniaki zbóż, wskaźniki efektywności rozdzielania.

A b s t r a k t

W pracy określono wpływ głębokości wgłębień kieszonkowych, wskaźnika statycznego obciążenia cylindra mieszaniną i kąta ustawienia roboczej krawędzi rynienki na uzysk orzeszków gryki, skuteczność wydzielania ziarniaków zbóż (pszenicy, żyta, jęczmienia i owsa) oraz skuteczność rozdzielania mieszaniny. Najlepsze efekty czyszczenia uzyskano dla wgłębień kieszonkowych o głębokości 2,4 mm, wskaźnika statycznego obciążenia cylindra mieszaniną 0,2 i kącie ustawienia roboczej krawędzi rynienki 30°. Przy tych parametrach tryjera uzysk orzeszków gryki wynosi 0,95, skuteczność wydzielania ziarniaków zbóż 0,83, a skuteczność rozdzielania mieszaniny 0,78.

Introduction

Threshed buckwheat nutlets contain various impurities, mostly wild radish siliques and cereal kernels (SEMCZYSZYN, FORMAL 1990). The effectiveness of graders equipped with a cylinder with indented pockets in the process of removing wild radish siliques from buckwheat raw material has been discussed in many publications (KALINIEWICZ, RAWA 2002a, 2002b, 2004). Yet to date there has been no study investigating the above grader's effectiveness in separating buckwheat nutlets from cereal kernels.

The objective of this study was to determine the impact of selected working parameters of a cylindrical grader with indented pockets on the efficiency of removing cereal kernels from the grain mixture where buckwheat nutlets constitute the main fraction.

Materials and Methods

The investigated material comprised nutlets of buckwheat cv. Luba with mass fraction of 80%, while the remaining fraction (20%) consisted of grain of 4 principal cereals: wheat cv. Nawra, rye cv. Bojko, barley cv. Blask and oat cv. Deresz, each accounting for 5% of the fraction. The relative moisture content of the investigated mixture components was as follows: buckwheat – 12.3%, wheat – 12.6%, rye – 11.8%, barley – 12.1% and oat – 11.5%. A high impurity content was adopted mainly due to the need to minimise measuring errors.

The study was conducted on a test stand presented in the work of KALINIEWICZ and RAWA (2004). It comprised a K-292 laboratory grader manufactured by Petrus, equipped with two cylinders with a length of 480 mm and internal diameter of 240 mm, each with indented pockets (KALINIEWICZ, RAWA 2002a, 2002b) with different indentation depth. The experiment was conducted in three replications with the following parameters:

1) constants:

- horizontal inclination angle of cylinder axis – 2° ,
- distance from the working edge of the trough to cylinder surface – 6 mm,
- cylinder's kinematic indicator – 0.25,
- impurity content of buckwheat raw material – 20%,

2) variables:

- working depth of indented pockets $s = 2.4$ mm and 2.8 mm,
- factor of static load of the cylinder with mixture $q_s = 0.1, 0.2$ and 0.3,
- setting angle of the working edge of the trough $\alpha = 10^\circ, 20^\circ, 30^\circ, 40^\circ$ and 50° ,

3) results:

- buckwheat nutlet yield ε_1 ,
- efficiency ε_{2p} of wheat grain removal,
- efficiency ε_{2z} of rye grain removal,
- efficiency ε_{2j} of barley grain removal,
- efficiency ε_{2o} of oat grain removal,
- efficiency ε_2 of impurities removal,
- efficiency ε of mixture separation.

The cylinder was filled with the mixture for around 60 s before every experiment. After the feeder and the grader were stopped, the trough and the waste container were removed and emptied. As the trough and the waste container were fitted back in place, the feeder and the grader were activated for 1 minute and the proper measurement was conducted. The waste which accumulated in the trough and in the waste container was separated into 5 fractions: buckwheat nutlets, wheat, rye, barley and oat kernels. Every fraction was weighed on laboratory scales with measuring precision of 0.01 g.

Buckwheat nutlet yield was determined based on the ratio of the weight of nutlets removed to the trough and the total weight of nutlets in the trough and in the waste container. The efficiency ε_{2i} of cereal grain removal was estimated based on the ratio of the weight of grain of every cereal species removed to the waste container and the total weight of cereal grain in the trough and in the waste container. The efficiency ε_{2i} of impurity removal was determined based on the ratio of the total weight of cereal grain removed to the waste container and the total weight of cereal grain in the trough and in the waste container. The efficiency of mixture separation ε was determined with the application of the formula (GROCHOWICZ 1994):

$$\varepsilon = \varepsilon_1 - (1 - \varepsilon_2) \quad (1)$$

Experimental results were processed with the use of Winstat and Statistica software. The functions describing dependent variables were determined by a multivariate regression analysis using a second-order polynomial model with stepwise elimination of non-significant variables and polynomial degree.

Results and Discussion

The highest efficiency $\varepsilon = 0.78$ (Fig. 1) of separation of the five-component mixture was reported in respect of indented pockets with a depth of $s = 2.4$ mm at the factor of static load of the cylinder with mixture of $q_s = 0.3$ and the setting angle of the working edge of the trough of $\alpha = 30^\circ$. Buckwheat grain loss

did not exceed 5% ($\varepsilon_1 = 0.95$), and impurity removal efficiency reached $\varepsilon_2 = 0.83$. The elimination efficiency of barley and oat kernels was slightly above the average, while below average results were observed in respect of wheat and rye kernels. A similar trend was observed within the entire range of variation of the analysed factors. A comparison of the obtained data with the results of other research studies indicates that graders with indented pockets may be effectively used to clean buckwheat material of grain impurities. The efficiency of mixture separation on a precision cleaning line in a buckwheat processing plant (SEM-CZYSZYN, FORMAL 1990) reached only 0.36. It should be noted, however, that the analysed mixture had a different composition – in addition to cereal kernels, it also comprised Tatarian buckwheat, bluebottle and vetch seeds, wild radish siliques as well as other organic and mineral impurities. KONOPKA (2006) separated a mixture consisting of buckwheat nutlets, kernels of four principal grain species and wild radish siliques in a separator whose cylindrical surface comprised adequately spaced circular-section rods. In the variant involving a separator with grooves, mixture separation efficiency reached around 0.63 with buckwheat loss of up to 14%. The highest efficiency of elimination was reported in respect of barley grains, and the lowest – in rye grains. When a separator without grooves was applied to separate a fraction with a thickness of $3.1 \div 3.5$ mm, mixture separation efficiency increased to 0.92 and the loss of buckwheat nutlets was minimised to 6%.

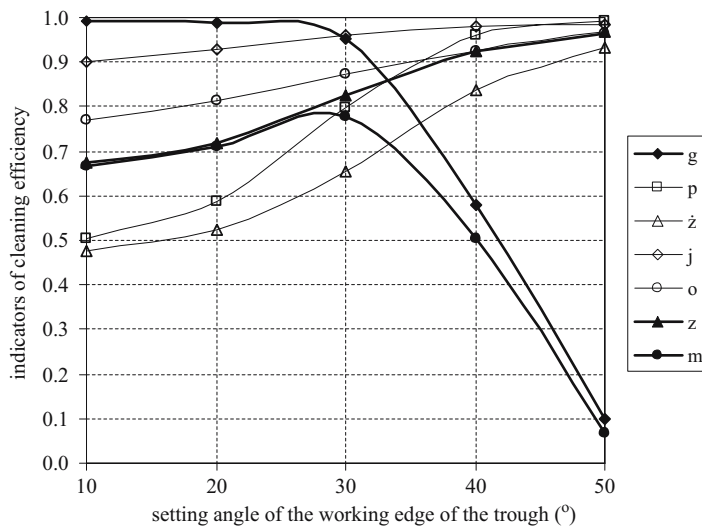


Fig. 1. Buckwheat nutlet yield (g) ε_1 , efficiency ε_{2p} of wheat grain removal (p), efficiency ε_{2r} of rye grain removal (z), efficiency ε_{2j} of barley grain removal (j), efficiency ε_{2o} of oat grain removal (o), efficiency ε_2 of cereal grain removal (z), efficiency ε of mixture separation (m) subject to the setting angle α of the working edge of the trough for indented pockets with a depth of $s = 2.4$ mm and the factor of static load of the cylinder with mixture of $q_s = 0.2$

Source: Author's calculations.

Straight-line correlation coefficients between dependent and independent variables are presented in Table 1. Within the analysed range of variation, the above coefficients ranged from 0.154 to 0.803. The investigated qualitative indicators of the separation process are most closely related to the setting angle of the grader trough. On the one hand, a higher setting angle reduces buckwheat nutlet yield and mixture separation efficiency, while on the other – it increases grain removal effectiveness. At the analysed level of significance, buckwheat nutlet yield is profoundly affected only by the setting angle of the working edge of the grader trough, and the efficiency of mixture separation – by the depth of indented pockets. There was no significant correlation between the efficiency of wheat grain removal and the factor of static load of the cylinder with mixture. In the remaining cases, correlation coefficients were higher than the critical value.

Table 1
Coefficients of straight-line correlation between variables

	ε_1	ε_{2p}	ε_{2z}	ε_{2j}	ε_{2o}	ε_2	ε
s	0.154	-0.529	-0.576	-0.475	-0.478	-0.526	-0.388
q_s	-0.162	0.347	0.385	0.433	0.504	0.427	0.267
α	-0.803	0.716	0.674	0.526	0.598	0.663	-0.319

Critical value of correlation coefficient – 0.361

Adopted level of significance – 0.05

Source: Author's calculations.

Since only two cylinders recommended for buckwheat cleaning were used in the experiment (with a different depth of indented pockets), second-order regression equations were developed separately for each cylinder. The functions describing qualitative indicators of the separation process within the analysed range of variation of independent factors are presented in Table 2. All equations are statistically significant at a level of 5%. The highest percentage of explained variation was recorded for the efficiency of rye grain removal (98.2) in the cylinder with $s = 2.4$ mm indented pockets, and the lowest for the efficiency of mixture separation (27.9) with the application of indented pockets with a depth of $s = 2.8$ mm. A comparison of the two tested cylinders shows greater consistency with the data specific for $s = 2.4$ mm indented pockets in respect of buckwheat nutlet yield, the efficiency of wheat and rye grain removal and the efficiency of mixture separation, while lower consistency was reported in respect of the efficiency of barley and oat grain removal and the efficiency of impurity removal. The above equations also indicate that despite an occasionally non-significant correlation between the factors, variable data may enter the equation in the form of a second-order effect or an interaction.

Table 2

Regression equations for qualitative indicators of the separation process

s [mm]	Regression equation	% explained variation	Standard deviation of residuals
2.4	$\varepsilon_1 = 0.04\alpha - 0.001\alpha^2 - 0.02q_s \cdot \alpha + 0.72$	96.91	0.07
	$\varepsilon_{2p} = 5.75q_s + 0.03\alpha - 6.28q_s^2 - 0.06q_s \cdot \alpha - 0.59$	97.50	0.05
	$\varepsilon_{2z} = 4.68q_s + 0.02\alpha - 5.39q_s^2 - 0.04q_s \cdot \alpha - 0.43$	98.18	0.04
	$\varepsilon_{2j} = 0.01\alpha + 0.75$	41.47	0.09
	$\varepsilon_{2o} = 0.03q_s \cdot \alpha + 0.66$	51.87	0.11
	$\varepsilon_2 = 5.27q_s + 0.02\alpha - 6.99q_s^2 - 0.05q_s \cdot \alpha - 0.26$	96.48	0.04
	$\varepsilon = 0.05\alpha - 0.001\alpha^2 + 0.15$	76.47	0.13
2.8	$\varepsilon_1 = 0.04\alpha - 0.001\alpha^2 - 0.02q_s \cdot \alpha + 0.67$	93.07	0.08
	$\varepsilon_{2p} = -0.02\alpha + 0.0004\alpha^2 + 0.05q_s \cdot \alpha + 0.11$	95.31	0.08
	$\varepsilon_{2z} = -0.02\alpha + 0.0004\alpha^2 + 0.04q_s \cdot \alpha + 0.16$	96.78	0.05
	$\varepsilon_{2j} = 0.05q_s \cdot \alpha + 0.38$	61.73	0.17
	$\varepsilon_{2o} = 0.06q_s \cdot \alpha + 0.26$	70.41	0.15
	$\varepsilon_2 = 2.48q_s + 0.0003\alpha^2 - 0.02q_s \cdot \alpha - 0.22$	97.45	0.05
	$\varepsilon = 1.20q + 0.08$	27.88	0.16

Adopted level of significance – 0.05

Source: Author's calculations.

Conclusions

1. The conducted experiment shows that a cylindrical grader with indented pockets may be applied in the separation process to improve the purity of buckwheat material. The highest impurity removal efficiency was reported in respect of barley kernels, and the lowest – in respect of rye kernels.

2. Within the analysed range of variation of indentation depth, the factor of static load of the cylinder with mixture and the setting angle of the working edge of the trough, the last parameter had the greatest impact on the qualitative indicators of the separation process. In the investigated case, the correlation coefficient ranged from 0.53 for the efficiency of barley grain removal to 0.80 for buckwheat nutlet yield.

3. The developed regression equations may be used to model the processes of separating buckwheat nutlets from impurities due to the high (in most cases) percentage of explained variation and relatively low standard deviation values of the residuals.

References

- GROCHOWICZ J. 1994. *Maszyny do czyszczenia i sortowania nasion*. Wydawnictwo Akademii Rolniczej. Lublin.
- KALINIEWICZ Z., RAWA T. 2002a. *Analiza teoretyczna skuteczności rozdzielania mieszaniny nasion gryki i tuszczyn rzodkwi świrzepy w tryjerze z wgłębieniami kieszonkowymi*. Problemy Inżynierii Rolniczej, 4: 43-50.
- KALINIEWICZ Z., RAWA T. 2002b. *Skuteczność czerpania nasion gryki klasycznymi i specjalnymi wgłębieniami tryjera*. Inżynieria Rolnicza, 5(38): 469-475.
- KALINIEWICZ Z., RAWA T. 2004. *Wyniki eksperymentalnej weryfikacji apriorycznego modelu matematycznego rozdzielczości tryjera do gryki*. Inżynieria Rolnicza, 3/58: 211-218.
- KONOPKA S. 2006. *Analiza procesu separacji nasion gryki przy wykorzystaniu prętowych powierzchni roboczych tryjerów*. Inżynieria Rolnicza. Rozprawy habilitacyjne, 21. Wyd. Polskie Towarzystwo Inżynierii Rolniczej. Kraków.
- SEMCZYSZYN M., FORMAL Ł. 1990. *Analiza skuteczności pracy urządzeń czyszczących stosowanych w liniach technologicznych czyszczenia ziarna gryki*. II. Wyniki badań jakości pracy urządzeń czyszczących. Acta Acad. Agricult. Techn. Olst., Aedif. Mech. 21: 111-121.

Accepted for print 6.12.2007 r.

OBLIGATORY INSPECTIONS OF THE EQUIPMENT TO PLANT PROTECTION CHEMICALS USING – LEGAL REGULATIONS, TESTING PROCEDURES AND CONTROVERSIES

Adam J. Lipiński

Department of Working Machines and Separation Processes
University of Warmia and Mazury in Olsztyn

Key words: spraying technique, sprayers, periodical investigations.

Abstract

The aim of the paper is to present legal regulations, procedures and some statements concerning obligatory inspections of sprayers in Poland. There are inaccuracies and controversies related to these subject matter shown. It was found incorrect that in the testing procedure there is a paragraph, where the law allows two different, incomparable methods of sprayers functioning valuation. Substantial misstatements in the testing procedures are the reason why users of sprayers often express negative opinions about the whole system of the periodical investigations of the equipment to plant protection chemicals using.

OBOWIĄZKOWE BADANIA SPRZĘTU DO STOSOWANIA ŚRODKÓW OCHRONY ROŚLIN – UREGULOWANIA PRAWNE, PROCEDURY BADAŃ I KONTROWERSJE

Adam J. Lipiński

Katedra Maszyn Roboczych i Procesów Separacji
Uniwersytet Warmińsko-Mazurski w Olsztynie

Słowa kluczowe: technika opryskiwania, opryskiwacze, badania okresowe.

Abstract

Celem pracy było zaprezentowanie regulacji prawnych, toku postępowania oraz spostrzeżeń, dotyczących obowiązkowych badań opryskiwaczy w Polsce. Przedstawiono nieścisłości oraz kontrowersje dotyczące tej problematyki. Uznano za niewłaściwe, że w procedurze badań opryskiwaczy polowych jest zapis, w którym ustawodawca dopuszcza dwie różne, nieporównywalne metody oceny funkcjonowania rozpylaczy. Zwrócono także uwagę, że nieścisłości merytoryczne w procedurze badań są często powodem negatywnej oceny przez użytkowników opryskiwaczy całego systemu obowiązkowych badań.

Introduction

Obligatory inspections of sprayers technical condition in Poland were initiated in 1999. Many users of sprayers wrongly connect that fact with Poland joining the European Union. In many of EU countries tests of sprayers are voluntary (Great Britain, Sweden, Austria, Portugal, Spain and France) or there is no system of periodical sprayers investigations at all (Ireland, Finland, Greece, Romania and Bulgaria) – after WEHMANN (2007). Therefore obligatory inspections of sprayers do not derive exactly from legal regulations in the European Union. EU machine directive in force defines fundamental requirements that fall within the domain of health care and safety of machines use, but the requirements of the directive concern every kind of agriculture machines in the same way.

Legal regulations

The obligation of sprayers technical state inspections comes out directly from the act about plant protection of the 12th July 1995 (Dz. U. z 1999 r., nr 66, poz. 751). According to the notations of the act, herbicides should be applied using strictly technically efficient equipment, which – if used appropriately – ensures effective killing harmful organisms and does not cause noisome effects on human's and animal's health or on environment. The act of the 1st January 1999 introduced obligatory inspections of the equipment to plant protection chemicals using (all types of sprayers, seed dressers etc.) which is in exploitation at agrarian producers in periods that not exceed two years. The regulation circumscribing detailed rules of the equipment to plant protection chemicals using inspections was enforced by the Ministry of Agriculture and Food Economy on the 11th February 1999 (Dz. U. nr 20, poz. 175).

In the previous period of sprayers inspections in Poland, the act about plant protection was emended twice. The first alteration to the act was executed on the 16th February 2001, with legal validity since the 25th July 2001 (Dz. U. nr 22, poz. 248). Amended act has ordered and specified many issues, which concerned particularly: requirements for the stations performing sprayers inspections, rules of the inspections, payments for the inspections and detailed technical requirements for sprayers. The obligation of testing new sprayers (introduced to trade) was imposed and the sprayers inspections were limited to tractor and self-propelled sprayers or fruit-growing sprayers only. Two years period between successive inspections was preserved. The weak point of the alteration was the fact that the regulation by the Ministry of Agriculture and Rural Development about sprayers inspections was published on the 15th

November 2001 (Dz. U. nr 137, poz. 1544). The time delay in publishing this regulation resulted that in the period between July and November 2001 there were no sprayers inspections performed, because of legal regulations missing.

The second alteration to the act about plant protection was enforced of the 18th December 2003 (Dz. U. z 2004 r. nr 11, poz. 94) with legal validity since the 1st May 2004, that is the date of Poland joining the European Union. In the subject matter concerning obligatory sprayers inspections there was only one change in amended act, it was the elongation of the period between consecutive sprayer tests up to three years.

Sprayers testing procedures

The procedure of sprayers testing consists of three stages:

1. The general inspection, where there is a visual valuation of the sprayer performed with drive turned off.

2. The inspection of the technical state of pump, agitator, container, measurement and control apparatus, liquid system, filters, field beam, atomizers and ventilator. The investigation of these subassemblies is performed twice: with drive of the particular elements turned off and on. In the first case there is a visual valuation executed, in the second case we use measurement and control equipment, in which – due to regulation by the Ministry of Agriculture and Rural Development of the 15th November 2001 (Dz. U. nr 137, poz. 1544) – every Station of Sprayers Inspection should be equipped.

3. Evidencing of the process.

The fact that in the sprayers inspections procedure there is many of control parts that are performed with sprayer drive turned off is sometimes interpreted as simplification that results in only rough valuation of sprayer (ZASIEWSKI, WIERZBICKI 1999). The procedure of sprayers inspections in Poland contains all important subassemblies (systems) of the sprayer and it has not significantly changed since the obligatory inspections were enforced. The only exception is the test of atomizers in field sprayers. During the period before the first amendment of the act about plant protection (1999-2001), the ending phase of the sprayer inspection was checking the distribution of transverse irregularity using the hand grooved table or the electronic table. After the act amendment (2001) it is also possible to test sprayers by checking the irregularity of liquid outflow from single atomizers at the whole length of the field beam.

Controversies

Since the day when the obligatory sprayers inspections were enforced, there is a discussion concerning this issue in Poland. The dispute concerns range of inspections, methods of specific sprayer's subassemblies tests and measurement equipment to be used during the investigations.

The range of obligatory inspections of sprayers technical state does not include the calibration of the sprayer. If sprayer is not calibrated, when there is only transverse irregularity checked, we can receive correct inspection result while the liquid dose would be overestimated (ZASIEWSKI, WIERZBICKI 1999). If the range of obligatory inspections is expanded with calibration, it will cause that sprayers investigations will have much more educative character. Authors experience acquired during the sprayers inspections indicates that the lack of skills is generally the reason why the calibration of sprayer is not performed. The opinions about the sprayers calibration in Poland and other European countries are divided (BALSARI et al. 2007, HOŁOWNICKI et al. 2007).

Most controversies of all is caused by the atomizers test, which can be performed using two different methods interchangeably: the first to valuate the transverse irregularity of liquid at the whole length of the field beam and the second to valuate the irregularity of liquid outflow from single atomizers at the whole length of the field beam. These methods are completely different and incomparable (SAWA et al. 2002). Poland is the only country in Europe, in which two methods are working at the same time – after HOŁOWNICKI et al. (2007). Furthermore, there are two criteria of verifying the distribution of transverse irregularity of liquid outflow. When testing sprayers using hand grooved table the criterion is the value of standard deviation ($\pm 15\%$) but when the test is performed using electronic table the criterion is the value of variability index (10%). The existing conjuncture is not the correct solution. In many European countries there are discussions concerning sprayers inspections. Unfortunately, discussions are frequently not based on logical arguments supported by scientific proofs (LANGENAKENS 2000, SAWA et al. 2002). It seems that the correct future solution should be hammering out the compromise, which brings together objectivity and recurrence of the tests with the guarantee of fulfilling quality requirements (after BALSARI et al. 2007).

The important element of sprayers equipment is the manometer indicating the working pressure value. During the manometer valuation we have to also check, due to regulation on technical requirements for sprayers by the Ministry of Agriculture and Rural Development of the 4th October 2001 (Dz. U. nr 121, poz. 1303), if the manometer has the proper scale. The scale

of the manometer is determined by the range of working pressure values and it is equal to: 0,02 MPa in range of 0-0,5 MPa; 0,1 MPa in range of 0,5-2,0 MPa and 0,2 MPa in range above 2,0 MPa. Acceptable values of single graduation on a manometer scale are too big, it particularly concerns pressure above 0,5 MPa. Furthermore, required kind of manometer is not connected with accuracy of manometer's reading (its class). It can result in big errors of working pressure value readings.

Statements and conclusions

1. In the obligatory system of sprayers testing procedures in Poland there were enforced changes, which have not always turned up in the executive regulations to the law. It is the reason why there was the time warp in inspections proceeding in 2001.

2. There is an improper paragraph in the field sprayers testing procedure, where the act allows two different – incomparable – methods of sprayers functioning valuation. There is no substantial reason for such notation.

3. In the author's judgement enforced changes in the law and some substantial misstatements – existing in the testing procedures – they are the reason why many farmers underestimate the whole system of obligatory sprayers inspections in Poland. The system is often perceived as inconvenient necessity.

References

- BALSARI P., OGGERO G., MARRUCCO P. 2007. *Proposal of a Guide for Sprayers Calibration*. Second European Workshop on Standardized Procedure for the Inspection of Sprayers, Straelen, s. 60-73.
- HOŁOWNICKI R., DORUCHOWSKI G., GODYŃ A., ŚWIECHOWSKI W. 2007. *Recommendations of SPISE 2004 and obligatory inspections of sprayers in Poland*. Second European Workshop on Standardized Procedure for the Inspection of Sprayers, Straelen, s. 43-47.
- LANGENAKENS J. 2000. *Inspekcja opryskiwaczy – stan unormowań europejskich*. Materiały z I Konferencji „Racjonalna technika ochrony roślin”, Skierniewice, s. 31-38.
- Rozporządzenie Ministra Rolnictwa i Gospodarki Żywnościowej z dnia 11 lutego 1999 r. w sprawie szczegółowych zasad przeprowadzania badań sprzętu do stosowania środków ochrony roślin. Dz. U. nr 20, poz. 175.
- Rozporządzenie Ministra Rolnictwa i Rozwoju Wsi z dnia 4 października 2001 r. w sprawie wymagań technicznych dla opryskiwaczy. Dz. U. nr 121, poz. 1303.
- Rozporządzenie Ministra Rolnictwa i Rozwoju Wsi z dnia 15 listopada 2001 r. w sprawie przeprowadzania badań opryskiwaczy. Dz. U. nr 137, poz. 1544.
- SAWA J., HUYGHEBAERT, KOSZEL M. 2002. *Metody praktycznej oceny rozpylaczy rolniczych*. Materiały z III Konferencji „Racjonalna technika ochrony roślin”, Skierniewice, s. 85-93.

-
- Ustawa o ochronie roślin uprawnych z dnia 11 sierpnia 1999 r. Dz. U. nr 66, poz. 751.
Ustawa o zmianie ustawy o ochronie roślin uprawnych z dnia 16 lutego 2001 r. Dz. U. nr 22, poz. 248.
Ustawa o ochronie roślin z dnia 18 grudnia 2003 r. Dz. U. nr 11, poz. 94, ze zm.
WEHMANN H.J. 2007. *Actual survey about inspection of sprayers in the European countries*. Second European Workshop on Standardized Procedure for the Inspection of Sprayers, Straelen, s. 22-28.
ZASIEWSKI P., WIERZBICKI K. 1999. *Zakres i metodyka przeprowadzania okresowej kontroli opryskiwaczy polowych w Polsce*. Mat. Konf. „Obowiązkowe badania techniczne opryskiwaczy”, Poznań, s. 7-12.

Accepted for print 1.10.2008 r.

THE PLASTIC EQUALIZATION METHOD FOR BENDING MOMENTS AND THE ROTATION CAPACITY OF PLASTIC HINGES IN CONTINUOUS REINFORCED CONCRETE BEAMS IN LIGHT OF EUROCODE REQUIREMENTS

Marek Jędrzejczak¹, Michał Knauff²

¹ Department of Civil Engineering and Building Structures
University of Warmia and Mazury in Olsztyn

² The Institute of Building Structures
Warsaw University of Technology

Key words: civil engineering, reinforced concrete constructions, redistribution of bending moments, plastic hinges.

Abstract

The method worked out by JĘDRZEJCZAK and KNAUFF in 2007 has been used to calculate rotation in plastic hinges of the continuous reinforced concrete beams. It has been stated that when the degree of redistribution of bending moments does not exceed the allowable limits described in the Eurocode, the rotation does not exceed the limit values indicated in the norm either. Using the plastic equalization method for bending moments according to the Polish norm – without limiting the degree of redistribution – leads to excessive rotation.

METODA PLASTYCZNEGO WYRÓWNIANIA MOMENTÓW A ZDOLNOŚĆ DO OBROTU W PRZEGUBACH PLASTYCZNYCH ŻELBETOWYCH BELEK CIĄGŁYCH W ŚWIETLE WYMAGAŃ EUROKODU

Marek Jędrzejczak¹, Michał Knauff²

¹ Katedra Budownictwa i Konstrukcji Budowlanych
Uniwersytet Warmińsko-Mazurski w Olsztynie

² Instytut Konstrukcji Budowlanych
Politechnika Warszawska

Słowa kluczowe: budownictwo, konstrukcje żelbetowe, redystrybucja momentów zginających, przeguby plastyczne.

A b s t r a k t

Do obliczania kątów obrotu w przegubach plastycznych żelbetowych belek ciągłych zastosowano sposób opracowany przez JĘDRZEJCZAKA i KNAUFFA (2007). Stwierdzono, że jeżeli stopień redystrybucji nie przekracza dopuszczalnych granic określonych w Eurokodzie, to kąty obrotu również nie przekraczają wartości granicznych wskazanych w tej normie. Zastosowanie plastycznego wyrównania momentów według polskiej normy – bez ograniczania stopnia redystrybucji – wywołuje nadmierne kąty obrotu.

Introduction

According to the Polish norm PN-B-03264:2002 it is possible to use several methods of nonlinear analysis of reinforced concrete construction. General principles of the plastic method of analysis and the elastic analysis with limited redistribution of moments in the Polish norm have been taken from Eurocode 2 (1992). Additionally, the Polish norm also contains the method of plastic equalization for moments in one way spanning slabs uniformly loaded and secondary continuous beams (point 9.1.2.3 in the norm). This method has been based on the 1970s editions of the norm.

The principles of the general, nonlinear method based on realistic models of reinforced concrete are not described in the Polish norm, but can be found in Eurocode 2 (from 1999 and 2008) and a manual (*Podstawy projektowania...* 2006).

The literature concerned with the application of the theory of plasticity to calculate concrete slabs, beams and frames is very extensive. The book by TICHY and RAKOSNIK (1971) contains 108 items listed in its bibliography. But the book of the greatest practical value in Poland was, for a long time, the one written by KOBIAK and STACHURSKI (part one issued in 1973, and part 2 issued in 1979). Both parts of the book, and the numerous articles included in it, did not, however, pay too much attention to the problem of rotation capacity in plastic hinges.

Due to the development in reinforced steel production and concrete technology, we now use materials that are much stronger but less ductile than the ones used at the time when the application of the theory of plasticity in reinforced concrete structures was rather rudimentary. This is why it is not wise to use methods assuming the redistribution of bending moments (e.g. in continuous reinforced concrete slabs and beams) in contemporary designs without checking rotation capacity in plastic hinges.

The Polish norm PN-B-03264:2002 states that if redistribution of moments calculated according to the linear elastic method is applied, it is necessary to provide the critical cross-sections with the rotation capacity, so that they can

adapt to the predicted redistribution. The norm does not contain any information about the allowable plastic rotation (such information can be found in the Eurocodes from 1992, 1999 and 2008) or calculation methods for such rotations. The only criterion mentioned in the Polish norm PN-B-03264:2002 (quoted after the 1999 edition of the Eurocode) in point 4.4.2 are the conditions referring to the allowable degree of the moments' redistribution. Details concerning calculating the rotation and the allowable degree of redistribution changed with each subsequent edition of the Eurocode (1992, 1999, 2008), and, as we have already mentioned, the Polish norm permits the use of the method developed forty years ago. Thus, the set of the current rules is not really coherent.

The method of plastic equalization of bending moments is of great practical importance in Poland. This method may be considered a very specific case of the linear-elastic method with redistribution, in which the moments in spans and supports have been equalized. In our article (JĘDRZEJCZAK, KNAUFF 2002) showed that using this method, the conditions concerning the allowable degree of the redistribution of moments are often (but not always) fulfilled – and then it is not necessary to control the plastic rotation capacity. There is, however, a question if the rotation appearing as a result of the redistribution predicted with the use of this method do not exceed the values permitted by Eurocode 2 (2008). The answer to this question is the subject of this article.

The calculation method of rotation

The rotation θ in a plastic hinge in a continuous beam may be calculated with a good approximation with the use of the method presented by (JĘDRZEJCZAK, KNAUFF 2007), by using the following formula

$$\theta = \frac{1}{12\alpha_w} \frac{1 - \delta}{\delta} \frac{l}{d} W \quad (1)$$

where:

- α_w – coefficient depending on static structure, i.e. the number of spans and the distribution of live load,
- δ – the degree of redistribution, i.e. the ratio of the redistributed moment to the elastic bending moment,
- l/d – span slenderness ratio (l – the length of span, d – the effective depth),
- W – coefficient depending on the reinforcement ratio and the characteristics of concrete and steel.

Coefficient α_w is calculated using the formula:

$$\alpha_w = \alpha_g \frac{g}{p} + \alpha_q \frac{q}{p} \quad (2)$$

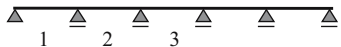
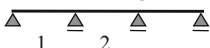
where:

g is dead load, q – live, p – total, α_g and α_q are coefficients to calculate extreme moments (e.g. according to Winkler's table).

Table 1 shows the values of α_w over supports B ($\alpha_g = -0.105$, $\alpha_q = -0.119$) and C ($\alpha_g = -0.079$, $\alpha_q = -0.111$) in a five-span beam and over support B in a three-span beam ($\alpha_g = -0.100$, $\alpha_q = -0.117$) for different ratios of loads q/g .

Table 1

Values of α_w

q/g	0.5	1.0	2.0	4.0	8.0
<div style="display: flex; align-items: center;"> <div style="margin-right: 20px;"> A B C  </div> <div> A five-span beam </div> </div>					
α_w (B)	0.110	0.112	0.114	0.116	0.117
α_w (C)	0.090	0.095	0.100	0.105	0.107
<div style="display: flex; align-items: center;"> <div style="margin-right: 20px;"> A B C  </div> <div> A three-span beam </div> </div>					
α_w (B)	0.106	0.109	0.111	0.114	0.115

Coefficient W is calculated using the following formulae

$$W = \frac{\xi_{eff}(1 - 0.5\xi_{eff}) f_{cd}}{E_{cd}j_{II}}, \quad j_{II} = \frac{J_{II}}{bd^3}, \quad \xi_{eff} = \rho \frac{f_{yd}}{f_{cd}} \quad (3)$$

where:

J_{II} is the moment of inertia of the cross-section in a clear phase II. The values of W are presented in diagrams a), b) and c) of Figure 1.

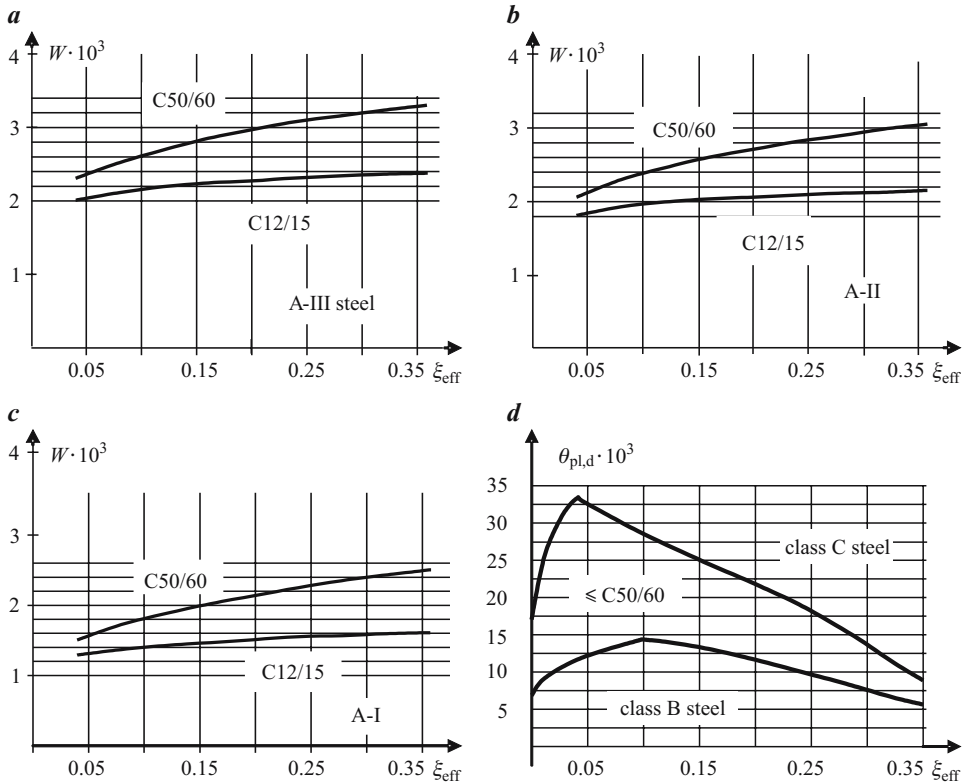


Fig. 1. Diagrams for checking the allowable plastic rotation – a, b, c) the values of expression W ; d) allowable plastic rotation $\theta_{pl,d}$ based on fig. 5.6N in Eurocode 2 (2008); (steel classes which are described in PN-B-03264:2002 except A-IIIN fulfill the requirements appropriate for B ductility class according to the Eurocode 2 from 2008)

Figure 1 d) shows the allowable plastic rotation $\theta_{pl,d}$ based on figure. 5.6N in the Eurocode (2008) calculated for shear slenderness $\lambda = 3,0$. If the shear slenderness is different, then the value of allowable plastic rotation $\theta_{pl,d}$ taken from figure 1 d) has to be multiplied by k_λ obtained from: $k_\lambda = \sqrt{\lambda/3}$, where $\lambda = a_q/d$, and a_q is the distance between point zero of the moments diagram and the support. For the sake of simplification, it can be assumed that $\lambda = M_{Sd}/(Vd)$.

Rotation in plastic hinges after equalizing the moments

In the method of plastic equalization, bending moments are calculated using the following formulae:

in the first and last spans and on the second and last but one supports:

$$M_1 = \frac{(g + q)}{11} l_{eff}^2 = 0.0909 p l_{eff}^2 \quad (4)$$

in intermediate spans and in intermediate supports:

$$M_2 = \frac{(g + q)}{16} l_{eff}^2 = 0.0625 p l_{eff}^2 \quad (5)$$

If live is equal to dead load (with different load ratios q/g , the values are different as well, but – as show in Table 1 – the influence of the q/g ratio has no significant meaning), then the coefficients α_w and the degree of redistribution δ as well as the coefficients of shear slenderness for the five-span beams are: over the second and last but one supports (B):

$$\alpha_w = 0.112, \delta = \frac{M_R}{M_e(p)} = \frac{0.0909 p l_{eff}^2}{\alpha_w p l_{eff}^2} = \frac{0.0909}{0.112} = 0.8116$$

$$\lambda = \frac{M_R}{Vd} = \frac{0.0909 p l^2}{0.5 p l d} = 0.1818 \frac{l}{d}$$

over the intermediate support (C):

$$\alpha_w = 0.095, \delta = \frac{0.0625 p l_{eff}^2}{\alpha_w p l_{eff}^2} = \frac{0.0625}{0.095} = 0.6579$$

$$\lambda = \frac{0.0625 p l^2}{0.5 p l d} = 0.125 \frac{l}{d}$$

The corresponding values for the three-span beams are:

$$\alpha_w = 0.109, \delta = \frac{0.0909}{0.109} = 0.8339, \lambda = 0.1818 \frac{l}{d}$$

Table 2 shows rotation over supports B and C in the five-span beam and over support B in the three-span beams, as well as the allowable plastic rotation according to the Eurocode (2008) for four values of ξ_{eff} and four slenderness ratios of the span l/d . Calculations have been done for B25 concrete and A-III steel. Table 3 shows a sample calculation for support B of a five-span beam, when $\xi_{eff} = 0.05$ and $\lambda = 2.0$ (formulae according to *Podstawy projektowania...* 2006).

Table 2

Rotation over supports

ξ_{eff}	λ	Three-span beam θ_B [mrad]	Five-span beam		$k_\lambda \cdot \theta_{pl,d}$ [mrad]
			θ_B [mrad]	θ_C [mrad]	
(1)	(2)	(3)	(4)	(5)	(6)
0.05	1.0	1.80	2.03	7.82	6.70
	2.0	3.59	4.06	15.65	9.47
	3.0	5.39	6.10	23.47	11.60
	4.0	7.19	8.13	31.30	13.39
0.10	1.0	1.92	2.17	8.36	8.02
	2.0	3.84	4.34	16.73	11.34
	3.0	5.76	6.52	25.09	13.90
	4.0	7.68	8.69	33.46	16.05
0.15	1.0	2.00	2.27	8.72	7.51
	2.0	4.00	4.53	17.43	10.61
	3.0	6.01	6.81	26.15	13.00
	4.0	8.01	9.07	34.87	15.01
0.20	1.0	2.07	2.34	9.01	6.64
	2.0	4.14	4.68	18.02	9.39
	3.0	6.21	7.02	27.03	11.50
	4.0	8.27	9.36	36.04	13.28
0.25	1.0	2.12	2.39	9.21	5.66
	2.0	4.23	4.79	18.43	8.00
	3.0	6.35	7.18	27.64	9.80
	4.0	8.46	9.57	36.85	11.32
0.30	1.0	2.15	2.43	9.37	4.56
	2.0	4.30	4.87	18.73	6.45
	3.0	6.45	7.30	28.10	7.90
	4.0	8.60	9.37	37.47	9.12
0.35	1.0	2.18	2.46	9.48	3.46
	2.0	4.35	4.92	18.95	4.90
	3.0	6.53	7.39	28.43	6.00
	4.0	8.70	9.85	37.90	6.93

Table 3

Sample calculation

$E_{cd} = \frac{E_{cm}}{\gamma_c}$	$E_{cd} = \frac{30}{1.2} = 25GPa$
$\alpha_e = \frac{E_s}{E_{cd}}$	$\alpha_e = \frac{200}{25} = 8$
$\rho = \xi_{eff} \frac{f_{cd}}{f_{yd}}$	$\rho = 0.05 \frac{13.3}{350} = 0.0019$
$\alpha_1 = \alpha_e \rho$	$\alpha_1 = 8 \cdot 0.0019 = 0.0152$
$\xi_{II} = \sqrt{\alpha_1^2 + 2\alpha_1} - \alpha_1$	$\xi_{II} = \sqrt{0.0152^2 + 2 \cdot 0.0152} - 0.0152 = 0.1598$
$j_{II} = \frac{\xi_{II}^3}{3} + \alpha_1 (1 - \xi_{II})^2$	$j_{II} = \frac{0.1598^3}{3} + 0.0152 \cdot (1 - 0.1598)^2 = 0.0121$
$W = \frac{\xi_{eff} (1 - 0.5\xi_{eff})}{j_{II}} \frac{f_{cd}}{E_{cd}}$	$W = \frac{0.05(1 - 0.5 \cdot 0.05)}{0.0121} \frac{13.3}{25 \cdot 10^3} = 2.145 \cdot 10^{-3}$
$\lambda = \frac{M_R}{Vd} = \frac{0.0909p_R l^2}{0.5p_R l d} = 0.1818 \frac{l}{d} \Rightarrow \frac{l}{d} = 5.5\lambda = 5.5 \cdot 2 = 11$	
$k_\lambda = \sqrt{\frac{\lambda}{3}}$	$k_\lambda = \sqrt{\frac{2}{3}} = 0.816$
$\theta = \frac{1}{12\alpha_w} \frac{1 - \delta}{\delta} \frac{l}{d} W \leq k_\lambda \theta_{pl,d}$	$\theta = \frac{1}{12 \cdot 0.112} \frac{1 - 0.8116}{0.8116} \cdot 11 \cdot 2.145 \cdot 10^{-3} = 4.06 \cdot 10^{-3} \leq$ $\leq 0.816 \cdot 11.6 \cdot 10^{-3} = 9.47 \cdot 10^{-3}$

Conclusion

As shown in the analysis (results presented in Table 2), while using the plastic equalization of bending moments, rotation in plastic hinges, which may then appear, are unacceptable according to Eurocode 2 (2008) (i.e. the rotation in columns 3, 4 or 5 are bigger than in column 6 of Table 2). Thus, this method – even though the norm PN-B-03264:2002 presents no objections to it – cannot be used without checking the rotation in plastic hinges.

Comparing the results with the conclusion of the article by JĘDRZEJCZAK, KNAUFF (2002), we have to state that the simple conditions offered in the norm PN-B-03264:2002, which exempt us from calculating the rotation in plastic hinges (with regard to the linear-elastic method with redistribution), are also appropriate for the method of plastic equalization for bending moments, because the values of rotation presented in Table 2 are exceeded only when the norm PN-B-03264:2002 does not exempt us from the obligation to control

these rotations. Exceeding the allowable plastic rotations appears, for example, in a three-span beam with significant reinforcement ($\xi_{eff} = 0.35$, when $\lambda \geq 3$) and in a five-span beam over the central support C, when $q/g > 0.5$.

References

- Eurocode 2: Design of Concrete Structures. Part 1-1: General Rules and Rules for Buildings. 1992.
- Eurocode 2: Design of Concrete Structures. Part 1-1: General Rules and Rules for Buildings, July 1999.
- Eurocode 2: Design of Concrete Structures. Part 1-1: General Rules and Rules for Buildings, December 2008.
- JĘDRZEJCZAK M., KNAUFF M. 2002. *Redystrybucja momentów zginających w żelbetowych belkach ciągłych – zasady polskiej normy na tle Eurokodu*. Inżynieria i Budownictwo, 8.
- JĘDRZEJCZAK M., KNAUFF M. 2007. *Kąty obrotu w przegubach plastycznych żelbetowych belek ciągłych w zależności od stopnia redystrybucji momentów*. Inżynieria i Budownictwo, 12.
- KOBIĄK J., STACHURSKI W. 1973. *Konstrukcje żelbetowe – część 1*. Arkady, Warszawa.
- KOBIĄK J., STACHURSKI W. 1987. *Konstrukcje żelbetowe – część 2*. Arkady, Warszawa.
- PN-B-03264:2002. *Konstrukcje betonowe, żelbetowe i sprężone. Obliczenia statyczne i projektowanie. Podstawy projektowania konstrukcji żelbetowych i sprężonych według Eurokodu 2*. 2006. Praca zbiorowa – koordynator M. Knauff. Dolnośląskie Wydawnictwo Edukacyjne, Wrocław.
- TICHY M., RAKOSNIK J. 1971. *Obliczanie ramowych konstrukcji żelbetowych z uwzględnieniem odkształceń plastycznych*. Arkady, Warszawa.

Accepted for print 2.08.2008 r.

RENOVATION OF BUILDINGS AND MODERNIZATION OF BUILT-UP AREAS – A CASE STUDY

Barbara M. Deja

Department of Civil Engineering and Building Structures
University of Warmia and Mazury in Olsztyn

Key words: civil engineering, renovation of buildings, modernization of a built-up area, engineering problems.

Abstract

The paper contains a description of three examples of the renovation of buildings and modernization of the surrounding area. The ownership rights of each premises were undisputable and the buildings were not registered as having special architectural or historic value. Nevertheless, it proved to be a complex and difficult task to undertake a decision concerning the extent and form of the revitalisation. In each case, the renovation works were preceded by a careful analysis of broad-scope profitability, which enabled the investor to minimize the risk involved.

WYBRANE PRZYKŁADY RENOWACJI BUDYNKÓW I MODERNIZACJI OBSZARÓW ZABUDOWANYCH

Barbara M. Deja

Katedra Budownictwa i Konstrukcji Budowlanych
Uniwersytet Warmińsko-Mazurski w Olsztynie

Słowa kluczowe: budownictwo, renowacja budynków, modernizacja obszaru zabudowanego, problemy inżynierskie.

Abstract

W artykule zaprezentowano trzy przedsięwzięcia z zakresu renowacji budynków i modernizacji towarzyszących im terenów. W każdym z analizowanych przypadków były uregulowane kwestie własności nieruchomości, tereny oraz budynki nie podlegały ochronie konserwatorskiej, mimo to podjęcie decyzji co do zakresu i formy rewitalizacji okazało się zadaniem złożonym i trudnym. Każde zadanie poprzedzono staranną analizą szeroko pojętej opłacalności, która pozwoliła zminimalizować ryzyko.

Introduction

Part of good development of urban areas involves projects aiming at renovation of dilapidated buildings and modernization of built-up areas. Such projects are undertaken in order to improve the spatial management and enhance the value of buildings in terms of their technical condition, aesthetics quality, functions and standards of use (BILIŃSKI 2003).

Very frequently renovation is more difficult than constructing new buildings as it has to take into consideration several aspects, such as the present condition of a building or the land parcel it stands on, the limitations caused by the original design, recommendations of the Building Conservation Officer¹, economic considerations, whether or not it is possible to stop using the building during the renovation works, how burdensome the works will be to the nearest neighbours, etc.

The paper presents three cases of renovation works carried out on three buildings alongside modernization of their immediate surroundings². The three cases involved the buildings and land used for different purposes, but none of the objects was a registered building. In each case, there was a different reason for undertaking the renovation works and making the decision about the extent of the improvements to the existing facilities.

The objective of this article has been to demonstrate that an optimum decision concerning modernization of old buildings needs to be preceded by a comprehensive analysis based on the guidelines of the revitalization programme for a whole town or a given area, inventory and evaluation of the initial state of the premises, expert technical opinion, a concept for repairs solutions as well as a preliminary costs analysis.

Modernization of the premises owned by the Institute of Animal Reproduction and Food Studies of the Polish Academy of Sciences

The first effort to modernize the buildings owned by Olsztyn-based Institute of Animal Reproduction and Food Studies, the Polish Academy of Sciences (PAN) was made in 2001.

At that time the Institute was seated in Bydgoska Street, in a building raised in the 1970s using traditional building technologies. It was a single-

¹ This applies only to registered buildings and land plots.

² The renovation projects of the buildings and built-up areas were prepared in Olsztyn-based architectural office ARCHE owned by Maciej Deja and Barbara Deja.

module, two-storey building with a basement and a ventilated flat roof (Fig. 1). The technical state of the building was satisfactory, but the building was too small for the institute, which was growing in size, and it failed to meet the standards regarding facilities and aesthetic values. What was necessary then was to renovate and expand the building.



Fig. 1. The building of the Institute of Animal Reproduction and Food Studies, the Polish Academy of Sciences (PAN) in Olsztyn, the north-eastern angle, as of 2002. Photo: B. DEJA



Fig. 2. The building of the Institute of Animal Reproduction and Food Studies, the Polish Academy of Sciences (PAN) in Olsztyn after the renovation and expansion. A view from the south-eastern angle. Photo: B. DEJA, 2008

The plans to modernize the complex of the PAN buildings (there are two other buildings on the grounds designated to be renovated: an animal house and a hotel, both in a similar technical state as the main building) complied with the urban revitalization programme.

“The Site Development Conditions” issued for the property in Bydgoska Street restricted the vertical expansion of the two-storey building to one additional floor, which would be a usable attic under a gable roof. Thus, it was necessary to analyse a possibility to expand the building horizontally.

The developed parcel, partly overgrown with trees, touched Bydgoska Street to the south and a compound of gardens to the west. It had a large westerly slope and very few spaces available for construction (Fig. 3).

By necessity, the expansion of the Institute’s main building concentrated along the south-western axis (also because it was necessary to preserve unobstructed front walls with windows in the existing building), while maintaining the required distance of 4 meters to the adjacent land plot.

Another essential aspect was to reduce to the necessary minimum any interference with the growing trees and plants (in the end, it was possible to save all the trees).

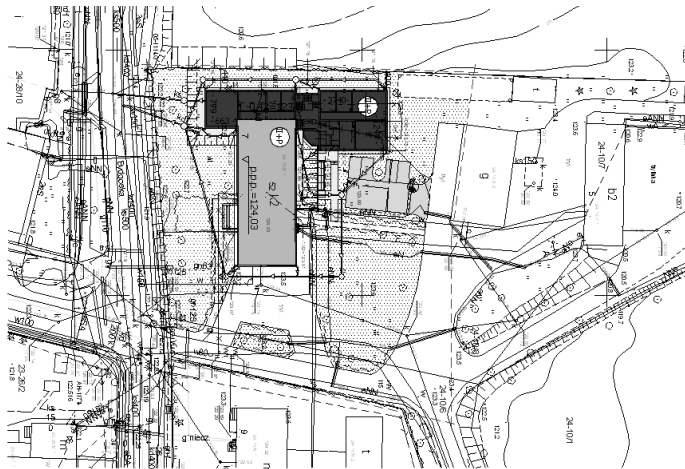


Fig. 3. The development plan for the land plot in Bydgoska Street. Designation: (II+p) – the expanded building of the Institute, (g) – the animal house, (b2) – the hotel building. Drawing: M. DEJA

The refurbished main building was designed as a three-storey building with a cellar and usable attic, built on an L-shaped plan (Fig. 4).

The interconnecting passages between the old and the new module of the building were designed on the ground floor and in the attic. In the newly added attic, the passage was included in the architectural design whereas in the existing ground floor it was made by changing one of the windows (seen in figure 4 in the top right-hand corner of the old building drawing) into a door.

The former entrance facing busy Bydgoska Street was abandoned. Instead, the main entrance was placed in the north wall, which made the building easily accessible from the car park (Fig. 5).

Common space was designed in the new module of the building, right behind the main door. It consisted of a lobby, a staircase and a lift, a cloak-room, a reception and a large staff room behind a glass-filled curtain wall. A similarly planned common space can be found on each floor, where it leads to the laboratories, office rooms and workrooms.

The expansion of the building was carried out using the traditional construction technology and locally available building materials. The old building was covered with a gable purlin-rafter roof supported on bearing walls (Fig. 6). A similar roof (also tiled with Dutch roof tiles) was made on the new building. The roof was supported by lengthwise bearing walls and binding joists, which along with the supporting posts constitute a load bearing structure for the floors in the part of the new module adjacent to the side wall of the old building (Fig. 4).



Fig. 4. The plan of the ground floor of the Institute of Animal Reproduction and Food Studies PAN in Olsztyn. Drawing: B. DEJA



Fig. 5. A view of the new building of the PAN Institute in Bydgoska Street, the north-eastern side. Photo: B. DEJA, 2008

The bearing walls of the new module were constructed from calcium-silicate brick and the foundation walls were made from C 12/15 class concrete. The aluminium-glass wall of the staff room was designed using Reynaers CW 50 2.1 panel walls system, according to DIN 4108 (Fig. 5). The joists, posts, ring beam and staircases were designed as monolithic concrete structures using C 16/20 class concrete reinforced with A-III class steel bars. Due to certain assembly limitations inside the old building, Leier Plus rib and slab floors were used.

Prior to designing the foundations of the new building, the foundations of the existing building were unearthed to determine their size and depth.

It was assumed that the expansion building would stand on footings and foundation walls made from C 16/20 class concrete reinforced with A-III class steel bars. Because of a high level of ground water (0.50 m below the footings), it was recommended to make the foundations using concrete mixed with Hydrobet and to carry out geotechnical monitoring while digging the foundation trenches.

All the office rooms and bathrooms were fitted with a gravitational ventilation system, whereas the laboratory rooms received mechanical ventilation supply/exhaust ventilation. The ventilation control rooms were placed in the attic.

Special ramps and an outdoor lift for the disabled (also wheelchair users) were added to the building. While planning the whole building project, the works were divided into stages so that the existing building was never put out of use. In January 2008 the construction works were completed and in spring this year the landscaping works will begin, including a new car park, a new

drive and some new plants (Fig. 7). The renovation of the other two buildings³ – the hotel and the animal house – will commence when the investor secures proper funds.

To the west side, the Institute of the Polish Academy of Sciences neighbours with a compound of gardens, which unfortunately spoil the view, as they contain a rather hectic composition of plants and many small garden sheds (Fig. 7). The value of the redesigned Institute building cannot be fully appreciated as long as this side of Bydgoska Street is not properly modernised.

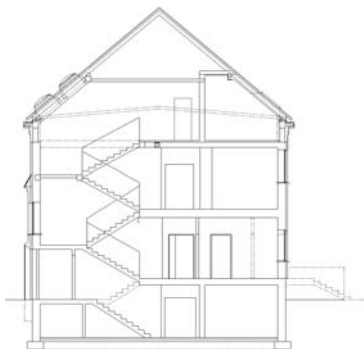


Fig. 6. A sectional view of the old building in Bydgoska Street. Visible are the existing flat roof and the new gable roof. Drawing: B. DEJA



Fig. 7. A view of the new building of the PAN Institute in Bydgoska Street, the western side. Photo: B. DEJA, 2008

Modernisation of Urania Sports and Convention Centre



Fig. 8. A view of the Urania Sports and Convention Centre from Piłsudskiego Avenue
Photo: B. DEJA, 2007

³ There is a project which covers these renovation works, prepared by ARCHE in Olsztyn.

The Urania Sports and Convention Centre⁴ in Olsztyn stands at 44 Piłsudskiego Avenue. It is not a protected building, but certainly is an interesting example of good aesthetic quality, construction solutions and functional values.

The Urania Arena lies in the central part of Olsztyn, on a small hill, near large open spaces and scattered houses, blocks of flats and single-storey shop buildings. It is separated from busy Piłsudskiego Avenue by a broad pavement and a steep slope overgrown with shrubs. There are broad steps and a ramp leading to the building. There is also a large car park in front.

The main arena is covered with a dome supported by 32 prefabricated reinforced concrete pillars joined at the top by a monolithic ring beam (Fig. 9). The 12-meter high supporting pillars are anchored in sleeve foundations, each of which was secured with four Franki piles.

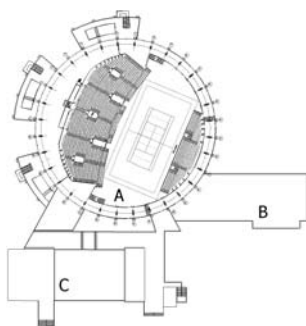


Fig. 9. A plan of the ground floor of the Urania. Drawing: B. DEJA

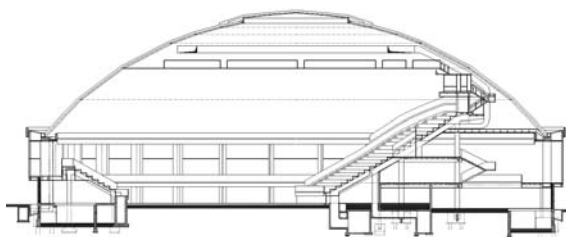


Fig. 10. A sectional view of the Urania main arena
Drawing: B. DEJA

The dome is a spheric ribbed structure, whose base diameter is 70.0 m, the rise of arch equals 17.45 m and the radius vector is 45.0 m. The subsequent rings of the dome (consisting of latitudinal bars) are joined with the longitudinal bars (ribs) forming equilateral triangular lacing, where the latitudinal bars are the base of the triangles. All the bars were made from two welded channel bars, which made tightly sealed box-sections (DEJA 2007).

The cap bearing ring (welded with plates anchored in the reinforced concrete ring beam) was made from welded sections of steel sheets.

⁴ The building design for this object was prepared in the Miastoprojekt General Construction Design Office in Olsztyn (architecture – Wiesław Piątkowski, construction – Henryk Żejmo). The arena was opened on 1st September 1978, almost 30 years ago.

The steel construction elements were covered with three layers of suitable paints. The cap bearing ring was lined with prefabricated sandwich boards and, along with the ring beam, covered with galvanized steel sheet scales, fitted to steel flat bars using timber laths.

The cap was covered with aluminium tin sheets fixed to prefabricated sandwich boards insulated with two layers of tar boards (the sandwich boards consisted of bearing ribs made of cold formed sections and pinewood boards hammered to wooden bracing frames).

The insulation of the dome roof was solved by hanging a wire net below the ceiling with rockwool boards, which was then lined with perforated tin panels.

At the topmost part of the cap there is a ring-shaped ventilation gap, which was obtained by rising the roof ends.

The outer walls of the main arena were made in the following fashion: at the ground floor level the whole walls are covered with marble plates; above, there is a ring beam with a gallery (ambulatory) lined with tinned steel sheet scales; from the first floor upwards the whole walls consist of Vitrolite sheets.

In the Vitrolite-made walls there are 24 ornamental elements, called "lunettes" by the designers. They consist of two three-dimensional parts made of welded tin sheets and fitted with windows.

Outside the main building, to the side occupied by the main rostrum and entrance lobbies, there are three emergency exit terraces connected with the first floor hallways by doors and equipped with steps which lead to an open square.

In 2001, the authorities of the Town of Olsztyn (the owner of the building) opened a competition for renovation of the Urania and modernization of the surrounding grounds.

For the purpose of this competition, the technical state of the building and the landscaping condition of the grounds were evaluated. The most important conclusions in this evaluation pertained to module A of the building no signs of poor technical condition of the bearing construction, including the pillars and reinforced concrete ring beams or the steel construction of the dome were observed.

However, other construction elements of the building showed many flaws:

- the Vitrolite wall was not weather proof, letting rain, wind and cold air through leaky seals made with a sealing mass called Olkit, which shrank and crumbled in winter while melting and flowing off the seals in summer. The glass panes in the window openings had been cut out carelessly and cracked as they tore against the channel bars in which they were set without any seals. The leaks in the seals were mended on many occasions with silicon or wooden boards, but as a result the surface of the whole wall was patchy and looked ugly;

– some of the coated tin scales which covered the lower and upper ring beams had fallen off as the wooden planks to which they had been attached had decayed and the steel flat bars in the bearing construction had corroded. In addition, the scales had become tarnished and some had bent because of winds;

– the lunettes were badly corroded and could fall off the wall because of the poor condition of their mounting construction (these elements were beyond any repair);

– the outer lining of the dome made of aluminium tin was not waterproof, which was evident during spring thawing, when melting snow leaked inside the building. This leakage was caused by the fact that the outer lining on the roof was sucked off from the sheathing and in some places strong winds would blow up the tin, which was weakly fixed to the decaying planking;

– the plaster on the emergency exit terraces had many holes and traces of repairs;

– the steps from the terraces were completely worn-out and needed major repair;

– the fixtures inside the building were designed in such a way that it was not possible to divide the building into zones and ventilate them separately. It was also impossible to adjust the heating power of the air heaters in particular parts of the building. Due to the faulty construction of the air filter station, which was out of use, the air inside the arena was not purified or humidified. Other flaws of the ventilation system included: the vents from the underground shafts making the air inside the arena cooler; the warm air from the upper levels of the arena not being sucked away, and the immense size of the ventilation control room;

– the heating system had many faults too. The major one was that the cost of heating power delivered by the municipal thermal power station was very high. The heating system failed to generate adequate temperatures inside the building (typically 13-14°C in the winter season). Old and inefficient thermal centres made it impossible to regulate the air temperature inside the building, while the radiators were corroded and filled with slime.

Below there are the main elements of the modernization plan for the Urania Arena. It is worth noticing that the underlying idea was to preserve the original aesthetic quality of the building while using modern materials in the main building it was advised to dismantle the Vitrolite wall, the lining of the upper and lower ring beams and the metal lunettes. A frame made from aluminium sections was to be mounted onto the existing steel bearing construction to support lining walls. The ornamental elements of the facade – the lunettes – should be made of aluminium tin and mounted in front of the facade using construction profiles.

The suggested solution for the outer wall provided the building with the thermal insulation, waterproofness and windtightness compliant with the standards. It also improved the aesthetic values of the building. Using small-sized facade elements guaranteed that the costs would be lower should any of the elements be damaged and needed replacement.

The renovation project included the replacement of the worn-out roof. The solution which was suggested did not require any strengthening of the roof bearing construction as it recommended using light aluminium profiles made by the German company Corus Bausysteme. The suggested insulation of the upper side of the dome would eliminate leakage through the untight suspended rockwool construction inside the dome. It would also facilitate the arrangement of acoustic elements and lining.

The suggested solution for the modernization of the mechanical ventilation system in the Urania relied on a general change in the use of this installation while preserving the existing air distribution system. Therefore, the idea of having a central machinery room was abandoned whereas some of the existing system of concrete channel which distributed fresh and used air as well as some air intakes and outlets would be preserved. The air should be prepared in 4 ventilation central units.

The concept for the modernization of the heating system comprised the following recommendations:

- instead of buying thermal power from the municipal thermal power station, the Urania should have its own power station powered by natural gas and fuel oil,
- there should be four independently controlled thermal zones in the compound, each working at different heating parameters. The zones are: building B, building C, main hall, lobby in hall A,
- convection heating in buildings B and C using panel radiators and thermoregulators,
- the heating of the main arena consisting of 10% convection heating (at present 60%), 50% automatic air heating system using Clima Heat equipment and 40% by mechanical ventilation with complete circulation of air,
- economical heating of the lobby in building A using Clima Heat radiators,
- the whole heating system integrated with the mechanical ventilation system and the thermal energy generation station by a central computer control system of the building compound BMS.

The concept for arranging the interior of the arena, in response to the expectations of the Urania administrator, contained suggestions which would increase the seat capacity and improve the aesthetic quality of the interior.

The exterior infrastructure of the Urania also needed to be modernized, for which purpose the project included such suggestions as: new surface of the

drives made of concrete pavers, setting car park spaces, new lighting of the drives and additional lights to illuminate the building; renovation of the terraces by making new silicon plaster and new exterior finish using coated steel sheets, adding new plants⁵.

All these renovation works could be completed rather easily and in stages, using modern technological solutions. The costs of the modernization were evaluated at about 10 million Polish zloty. Building a new sports and convention centre would be several-fold more expensive. Should a decision be made to construct a new compound, the additional costs incurred by the demolition works would be very high, too.

The refurbishment and expansion of the Urania based on the existing construction would not cause such big inconvenience to the environment and the people living nearby as constructing a new centre (transport and traffic around the building site, foundation piling, etc.)

Irrespective of the advantages of the modernization, no decision has been made as of present to give it the green light (mainly because of financial reasons). Recently, an opportunity has occurred to apply for EU funds dedicated to infrastructure revalorization. This has brought back the question of the refurbishment of the Urania when discussing investment projects managed by the Council. However, it has been seven years since 2001, when the compound underwent technical evaluation, so it is now necessary to update the modernization solutions, taking into consideration the current technical state of the building as well as some newer technologies.

Modernization plans to convert a fodder store to an office building of the Centre of Environmental Biotechnology of the University of Warmia and Mazury in Olsztyn

The Faculty of Environmental Protection and Fisheries at the University of Warmia and Mazury in Olsztyn, which in 2002 started research in biotechnology, needed a well equipped building to house rooms for the new laboratories to open, such as technological, chemical analysis, genetic engineering, biochemical, toxicological, low temperatures, microbiological, fermentation, hydrobotanic, reagents preparation, computer, audiovisual processing labs (*The Functional Programme of the Centre... 2002*).

As the Faculty did not have a proper building, it undertook an effort to adapt for this purpose an old fodder storehouse (built in the 1960s), located at the corner of Dybowskiego and Słoneczna Streets, in Kortowo II.

⁵ The suggested modernization of the surrounding land could only regard the immediate surroundings of the arena because of the prospective construction of a new road nearby. It is only after the road is built that the renovation of the whole area will be possible.

The building underwent a technical evaluation, which showed that it was in very bad technical state. The unheated building, which had been used to store loose animal fodders, had very moist walls, attacked by fungus. Besides, the height of the ground floor was very low and certain construction limitations excluded a possibility to expand the building vertically, whereas the small size of the land parcel on which the building stood limited its horizontal expansion.

Thus, a cost analysis was carried out to determine the profitability of refurbishment and modernization of the existing building as well as to indicate possible effects of the renovation works. Based on this analysis, a decision was made to demolish the old building and raise a new one – the Centre of Environmental Biotechnology.

After the demolition the whole land plot was available providing enough room to locate two underground tanks. One of them was to collect wastewater, which would be passed to a laboratory equipped with a semi-technological SBR reactor, and that would enable researchers to monitor wastewater treatment for scientific purposes (an additional advantage of this solution was that the municipal sewage system would receive treated wastewater).

The rainwater collected in the other tank was to be used to water the green grounds around the building and flush the toilets.



Fig. 11. The development plan for the Centre of Environmental Biotechnology UWM. Designation: III – a three-storey building of the Centre, the thin line shows the outline of the demolished fodder storehouse, 1 – a roofed bicycle stand, 2 – a trash bin. Drawing: M. DEJA

Figure 11 shows the plan for landscaping the grounds around the Centre of Environmental Biotechnology. The modernization of the land plot consisted of setting a comfortable car park with an access drive from Świetlista Street and

designing beautifully kept green areas. Noteworthy is the fact that while landscaping the grounds, not a single tree was cut down. Other objects located on the premises include a roofed bicycle rack and a dustbin hidden behind shrubs.



Fig. 12. The fodder storehouse at 46 Słoneczna Street as of 2001. Photo from the archives of the Real Estate Management Department of the UWM



Fig. 13. A view of the Centre of Environmental Biotechnology from the south-eastern side. In the foreground, the fence, gate and part of the landscaped ground. Photo: B. DEJA, 2008

Figures 12 and 13 show the old fodder storehouse designated to be demolished and the building raised on the recovered land plot. The drastic decision made by the architect (and accepted by the investor) made it possible to raise a functional building, which serves the purposes of the users very well and is liked by the people living nearby. The modernization of the land plot to house the Centre improved the aesthetic quality of this part of the university campus.

The University has more plans to revalorise the grounds near the Centre, which means that the modernization of the Centre is just a step in a broader plan, whose final execution (depending on the acquisition of external funds) will certainly improve the spatial management of Kortowo II.

Summary

The paper presents three cases of the renovation of buildings and modernisation of the grounds around. In each case, the ownership rights were undisputable and the buildings were not registered as having special architectural or historic value. Nonetheless, the decision regarding the extent and form of the revitalization of each building was a difficult one, preceded by a careful analysis of the profitability of the undertaking, which enabled the investors to minimize the risk involved (BILIŃSKI 2007).

Only one of the three cases consisted of the renovation and expansion of an existing building as well as the modernization of the whole premises (the Polish Academy of Sciences Institute in Bydgoska Street).

The owner of the Urania Sports and Convention Centre accepted the revalorization project but did not carry it out due to financial reasons. As the renovation works were postponed, the degradation of the building and its surroundings continues to the present day.

In the last case – modernization and adaptation of a storehouse in Kortowo II (to house the Centre of Environmental Biotechnology) – the expert opinion regarding the technical state of the old building along with the economic analysis of the enterprise showed that the best solution would be to pull down the existing construction, raise a new building and renovate the grounds. These plans have been put to life, thus obtaining a new value – an aesthetically beautiful and functional building located on a well-kept land plot.

Regardless of the difficulties encountered while undertaking renovation of old buildings – preliminary analysis, designing, and executing the project – revitalisation efforts are well-grounded and should be treated as part of the development strategy (BILIŃSKI 2005), especially in towns, where such works improve the value of a real estate being modernized and, whenever the prospects of obtaining new lands to be developed are slim, revitalization is an only chance for urban development.

References

- BILIŃSKI T. 2003. *Modernizacja obszarów zabudowanych*. Materiały Budowlane, 11: 15-19.
- BILIŃSKI T. 2005. *Rewitalizacja obszarów miejskich instrumentem strategii rozwoju miasta*. W: *Renowacja budynków i modernizacja obszarów zabudowanych*. T. 1. Oficyna Wydawnicza Uniwersytetu Zielonogórskiego, Zielona Góra, ss. 23-33.
- BILIŃSKI T. 2007. *Rewitalizacja obszarów miejskich. Program i ryzyko jego realizacji*. W: *Renowacja budynków i modernizacja obszarów zabudowanych*. T. 3. Oficyna Wydawnicza Uniwersytetu Zielonogórskiego, Zielona Góra, ss. 37-46.
- DEJA B. M. 2007. *Dlaczego należy zmodernizować halę widowiskowo-sportową Urania w Olsztynie?* Materiały Budowlane, 12: 34-38.
- Program funkcjonalno-użytkowy Centrum Biotechnologii Środowiska UWM w Olsztynie*. 2002. Maszynopis przygotowany na Wydziale Ochrony Środowiska i Rybactwa UWM.
- Program funkcjonalno-użytkowy budynku PAN przy ul. Bydgoskiej w Olsztynie*. 2002. Maszynopis przygotowany w Instytucie Rozrodu Zwierząt i Badań Żywności PAN.

Accepted for print 2.08.2008 r.

POSSIBLE APPLICATIONS OF NETWORK METHODS TO OPTIMALIZATION OF CERTAIN ASPECTS IN THE CONSTRUCTION INDUSTRY MANAGEMENT

Elżbieta Szafranko

Department of Civil Engineering and Building Structures
University of Warmia and Mazury in Olsztyn

Key words: construction industry, construction industry management, decision problems, theory of networks and graphs.

A b s t r a c t

The construction industry, in a broad scope of works and services it renders, encounters many problems where optimization of an outcome is needed. At all the stages of a construction project, such as planning, designing and building, there are many problems which are difficult to solve directly. However, they can be handled with an aid of mathematical methods designed to support decision making processes. Such processes, apart from being space- and time-dependent, are very complex as they involve many factors which condition success or failure of a given task. Hence, methods based on the network theory are very useful. Decision-supporting network methods are applicable at any stage of a construction project. This paper presents how the theory of networks can be applied to solving certain decision problems in the construction industry.

MOŻLIWOŚCI ZASTOSOWANIA METOD SIECIOWYCH W OPTYMALIZACJI NIEKTÓRYCH ZAGADNIENI Z DZIEDZINY ZARZĄDZANIA W BUDOWNICTWIE

Elżbieta Szafranko

Katedra Budownictwa i Konstrukcji Budowlanych
Uniwersytet Warmińsko-Mazurski w Olsztynie

Słowa kluczowe: budownictwo, zarządzanie w budownictwie, problemy decyzyjne, teoria sieci i grafów.

A b s t r a k t

W szeroko pojętej działalności budowlanej istnieje wiele zagadnień wymagających optymalizacji efektów podjętej działalności. Zarówno na etapie planowania i projektowania, jak i w trakcie realizacji zaprojektowanych obiektów, pojawia się wiele problemów, które trudno rozwiązać bezpośrednio.

Można je rozwiązać, stosując matematyczne metody wspomagania procesów decyzyjnych. Bardzo przydatne są metody oparte na teorii sieci, ze względu na złożoność procesów, wiele czynników warunkujących powodzenie przedsięwzięć, ich przestrzenny charakter oraz fakt, że procesy te przebiegają w czasie. Są one możliwe do wykorzystania na każdym etapie działalności inwestycyjnej. W artykule przedstawiono możliwości wykorzystania teorii sieci do rozwiązania niektórych problemów decyzyjnych w budownictwie.

Introduction

Typically, problems occurring while designing a construction project can be solved in a variety of ways, i.e. the expected aim can be attained via alternative solutions (variants). Thus, the designing stage often includes the question of selecting a proper design variant. A similar task of choosing a variant solution will arise in the pre-design phase, and the choice of one of the variants will often have a significant influence on the economic effects of the project based on the solution chosen.

The need to choose a variant solution occurs also during the construction works, when it is necessary to select, for example, a building materials supplier, building equipment and tools.

A typical example of optimization during a decision making process in the construction industry is the question of locating industrial plants which make building materials (SZAFRANKO 1999). The construction and building materials industry is one of these branches of industries which are vulnerable to space-related conditions, with the issue of localization being one of the major aspects. It is so because the construction industry uses large quantities of building materials, and some of the construction materials, such as prefabricated components or construction elements, can be huge and heavy, which means they need to be transported using heavy-duty, specialist vehicles. Consequently, wrong location (not optimal) of construction materials factories can result in the costs of transport being exponentially high versus the value of the building materials (SZAFRANKO 1999).

Another common problem is the choice of a land plot on which to raise a designed object (SZAFRANKO 1999). Wrong location can add to the costs of the project. As before, several variant solutions need to be considered including all possible factors which can affect the final outcome.

All the above problems have some features in common. They all involve the need to choose one, potentially the best solution, and the choice relies on a number of factors, for example constraints regarding the availability of resources (materials, means, land, etc.). Besides, there can be various dependencies between particular variants, such as the execution of certain elements of one variant exclude others and vice versa – the realization of some other elements does not make sense unless other elements are realized too.

What is characteristic of all these problems is that most of them occur at a specific time and can be modified during an ongoing construction project. When a project comprises large objects or compounds of buildings, for practical reasons the whole undertaking is divided into stages, each of which is designated specific execution requirements (KORZAN 1978).

For such projects, the best decision supporting method seems to be the one which will take into account the dynamic character of the problem and allow the decision makers to observe the effects of potentially possible modifications of the processes while they are being executed. At the same time, it should make it possible to consider certain restricting conditions and logical dependencies. It seems that a method based on the theory of traditional networks and neural networks, the latter being increasingly more frequently recommended in the relevant literature, is an answer (FORD, FULKERSON 1967).

An example of the application of network theories to an optimization task can be presented as an investment project consisting of several objects, which are constructed over a certain time period as the need arises. Each object is a separate entity in the whole construction project and can be built and opened independently from the others. As the expected technical parameters change while buildings are being used, several stages can be distinguished. It is assumed that the number of stages and their duration are known. All the objects which are put to use at a given stage should be characterized by the technical parameters no lower than the minimal requirements specified for this stage.

The whole investment project can be realized in a number of ways and it is possible to use any strategy that will fulfill the demands of the subsequent stages. Each project execution method is different from the others in costs and cost distribution during the execution of the project.

Formulation of a problem using the network theory

Preparation and development of land parcels is a process of certain duration. The decisions made during a land development project are affected by such factors as the growth rate in residential space demand, which is a consequence of effective demand, or a time when particular land plots are made available for development. Another important issue is the distribution of capital expenditures and cost of the capital.

The time factor is included by dividing the time horizon into several sections (stages), not necessarily equal in length. The number and duration of such stages depend on the forecasted growth rate of the town, the growing demand for residential space and the corresponding demand for land available

for development. All these values are time distributed and estimated for each time period. In every time period, the number of wanted flats is determined. The land plots available for development can be used completely or in part, in one or a few stages. It is assumed that the land plots will be made available for development at the beginning of each stage. The realization time is the time moment corresponding to the half-time of a subsequent stage.

Designations

- $k = \overline{1, m}$ – subsequent number of a project execution stage,
 T_0 – onset of the project execution,
 T_k – termination of stage k and onset of stage $k+1$,
 T_m – termination of the project execution (time horizon of the analysis)
 Q_k – number of flats to be built during stage k
 (in the time period $T_{k-1} \div T_k$)
 $j = \overline{1, n}$ – subsequent numbers of land plots
 q_j – number of flats which can be built on land plot j ,
 d_j – fixed costs of making available land plot j ,
 c_j – variable costs related to building up land plot j ,
 d_j^k – costs of making available land plot j at stage k ,
 ($d_j^k = d_j \alpha_{T_{k-1}}$),
 c_j^k – variable costs of building up land plot j at stage k
 ($c_j^k = c_j \alpha_{T_k}$),
 x_{jl}^k – number of flats built on land plot j during stage l when the land plot was made available at stage k ,
 T_k' – contractual time for variable cost accounting at k^{th} stage of the project realization,
 y_j^k – binary variable which determines the intensity of preparing land plot j for development during stage k .

Assumptions

A complete urban development programme is expected to be realized in a long time perspective, e.g. several years, which means that land plots to be developed can be made available to contractors successively. For the evaluation of particular variant solutions and, ultimately, choosing the optimum one, it is important to know when particular land plots will be made available for development and how the capital outlays will be distributed in time.

In order to take into account the time factor, the project realization time is divided into m stages. Stage k is between T_{k-1} and T_k moments of time. For each

stage, the demand for flats is determined. At stage k ($k = 1, m$) it is Q_k . It is assumed that the investment project begins at T_0 moment and terminates at T_m . Any land plot, for example land plot j , can be made available for development at any moment in the time period (T_0, T_m) (KUBALE 2002, TARAPATA 2003).

Another assumption is that the moment any stage, e.g. k^{th} stage, begins is the latest moment for making the land available for development at this stage. As it is not economically valid to prepare land plots for development earlier than that, it is assumed that land plots are made available for development at the early time of each project realization stage, that is at T_k ($k = 0, m-1$) moments. A plot which is made available at stage k can be used for development at all the later stages which remain until the termination of the project. Thus, plot j is available at T_0 moment and can be successively developed and built up throughout the whole investment project execution time. The same land plot made available at stage k can be used at all the successive stages.

It is assumed that each land plot can be made available at any of the possible time moments. The dates when the land plots are made available for development will affect the fixed costs and the dates when they are built up will influence the variable costs. The effect of time on costs is included in the analysis using the discount technique. For comparison of the outlays in different time periods, the starting moment of the investment project execution T_0 is taken as a reference.

For determination of the discount factors, it is assumed that the all-in outlays involved in making the land plot available for development at stage k are incurred at the moment when this stage begins, that is at T_{k-1} moment. Thus,

$$d_j^k = \alpha_{T_{k-1}} d_j \quad (1)$$

where:

$\alpha_{T_{k-1}}$ – discount factor calculated for T_{k-1} moment

$$\alpha_{T_{k-1}} = (1 + r)^{-T(k-1)} \quad (2)$$

r – cost of the capital involved,

d_j – capital expenditures (in nominal value) on preparing the land plot for development,

and:

$$c_j^k = \alpha_{T_K} c_j \quad (3)$$

where:

T_K corresponds to the half duration of the stage.

We designate the following as:

x_{jl}^k – extent of the development of land plot j at the l^{th} stage of the project execution when the plot was made available for development during the k^{th} stage

$$(k = 1, m.) (l = k, m.)$$

As it is not possible to build flats on a given land plot in excess of its capacity, the following conditions are given:

$$\sum_{l=k}^m x_{jl}^k \leq q_j \quad (k = \overline{1, m.}) (j = \overline{1, n}) \quad (4)$$

Each land plot can be made available for development no more than once (at one specific time) and built up in only one way, therefore particular dates of making this land plot available exclude each other. To account for this, each possible time moment of making each of the land plots available is designated binary variables y_j^k : defined as follows:

$$y_j^k = \begin{cases} 1, & \text{when the land plot is prepared for development at stage } k \\ & \text{and consecutive stages} \\ 0, & \text{when it is not} \end{cases}$$

The condition stating that different dates of making the same land plot available are mutually exclusive can be formulated as:

$$\sum_{k=1}^m y_j^k \leq 1 \quad (j = \overline{1, n}) \quad (5)$$

The problem consists in defining particular dates when the land plots are to be made available and precise determination of the development rate in such a way as to minimize the outlays, brought down to comparable values, on the preparation and development of the land plots.

The mathematical model of the problem

The above problem can be expressed in the form of the following mathematical programming (KORZAN 1978):

Determine the values of the variables y_j^k and x_{jl}^k , for which the objective function is:

$$\sum_{j=1}^n \sum_{k=1}^m y_j^k d_{jk} + \sum_{j=1}^n \sum_{k=1}^m c_j^k x_{jl}^k \rightarrow \min \quad (6)$$

and the set of restrictions is met:

$$\sum_{j=1}^n \sum_{k=1}^m x_{jl}^k \geq Q_l \quad (l = \overline{1, m}) \quad (7)$$

$$\sum_{k=1}^m x_{jl}^k \leq q_j \quad (k = \overline{1, m}) \quad (j = \overline{1, n}) \quad (8)$$

$$\sum_{k=1}^m y_j^k \leq 1 \quad (j = \overline{1, n}) \quad (9)$$

$$x_{jl}^k \geq 0 \quad (j = \overline{1, n}) \quad (l = \overline{1, m}) \quad (k = \overline{1, m}) \quad (10)$$

$$y_j^k \in \{0, 1\} \quad (j = \overline{1, n}) \quad (k = \overline{1, m}) \quad (11)$$

The conditions (7) guarantee the necessary supply of land for construction at each stage; conditions (8) guarantee that the capacity of any of the land plots will not be exceeded in terms of the number of flats built, and the remaining conditions describe logical requirements.

Model (6) – (11) will be large in size even for a relatively small number of potential land plots and number of stages in an investment project, and that means that any attempt at solving the model with mathematical programming methods will be cumbersome. Finding a solution will be much easier if network theory based methods are applied.

Figure 1 illustrates a network which comprises a set of all possible variants for the development of land plot number j ($j = \overline{1, n}$). In this paradigm all possible dates of making the land plot available for development are treated as a potential store. All stores are identified by numbers corresponding to the stages in the project execution. The number of a potential source is identical to the lowest number of the stage in the project execution when this plot can be used for construction. All the stores are preceded by a common source

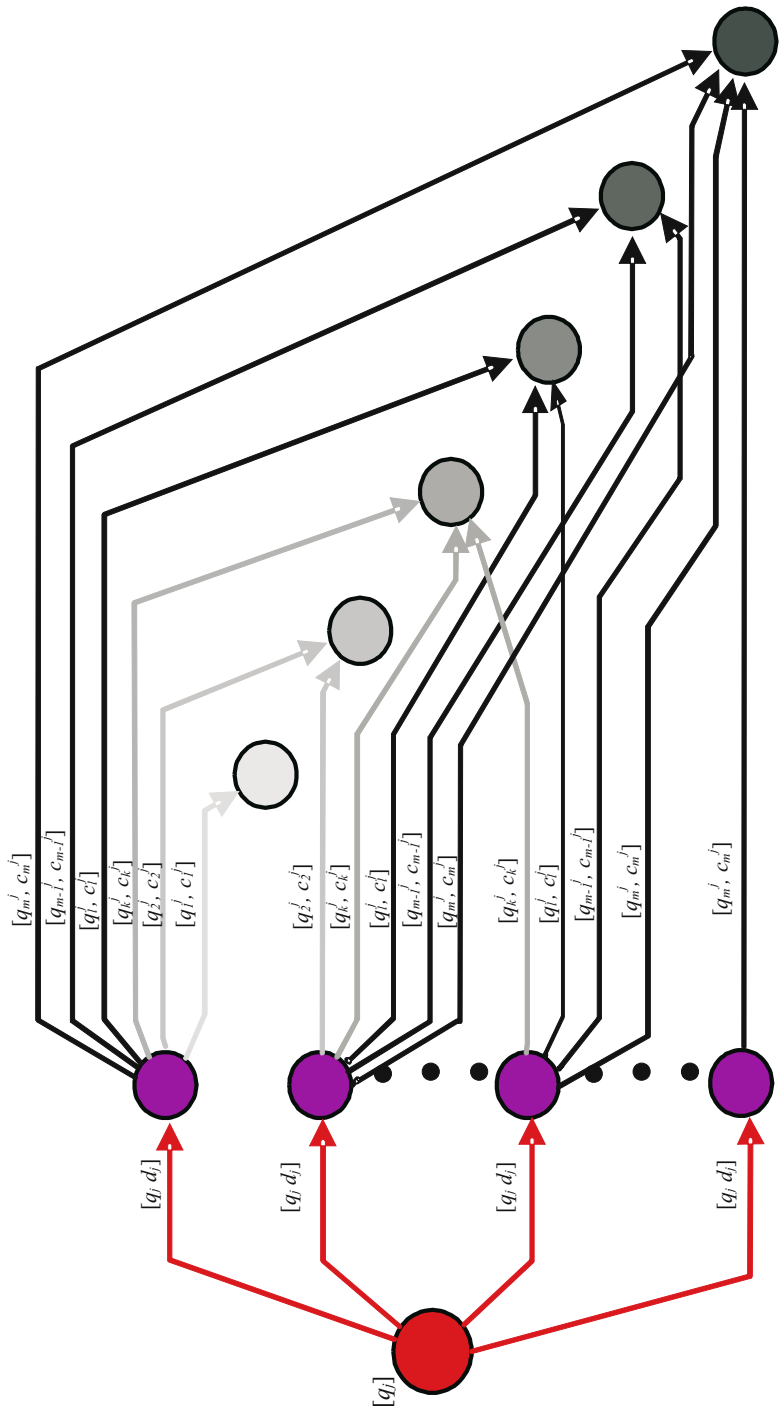


Fig. 1. A set of variants for development of a land plot in the investment project execution

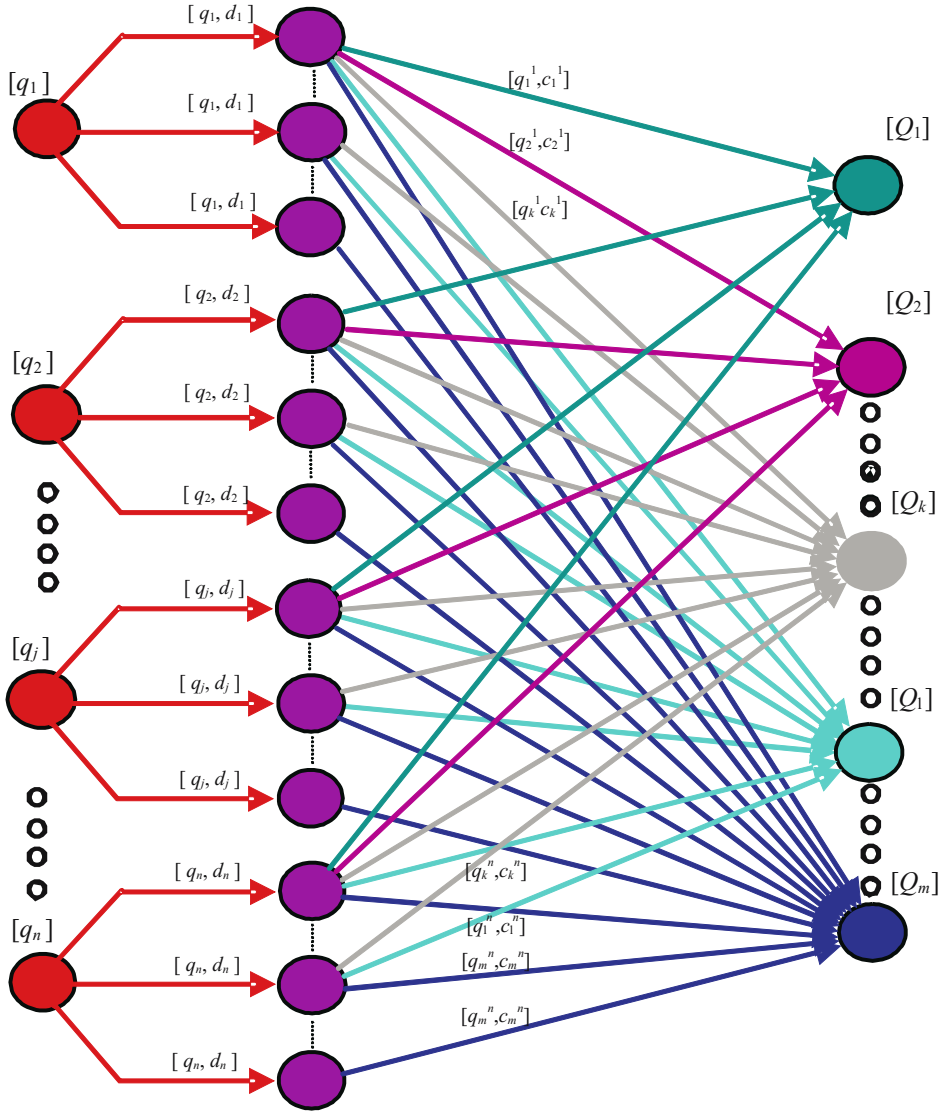


Fig. 2. The decision network including time factor

of efficiency marked as q_j . The arcs joining the source with the stores are designated bandwidth q_j and discounted value of making the land plot available d_j^k . The demand for flats at each stage is interpreted as outflows in the network of expenditures Q_k . Each store is connected by arcs with all the outflows of the same and higher order numbers. The bandwidth of each arc is

q_j and a unit transport cost equals c_j^k , i.e. the discounted value of unit variable costs of developing the land plot.

The network illustrated in Figure 1 and expanded by inclusion of possible variants of using the other land plots can be seen in Figure 2. The determination of a satisfying flow at the minimum cost in this network will correspond to the determination of the time when these land plots should be developed and the extent of the construction works.

Conclusions

As a formal concept, a network can serve as a natural and illustrative model for many problems. By presenting an investment project in the form of a graph it is possible to analyze the inner structure of a problem we need to deal with. In addition, in this case a solution to the problem can involve algorithms based on the theory of graphs, which are usually more effective than algorithms based on other mathematical theories. Besides, they simplify and accelerate the calculations. Proper formulation of the data enables decision makers to answer many questions. Most importantly, network-based paradigms can determine the sequence in which land plots should be developed so as to respond to the demand for housing space. Besides, they facilitate ongoing control of the size and structure of expenditures incurred by a given project. By describing arcs in a network with a cost function, it is possible to account for all the expenses which relate to the land utility criteria and economic conditions.

To recapitulate, it needs to be stated that methods based on the theory of networks and graphs can be an efficient and convenient tool, which will support decision makers while planning an investment project.

References

- FORD J.R., FULKERSON D.R. 1967. *Flows in Networks*. Princeton, New Jersey.
KORZAN B. 1978. *Elementy teorii grafów i sieci*. WNT, Warszawa.
KUBALE M. 2002. *Optymalizacja dyskretna. Modele i metody kolorowania grafów*. WNT, Warszawa.
SZAFRANKO E. 1999. *Możliwości sterowania kosztami inwestycji za pomocą metod sieciowych*. Problemy Rozwoju Budownictwa, 4.
TARAPATA Z. 2003. *Zliczanie dróg w grafach regulowanych*. Biuletyn WAT, Warszawa.

Accepted for print 1.07.2008 r.

METHODS OF CALCULATING CONCRETE STRAIN TAKING INTO ACCOUNT THE NONLINEAR CREEP

Krzysztof Klempka

Department of Civil Engineering and Building Structures
University of Warmia and Mazury in Olsztyn

Key words: nonlinear creep of concrete, reinforced concrete, strain, stress.

Abstract

In the following article we present the law of nonlinear creep and simplified methods of calculating strains after t time. Next, we propose a constitutive rule for concrete, which may be used in analyzing strains of construction elements, where stress exceeds the limit of linear creep.

METODY OBLICZANIA ODKSZTAŁCEŃ BETONU Z UWZGLĘDNIENIEM NIELINIOWEGO PEŁZANIA

Krzysztof Klempka

Katedra Budownictwa i Konstrukcji Budowlanych
Uniwersytet Warmińsko-Mazurski w Olsztynie

Słowa kluczowe: nieliniowe pełzanie betonu, konstrukcje żelbetowe, odkształcenia, naprężenia.

Abstrakt

W artykule omówiono prawo nieliniowego pełzania oraz uproszczone metody obliczania odkształceń po czasie t . Zaproponowano prawo konstytutywne dla betonu. Może być ono wykorzystane w analizach odkształceń elementów konstrukcji, w których naprężenia przekraczają granicę liniowego pełzania.

Introduction

According to the current regulations of the Polish norm PN-B-03264 based on the Eurocode EN 1992-1-1 (or EC2), it is necessary to take into account the

nonlinear creep and to do so the creep coefficient $\phi(t, t_0)$ is substituted with coefficient $\phi_k(t, t_0)$ obtained from the following formula:

$$\phi_k(t, t_0) = \phi(t, t_0) e^{1,5(k_\sigma - 0,45)} \quad (1)$$

where:

k_σ is a ratio of stress in concrete σ to the mean compressive strength at the time of applied loading $f_{cm}(t_0)$. The limit of linear creep is assumed to be the value of stress equal to $0,45 f_{cm}(t_0)$. The current version of the Eurocode has been corrected by changing that value of the limit to $0,45 f_{ck}$. It means that there is now a necessity to take into account the nonlinear creep even with smaller stresses. The rules and regulations of the Eurocode that are going to be binding in Poland as of 2010 include the new guidelines regarding the nonlinear creep. This is why we have to find new calculation methods for long term strains of selected construction elements (e.g. slender columns, pre-stressed concrete beams) with the use of the nonlinear theory, then comparing the results obtained by using these new methods with the results obtained by using the simplified method based on applying formula (1). Further in the paper we present the nonlinear creep law and the simplified methods for calculating strains after t time, as well as the constitutive law for concrete formulae (5) and (14) which may be used in numerical analyses of constructions.

The nonlinear creep law

The strain in the time function t is expressed by formula (2) (presented in ARUTIUNIAN'S paper from 1952)

$$\varepsilon(t) \frac{\sigma(t_0)}{E(t_0)} + F[\sigma(t_0)]C(t, t_0) + \int_{t_0}^t \left\{ \frac{d\sigma(\tau)}{d\tau} \frac{1}{E(\tau)} + \frac{dF[\sigma(\tau)]}{d\tau} C(t, \tau) \right\} d\tau \quad (2)$$

where:

- | | |
|--|--|
| $C(t, \tau) = \frac{\phi(t, \tau)}{E(\tau)}$ | – coefficient described as specific creep, |
| $\phi(t, \tau)$ | – creep coefficient, |
| $E(\tau)$ | – instantaneous elastic modulus in time τ , |
| $\sigma(t_0)$ | – initial stress at the time t_0 , |
| $E(t_0)$ | – modulus of initial deformation at time t_0 , |

- $F[\sigma(t_0)]$ – the value of nonlinear stress function at time t_0 ,
 $F[\sigma(\tau)]$ – nonlinear stress function dependent on time τ .

Nonlinear stress function $F[\sigma(t)]$

ARUTIUNIAN (1952), JACENKA et al (2000), ULICKIJ (1967) all propose different expressions describing the nonlinear stress function $F[\sigma(t)]$. In our further analyses we use a very simple dependence described in Arutiunian's book from 1952 by the following relation (3).

$$F[\sigma(t)] = \sigma(t) + \beta \sigma^2(t) \quad (3)$$

where coefficient β is the stress function (Fig. 1).

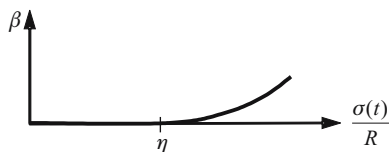


Fig.1 Dependence of coefficient β on stress $\sigma(t)/R$

The denomination of β is 1/MPa. According to [6] the value of β may be calculated from the following dependence

$$\beta = \begin{cases} 0 & \text{for } \sigma(t) \leq \eta R \\ \nu \left[\frac{\sigma(t)}{R} - \eta \right]^n & \text{for } \sigma(t) > \eta R \end{cases} \quad (4)$$

where:

- f_c – compressive strength of concrete (in ULICKIJ'S paper from 1967 compressive strength of concrete was marked by R),
 η – the ratio of the value of the stress which causes linear creep to change into nonlinear creep to compressive strength of concrete f_c .
 ν, n – parameters assumed for the sake of experiment

According to EC2 the limit of the linear creep is assumed to have the value of stress equal to $0,45 f_{ck}$ (f_{ck} – characteristic compressive cylinder strength of concrete at 28 days). In this article we assume average values of compressive strength of concrete. Thus, further in the article the assumed value of the linear creep's limit is $0,45 f_c$. Taking into account the mention assumption, dependence (4) may be expressed as follows

$$\beta = \begin{cases} 0 & \text{for } \sigma(t) \leq 0,45 f_c \\ \nu \left[\frac{\sigma(t)}{f_c} - 0,45 \right]^n & \text{for } \sigma(t) > 0,45 f_c \end{cases} \quad (5)$$

For the sake of further analyses we assumed the values of parameters $\nu = 0,15$ [1/MPa] and $n = 1,00$ from E.A. Jacenka's experiments described in ULICKIJ (1967).

Concrete strain under the constant stress

Creep in time (t_0, t) is taken into account. It is assumed that as a result of axial compression the stress in concrete at the initial moment t_0 is $\sigma(t_0)$ and does not change with time. The value of stress functions $F[\sigma(t_0)]$ is also constant in time (Fig. 2). The strain in time t is calculated from formula (2), which may be presented as formula (6) in case of constant stress

$$\varepsilon(t) = \varepsilon^{in}(t_0) + \varepsilon^{cr}(t) = \frac{\sigma(t_0)}{E(t_0)} + F[\sigma(t_0)] C(t, t_0) \quad (6)$$

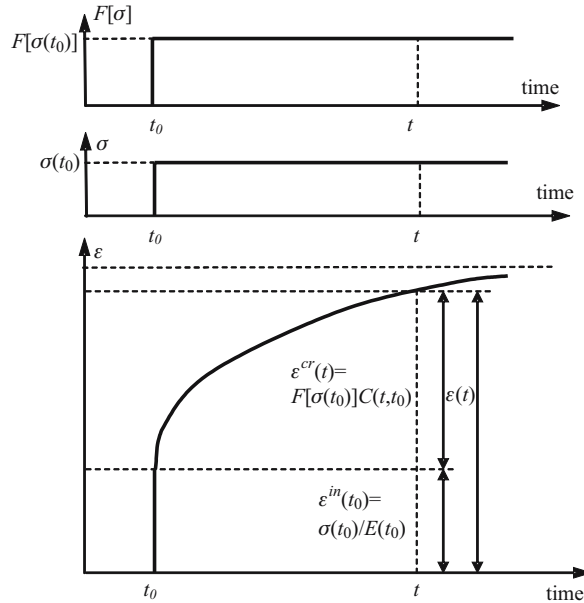


Fig. 2. Total strain $\varepsilon(t)$ at the moment t with constant stress; $\varepsilon^{in}(t_0)$ – elastic strain, $\varepsilon^{cr}(t_0)$ – creep strain

Concrete strain under changeable stress when stress is given in time function

Exact, numerical calculation of strain may be done by dividing the considered time into short periods and summing up the subsequent increments. Assuming that after time t_0 there are changes in stresses $\Delta\sigma(t_i)$, and increments of stress function $\Delta F[\sigma(t_i)]$ in subsequent time periods $\Delta t_i = t_i - t_{i-1}$, the integral in formula (2) is approximated by the following sum:

$$\int_{t_0}^t \left\{ \frac{d\sigma(\tau)}{d\tau} \frac{1}{E(\tau)} + \frac{dF[\sigma(\tau)]}{d\tau} C(t, \tau) \right\} d\tau = \sum_{i=1}^n \frac{\Delta\sigma(t_i)}{E(t_i)} + \Delta F[\sigma(t_i)] C(t, t_i) \quad (7)$$

After taking into account the relation (7), the dependence (2) may be expressed as the formula (8)

$$\varepsilon(t) = \frac{\sigma(t_0)}{E(t_0)} + F[\sigma(t_0)] C(t, t_0) + \sum_{i=1}^n \frac{\Delta\sigma(t_i)}{E(t_i)} + \Delta F[\sigma(t_i)] C(t, t_i) \quad (8)$$

Formula (8) enables the exact calculation of strain. The method based on dependence (8) was named a 'step by step' method in the paper of CHIORINO et al. (1980). Depending on using different methods of approximating the integral in formula (2) we can distinguish the following simplified methods of calculating strain in time t :

1. Effective modulus method (EM)
2. Mean stress method (MS)
3. Age adjusted effective modulus method (AAEM)

The analysis of these methods in case of linear creep was presented in the paper by CHIORINO et al (1980). Below we present formulae for concrete strains in time t for nonlinear creep derived for these methods and based on the assumptions of CHIORINO et al (1980).

Effective modulus method (EM)

Assuming one time period with the use of the rectangular rule, the integral in dependence (2) may be approximated by the following expression:

$$\int_{t_0}^t \left\{ \frac{d\sigma(\tau)}{d\tau} \frac{1}{E(\tau)} + \frac{dF[\sigma(\tau)]}{d\tau} C(t, \tau) \right\} d\tau \equiv (\sigma(t) - \sigma(t_0)) \frac{1}{E(t_0)} + (F[\sigma(t)] - F[\sigma(t_0)]) C(t, t_0) \quad (9)$$

After taking into account (9), dependence (2) may be expressed by formula (10)

$$\varepsilon(t) = \frac{\sigma(t)}{E(t_0)} + F[\sigma(t)] C(t, t_0) \quad (10)$$

Substituting (11) and (12)

$$E(t_0) = E_{cm} \quad (11)$$

$$C(t, t_0) = \varphi(t, t_0)/E_{cm} \quad (12)$$

in (10) we obtain dependence (13)

$$\varepsilon(t) = \frac{\sigma(t)}{E_{cm}} + \frac{F[\sigma(t)]}{E_{cm}} \varphi(t, t_0) \quad (13)$$

Substituting (3) in (13) we obtain a relationship between stresses and strains in concrete at the moment t :

$$\varepsilon(t) = \beta \frac{\sigma^2(t)}{E_{cm}} \varphi(t, t_0) + \frac{\sigma(t)}{E_{cm}} (\varphi(t, t_0) + 1) \quad (14)$$

With the stress growing in time, the strains calculated according to (14) come with excess. Using The method does not require calculating the value of initial stresses $\sigma(t_0)$.

In case of linear creep, the nonlinear stress function $F[\sigma(t)]$ equals the value of $\sigma(t)$, and thus dependence (14) may be expressed as this commonly known formula:

$$\varepsilon(t) = \frac{\sigma(t)}{E_{c,eff}} \quad (15)$$

where:

$$E_{c,eff} = \frac{E_{cm}}{1 + \varphi(t, t_0)} \quad (16)$$

Due to its simplicity, the EM method is used in the Eurocode and the Polish norm for calculating deflections of bent elements. Application of this method is based on substituting (in formulae of the linear theory of reinforced concrete) the modulus of concrete elasticity E_{cm} with the effective modulus $E_{c,eff}$.

Mean stress method (MS)

Assuming one period of time and using the trapezoidal rule, the integral in formula (2) is approximated by the following expression

$$\int_0^t \left\{ \frac{d\sigma(\tau)}{d\tau} \frac{1}{E(\tau)} + \frac{dF[\sigma(\tau)]}{d\tau} C(t, \tau) \right\} d\tau \cong \frac{(\sigma(t) - \sigma(t_0))}{2} \left(\frac{1}{E(t)} + \frac{1}{E(t_0)} \right) + (F[\sigma(t)] - F[\sigma(t_0)]) \frac{C(t, t) + C(t, t_0)}{2} \quad (17)$$

Taking into account (17) and dependence (2) may be expressed as follows:

$$\varepsilon(t) = \frac{\sigma(t_0)}{E(t_0)} + \frac{F[\sigma(t)] + F[\sigma(t_0)]}{2} C(t, t_0) + \frac{(\sigma(t) - \sigma(t_0))}{2} \left(\frac{1}{E(t)} + \frac{1}{E(t_0)} \right) \quad (18)$$

In case of linear creep, relations (3) and (5) result in dependences (19) and (20)

$$F[\sigma(t)] = \sigma(t) \quad (19)$$

$$F[\sigma(t_0)] = \sigma(t_0) \quad (20)$$

Taking into account the relation of (19) and (20), dependence (18) may be expressed as formula (21)

$$\varepsilon(t) = \frac{\sigma(t_0)}{E(t_0)} + \frac{\sigma(t) + \sigma(t_0)}{2} C(t, t_0) + \frac{(\sigma(t) - \sigma(t_0))}{2} \left(\frac{1}{E(t)} + \frac{1}{E(t_0)} \right) \quad (21)$$

Using the relation of (11) and (12), dependence (21) may be expressed as (22) derived in the paper by CHIORINO et al. (1980).

$$\varepsilon(t) = \frac{\sigma(t)}{E_{cm}} + \frac{\sigma(t) + \sigma(t_0)}{E_{cm}} \varphi(t, t_0) \quad (22)$$

Age adjusted effective modulus method (AAEM)

Using one period of time and the aging coefficient χ , the integral in formula (2) may be substituted with the following expression

$$\int_{t_0}^t \left\{ \frac{d\sigma(\tau)}{d\tau} \frac{1}{E(\tau)} + \frac{dF[\sigma(\tau)]}{d\tau} C(t, \tau) \right\} d\tau \equiv (\sigma(t) - \sigma(t_0)) \frac{1}{E(t_0)} + (F[\sigma(t)] - F[\sigma(t_0)]) \chi C(t, t_0) \quad (23)$$

Taking into account (23), dependence (2) may be expressed as formula (24)

$$\varepsilon(t) = \frac{\sigma(t_0)}{E(t_0)} + F[\sigma(t_0)] C(t, t_0) + (\sigma(t) - \sigma(t_0)) \frac{1}{E(t_0)} + (F[\sigma(t)] - F[\sigma(t_0)]) \chi C(t, t_0) \quad (24)$$

Using dependences (11), (12) as well as (19) and (20), and taking into account linear creep, formula (24) may be expressed as (25)

$$\varepsilon(t) = \sigma(t_0) \left[\frac{1}{E_{cm}} + \frac{\varphi(t, t_0)}{E_{cm}} \right] + [\sigma(t) - \sigma(t_0)] \left[\frac{1}{E_{cm}} + \chi \frac{\varphi(t, t_0)}{E_{cm}} \right] \quad (25)$$

Based on analyses presented in CHORINO'S et al. (1980), this theory gives good results in cases where stresses do not change quickly in a given time.

Relation between stresses and strains in time t function – effective modulus method EM

A relation between stresses and strains in the time t function has been presented in figure 3. Assuming that $t = t_0$, $\varphi(t, t_0) = 0$, formula (14) is transformed into a linear dependence (26) (straight line I, figure 3)

$$\varepsilon(t_0) = \frac{\sigma_c(t_0)}{E_{cm}} \quad (26)$$

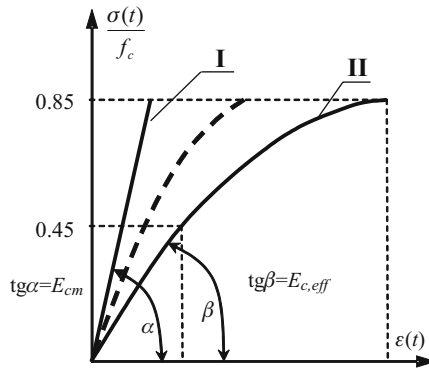


Fig. 3. Dependence $\frac{\sigma(t)}{f_c} - \varepsilon(t)$; I – linear dependence for $t = t_0$ for a short-term load, II – nonlinear dependence for $t \rightarrow \infty$ (boundary curve) for long-term loads

If $t \rightarrow \infty$, then the relation between stresses and strains is linear only for stresses $\sigma \leq 0,45 f_c$ and can be expressed with formula (15). For stresses greater than $0,45 f_c$ the dependence is nonlinear (curve II, figure 3). The curve marked with a broken line reflects dependence $\sigma(\tau) - \varepsilon(t)$ defined for any moment t from the interval (t_0, t_∞) . Because compressive strength of concrete decreases in case of long-term loading, the range of stresses considered here has been limited to $0,85 f_c$.

Straight line I shows a dependence resulting from immediate loading of only one concrete sample (strain is defined when loading is increasing). Dependences presented by curve II cannot be determined with only one experiment, but with a series of them. To run just one experiment, we would have to apply to the sample an axial load which causes stress $\sigma(t)$, and then, after an infinite time ($t \rightarrow \infty$) of being loaded, define strain $\varepsilon(t)$. Successive experiments would have to be carried out in a similar way, but using different samples, each one loaded with increasing force. Such a series of experiments would result in obtaining the dependence presented by curve II.

Conclusion

1. We have presented in this article three simplified methods which enable to calculate strains resulting from concrete creep after t time under the influence of great stresses ($\sigma > 0,45 f_c$).

2. Approximating the integral in formula (2) with expression (9) (effective modulus method) and using expression (3) which describes the stress function we obtained dependence (14). Dependence $\sigma(t) - \varepsilon(t)$ presented by formulae (5) and (14) (curve II, figure 3) may be used while analysing strain in construction elements where stresses exceed the limit of linear creep.

References

- ARUTUNIAN N. 1952. *Niekatoryje waproxy teorii potzuczestii*. Moskwa.
- CHIORINO M., NAPOLI P., MOLA F., KOPRKA M. 1980. *Structural effects of time-dependent behaviour of concrete*. Comité Euro-International du Béton: CEB Design Manual. Bulletin d'Information 136.
- Eurocode 2: Design of Concrete Structures. Part 1-1. General Rules and Rules for Buildings. EN 1992-1-1: 2008.
- JACENKO E., KORNIŁOWA S., BOWIN A., SOSSU G. 2000. *Teoria potzuczestii żeliezobietonnych konstrukcji*. Dniepropietrowsk.
- Konstrukcje betonowe, żelbetowe i sprężone. Obliczenia statyczne i projektowanie*. PN-B-03264: 2002.
- ULICKI I. 1967. *Teoria i rasczot żeliezobietonnych stierzniewych konstrukcji s uczotom dlitieelnych prociesow*. Izdatielstwo Budiwielnik. Kijew.

Accepted for print 23.05.2008 r.

**THE QUESTION OF DESIGNING MODERN
ARCHITECTURE IN CONSERVATION AREAS:
A CASE STUDY OF KORTOWO, THE CAMPUS
OF THE UNIVERSITY OF WARMIA AND MAZURY
IN OLSZTYN**

Joanna Pawłowicz, Marek Zagroba

Department of Civil Engineering and Building Structures
University of Warmia and Mazury in Olsztyn

Key words: architecture, urbanism, spatial composition, campus, Kortowo.

A b s t r a c t

This paper is a presentation of the problems which appear when shaping space in architectural and urbanistic areas of special historic interest, with the campus of the University of Warmia and Mazury in Olsztyn taken as a case study. Each new construction project in a conservation area must comply with a number of restricting conditions, whose aim is to adjust new buildings to the existing environment. Unfortunately, good exposition of the existing architectural composition not an easy task, and on many occasions construction projects carried out in historical sites introduce an element of chaos to space.

By analyzing how the university campus in Kortowo has been developed, we have arrived at the conclusion that the future spatial development of this area should focus on revalorization of the existing buildings – that is the overriding objective should be to bring order to the functions, forms and surroundings of the buildings on the campus grounds. This is a reflection of the complex nature of problems encountered when shaping a spatial composition in a conservation area. Eliminating ‘foreign’ shapes as well as creating new architecture that will blend well with the historical buildings would enhance the spatial values of the old part of Kortowo, which in turn could emphasize the prestige of the campus.

**PROBLEMATYKA PROJEKTOWANIA WSPÓŁCZESNYCH OBIEKTÓW ARCHITEKTURY
W STREFACH OCHRONY KONSERWATORSKIEJ NA PRZYKŁADZIE KAMPUSU
UNIwersYTETU WARMIŃSKO-MAZURSKIEGO W OLSZTYNIE**

Joanna Pawłowicz, Marek Zagroba

Katedra Budownictwa i Konstrukcji Budowlanych
Uniwersytet Warmińsko-Mazurski w Olsztynie

S ł o w a k l u c z o w e: architektura, urbanistyka, kompozycja przestrzenna, strefa ochrony konserwatorskiej, miasteczko akademickie, Kortowo.

A b s t r a k t

W artykule przedstawiono problemy kształtowania przestrzeni w historycznych założeniach architektoniczno-urbanistycznych na przykładzie miasteczka akademickiego Uniwersytetu Warmińsko-Mazurskiego w Olsztynie. Każda inwestycja powstająca na terenach objętych ochroną konserwatorską podlega wielu rygorom, które mają zapewnić dostosowanie nowo powstających obiektów do istniejącego otoczenia. Niestety ekspozycja kompozycji istniejących form nie jest zagadnieniem łatwym i niejednokrotnie w miejscach o historycznym rodowodzie można zaobserwować działania wprowadzające chaos w przestrzeni.

Analizując sposób i intensywność zagospodarowania kampusu uniwersyteckiego, należy stwierdzić, że dalszy rozwój przestrzenny powinien skupiać się wokół działań rewaloryzacyjnych istniejących obiektów – uporządkowania ich funkcji, formy i otoczenia. Działania te odzwierciedlają złożoność problemów w kształtowaniu przestrzeni w strefach ochrony konserwatorskiej. Eliminowanie „wyobcowanych” form kubaturowych oraz tworzenie i powiązanie nowej architektury z historyczną wpłynęłoby na podniesienie przestrzennych walorów tej części Kortowa, co dodatkowo podkreślałoby jego prestiż.

Introduction

Designing modern architectural forms in a historical setting usually creates a series of problems, which must be solved in order to pay respect to the cultural heritage of a given area. This is unquestionably a necessary condition, which governs all actions conducted in conservations areas, both urbanistic and architectural ones. Unfortunately, good exposition of the composition of existing elements is not an easy task and therefore in many historical areas we can observe actions which introduce spatial chaos. The oldest part of the university campus in Olsztyn can serve as a good example of the above problems, which are the subject of the present article.

Kortowo¹, an area in the south-western part of Olsztyn, preserves the remains of a psychiatric hospital compound, built at the end of the 19th century. Today, it is the seat of the University of Warmia and Mazury.

As an urbanistic and architectural complex, the historical part of Kortowo is rich in the material culture elements, which can be put into mutually interacting groups of values, such as:

- archaeological – archeological sites,
- urbanistic – the composition plan, interiors, compositional axes,
- architectural – single architectural objects as well as their groups,
- natural – natural monuments, landscaped green spaces.

¹ This part of the campus which contains the oldest architecture is known as Kortowo I. It belongs to the university and is delineated by Warszawska Avenue to the east, a military zone to the north, Kortowskie Lake to the west and the Kortówka River to the south.

Spatial management elements

The spatial composition of historical Kortowo has maintained, to some extent, the original plan (Fig. 1) although the urbanistic setting – regular, symmetrical and developed along an axis running from the north-east to the south-west – has been largely obscured. However, the central part of the compound, around the Rector's Office and Cieszyński Square, has been preserved rather clearly.

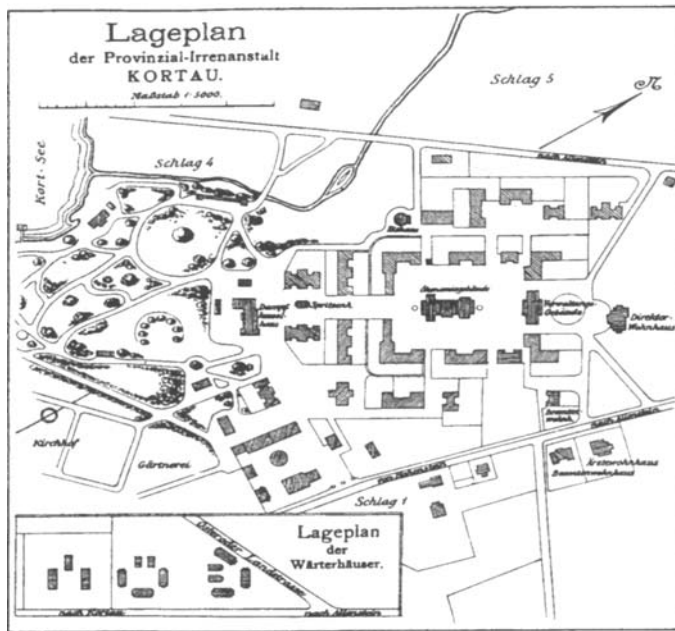


Fig. 1. Kortowo as a psychiatric hospital, plan of 1913

Source: PIECHOCKI (1993)

Changes in the urbanistic design of Kortowo are mainly due to the events that happened here at the end of World War Two, when many of the hospital buildings were damaged and devastated. The new buildings constructed shortly after the war were raised on the old foundations, with much care taken to maintaining their historical plan and shape. However, the architectural design of these buildings was an expression of the Social Realism style. Moreover, little attention was paid to the architectural detail and the buildings were often ineptly adapted to new functions. As a result, the spatial composition was degraded.

Although car transport has developed enormously over the last hundred years, the road pattern seen in today's Kortowo largely corresponds to the solution created at the end of the 19th century. Owing to many restrictions imposed on motor traffic on the campus, the original street plan of Kortowo, with the streets, squares and urbanistic interiors it included, has not been considerably modified. On the other hand, the fact that in the post-war years Kortowo began to serve educational purposes has made it necessary to design new routes for pedestrians and motorists as well as new car parks. This in turn has resulted in a number of uncontrolled solutions, divergent from the historical street plan, which should be now remodelled.

The construction investments completed in the post-war years have made diverse impact on the spatial structure of old Kortowo. The original axis of the whole composition has been severed in its southern section by a building (Fig. 2) completely different (foreign) in character from the existing edifices.



Fig. 2. A university building in Cieszyński Square, photo: M. ZAGROBA

Also the northern end of this axis has been cut off with a large, one-storey pavilion, which looks foreign to the surrounding environment. The cemetery, which was situated in the south-western part of the hospital compound, was transformed into a university park. Several other buildings,

larger and smaller ones, seem to have been constructed without any underlying complex analysis, which should be obligatory for any actions undertaken in a conservation area².

Architectural objects

Architecture has a profound effect on shaping the space in the old part of Kortowo, an area under protection of the Conservation Office. Most of the buildings reveal features typical of the architecture of Warmia and Mazury – they are built of red brick on rectangular, horseshoe or L-shaped plans (Fig. 3) and covered with ceramic tiled gable roofs. Their facades are divided with risalits and they possess many interesting architectural details, such as brick cornices and risalit tops or timber elements of the roofs (Fig. 4). The original setting and form of the buildings preserved until our days along with the materials used emphasize their historical value.



Fig. 3. A women's ward building of the psychiatric hospital – building no 31, photo: M. ZAGROBA

² The area of the former psychiatric hospital was converted into a conservation area and registered on 23rd April 1985 at number 3626 on the list of historical buildings as an architectural and urbanistic complex. Other protected elements comprise: the park, which lies on Kortowskie Lake, the grounds which contained the former Higher School of Agriculture and the complex of halls of residence as far as the Kortówka River. This protection zone 'B' also includes two buildings and the land plots on which they stand in Warszawska Street, opposite Kortowo.



Fig. 4. A women;s ward building, typical architecture of the historical part of Kortowo,
photo: M. ZAGROBA



Fig. 5. A hospital building, a historical building in Kortowo, raised in the early 20th century and
'modernized' in the 1970s, photo: M. ZAGROBA

Newer buildings, erected after World War Two, demonstrate a distinctly different type of architecture. With their shapes and form, construction solutions and design as well as the building materials used, they diverge from the harmonic, historical buildings, thus introducing some chaos to the well-designed compositional space. This is particularly true about the large buildings, which bear close semblance to the architecture of Social Realism (Fig. 2, 5). But many smaller, one-storey buildings covered with flat roofs are also in discord with the old architecture. This inconsiderate manner of adding new buildings greatly depreciates the value of the space, which is protected as a conservation area.



Fig. 6. University buildings in Prawocheńskiego Street, photo: M. ZAGROBA

Several observations can be made at this point. First of all, the new buildings are not examples of unpermitted construction work. Contrary to this, they all had building permits. The local development plan, however, is not short of explicit written rules regarding the adjustment of new construction investment projects (construction of a new building, extension, addition of floors, reconstruction as well as demolition of old buildings) to the forms, sizes and architecture of historical buildings.

In practice, it proves to be a challenging task to choose the right colours for a façade or to replace old windows, for example, when the role of an architect is often reduced to an ability of graphic presentation of design solutions rather

than making designs and choices. Doubtless, this characterizes the current state and problems of architecture in Poland.

All the elements of the present spatial management in the historical part of the campus – architectural, landscape and urbanistic ones – require revalorization, with an aim of preserving the culturally valuable complex of the buildings. Another reason why Kortowo is so valuable is its location (on a lake, next to a park), which is why it is considered to be one of the most picturesquely set university campuses in Poland.

Designing architectural objects

The oldest part of the university campus, today, set out as a conservation area owing to its spatial design, excludes construction of large objects in the available space. But this does not mean that the whole area is protected from any construction investment projects. The local development plan states it very clearly that the form of new buildings cannot be in discord with the existing design and their size must not be overwhelmingly large in the space which was defined in the past. Such recommendations should eliminate construction or reconstruction of the likes of Social Realism or erection of flat-roofed, one- or two-storey pavilions (Fig. 7).



Fig. 7. A historical building of the post office, against the background of post-war buildings, in Heweliusza Street, photo: M. ZAGROBA



Fig. 8. A one-storey pavilion at 4 Heweliusza Street, photo: M. ZAGROBA

Having analyzed the manner and intensity of the development of this area, it needs to be suggested that any future spatial development should focus on revitalization of the existing buildings in a way that will bring order to their functions, forms and surrounding grounds (Fig. 8). Elimination of ‘foreign’ forms as well as creation of new architecture related to the historical buildings would improve the spatial values of this part of Kortowo, which in turn could add to its prestige. For such activities it is necessary to formulate certain recommendations, which reflect the complexity of spatial management in conservation areas. The recommendations can be summarized as follows:

- based on some analytical work – monitoring of modifications made to the urbanistic setting – streets, squares, building alignments, composition of interiors,
- elimination of ‘accidental’ objects, ‘accidental’ in terms of their form, scale, expression, spatial context, in short – buildings which disturb the uniform character of the whole complex of buildings,
- adjusting new construction projects to the historical forms by maintaining the same scale, architectural expression, materials and solutions. New architecture should not copy the historical forms but it needs to be suited to the developed space.
- when renovating the existing buildings, the applied design solutions should correspond to the historical forms of the buildings. The materials used ought to include traditionally used building materials (brick, timber, ceramic roof tiles).

Preservation of cultural values – urbanistic, architectural, archaeological and natural – should be combined with analyses of the impact produced by new

construction investment projects on the maintained historical spatial plan of the area. This means that both the architects and the conservation officers, who supervise the design and construction stages, are greatly responsible for the protection of the cultural heritage. Unfortunately, this shared responsibility for our common heritage does not always assume the form of partner cooperation. Thus, it is evident that the question of designing modern architecture in conservation areas is a multi-facet issue.

References

- CIELĄTKOWSKA R. 2003. *Miasteczko Akademickie Uniwersytetu Warmińsko-Mazurskiego w Olsztynie w kontekście funkcjonowania kampusów uniwersyteckich w świecie*. W: *Kortowo – Miasteczko Akademickie Uniwersytetu Warmińsko-Mazurskiego w Olsztynie. Kontekst – Historia – Stan obecny*. Red. R. Cielątkowska, Olsztyn, s. 34-37.
- Karta ewidencyjna rejestru zabytków województwa warmińsko-mazurskiego nr 3626 z dnia 23.04.1985 r., archiwum SOZ w Olsztynie.
- PIECHOCKI S. 1993. *Czyściec zwany Kortau*. Książnica Polska, Olsztyn, s. 30.

Accepted for print 4.07.2008 r.

MODELLING OF THE SILTING UP PROCESSES IN WATER ROUTES OF ŁEBA AND TOLKMICKO PORTS

Leszek M. Kaczmarek¹, Szymon Sawczyński²

¹ Department of Civil Engineering and Building Structures

University of Warmia and Mazury in Olsztyn

Institute of Hydroengineering of the Polish Academy of Sciences (IBW PAN) in Gdańsk

² Department of Civil Engineering and Building Structures

University of Warmia and Mazury in Olsztyn

Key words: sediment transport, grain-size distribution, bathymetry, hydrodynamic parameters, silting.

Abstract

A theoretical three-layer model of non-uniformly graded sediment transport has been used to analyse the silting up of water routes in the port of Łeba and Tolkmicko. Comparison of the results derived from model calculations with the measurements and dredging work data has demonstrated that the model is useful for prediction of the silting up extent as well as the distribution of grain-size fractions in sediments captured in water routes of ports, which are different in bathymetric as well as hydrodynamic parameters, and where sea bottom deposits are different in nature.

MODELOWANIE ZAPIASZCZANIA TORÓW WODNYCH PORTÓW W ŁEBIE I TOLKMICKU

Leszek M. Kaczmarek¹, Szymon Sawczyński²

¹ Katedra Budownictwa i Konstrukcji Budowlanych

Uniwersytet Warmińsko-Mazurski w Olsztynie

Instytut Budownictwa Wodnego PAN w Gdańsku

² Katedra Budownictwa i Konstrukcji Budowlanych

Uniwersytet Warmińsko-Mazurski w Olsztynie

Słowa kluczowe: transport osadów, rozkład granulometryczny, batymetria, parametry hydrodynamiczne, zapiaszczanie.

Abstrakt

Do analizy zapiaszczania torów wodnych portów w Łebie i Tolkmicku wykorzystano trójwarstwowy model teoretyczny transportu osadów niejednorodnych granulometrycznie. Porównanie wyników obliczeń z pomiarami i wielkościami robót czerpalnych wykazało przydatność modelu do predykcji zarówno wielkości zapiaszczania, jak i rozkładów uziarnienia osadów zatrzymywanych w torach portów o różnych reżimach batymetryczno-hydrodynamicznych oraz różnym charakterze osadów budujących dno morskie.

Introduction

Good prediction of the volume of sediments transported near various types of hydrotechnical facilities, both existing and planned ones, is essential to maintain the shoreline and man-made constructions. This paper presents a possibility of using a three-layer model of non-uniformly graded sediments, which for many years has been elaborated at the IBW PAN in Gdańsk by a team of researchers supervised by Leszek M. Kaczmarek, to solve specific engineering problems, using two ports, in Łeba and in Tolkmicko, as case studies. These issues have also been discussed in Master Degree theses (ZDUNEK 2006, BOŻOMAŃSKI 2007) written at the University of Warmia and Mazury in Olsztyn, under the supervision of L.M. Kaczmarek and J. Kaczmarek, respectively.

Methods

The three-layer model of non-uniformly graded sediment motion

The theoretical three-layer model has been used to analyse the silting up in water routes (KACZMAREK 1999, KACZMAREK, OSTROWSKI 2000, 2002). This model distinguishes the bedload layer, the transient (contact load) layer and the outer region, in which sediments are transported as suspension. The nature of interactions between water and sediments in each of these layers is different, which is why it is described with a different set of equations, folded at the contact between the layers so as to provide a complete theoretical description of the structure of sandy sediment transport.

For the mathematical modelling it has been assumed that all the fractions in the bedload layer move at identical velocity in the form of a dense water and ground mixture, and that sediments are not sorted out in this layer. Another assumption is that interactions between sediment fractions are so strong that finer fractions are retarded by coarser ones – as a result all fractions travel at

the same speed. Thus, in this layer simple totalling of transport tensions of particular fractions, treated as uniform sediment, is not valid.

The mathematical model has also accounted for the fact that the most intensive vertical sorting occurs by picking up sand grains in the contact layer near the sea bed. In the contact load layer, turbulent pulsations as well as chaotic collisions among grains cause very strong diversity in transport of particular fractions. Very close to the sea bed – in the sub-layer, where the sliding friction features strongly in the distribution of velocity of i^{th} fraction – there is very strong interaction between particular fractions caused by their mutual chaotic collisions. Further away from the sea bed, these interactions between fractions weaken. However, the concentration of the i^{th} fraction is big enough to suppress the turbulence, with the actual suppression strength depending on the diameter of grains d_i . It can therefore be expected that each i^{th} fraction, because of the mutual interactions, moves at its own velocity and is characterised by its own concentration.

The velocities and concentrations of coarser fractions calculated in the contact load layer are larger than the values these fractions would obtain, should the sea bottom be uniform and built of one corresponding fraction.

In the outer layer, above the contact load layer, no change in the grain-size distribution of the transported sediment is expected. The vertical distribution of sediment concentration in this layer is described with a power function.

Calculation procedure

The transformation of surface waves and sea currents in the marine shoreline zone has been calculated using the programme CROSMOR, whereas the transport of sediments has been analysed with the programme KLEPSYDRA, which takes advantage of the three-layer model of non-uniformly graded sediments.

CROSMOR is a software application developed at Utrecht University by a team headed by professor Leo van Rijn and dr Bart Grasmeijer. It allows the user to determine the transformation of surface waves in a cross-shore transect. The surface wave and sea current parameters obtained with this programme are used in the application KLEPSYDRA, prepared at the Institute of Hydroengineering of the Polish Academy of Sciences (IBW PAN) in Gdańsk, by a team supervised by L.M. Kaczmarek. This software package runs calculations of the intensity transport for each sediment fraction in the three layers, i.e. bedload, contact load and outer layer. The calculations are performed along the two edges of a water route, i.e. on the windward and leeward sides. Along the windward (updrift) side of an approach route, sediments are transported

during the wave crest phase in the bedload and contact load layers; along the leeward (downdrift) side, sediments are conveyed under the effect of the resultant current only during the trough wave phase in the bedload and contact load layers.

The data produced by the two programmes can be used to calculate the amount of sediment transported over a time period and to determine changes in the grain-size distribution of sediment captured in a water route. Knowing the figures, such as the values of transport intensity for each sediment fraction, in the bedload and contact load layers as well as in the outer region, where sediment is present as suspension, it is possible to determine the amounts of transported material along both edges of an approach route which is being silted up. The calculations must include the mutual location between the approach route, the cross-shore profile and the incident wave angle along the edges of the route.

Comparison of the calculations and measurements

The paper contains a comparison of the results of calculations of the mean annual grain-size distribution of sediments captured in the approach channels with the actual grain-size distributions of sediments sampled in these navigation channels near Łeba and Tolkmicko. In addition, the results of the modelling of mean annual volumes of silt deposited in the routes were compared with the actual size of dredging work completed in these routes. This means that a complex comparative analysis has been made, both in terms of grain-size distribution and the rate of silting up.

Such complex verification has been possible owing to the three-layer model of non-uniformly graded sediments.

Description of the analysed areas

Each of the ports (Łeba and Tolkmicko) has been selected for our analyses because of its unique location. The port in Łeba lies on the Middle Coast at the mouth of the Łeba River; the port in Tolkmicko is situated on the Vistula Lagoon. In general, both ports share the same problem, that is excessive silting up of their navigation channels. The approach routes to these ports are constantly silted up. Łeba port has a particularly difficult situation in this respect. Tolkmicko port is in a slightly different position, as it stands on a shallow closed water body, which adds to the difficult task of maintaining a sufficiently deep approach route.

Silting up analysis

Hydrodynamic parameters

The analyses included parameters of the seaward wind typical for each region. Next, the deep water wave parameters were added to these values as well as parameter of the shallow wave after transformation and sea currents. The wind conditions in Łeba were determined on the data for 1951-1978 (KACZMAREK et al., 1996, 1997).

The wind parameters necessary to calculate the wind wave on the Vistula Lagoon near Tolkmicko were found in the relevant references (ŁAZARENKO, MAJEWSKI 1975) and the data stored at the Port Office in Tolkmicko. The data were converted to mean annual values and then used for calculations (Krylov method) of the parameters of the wind wave.

The calculations were completed for four wind velocity classes (2.5 m/s, 7.5 m/s, 13 m/s and 18 m/s) blowing from five wind direction classes (N, NE, E, NW and W).

Bathymetry and sediments

Another set of the input data necessary for our analyses consisted in the bathymetric profile and grain-size composition of the sediments. The bathymetric data, illustrated in Figures 1 and 2, originated from the information provided by the Maritime Offices in Słupsk and Gdynia and the Maritime Institute in Gdańsk for two master degree theses (ZDUNEK 2006, BOŻOMAŃSKI 2007).

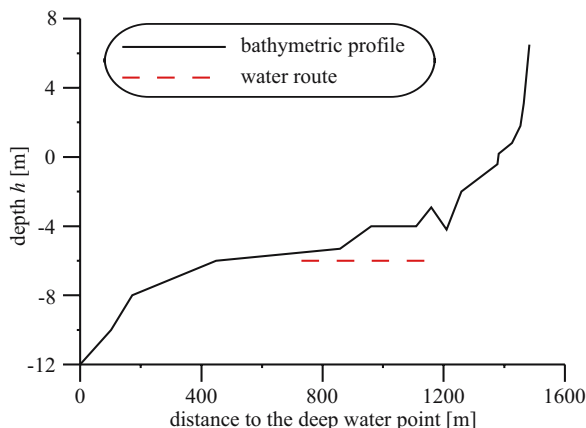


Fig. 1. Łeba – the bathymetric profile including the water route

For the calculations presented in this article, the grain-size distribution from a site designated as 'k10' was taken (Fig. 3). This is the distribution of the sediment sampled at the upper edge of the water route. Additionally, for comparison with the calculations, the results of sieve analysis of three sediment samples collected in 2003 inside the port channel, marked as no 1, 2 and 3, were used.

The grain-size distributions (Fig. 4) from Przebrno (nos 1 and 2) and Krynica Morska (nos 3 and 4) were used to calculate the mean annual grain-size distribution, which served as an input datum for the calculations run for Tolkicko Port.

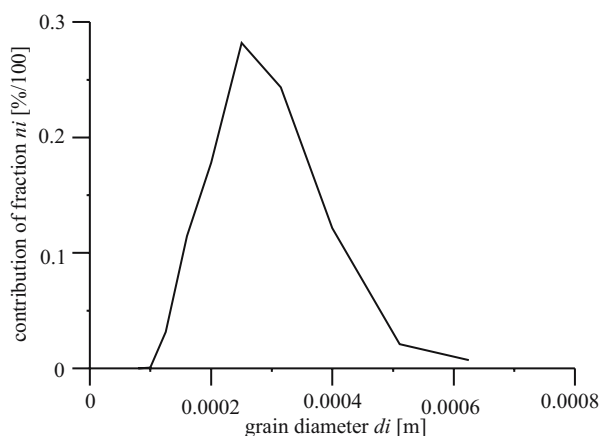


Fig. 3. Grain-size distribution of sediments in Łeba taken for the calculations

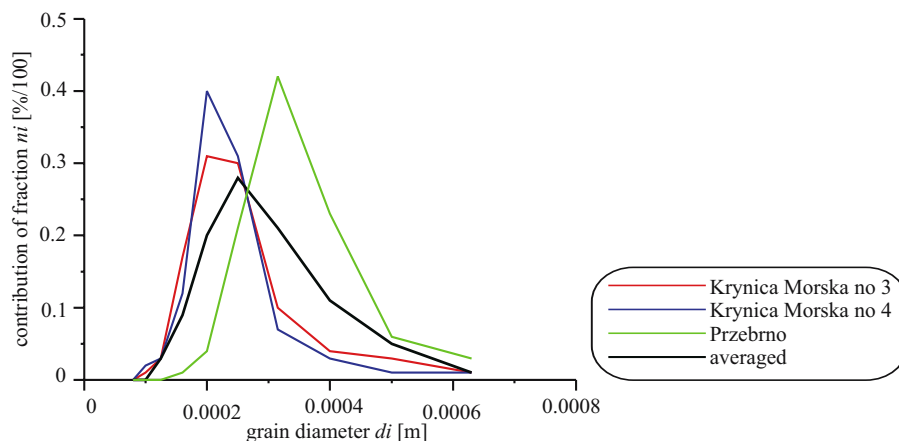


Fig. 4. Tolkicko – grain-size distribution of sediments

Łeba

This sub-section presents results of the calculations of sediment transport intensity and changes in the grain-size distribution of the sediments captured in different sites along the approach route in Łeba, on each of its sides, for various wave formation conditions. Figures 5 and 6 illustrate the results obtained under storm conditions. In addition, Figures 5 and 6 contain the results of the calculations of transformation of waves (H_{rms}) and valued (averaged over depth) of longshore and cross-shore currents, produced by the programme CROSMOR.

It is evident that under intensive wave formation conditions, the transformation of waves starts at the deep water limit and consequently the whole shoreline zone experiences very intensive sediment transport. Figures 5 and 6 indicate that under intensive wave formation conditions, suspended sediment transport (q_0) prevails over the transport of sediments in the bedload (q_b) and contact load (q_c) layer. The symbols $q_{c,G}$, $q_{b,G}$ are assigned to the intensity of sediment transport during the crest wave phase in the contact load and bedload layers, respectively. The symbols $q_{c,D}$, $q_{b,D}$ designate the intensity of transport of sediments during the trough wave phase in the contact load and bedload layers, respectively.

Based on the information contained in Figures 5 and 6 it can be seen that the grain-size distributions of the sediment silting up the approach route depend on the position of the edge (windward or leeward) of the route as well as on the direction and height of the incident wave.

On the windward side of the route edge, i.e. facing approaching waves, grain-size distributions imply that the sedimentation material is much smaller in size, dominated by the fine fractions. This suggests that there is a large percentage of suspended sediments, transported by the longshore current.

On the leeward side, the silting up of the route is much weaker and caused only by the motion of bedload sediments and sediments suspended just above the seabed during the returning wave phase. The transport of bedload sediments does not modify the grain-size distribution of sediments. Thus, the grain-size distribution of sediments in the water route by the leeward side of the water route remains hardly changed versus the sediments found along the leeward edge of the route.

It should be emphasized that a considerable contribution of suspended sediment transport changes the grain-size distribution in the water route as only small fractions are transported in the form of suspension by the longshore current. Another interesting fact is that on the windward side the grain-size distributions of sediments are bimodal, with the fine-grain fractions being clearly dominant. In contrast, on the leeward side, the distributions are unimodal and dominated by coarser fractions.

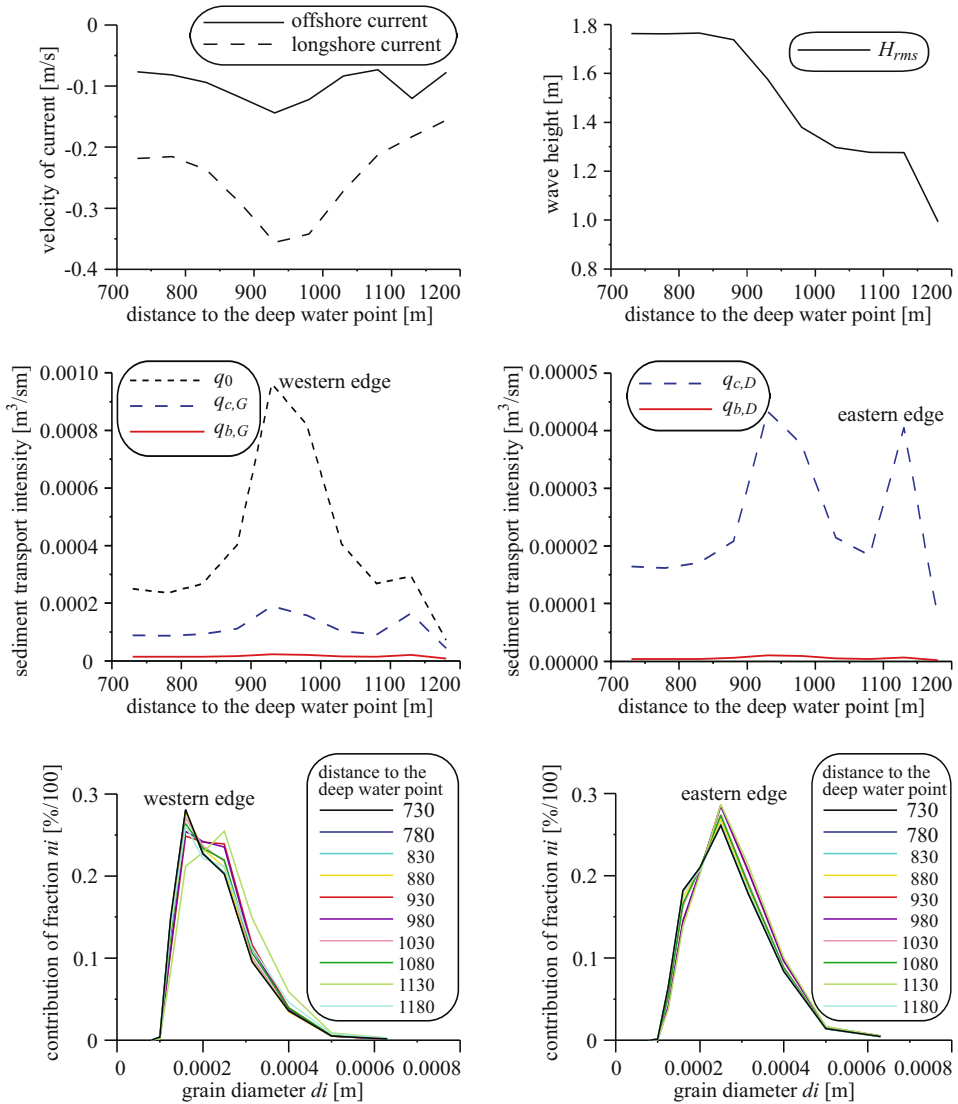


Fig. 5. Results of the calculations of wave formation, currents, sediment transport and grain-size distribution in the approach route in Leba for the NW wind velocity of 17 m/s

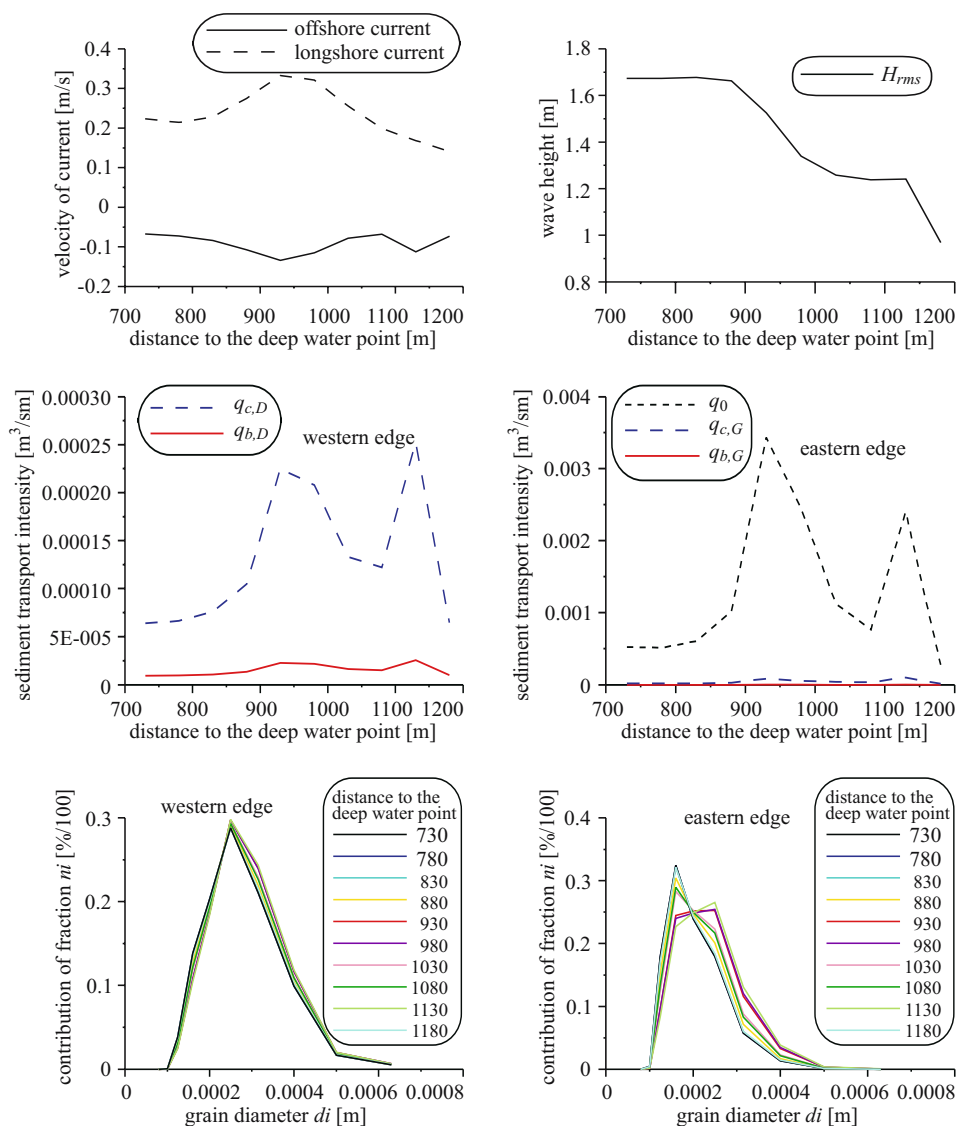


Fig. 6. Results of the calculations of wave formation, currents, sediment transport and grain-size distribution in the approach route in Łeba for the NE wind velocity of 17 m/s

Figure 7 shows the results of a comparison made between the calculations of the grain-size distributions of sediments silting up the water route in Łeba with the measurements carried out in 1998 and 2003. The agreement between these results is very good.

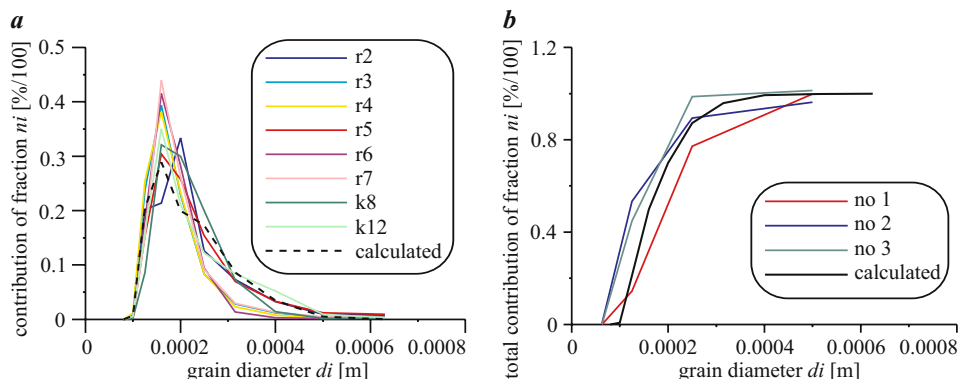


Fig. 7. Comparison of the results of modelling grain-size distribution of sediments silting up the water route in Łeba with the measurements of a) 1998, b) 2003

Tolkmicko

The results of the calculations of mean annual grain-size distributions along the length of the approach route and averaged over the transect of the route are shown in Figure 8.

In addition, Figure 8 presents the grain-size distribution averaged over the whole length of the route. It is evident that the calculated grain-size distributions are only slightly varied along the whole length of the channel. Figure 9 illustrates a comparison of the calculated mean annual grain-size distribution with the parameters obtained from Krynica Morska (Krynica 3 and 4). In addition, Fig. 9 shows the grain-size distribution which is an average distribution from the samples collected near Przebrno (1 and 2) and Krynica Morska (3 and 4). The average distribution was taken as an input distribution

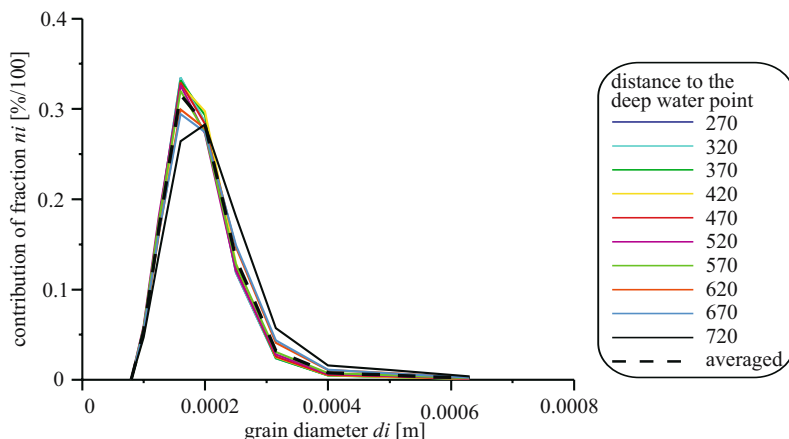


Fig. 8. Tolkmicko – calculated mean annual grain-size distributions in the approach route

for the calculations. The agreement between the calculations and measurements is good.

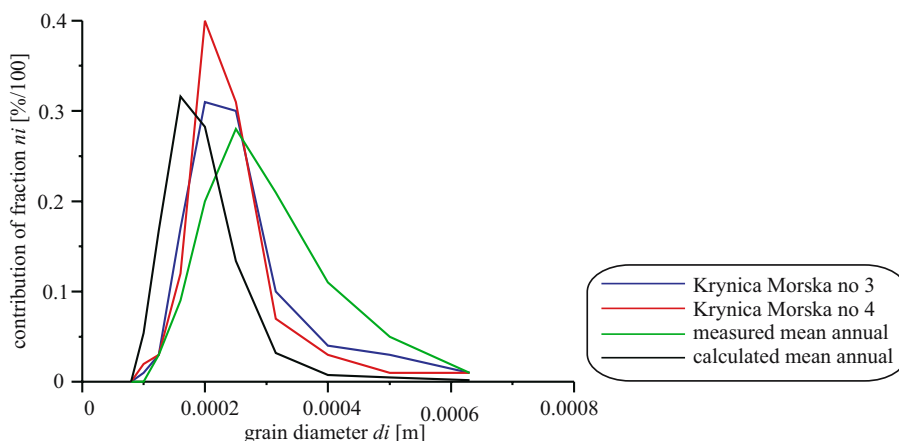


Fig. 9. Comparison of the calculated mean annual grain-size distribution with the measured grain-size distributions in Krynica Morska (nos 3 and 4)

Silting-up rate

Łeba

Figure 10 illustrates the extent of the dredging and silting works in the approach route of Łeba port. The data of 1915-1974 were found in the article by KACZMAREK et al. (1997), whereas the data of 2004-2005 were provided by the Maritime Office in Słupsk. The figure also contains the value of a mean annual silting-up of the approach route, which was calculated from the three-layer model of sediment transport. The agreement between the calculations and the empirical data seems to be very good.

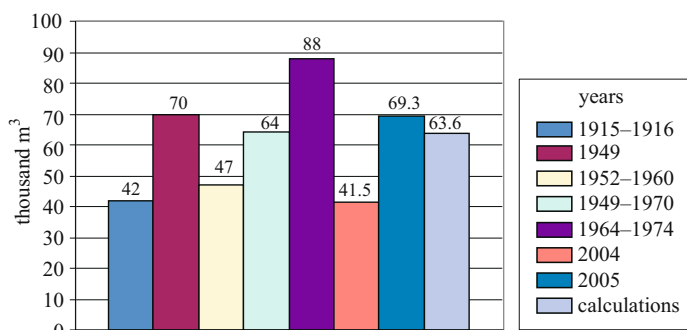


Fig. 10. Mean annual dredging work volume in the water route of Łeba port

Tolkmicko

Figure 11 contains a comparison of the results of calculations of a mean annual transport of debris halted in the approach route, depending on the grain-size distribution (e.g. for the distributions taken for the calculations from different sites in the Lagoon: Przebrno 1 and 2, Krynica Morska 3 and 4, and the averaged distribution for these sites) with the extent of the dredging works carried out in the approach route of Tolkmicko port in 2005.

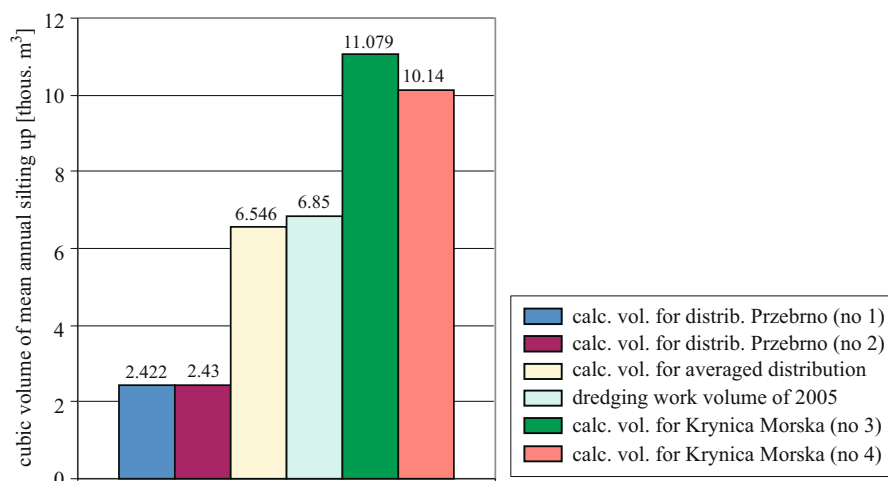


Fig. 11. Tolkmicko – comparison of the calculated mean annual cubic volumes of sediments and dredging work volume

The results shown in figures 9 and 11 demonstrate that the suggested theoretical model is good at depicting both grain-size distributions of sediments captured in the approach route of Tolkmicko port and the capacity of sediments silting up this navigation channel. Thus, the model can be recommended for use in engineering practice at closed shallow water bodies.

Summary

The paper deals with the hydrodynamic analysis of silting up of the approach routes in two ports: Łeba and Tolkmicko. For the purpose of such analysis, the three-layer model of non-uniformly graded sediment transport, developed for many years under the supervision of Leszek M. Kaczmarek at the IBW PAN in Gdańsk, has been applied. The article contains a comparison

of the calculations of mean annual grain-size distributions of sediments captured in the two water routes with the empirical data. Besides, the authors carried out a comparative analysis of the model determinations of mean annual silting up in these water routes with the actual extent of the dredging works carried out at Łeba and Tolkmicko. It has been demonstrated that the suggested three-layer model is suitable for prediction of both silting-up rate and grain-size distributions of sediments which settle down in water routes of ports different in bathymetric and hydrodynamic characteristics as well as seabed deposits.

The research results presented in this paper are a stage in the execution of a research and development grant number R0401703 on the hydrodynamic aspects of the plan to build a canal to the Vistula Lagoon.

References

- BOŻOMANSKI K. 2007. *Hydrodynamiczna ocena transportu rumowiska w Zalewie Wiślanym i zapiaszczania toru podejściowego do portu w Tolkmicku*. Praca magisterska. Uniwersytet Warmińsko-Mazurski, Olsztyn.
- KACZMAREK L.M., MIELCZARSKI A., NAGUSZEWSKI A., OSTROWSKI R., PRUSZAK Z., SKAJA M., SZMYTKIEWICZ M. 1996. *Badanie ruchu rumowiska w Porcie Łeba. Ocena przewidywanego wpływu projektowanej przebudowy układu falochronów na warunki zapiaszczania portu i na kształtowanie się brzegu*. Opracowanie wewnętrzne, IBW PAN, Gdańsk.
- KACZMAREK L.M., MIELCZARSKI A., OSTROWSKI R. 1997. *Zastosowanie nowego modelu transportu osadów do oceny zapiaszczania portowych torów podejściowych*. Inżynieria Morska i Geotechnika, 21: 113-117.
- KACZMAREK L.M. 1999. *Moveable Sea Bed Boundary Layer and Mechanics of Sediment Transport*. IBW PAN, Gdańsk, ISBN 83-85708-35-9.
- KACZMAREK L.M., OSTROWSKI R. 2000. *Wzdłużbrzegowy transport osadów morskich w świetle modelu mieszaniny wodno-gruntowej i danych terenowych*. Inżynieria Morska i Geotechnika, 3: 128-133.
- KACZMAREK L.M., OSTROWSKI R. 2002. *Modelling intensive near-bed sand transport under wave-current flow versus laboratory and field data*. Coastal Engineering, 45(1): pp. 1-18.
- ŁAZARENKO N.N., MAJEWSKI A. 1975. *Hydrometeorologiczny ustrój Zalewu Wiślanego*. Warszawa.
- ZDUNEK A. 2006. *Analiza hydrodynamiczna zapiaszczania toru podejściowego do portu Łeba w aspekcie projektowania budowli i optymalizacji prac pogłębiarskich*. Praca magisterska, Uniwersytet Warmińsko-Mazurski, Olsztyn.

Accepted for print 4.07.2008 r.

MODELLING OF THE SILTING UP OF NAVIGATION CHANNELS

Leszek M. Kaczmarek

Institute of Hydroengineering of the Polish Academy of Sciences (IBW PAN) in Gdańsk
Department of Civil Engineering and Building Structures
University of Warmia and Mazury in Olsztyn

Key words: transport of bedload and suspended sediments, grain size distribution, surface waving, sea currents, silting up of water routes.

Abstract

A mathematical model describing transport of non-uniformly graded sediments has been applied to analyzing the silting up of approach routes (navigation channels) leading to ports. This model distinguishes three layers in the movement of sediments, assuming that the vertical sorting occurs only in the process of picking up grains in the contact layer. It is also assumed that along the windward edge of the route sediments are transported in the bedload and contact layers during the wave crest phase and – as suspended sediments – in the outer region under the influence of the resultant current. On the leeward side sediments are transported only during the wave trough phase in the bedload and contact layer. The computations have demonstrated that the above model can be a useful tool for predicting both the rate and volume of sediments silting up navigation channels as well as grain-size distribution of sediments which fill up a water route.

MODELOWANIE PROCESÓW ZAPIASZCZANIA KANAŁÓW NAWIGACYJNYCH

Leszek M. Kaczmarek

Instytut Budownictwa Wodnego PAN w Gdańsku
Katedra Budownictwa i Konstrukcji Budowlanych
Uniwersytet Warmińsko-Mazurski w Olsztynie

Słowa kluczowe: transport osadów wleczonych i zawieszonych, rozkład granulometryczny, falowanie powierzchniowe, prądy morskie, zapiaszczanie torów wodnych.

Abstract

Model matematyczny transportu osadów niejednorodnych granulometrycznie zastosowano do analizy zapiaszczania torów podejściowych (kanałów nawigacyjnych) do portów. Wyszczególnia on trzy warstwy ruchu osadów, przy czym założono, że pionowe sortowanie odbywa się tylko w procesie

podrywania ziaren w warstwie kontaktowej. Zakłada się, że na krawędzi nawietrznej toru osady transportowane są w fazie grzbietu fali w warstwie wleczenia i kontaktowej oraz zewnętrznej – w formie zawieszonej – pod wpływem wypadkowego prądu. Na krawędzi zawiętrznej osady transportowane są tylko w fazie doliny fali w warstwie wleczenia i kontaktowej. Przeprowadzone obliczenia pokazują, że zastosowany model może być użytecznym narzędziem w predykcji zarówno wielkości i tempa zapiaszczania, jak i określaniu rozkładów granulometrycznych osadów wypełniających tor wodny.

Introduction

The mathematical model of sediment transport, which for years has been developed at the Institute of Hydroengineering of the Polish Academy of Sciences (IBW PAN) in Gdańsk, Poland, has been applied to analyze the rate and extent of silting up in approach routes to ports. A three-layer theoretical model (KACZMAREK 1999, KACZMAREK, OSTROWSKI 2000, 2002) has been used. This model distinguishes between the bedload layer, contact load (transient) layer and the outer region (Fig. 1). The nature of interactions between water

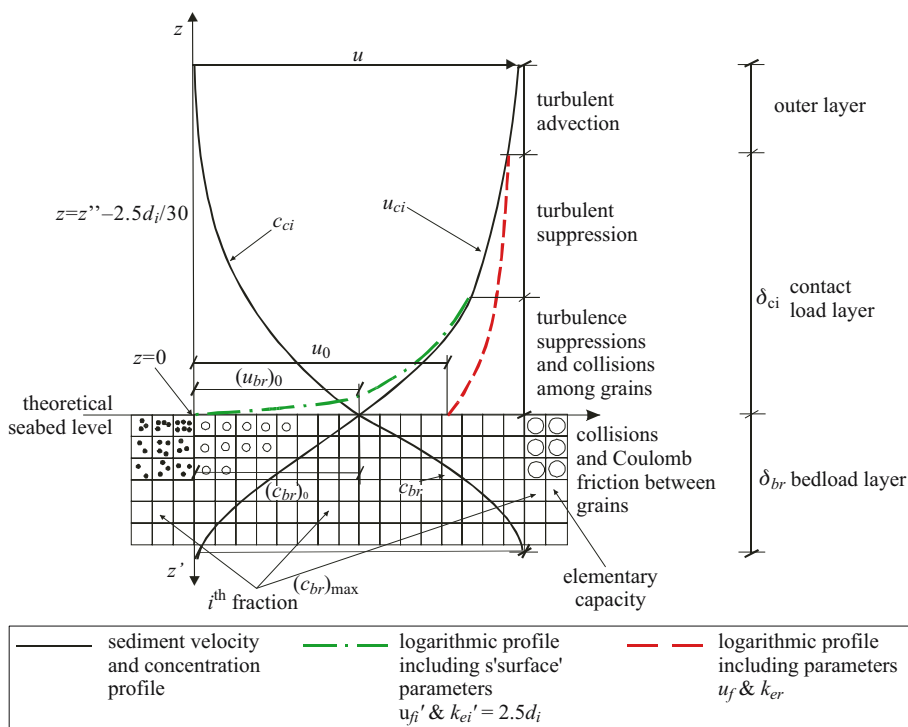


Fig. 1. Diagram of the three-layer momentum exchange model

and sediments is different in each of these layers, therefore they are described using different equations although at the contact of these layers the equations are folded, thus providing a complete theoretical description of the structure of sandy sediment transport.

In 1997, this model (in its simplified version albeit with a well-recognized bedload layer) was applied to analyze the silting-up of an approach route in Łeba port (KACZMAREK et al. 1996, KACZMAREK et al. 1997). The results were highly promising, although it needs to be recalled that at that stage of its development the model was constrained to descriptions of uniformly graded sediments.

However, in order to plan and carry out dredging and silting work, it seems necessary to have sound knowledge of mechanisms governing movements of non-uniformly graded sandy sediments and to be able to predict transport of each fraction as well as grain-size distribution of sediments which fill in a given approach route. Not infrequently, silt dredged from a navigation channel is used to strengthen shores near the harbour, in which case it is absolutely necessary to know the grain-size distribution of such silt, as it can be a futile and uneconomical effort to try and support the shores using sand which is too fine.

This paper relies on a three-layer mathematical model elaborated by KACZMAREK et al. (2004) and KACZMAREK and BIEGOWSKI (2006). This model enables description and prediction of non-uniformly graded shoreface debris movements.

Sediment transport model

For the mathematical modelling it has been assumed that all the fractions in the bedload layer move at identical velocity in the form of a dense mixture of water and soil, and that sediments in this layer are sorted. In addition, the model accounts for the fact that the most intensive vertical sorting occurs while grains are being picked up in the contact load layer above the sea bottom. Higher than this layer the grain-size distribution of sediments hardly changes.

Taking advantage of SAYED and SAVAGE'S dependencies (1983) for viscosity tensions and tensions caused by Coulomb friction, a set of equations has been obtained to describe the rate and concentration of sedimentation in the bedload layer, which can be presented as:

$$\alpha^0 \left(\frac{c_b - c_0}{c_m - c_b} \right) \sin \varphi \sin 2\psi + \mu_1 \left(\frac{\partial u_b}{\partial z} \right)^2 = \rho u_f^2 \quad (1)$$

$$\begin{aligned}
 \alpha^0 \left(\frac{c_b - c_0}{c_m - c_b} \right) (1 - \sin \phi \sin 2\psi) + (\mu_0 + \mu_2) \left(\frac{\partial u_b}{\partial z'} \right)^2 = \\
 = \left(\frac{\mu_0 + \mu_2}{\mu_1} \right) \Big|_{c=c_0} \rho u_f^2 + (\rho_s - \rho) g \int_0^{z'} c_b dz'
 \end{aligned} \tag{2}$$

The coefficients μ_0 , μ_1 and μ_2 are sediment concentration c functions, defined by the formulas

$$\frac{\mu_1}{\rho_s d^2} = \frac{0.03}{(c_m - c_b)^{1.5}} \tag{3}$$

$$\frac{\mu_0 + \mu_2}{\rho_s d^2} = \frac{0.02}{(c_m - c_b)^{1.75}} \tag{4}$$

where $c_m (= 0.53)$ is the maximum concentration of inert sediment, when grains closely adhere to one another; c_b is sediment concentration and u_b is the velocity of sediment motion in the bedload layer while c_0 is the sediment concentration at the theoretical seabed level; ($c_0 = 0.32$), $\alpha^0 / \rho_s g d = 1$, ϕ is a quasi-static inner friction angle $\psi = \frac{\pi}{4} - \frac{\phi}{2}$.

Because of strong interactions between grains of particular fractions in the bedload layer, it was assumed that all fraction moved at the same velocity [$u_{br}(z', t)$] and had the same concentration [$c_{br}(z', t)$] at a given level z' . From this assumption it follows that sediment is not sorted in the bedload layer and it is possible to describe sediment transport using the representative diameter ($d_r = d_{50}$). Thus, taking the representative diameter d_r the effective roughness $k_e = k_{er}$ is derived from the formula suggested by KACZMAREK (1999) and then, from the integral model developed by FREDSSØE (1984), temporary friction velocities $u_f(t)$ on the sea bed surface are obtained. From equations (1) ÷ (4) temporary values of velocity $u_{br}(z', t)$ and concentration $c_{br}(z', t)$ of sediments in the bedload layer of the thickness δb_r are obtained. Noteworthy is the fact that the above model removes from the bedload layer the largest simplification used so far when modelling non-uniformly graded sediment motions. The present model assumes that interactions between sediment fractions are so strong that as a result smaller fractions are retarded by larger ones and that means that all

the fractions travel at identical speed. Thus, simple totalling of transport intensities of particular fractions, treated as uniform sediment, does not apply to sediment motions in the bedload layer. This conclusion is in accord with many laboratory observations (cf. HASSAN et al. 2001).

In the contact load layer, numerous turbulent pulsations and chaotic collisions among grains cause large variation in the transport of particular sediment fractions. Very close to the sea bottom – in the sub-layer where the distribution of velocities of the i^{th} fraction of sediments evidently reveal the occurrence of sliding velocity u_{br} – there is very strong interaction between the fractions, evoked by mutual chaotic collisions. Further away from the sea bottom, these interactions between the fractions weaken. However, the concentration of the i^{th} fraction is big enough to suppress turbulences, and this effect is dependent on the grain diameter d_i . Thus, it can be expected that each i^{th} fraction, owing to mutual interactions, moves at its own speed $u_{ci}(z'', t)$ and is characterised by its own concentration $c_{ci}(z'', t)$. In this model, temporary vertical velocity and concentration distributions are derived from the equations suggested by KACZMAREK (1999), knowing the friction velocity $u_{\tau i}'(t)$, which is variable during the surface wave period:

$$\left[\frac{3}{2} \left(\alpha_s \frac{d}{w_s} \frac{\partial u_c}{\partial z''} \frac{2}{3} \frac{s + c_M}{c_D} + \beta_s \right)^2 d^2 c_c^2 (s + c_M) + l^2 \right] \left(\frac{\partial u_c}{\partial z''} \right)^2 = u_{\tau i}'^2(t) \quad (5)$$

$$\left[3 \left(\alpha_s \frac{d}{w_s} \frac{\partial u_c}{\partial z''} \frac{2}{3} \frac{s + c_M}{c_D} + \beta_s \right)^2 d^2 \frac{du_c}{dz''} c_c + l^2 \frac{du_c}{dz''} \right] \frac{dc_c}{dz''} = -w_s c_c \quad (6)$$

where c_D is the resistance coefficient and c_M is the added mass coefficient. DEIGAARD (1993) assumed that $(s + c_M) = 3.0$, and $c_D = 1.0$. The proportionality coefficients α_s and β_s remain unknown and have to be determined by the model calibration; l is the mixing length expressed as $l = \kappa z'' = 0.4z''$.

The value $u_{\tau i}'(t)$ is calculated from FREDSTØE'S integral model (1984), assuming that the surface height of roughness k'_{ei} is determined from the equation $k'_{ei} = 2.5d_i/30$. The boundary conditions for all the fractions are the same:

$$u_{ci}(z'' = 2.5d_i / 30, t) = u_{br}(z' = 0, t) \quad (7)$$

$$c_{ci}(z'' = 2.5d_i / 30, t) = c_{br}(z' = 0, t) = 0.32 \quad (8)$$

The topmost limit of the contact load layer – common for all the fractions (δ_{cr}) – is determined using FREDSTØE'S integral model (1984) including the

effective surface roughness determined for the representative diameter $k'_{er} = 2.5d_r = 2.5d_{50}$. As has been demonstrated by KACZMAREK (1999) this thickness can be expressed by the dependence $\delta_{cr} = \delta_1'/2$, where δ_1' represents the wall adjacent thickness (found from the solution suggested by FREDSE (1994) for $k'_{er} = 2.5d_r = 2.5d_{50}$), at the moment of the maximum (during the wave period) orbital velocity at the sea bottom.

It should be noticed here that in the suggested model the velocities and concentrations of rougher fractions are larger than the values these fractions would obtain should the sea bed be uniform, consisting of just one corresponding fraction. This increase in velocities in a mixture results from mutual interactions between the fractions, where rougher fractions are accelerated by finer grains. This finding agrees with laboratory observations (cf. DE MEIJER et al. 2002), which prove that larger fractions of sediments are transported more intensively in a non-uniform mixture than in a uniformly graded sediment.

Recapitulating, it needs to be stressed that simple aggregation of stresses occurring in the transport of all fractions, treated as uniform sediment, is not applicable to the contact load layer model (same as the bedload layer). Thus, the contribution of the i^{th} fraction to the transport of mixture $n_i q_{ci}$ does not equal an 'independent' transport $n_i q_i$, that is $n_i q_i \neq n_i q_{ci}$.

In the outer layer, due to the adopted transport model, the grain-size distribution of the transported sediment does not alter. The grain-size distribution of suspended sediment

$$c(z) = c_z(z = \delta_{cr}) \left(\frac{z}{\delta_{cr}} \right)^{-\alpha_1} \quad (9)$$

is dependent exclusively on the grain-size distribution at the reference level, i.e.

$$c_z(z = \delta_{cr}) = \bar{c}_z(z = \delta_{cr}) = \sum_{i=1}^N [\bar{c}_{ci}(z = \delta_{cr}) n_i] \quad (10)$$

where:

$$\bar{c}_{ci}(z = \delta_{cr}) = \frac{1}{T} \int_0^T c_{ci}(z = \delta_{cr}, t) dt \quad (11)$$

BIEGOWSKI (2006) demonstrated that the power function exponent is $\alpha_1 = 0.6$.

Therefore, including the assumptions pertaining to flows of sediments, the following equations can be suggested to describe the resultant (over the wave period) transport of non-uniformly graded sediments:

$$\begin{aligned}
q_{net} &= \sum_{i=1}^N n_i \bar{q}_{1i} - \sum_{i=1}^N n_i \bar{q}_{2i} = \\
&= \sum_{i=n}^N n_i \frac{1}{T} \int_0^T \left(\int_0^{\delta_{br}} u_{br}(z', t) c_{br}(z', t) dz' \right) dt + \\
&+ \sum_{i=n}^N n_i \frac{1}{T} \int_0^T \left(\int_0^{\delta_{1/2} + 2.5d_i/30} u_{ci}(z'', t) c_{ci}(z'', t) dz'' \right) dt - \\
&- \sum_{i=1}^N n_i \int_{\delta_{1/2}}^{h_i} u_z(z) c_z(z) dz = \tag{12} \\
&= \frac{1}{T} \int_0^T \left(\int_0^{\delta_{br}} u_{br}(z', t) c_{br}(z', t) dz' \right) dt + \\
&+ \sum_{i=n}^N n_i \frac{1}{T} \int_0^T \left(\int_0^{\delta_{1/2} + 2.5d_i/30} u_{ci}(z'', t) c_{ci}(z'', t) dz'' \right) dt - \\
&- \int_{\delta_{1/2}}^{h_i} u_z(z) c_z(z) dz
\end{aligned}$$

where h_i is the height from the sea bed to the wave trough level while u_z is the value of the resultant of the cross-shore and longshore currents.

By including to the first two components of equation (12) temporary values of velocities and concentrations of sediments for the crest and trough wave respectively, the average intensity of sediment transport in the bedload layer during the wave period and in the contact load layer during the wave crest and trough can be described.

Computation procedure

For calculating the transformations of wave formation and currents, a procedure based on the CROSMOR software was suggested. The software package KLEPSYDRA, which uses the three-layer model of non-uniformly graded sediment motions and is described by equations (1) ÷ (12) was applied to calculate sediment transport values.

CROSMOR, which has been elaborated at Utrecht University by a team of researchers supervised by professor Leo van Rijn and dr Bart Grasmeijer, allows the determination of surface wave transformation in a shore cross-section profile. The transformation is described by several parameters, of

which the major ones are: the mean-square average height (H_{rms}), incident wave angle (α) (Fig. 2) and depth-averaged cross-shore and longshore velocities.

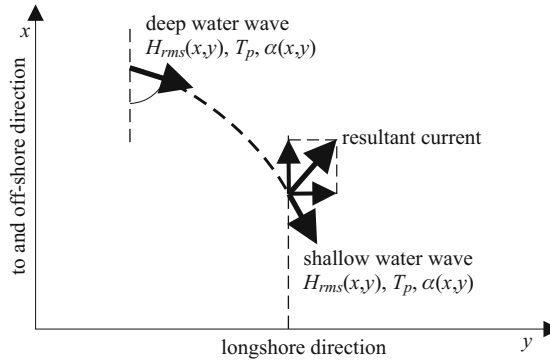


Fig. 2. Wave transformation pattern

The parameters for wave and current formation obtained from CROSMOR are then fed to the software programme KLEPSYDRA, elaborated at the Institute of Hydroengineering of the Polish Academy of Sciences (IBW PAN) in Gdańsk by a team headed by Leszek Kaczmarek. Based on the equations (1) ÷ (12) this programme performs calculations of the transport intensity for each fraction in the three layers, i.e. bedload, contact load and outer layers. The calculations are carried out along the two edges of an approach route, i.e. the windward and leeward sides of the channel (cf. Fig. 3). It is assumed that each wave characterised by the parameters H_{rms} and T_p can be described by Stokes second approximation, with a heightened crest and flattened trough. Near the sea shorelines, sediment transport is most often described using the above description of waves (cf. KACZMAREK 1999).

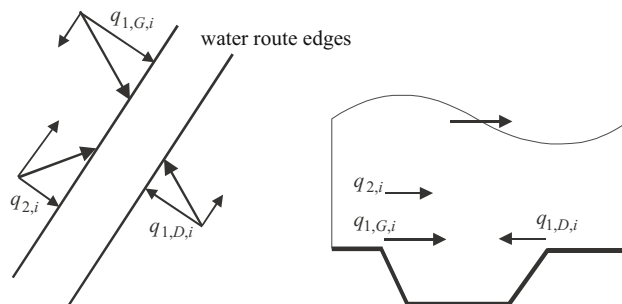


Fig. 3. Diagram of the i th sediment fraction transport intensity at the edges of a water route in the crest (G) and trough (D) wave phase

Having performed the calculations, the following are obtained:

- transport intensity of the i^{th} fraction in the bedload layer during the wave crest phase ($q_{b,G,i}$),
- transport intensity of the i^{th} fraction in the bedload layer during the wave trough phase ($q_{b,D,i}$),
- transport intensity the i^{th} fraction in the contact load layer during the wave crest phase ($q_{c,G,i}$),
- transport intensity the i^{th} fraction in the contact load layer during the wave trough phase ($q_{c,D,i}$),
- transport intensity of the i^{th} fraction during the wave crest phase ($q_{1,G,i}$)

$$q_{1,G,i} = q_{b,G,i} + q_{c,G,i} \quad (13)$$

- transport intensity of the i^{th} fraction during the wave trough phase ($q_{1,D,i}$)

$$q_{1,D,i} = q_{b,D,i} + q_{c,D,i} \quad (14)$$

- transport intensity of the i^{th} fraction of sediments suspended under the influence of the resultant (cross-shore and longshore) current in the outer layer ($q_{2,i}$).

As illustrated in Figure 3, at the windward (updrift) edge of the approach route, the sediments are conveyed during the wave crest phase in the bedload and contact load layers and in the outer layer they are transported by the resultant current. On the leeward (downdrift) edge, the sediments are transported only during the wave trough phase in the bedload and contact load layers.

The above results are applied to calculations of volumes of sediment transported over periods of time and determinations of grain-size composition of the sediment captured in a navigation channel. Knowing these results, i.e. the values of transport intensity for each sediment fraction both in the bedload, contact load and outer layers, with the sediment being suspended in the latter layer, it is possible to determine quantities of material carried along both edges of a water route. The calculations should include such factors as the mutual location of the approach route, the shore cross-section profile and the incident wave angle to the shoreline along the edge of the water route.

Changes in the grain-size composition of sediment halted in a water route on its windward side are expressed by the equation:

$$n_{i,naw.} = \frac{q_{1,G,i} + q_{2,i}}{\sum_i (q_{1,G,i} + q_{2,i})} = \frac{q_{1,G,i} + q_{2,i}}{q_{1,G} + q_2} \quad (15)$$

By analogy, for the leeward side, the following equation is valid;

$$n_{i,zaw.} = \frac{q_{1,D,i}}{\sum_i q_{1,D,i}} \quad (16)$$

The quantities and grain-size distribution of sediments which silt up both sides of a water route at a length of L over a time interval t can be calculated from the formulas:

$$Q = \sum_i (q_{1,G,i} + q_{2,i} + q_{1,D,i}) \cdot t \cdot L \quad (17)$$

$$n_i = \frac{Q_i}{Q}$$

Computations: a case study

In order to analyze the effect of grain-size distribution on the silting up of a water route, case computations have been performed for the approach route to Łeba port. In the initial stage, the effect of one parameter only, i.e. d_{50} , was analyzed. It was therefore assumed that the bottom sediments are perfectly sorted out and consist of just one fraction measuring d_{50} in diameter. The calculations of the mean annual silting up were done for two grain diameters: $d_{50} = 0.2$ mm and $d_{50} = 0.25$ mm. The following volumes of silting were obtained: for $d_{50} = 0.2$ mm $\rightarrow Q = 74$ thousand m³/year and for $d_{50} = 0.25$ mm $\rightarrow Q = 40$ thousand m³/year.

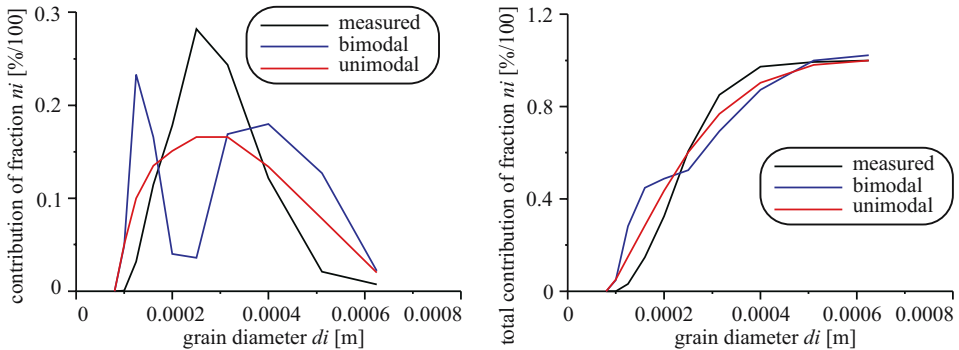


Fig. 4. Grain-size distributions taken for the calculations

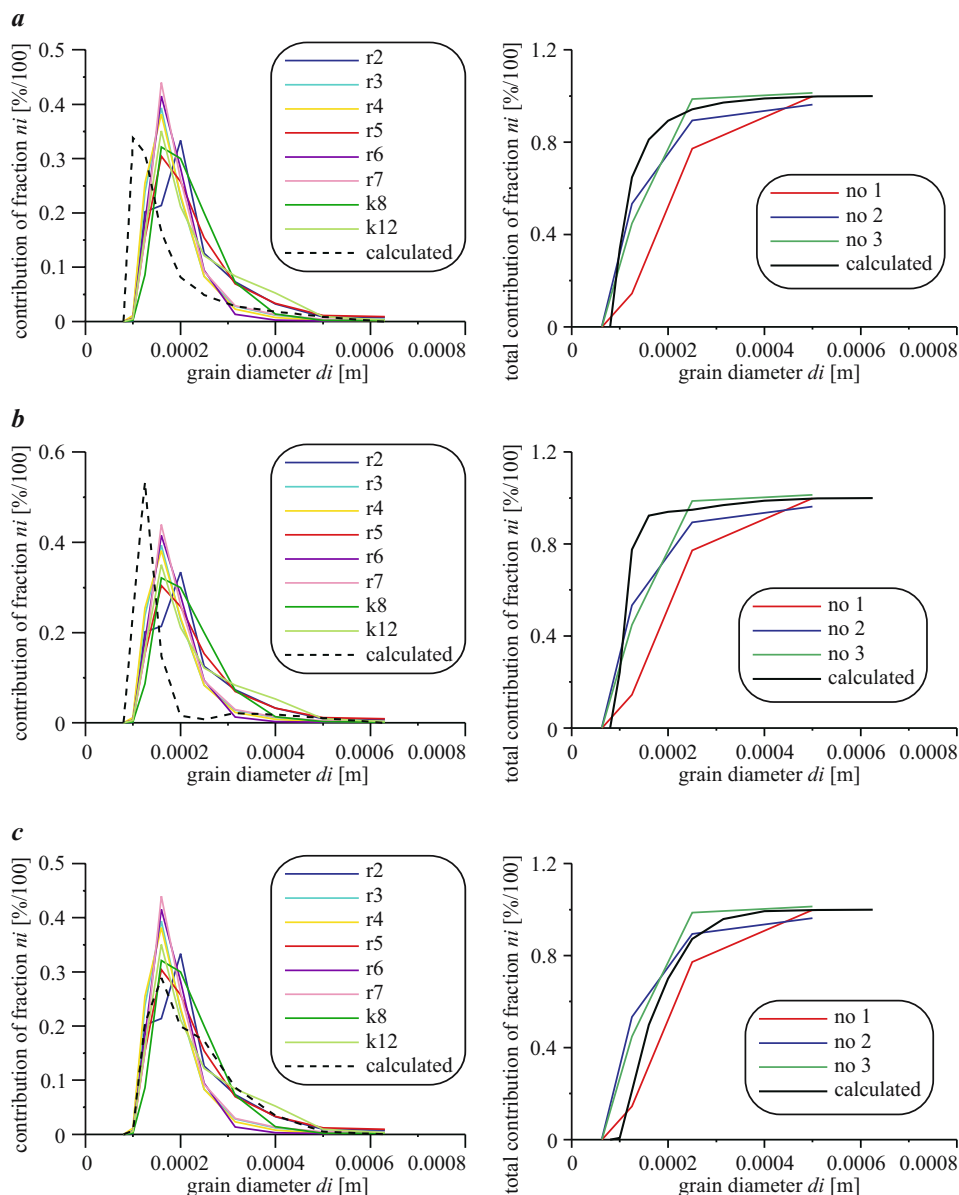


Fig. 5. Comparison of the measurements with the modelling of grain-size distribution of sediments silting up a water route for a) unimodal, b) bimodal, c) measured distribution (r2-r7, k8, k12 – designations of surface sediment samples taken from the approach route in Łeba)

The second stage comprised an analysis of the influence of the shape of grain-size distribution on the volume of mean annual silting of this approach route. The calculations involved the grain-size distribution patterns which differed in the shape but had a constant value of d_{50} . The grain-size distributions taken for these calculations are shown in Figure 4 against the background of the grain-size distribution measured along the edge of the route and used for the calculations presented in this paper. The following values of the mean annual silting up of the water route have been obtained: for a bimodal distribution with a significant mode within the fine-grained fractions $Q = 170$ thousand m^3/year ; for a unimodal distribution $Q = 126$ thousand m^3/year ; for the distribution measured along the edge of the route $Q = 63,609 \text{ m}^3/\text{year}$. For comparison, the dredging and silting work in 2005 removed 69,300 m^3/year (the data given by the Maritime Office in Słupsk).

As seen from the above, increased contribution of fine fractions, even at the constant value d_{50} , has a considerable influence on the silting up of a water route. Figure 5 illustrates a comparison between the computed results for grain-size distribution of sediments silting up the route as uni- and bimodal calculations and these measured along the edge of the water route. Very good agreement was obtained between the computations and the measurements of the grain-size distribution measured at the edge of the water route. It is evident that the calculated grain-size distributions for uni- and bimodal distribution models are considerably different from those measured in the water route.

To recapitulate, it should be emphasized that knowledge of only one parameter, i.e. d_{50} may not suffice for a reliable evaluation of sediment transport and analysis of silting up of water routes. Apart from the value of d_{50} , the shape of grain-size distribution is another important component. The meaning of this element becomes ever more important as the contribution of fine-grained fractions increases.

Summary

The aim of this paper has been to describe a model of non-uniformly graded sediment transport and to present how this model can be helpful in describing the process of silting up of navigation channels.

The mathematical model has been presented in the form of a set of numerical algorithms. The calculations that have been executed show that it is possible to predict the amounts of transported sediments of different grain size and to assess the transport intensity of particular fractions. Consequently, it is possible to detect the grain-size distributions of the sediments which fill up an

approach route to a port. Such information can be used to plan and carry out dredging and silting work, which is associated with artificial maintaining of seashores. The material picked up from water routes as a result of dredging is used to support the shores near ports, which means that it is essential to have good knowledge of its grain-size distribution.

The analysis of the effect of grain-size distribution on the silting up of a water route has revealed that in order to be able to successfully assess the rate of silting up it is not enough to know the parameter d_{50} . Another essential factor is the grain-size distribution shape. Knowing this component becomes even more important when sediments contain large proportions of fine sands.

The research results presented in this paper are a stage in the execution of a research and development grant number R0401703 on the hydrodynamic aspects of the plan to build a canal to the Vistula Lagoon.

References

- BIEGOWSKI J. 2006. *Dynamika osadów morskich o niejednorodnym uziarnieniu w świetle teorii i eksperymentu*. Praca doktorska, IBW PAN.
- DEIGAARD R. 1993. *Modelling of sheet flow: dispersion stresses vs. the diffusion concept*. Prog. Rep., 74, Inst. Hydrodyn. and Hydraulic Eng., Tech. Univ. Denmark, pp. 65-81.
- DE MEIJER R.J., BOSBOOM J., CLOIN B., KATOPODI I., KITOU N., KOOMANS R.L., MANSO F. 2002. *Gradation effects in sediment transport*. Coastal Engineering, 47: 179-210.
- FREDSOE J. 1984. *Turbulent boundary layer in combined wave-current motion*. J. Hydraulic Eng., ASCE, Vol. 110, No. HY8: 1103-1120.
- HASSAN W.N., KROEKENSTOEL D.K., RIBBERINK J.S. 2001. *Size-gradation effect on sand transport rates under oscillatory sheet-flows*. Proc. Coastal Dynamics '01, ASCE, Reston VA, pp. 928-937.
- KACZMAREK L.M., MIELCZARSKI A., NAGUSZEWSKI A., OSTROWSKI R., PRUSZAK Z., SKAJA M., SZMYTKIEWICZ M. 1996. *Badanie ruchu rumowiska w Porcie Łeba. Ocena przewidywanego wpływu projektowanej przebudowy układu falochronów na warunki zapiaszczania portu i na kształtowanie się brzegu*. Opracowanie wewnętrzne, IBW PAN, Gdańsk.
- KACZMAREK L.M., MIELCZARSKI A., OSTROWSKI R. 1997. *Zastosowanie nowego modelu transportu osadów do oceny zapiaszczania portowych torów podejściowych*. Inżynieria Morska i Geotechnika, 21: 113-117.
- KACZMAREK L.M. 1999. *Moveable Sea Bed Boundary Layer and Mechanics of Sediment Transport*. IBW PAN, Gdańsk.
- KACZMAREK L.M., OSTROWSKI R. 2000. *Wzdłużbrzegowy transport osadów morskich w świetle modelu mieszaniny wodno-gruntowej i danych terenowych*. Inżynieria Morska i Geotechnika, 3: 128-133.
- KACZMAREK L.M., R. OSTROWSKI 2002. *Modelling intensive near-bed sand transport under wave-current flow versus laboratory and field data*. Coastal Engineering, 45(1): 1-18.
- KACZMAREK L.M., BIEGOWSKI J., OSTROWSKI R. 2004. *Modelling cross-shore intensive sand transport and changes of grain size distribution versus field data*. Coastal Engineering, 51: 501-529.
- KACZMAREK L.M., BIEGOWSKI J. 2006. *Modelowanie segregacji osadów wzdłuż profilu poprzecznego brzegu w porównaniu z pomiarami w naturze*. Inżynieria Morska i Geotechnika, 2: 79-87.
- SAYED M., SAVAGE S.B. 1983. *Rapid gravity flow of cohesionless granular materials down inclined chutes*. J. Applied Mathematics and Physics (ZAMP), 34: 84-100.
- ZDUNEK A. 2006. *Analiza hydrodynamiczna zapiaszczania toru podejściowego do portu Łeba w aspekcie projektowania budowy i optymalizacji prac pogłębiarskich*. Praca magisterska, Uniwersytet Warmińsko-Mazurski, Olsztyn.

INFLUENCE OF AIR ENTRAPMENT ON FLOOD EMBANKMENT FAILURE MECHANISM – MODEL TESTS

Piotr Bogacz¹, Jarosława Kaczmarek¹, Danuta Leśniewska²

¹ Department of Civil Engineering and Building Structures
University of Warmia and Mazury in Olsztyn

² Institute of Hydro-Engineering, Polish Academy of Sciences, Gdansk
Koszalin University of Technology, Koszalin

Key words: flood embankment, air trapping, failure mechanism.

Abstract

The paper describes model tests on flood embankments, performed within the frame of EC 6th Framework Integrated Project FLOODsite (LEŚNIEWSKA et al. 2007). It is focussed mainly on presenting physical phenomena observed during the tests and related to air entrapment within embankment body and its subsequent release. The most important conclusion derived from recent tests is the existence of clear relationship between air entrapment and release and failure of internal embankment structure. Primary results of deformation of the embankment with a help of PIV analysis are also presented in the paper, showing air trapping influence on the embankment global failure mechanism.

WPŁYW ZAMYKANIA POWIETRZA NA MECHANIZM ZNISZCZENIA WAŁU PRZECIWPOWODZIOWEGO – BADANIA MODELOWE

Piotr Bogacz¹, Jarosława Kaczmarek¹, Danuta Leśniewska²

¹ Katedra Budownictwa i Konstrukcji Budowlanych
Uniwersytet Warmińsko-Mazurski w Olsztynie

² Instytut Budownictwa Wodnego PAN w Gdańsku,
Politechnika Koszalińska

Słowa kluczowe: wały przeciwpowodziowe, zamykanie powietrza, mechanizm zniszczenia.

Abstrakt

Praca zawiera wyniki badań modelowych wału przeciwpowodziowego, przeprowadzonych w ramach zintegrowanego projektu 6 PR UE FLOODsite (LEŚNIEWSKA i in. 2007). Zaprezentowano

zjawisko fizyczne zaobserwowane w trakcie badań, związane ze zjawiskiem zamykania i uwalniania powietrza w korpusie wału. Najważniejszym wnioskiem wynikającym z dotychczasowych badań jest wyraźny związek między zamykaniem i uwalnianiem powietrza a niszczeniem wewnętrznej struktury wału. W pracy przedstawiono również wyniki wstępnej analizy przebiegu deformacji wału metodą PIV, która pozwoliła na zbadanie wpływu zamykania powietrza na uaktywnienie się globalnego mechanizmu zniszczenia wału.

Introduction

Flood embankments are very important from a safety point of view. They are mainly the earth structures and as such are intensively studied by soil scientists and engineers for many years. The history of flood embankments is quite long – in spite of this fact mechanisms of their internal structure failure and possible reasons of activating these mechanisms are still not recognised properly.

European Commission, within the framework of FLOODsite Integrated Project (2004-2009), addressed flood problems in a global way. One of the particular contributions to this project is the influence of air entrapped within a flood embankment on its failure mechanism. This particular problem is investigated from 2004 by common research team of Institute of Hydro-Engineering PAS in Gdańsk and University of Warmia and Mazury Civil Engineering Division. Within the frame of this cooperation a series of model tests were performed in Institute of Hydro-Engineering laboratory. The results of the tests are presented in this paper.

Test apparatus

The overall view of the test apparatus for model embankments is presented in Figure 1. It consists of the test box 200 cm long, 100 cm high and 4.5 cm wide, equipped with two transparent perplex walls, overflow device, gravel filter, vertically moving set of hoppers, enabling to form a model by sand pouring, pressure gauges mounted in the front perplex wall and connected to a computer recording system and water supply system (including rain generator).

The tests were recorded using digital cameras: SONY CYBERSHOT (2560 x 1920 pixels), HP PhotoSmart C850 (2272 x 1712 pixels) and PENTAX Optio T10, 2816 x 2112 pixels). During each test one of the cameras, named Camera 1, was covering the whole area of the test box (Fig. 2.), the other one (Camera 2) was located closer to the model to catch the details of deformation and produce a picture suitable for later image analysis (PIV).

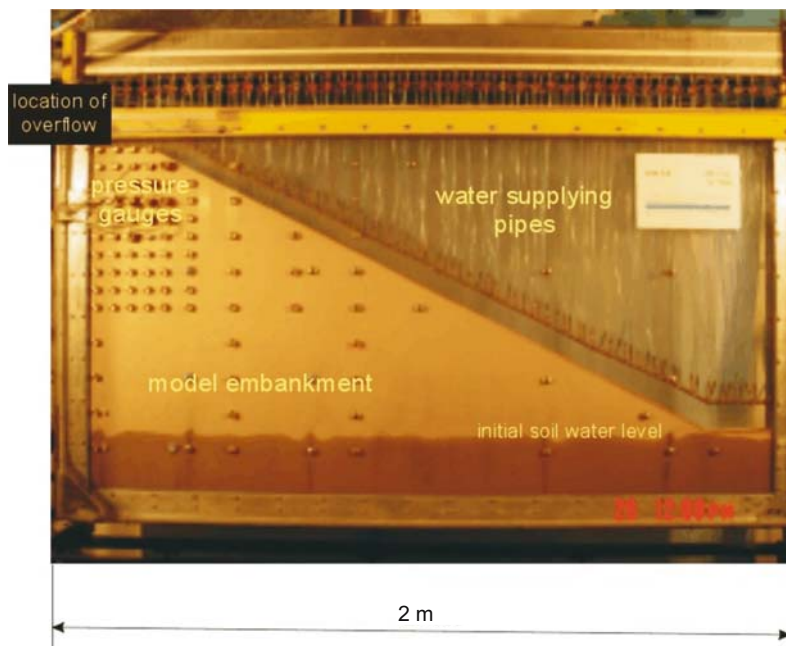


Fig. 1. Model embankment in the test box

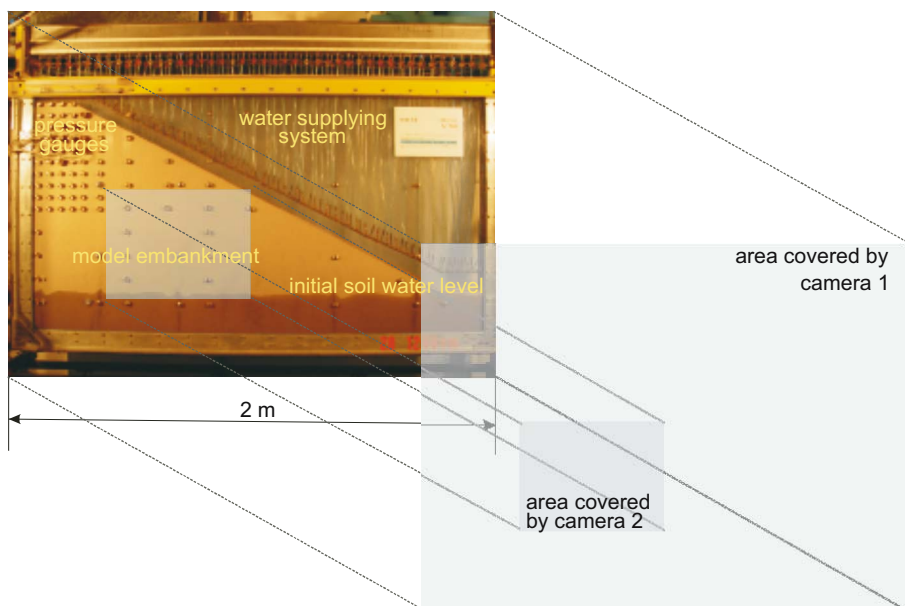


Fig. 2. Areas of the test box covered by Camera 1 and Camera 2

Sand used to build the embankment models was natural beach sand from Lubiatoŵo – a village placed 70 km north west from Gdańsk, at the open sea. It was a fine sand, characterised by $d_{50} = 0.25$ mm, well sorted. Results of sieve analysis made for this sand is presented in Table 1. Its water conductivity is $k_s = 0.016$ cm/s (ABO ELELA 1996), its initial moisture content 0.1% for all the tests performed. Sand built in a model was mostly in a dense state, characterised by average unit weight equal to 17.0 kN/m³ and internal friction angle equal to 34° .

Table 1

Sieve analysis for Lubiatoŵo sand

Grain diameter (mm)	Sand fraction (%)	Summa (%)
0.50	0.072	0.072
0.40	0.684	0.756
0.315	9.328	10.084
0.25	28.060	38.144
0.20	28.360	66.504
0.16	26.224	92.728
0.10	6.940	99.668
0.08	0.272	99.940
< 0.08	0.060	100.000

Model embankments were formed by sand pouring (Fig. 3) in the following steps:

1. Installing and calibrating the pressure gauges.
2. Preparing proper amounts of sand to fill in 20 containers in 4 hoppers placed above the test box.
3. Pouring sand from hoppers to obtain the embankment model built of dense sand (Fig. 3).
4. Correction of the model profile with a help of special vacuum cleaner (if necessary).
5. Setting initial water table (Fig. 4).

Method of forming an embankment model by sand rain consists in pouring sand from hoppers from constant height (equal to 0.7 m in case of the tests presented in this paper), what can be achieved by vertical movement of the set of hoppers with constant speed. It was not possible to pour sand evenly in horizontal layers. The sand flow was sometimes turbulent, mainly due to apparent electric charge of sand grains, causing horizontal deviation of gravitational sand flow, what resulted in “waved” soil surface, far from horizontal. This effect was additionally strengthened by random to some extent character

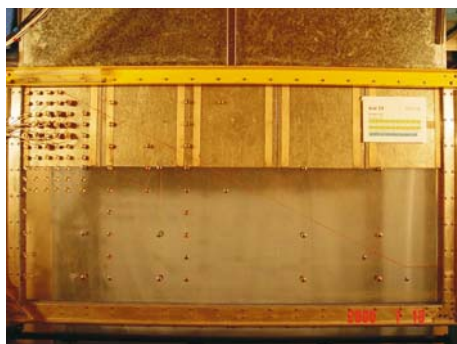
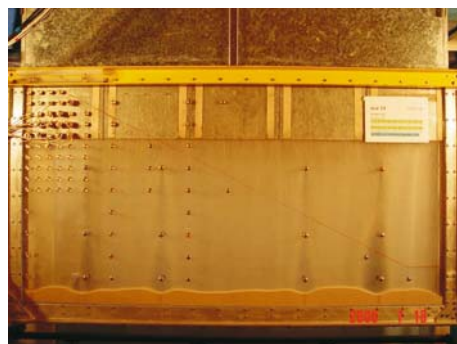
1 – $t = 0$, test 14, Phot. 2689, camera 12 – $t = 3$ min, Phot. 2692, camera 13 – $t = 5$ min, Phot. 2696, camera 14 – $t = 7$ min, Phot. 2700, camera 15 – $t = 7.5$ min, Phot. 2701, camera 16 – $t = 8$ min, Phot. 2702, camera 1

Fig. 3. Example of building the embankment model by pouring (test 14)

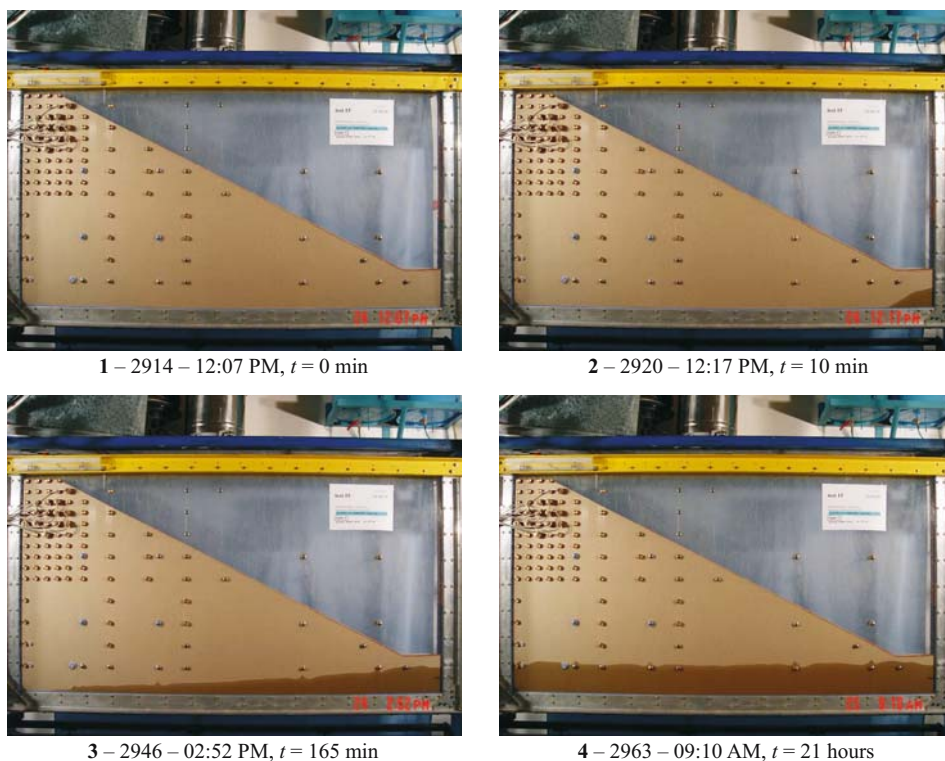


Fig. 4. Example of setting initial soil water table (Test 15)

of the flow from hoppers. As a result the internal structure of the embankment model was rather complex, but steady from test to test, giving not perfectly uniform, but highly repeatable internal structure of the model.

Setting of the initial water table was made through the inlet placed at the right down corner of the test box. The proper tests were performed 2-3 days after setting the initial soil water table. The tests were made on a model of landward embankment slope of inclination 1:2, 0.8 m high and 1.60 m long. It was situated on a subsoil layer 0.2 m thick, made of the same sand. The width of the embankment crown was 0.2 m.

Two types of tests were performed, for which two ways of supplying water to the model were employed:

- **type A** – water supplied to the embankment body by rain generator, along the whole slope length. This type of test can simulate both conditions created by overflow (without significant surface erosion) and by heavy rainfall,
- **type B** – water supplied to the model from its top by rising water level in overflow vessel (real overflow).

Test results

Due to a big number of tests performed three representative tests were chosen to present typical results: test 14, test 15 and test 17. Data collected during these test illustrate best the process of air trapping and its influence on the embankment internal structure.

- Test 14 – type A test (rain generator used to supply water along the whole length of the embankment slope), intensity of water supply $q \sim 10$ ml/s.
- Test 15 – type B test (water supplied by overflow vessel from the top of the embankment model), $q \sim 4$ ml/s.
- Test 17 – type B test, $q = 9.25$ ml/s.

Original numbers given by the digital cameras are left in the photographs descriptions.

Test 14

Course of test 14 is shown in Figure 5. Photographs taken by the two cameras are put on together in this figure for the purpose of further analysis. The darker areas visible on photographs are wet, the lighter ones are dry. Several zones of entrapped air were created and lasted for some time during the test. Most of them disappeared in later stage of the test (air escaped to the atmosphere). At 22 min of water supplying to the embankment body the first traces of slope failure were noticed some distance from the toe of the model. Also about this moment the first cracks were observed to form and later open in isolated dry areas, surrounded by saturated soil.

Test 15

Course of the test 15 is presented in Figure 6. Water was supplied to the embankment not by the rain generator along the whole slope length, like it was in previous case, but from the top of the model by overflow vessel. Intensity of overflow was about 4 ml/s. For this intensity no air trapping occurred. Start of the slope failure was observed later than in case of test 14 (after 81 min), but its shape and location were similar.

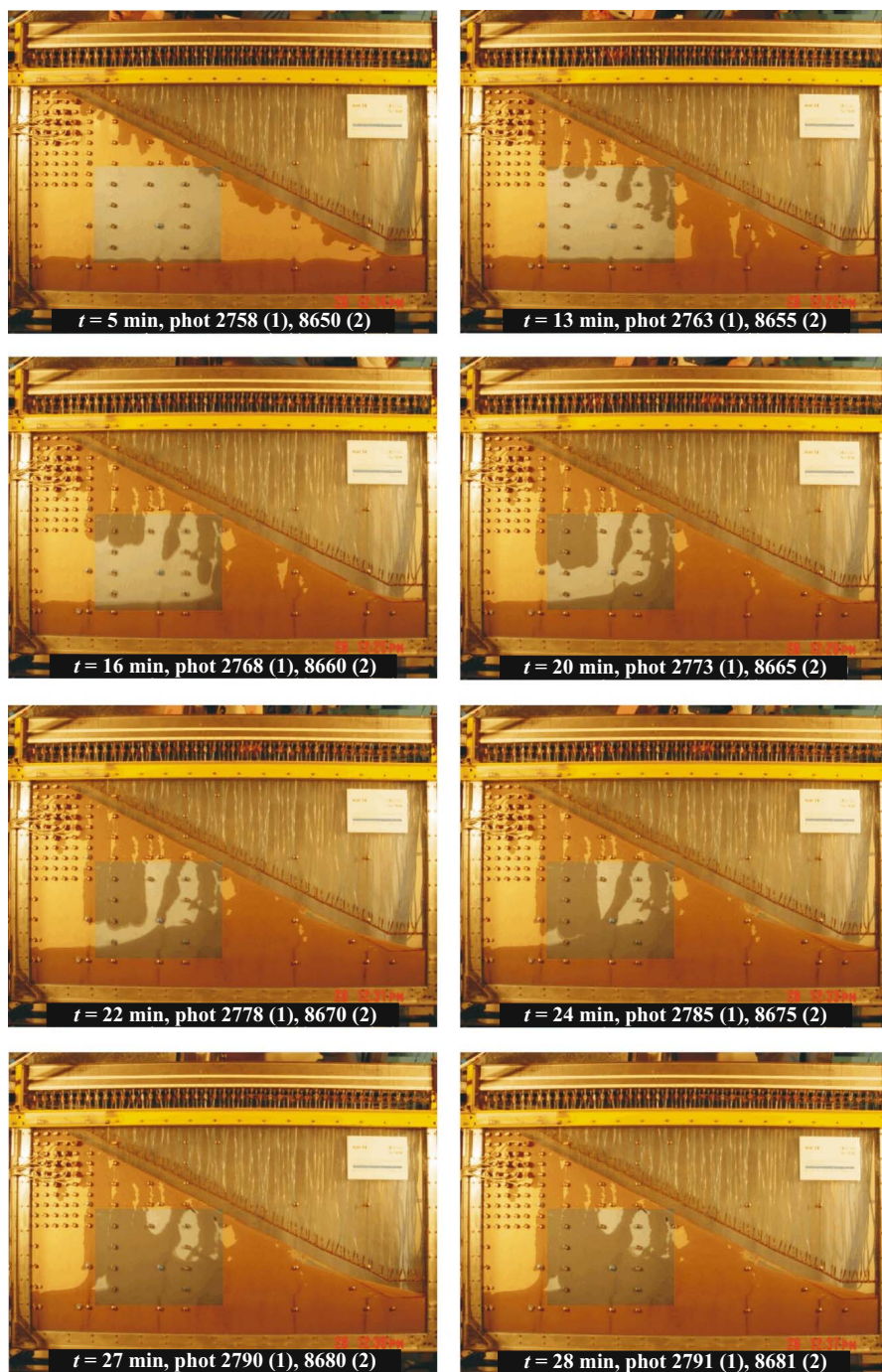
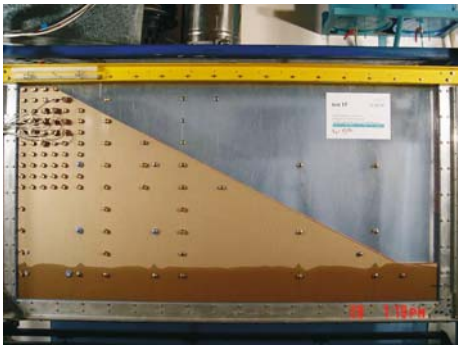
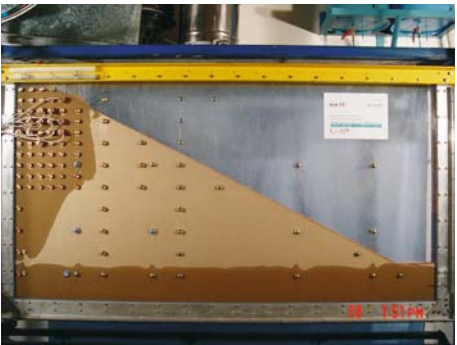


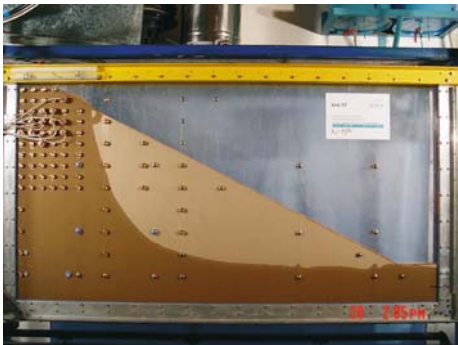
Fig. 5. Course of test 14



1 – 2968 – 01:19 PM, $t = 0$ min



2 – 2995 – 01:51 PM, $t = 32$ min



3 – 3007 – 02:05 PM, $t = 46$ min



4 – 3098 – 03:52 PM, $t = 153$ min

Fig. 6. Course of test 15

Test 17

Test 17 is presented in Figure 7. It was a repeat of test 15 with greater overflow intensity ($q = 9.25$ ml/s). Air entrapment occurred after 19 min of water supply. Some of the entrapped air zones resulted in cracks opening,. The opened cracks proved to be very stable and lasted even after drying an rising again water table.

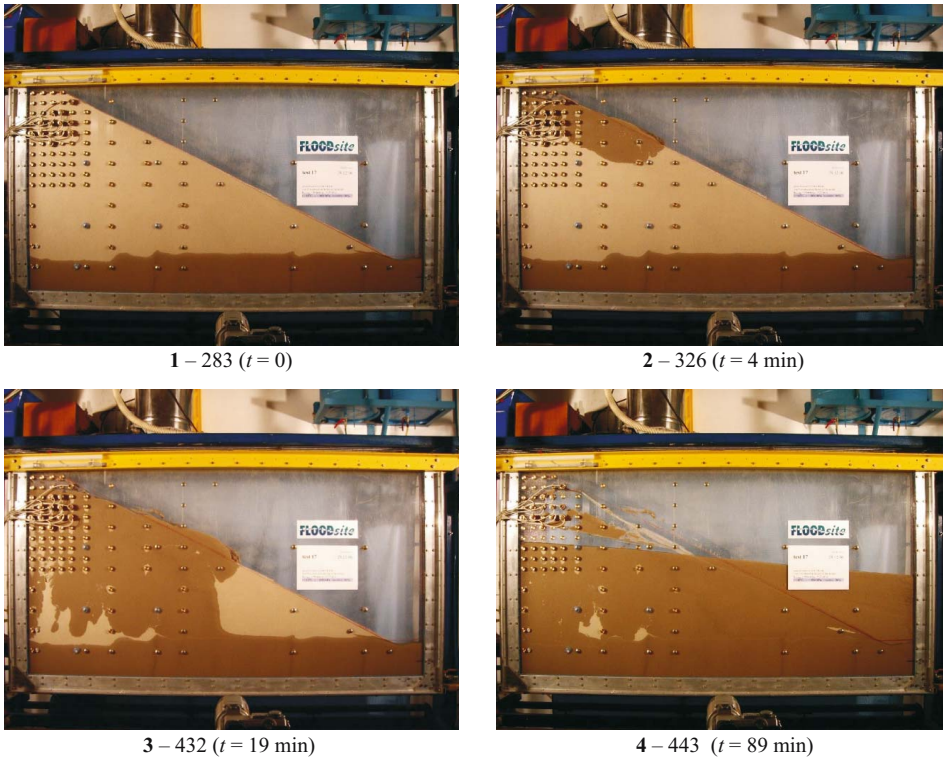
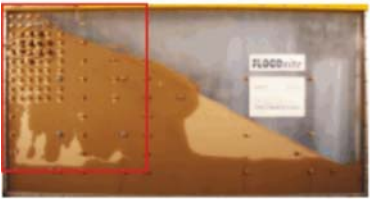
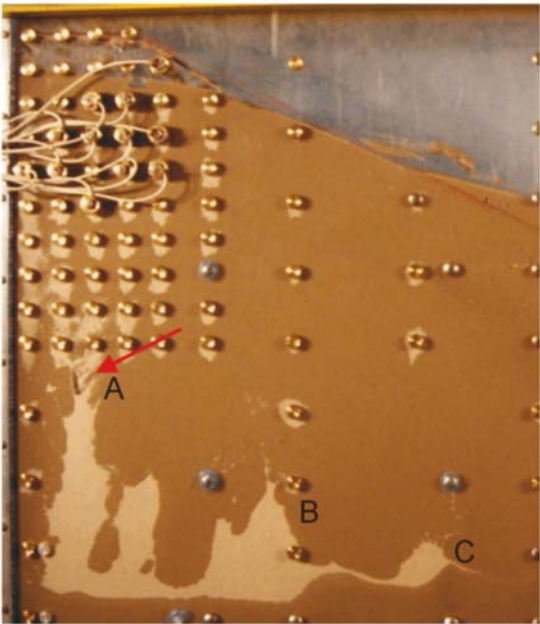


Fig. 7. Course of test 17



camera 1
phot. 433
 $t = 59 \text{ min (2)}$



camera 1
phot. 434
 $t = 60 \text{ min}$

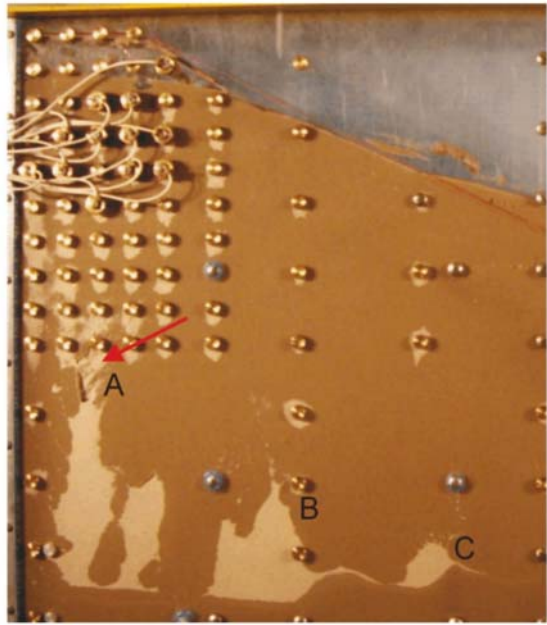


Fig. 8. Example of entrapped air release

Analysis of the tests results

Two types of analysis were made on test 14 and test 17 data, for which air trapping occurred. The first was related to soil air pressure measurements, the second to deformations of model embankment during water infiltration.

Entrapped air pressures

Measuring entrapped air pressure was not easy, as the location of air entrapment was random and varied from test to test. It was expected however, on the basis of previous works (ZARADNY 1994, 1999, ABO ELELA 1996), that the most probable location for air entrapment was the area below the top of embankment and the pressure sensors were located there. This assumption proved to be true in most cases, but sometimes air was closed also in the central part of the model. In some cases rapid escape of air was observed, so sudden, that not possible to catch by a camera. Spectacular escape of air bubble accompanied by successful record of air pressures was observed during test 17 (Fig. 8). Comparison of pressure graphs and relevant photographs shows that air pressure changes reflect properly consecutive test stages. Stable parts of pressure graphs coincides with air bubble of stable dimensions, sudden pressure rises correspond to rapid air escape to the atmosphere.

Displacements and strain fields

Displacement and strain fields were analysed, using image processing software geoPIV, based on the PIV (particle image velocimetry) method. Preliminary results obtained for test 14 are presented in Fig. 9.

Conclusions

Measurements made during flood embankment tests proved that the entrapped air pressure is higher than atmospheric. The measured difference was about 25 hPa at peak. It was enough to induce internal cracks forming and opening within an embankment body.

Analysis of test results by the PIV method shows that the first measurable displacements and strains in flood embankment model can be observed already during setting the initial ground water level. It proves that ground water level variations introduce significant and irreversible changes of embankment

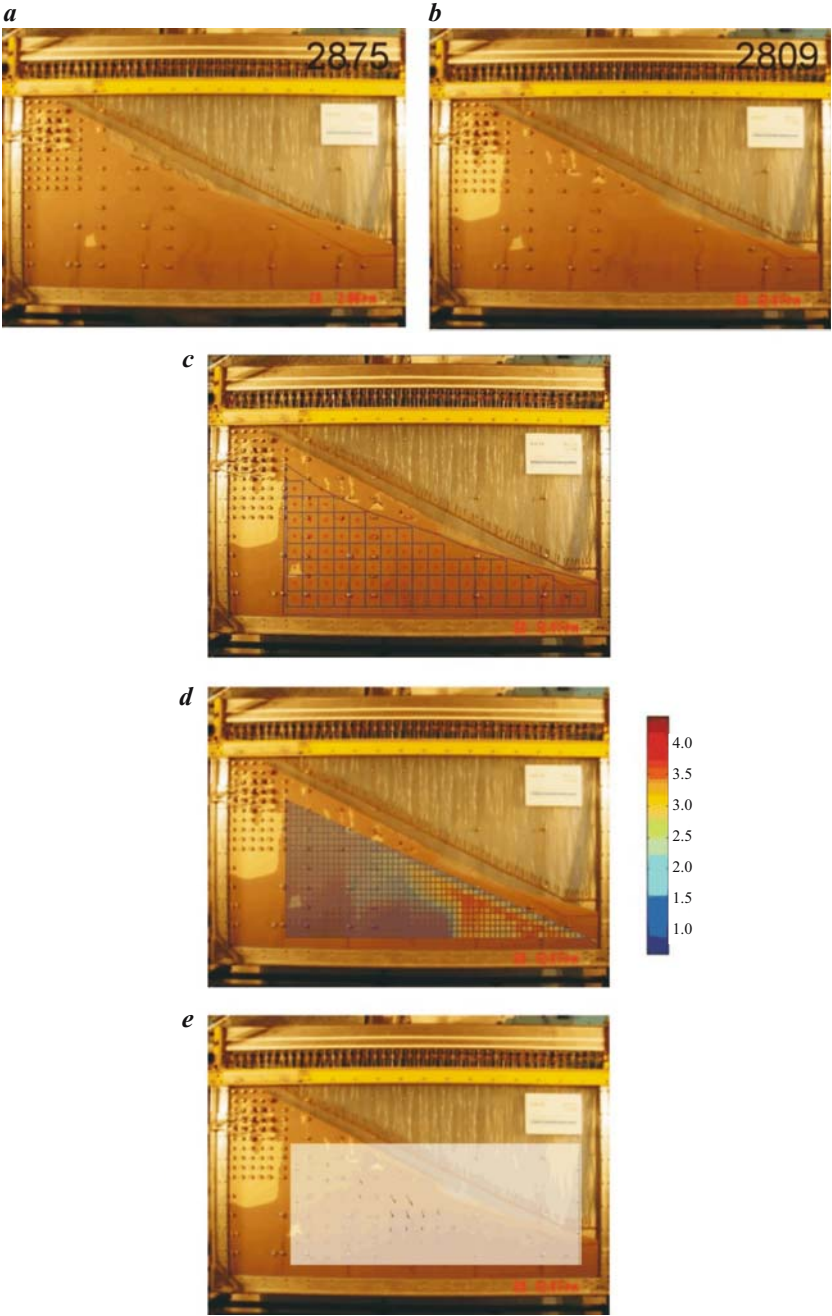


Fig. 9. Final failure displacements and strains – global failure mechanism

internal structure, which can in turn, in favourable conditions, activate global sliding embankment failure.

Acknowledgement

The work described in this publication was supported by the European Community's Sixth Framework Programme through the grant to the budget of the Integrated Project FLOODsite, Contract GOCE-CT-2004-505420.

Disclaimer

This document reflects only the authors' views and not those of the European Community. This work may rely on data from sources external to the FLOODsite project Consortium. Members of the Consortium do not accept liability for loss or damage suffered by any third party as a result of errors or inaccuracies in such data. The information in this document is provided "as is" and no guarantee or warranty is given that the information is fit for any particular purpose. The user thereof uses the information at its sole risk and neither the European Community nor any member of the FLOODsite Consortium is liable for any use that may be made of the information.

References

- ABO ELELA M.M.I. 1996. *Filtration phenomena in earth dike during intensive precipitation*. PhD Thesis, Polish Academy of Sciences, Institute of Hydro-Engineering, Gdańsk.
- LEŚNIEWSKA D., BOGACZ P., KACZMAREK J., ZARADNY H. 2007. *Air trapping phenomenon and cracking*. FLOODsite Raport T04 07.
- WHITE D.J., TAKE W.A. 2002. *GeoPIV: Particle Image Velocimetry (PIV) software for use in geotechnical testing*. Cambridge University Engineering, Department Technical Report, D-SOILS-TR322.
- ZARADNY H. 1994. *Physical modelling of infiltration into dikes for stability purposes*. Road and Hydraulic Engineering Division, Rijkswaterstaat, Delft, Contract DWW-510 Final Report.
- ZARADNY H. 1999. *Entrapped air – reason for the unexpected pore pressure behaviour in levees and earth dams*. Proceedings of XXVIII IAHR Congress – Hydraulic Engineering for Sustainable Water Resources Management at the Turn of the Millenium, Graz, Austria, pp. 7.

Accepted for print 27.06.2008 r.

SPLIT ESTIMATION OF PARAMETERS IN FUNCTIONAL GEODETIC MODELS

Zbigniew Wiśniewski

Institute of Geodesy
University of Warmia and Mazury, Olsztyn

Key words: adjustment, M -estimation.

Abstract

The method of estimation presented in the paper is based on the assumption that every measurement result can be a realization of either of two different, random variables (differing from each other in expected values). Supposing it, the functional model $\mathbf{v} = \mathbf{y} - \mathbf{A}\mathbf{X}$ is split into two competitive ones $\mathbf{v}_\alpha = \mathbf{y} - \mathbf{A}\mathbf{X}_\alpha$ and $\mathbf{v}_\beta = \mathbf{y} - \mathbf{A}\mathbf{X}_\beta$, that concern the same vector of observation \mathbf{y} (\mathbf{A} is a common coefficient matrix, \mathbf{v}_α and \mathbf{v}_β are competitive vectors of random errors, \mathbf{X}_α and \mathbf{X}_β – competitive parameter vectors, respectively). The estimation process proposed here is based on the principle of crossing (mutual) weighting of competitive random errors $v_{i\alpha}$ and $v_{i\beta}$ (concerning the same observation y_i).

The proposed method is essential extension of M -estimation class. However, its practical application is not limited to a robust estimation of the parameter \mathbf{X} ($\hat{\mathbf{X}}_\alpha$ estimator) and extended with estimator $\hat{\mathbf{X}}_\beta$ (concerning outliers). The presented method can be also applied to a joint adjustment of two observation sets measured in two, different epochs. Differences between competitive estimates $\hat{\mathbf{X}}_\alpha$ and $\hat{\mathbf{X}}_\beta$ can indicate displacements of network points. The paper presents some basic, numerical examples that illustrate principles of the split estimation in functional geodetic models.

ROZSZCZEPIONA ESTYMACJA PARAMETRÓW W FUNKCJONALNYCH MODELACH OBSERWACJI GEODEZYJNYCH

Zbigniew Wiśniewski

Instytut Geodezji
Uniwersytet Warmińsko-Mazurski w Olsztynie

Słowa kluczowe: metody wyrównania, M -estymacja.

Abstrakt

Przedstawiona w pracy metoda estymacji wynika z założenia, że każdy z wyników pomiaru może być realizacją jednej z dwu zmiennych losowych różniących się wartościami oczekiwanymi. Takie

założenie doprowadziło do rozszczepienia modelu funkcjonalnego $\mathbf{v} = \mathbf{y} - \mathbf{A}\mathbf{X}$ na dwa konkurencyjne modele: $\mathbf{v}_\alpha = \mathbf{y} - \mathbf{A}\mathbf{X}_\alpha$, $\mathbf{v}_\beta = \mathbf{y} - \mathbf{A}\mathbf{X}_\beta$, dotyczące tego samego wektora obserwacji \mathbf{y} (\mathbf{A} – znana macierz współczynników, \mathbf{v}_α i \mathbf{v}_β – konkurencyjne wektory poprawek, \mathbf{X}_α i \mathbf{X}_β – konkurencyjne wektory parametrów). W procesie estymacji szczególną rolę odgrywa zasada krzyżowego (wzajemnego) wagowania konkurencyjnych poprawek v_α i v_β dotyczących tej samej obserwacji y_i .

Proponowana metoda estymacji jest istotnym rozszerzeniem M -estymacji. Jej praktyczne zastosowania nie ograniczają się jednak do odpornej estymacji parametru \mathbf{X} . Metoda może być zastosowana także do wspólnego wyrównania obserwacji z dwu epok pomiarowych sieci geodezyjnych. Różnica między konkurencyjnymi estymatorami $\hat{\mathbf{X}}_\alpha$ i $\hat{\mathbf{X}}_\beta$ będzie wówczas wskazywać na przemieszczenie punktów tej sieci. W pracy zamieszczono proste przykłady numeryczne ilustrujące podstawowe właściwości rozszczepionej estymacji parametrów funkcjonalnych modeli obserwacji geodezyjnych.

Introduction

In estimation theories, it is usually assumed that measurement results are a set of realizations of one random variable ξ with the expected value $E(\xi) = \mathbf{A}\mathbf{X}$ ($\mathbf{A} \in \mathbb{R}^{n,r}$ – known coefficient matrix, $\mathbf{X} \in \mathbb{R}^{r,1}$ – parameter vector). Then, the following functional model $v_i = y_i - \mathbf{a}_{(i)}\mathbf{X}$, $i = 1, \dots, n$, can be formulated for every observation y_i (v_i – random error, $\mathbf{a}_{(i)}$ – i th row of the matrix \mathbf{A}). In geodetic practice, it is sometimes possible that measurement results are realizations of either of ξ_α or ξ_β different, random variables differing from each other in expected values $E(\xi_\alpha) = \mathbf{A}\mathbf{X}_\alpha$ and $E(\xi_\beta) = \mathbf{A}\mathbf{X}_\beta$. For example, it can occur that an observation set contains some outliers. Then, one can assume that “good” observations are realizations of the variable ξ_α and outliers, the other one, ξ_β . The essential problem is how to identify a particular measurement result with either of random variables objectively.

Robust M -estimation solves the problem by applying specially designed attenuation functions. Such functions decrease weights of observations, which are supposed to be realizations of the variable ξ_β (such suspicion is based on values of residuals v_i) (e.g. HUBER 1981, HAMPEL et al. 1986, YANG 1994, YANG et al. 2002). In that case, estimation results depend on arbitrarily assumed attenuation functions or more generally on assumed weight functions (various examples of attenuation or weight functions are presented in e.g. HAMPEL et al. 1986, KADAJ 1988, KOCH 1996, 1999, GUI, ZHANG 1998, CASPARY, HEAN 1990, WIŚNIEWSKI 1999).

Similarly, results of geodetic network measurements obtained in two different epochs can be an example of a set that consists of realizations of two random variables differing from each other in expected values. Up to now, in the classical estimation methods, results obtained in the first epoch are arbitrarily taken as realizations of the first variable ξ_α , and in the second one as realizations of the other ξ_β . Thus, it is necessary to assume two coexisting functional models: for one part of the observation set $v_{i\alpha} = y_i - \mathbf{a}_{(i)}\mathbf{X}_\alpha$, $i = 1, \dots, n_\alpha$

and for the other $v_{i\beta} = y_i - \mathbf{a}_{(i)}\mathbf{X}_\beta$, $i = n_\alpha + 1, \dots, n$, where \mathbf{X}_α and \mathbf{X}_β are two states of network point coordinates. Now, let us assume that some network points are not displaced. Then, some observations described classically with the model $v_{i\beta} = y_i - \mathbf{a}_{(i)}\mathbf{X}_\beta$, can be interpreted as realizations of the variable ξ_α and can support estimation of the parameter \mathbf{X}_α .

Let us consider the above examples or other similar situation when a set of measurement results may be a realization of either of two random variables. It is assumed here that to identify observations objectively, which is equivalent with objective estimation of parameters \mathbf{X}_α and \mathbf{X}_β , the random variables should rival each other. It means that, two functional models as well as two competitive random errors $v_{i\alpha}$ and $v_{i\beta}$ should exist for each observation y_i . The concept described here is explained with the following elemental and rather “idealistic” example.

Let $y = 1, 2, 3, 6, 8$ be measurement results of some quantity X with the model $v_i = y_i - X$. One can assume \hat{X}_α as the estimator that accepts realizations of the random variable $\xi_\alpha = 1, 2, 3$ (in the robust estimation ξ_α would be a “good” variable) and ignores realizations of the variable $\xi_\beta = 6, 8$ (in the robust estimation – “strange” variable). The following residuals: $\hat{v}_{1\alpha} = -1$, $\hat{v}_{2\alpha} = 0$, $\hat{v}_{3\alpha} = 1$, $\hat{v}_{4\alpha} = 4$, $\hat{v}_{5\alpha} = 6$ respond to that estimator. Another possible and competitive solution is an estimate $\hat{X}_\beta = 7$. This time one assumes that ξ_α is the “strange” variable. Thus, another version of residuals can be obtained: $\hat{v}_{1\beta} = -6$, $\hat{v}_{2\beta} = -5$, $\hat{v}_{3\beta} = -4$, $\hat{v}_{4\beta} = -1$, $\hat{v}_{5\beta} = 1$.

If two competitive assumptions about identifying measurement results with either of random variables is considered then the classical functional model of geodetic observations must be split. This paper proposes the way how to estimate parameters of such, split models. The optimisation problem formulated here refers to the principles of M -estimation but it is also an important extension of this estimation class. The proposed method is illustrated with two numerical examples: The first one concerns the observation set presented earlier (with the solutions indicated) and the second one refers to estimation of coordinates of geodetic points in a network with a “mixed” set of measurement results (measurement results obtained in two epochs).

Assumptions

Split functional model

The following optimisation problem:

$$\min_{\mathbf{X}} \quad \varphi(\mathbf{X}) = \sum_{i=1}^n \rho(\hat{v}_i), \quad \hat{v}_i = y_i - \mathbf{a}_{(i)}\hat{\mathbf{X}} \quad (1)$$

is the basis for many estimation methods that belong to the M -estimation class; where $\rho(v_i)$, $i = 1, \dots, n$, are some symmetric, convex, arbitrarily assumed functions (HUBER 1981, HAMPEL et al. 1986, KADAJ 1988, KRARUP, KUBIK 1983, HUANG, MARTICAS 1995, KOCH 1996, ZHU 1996, XU 1989, YANG 1994, YANG et al. 2002). In the least squares method, which is a neutral M -estimation, it is assumed that

$$\rho(v_i) = v_i^2 p_i \quad (2)$$

where p_i is the weight of i th observation assigned, within the function $\rho(v_i)$ to the random error v_i . According to the robust M -estimation, the weights p_i are replaced with equivalent weights \hat{p}_i , which values are equal to values of concave or quasi-concave weight functions $w(v_i)$ whereat $\forall v_i \neq 0: w(v_i) \leq w(0)$. The above properties of weight functions correspond to the assumption that the M -estimator should be function of realizations of “good” variable ξ_α only. Outliers, realizations of “strange” variable ξ_β , should be rejected.

The concept of equivalent weights follows the assumptions that variables ξ_α and ξ_β share one expected value $E(\xi_\alpha) = E(\xi_\beta) = E(\xi) = \mathbf{AX}$ and differ from each other much in standard deviations σ . Values of the standard deviation σ_α (variable ξ_α) are reasonable and depend on measurement accuracy, technique etc. In contrast, values of the standard deviation σ_β (“strange” variable ξ_β) are assumed as adequately bigger than σ_α hence not to influence the M -estimator computation. In practice, weight functions, which follow the concept described above, are not so restrictive (influence of realizations identified as outliers is “eliminated” softly). It is because observation residuals are known only (real errors stay unknown) and sets of realizations ξ_α and ξ_β can share some intersections. Huber’s function is a good example of such practical weight function (HUBER 1986)

$$\hat{p}_i = w(v_i) = \begin{cases} p_i & \text{for } |v_i| \leq c \\ \frac{c}{|v_i|} & \text{for } |v_i| > c \end{cases} \quad (3)$$

where $p_i = 1 / \sigma_\alpha^2$ are original weights while equivalent weights $\hat{p}_i = c/|v_i|$ approach some small value referred to standard deviation σ_α (usually $c = 2\sigma_\alpha$). One can notice that values of σ_β should be at an adequately high level. It is because of the assumption concerning expected values $E(\xi)$ of the random variables ξ_α and ξ_β .

This paper proposes more natural concept that accepts expected value $E(\xi) = E(\xi_\beta)$ different from $E(\xi) = E(\xi_\alpha)$ and that makes standard deviation σ_β reasonable, too. Such assumptions lead to the split of the random variable realizations (concerning ξ_α and ξ_β , respectively) and to other following consequences, described later on.

Thus, if a set of random variable realizations is split into two competitive ones, which are identified with variables ξ_α and ξ_β , then two competitive, functional models $v_{i\alpha} = y_i - \mathbf{a}_{(i)}\mathbf{X}_\alpha$ and $v_{i\beta} = y_i - \mathbf{a}_{(i)}\mathbf{X}_\beta$ (where $E(y_i) - \mathbf{a}_{(i)}\mathbf{X}_\alpha$ and $E(y_i) - \mathbf{a}_{(i)}\mathbf{X}_\beta$) are assigned to every observation y_i . The split of the functional model that concerns whole observation set can be written as follows:

$$\text{split } (\mathbf{v} = \mathbf{y} - \mathbf{AX}) \begin{cases} \mathbf{v}_\alpha = \mathbf{y} - \mathbf{AX}_\alpha \\ \mathbf{v}_\beta = \mathbf{y} - \mathbf{AX}_\beta \end{cases} \quad (4)$$

Weight functions and target function components

Estimation of competitive parameters \mathbf{X}_α and \mathbf{X}_β by using the same vector of observations \mathbf{y} , requires specially formulated target function of the optimisation problem. This paper proposes to replace function $\rho(v)$ with functions $\rho_\alpha(v_\alpha)$ and $\rho_\beta(v_\beta)$, according to the model in Eq. (4) and in compliance with the principle of crossing, mutual weighting of competitive residuals v_α and v_β . That cross-weighting is guaranteed when the weight functions $w_\alpha(v_\beta)$ and $w_\beta(v_\alpha)$ are obtained as

$$w_\alpha(v_\beta) = \frac{\partial \rho_\alpha(v_\alpha)}{\partial (v_\alpha^2)}, \quad w_\beta(v_\alpha) = \frac{\partial \rho_\beta(v_\beta)}{\partial (v_\beta^2)} \quad (5)$$

The functions ρ_α and ρ_β , as well as the weight functions, should also own the following properties (considering the optimisation target):

$$\left. \begin{aligned} \min_{v_\alpha} \rho_\alpha(v_\alpha) &\equiv \sup_{|v_\alpha| \leq \delta_v} w_\alpha(v_\beta), & \min_{v_\beta} w_\alpha(v_\beta) &\equiv \sup_{|v_\alpha| \leq \delta_v} \rho_\alpha(v_\alpha) \\ \min_{v_\beta} \rho_\beta(v_\beta) &\equiv \sup_{|v_\beta| \leq \delta_v} w_\beta(v_\alpha), & \min_{v_\alpha} w_\beta(v_\alpha) &\equiv \sup_{|v_\beta| \leq \delta_v} \rho_\beta(v_\beta) \end{aligned} \right\} \quad (6)$$

where $\delta_v = v_\beta - v_\alpha$. The following functions of standardized random errors v_α, v_β :

$$\left. \begin{aligned} \rho_\alpha(v_\alpha) &= v_\alpha^2 v_\beta^2 & w_\alpha(v_\beta) &= \frac{\partial \rho_\alpha(v_\alpha)}{\partial (v_\alpha^2)} = v_\beta^2 \\ \rho_\beta(v_\beta) &= v_\beta^2 v_\alpha^2 & w_\beta(v_\alpha) &= \frac{\partial \rho_\beta(v_\beta)}{\partial (v_\beta^2)} = v_\alpha^2 \end{aligned} \right\} \quad (7)$$

own mentioned properties in natural way (Fig. 1).

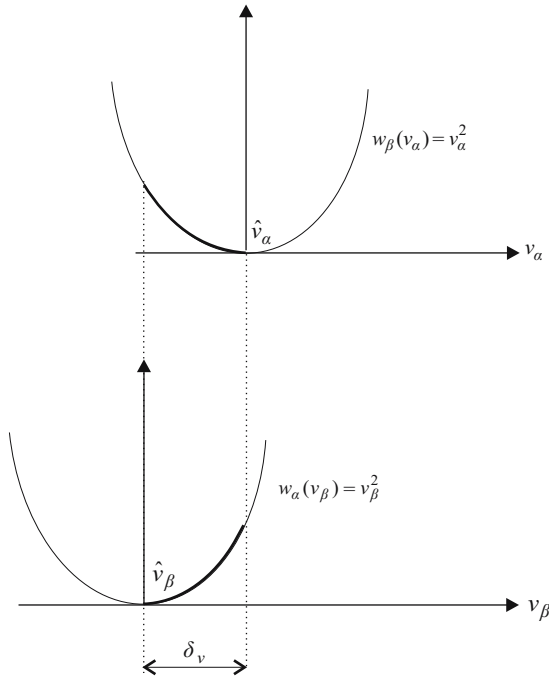


Fig. 1. Illustration to cross-weighting

Optimisation Problem and Solution

The following optimisation problem is formulated on the basis of the model Eq. (4) and functions from Eq. (7):

$$\left. \begin{aligned} \mathbf{v}_\alpha &= \mathbf{y} - \mathbf{A}\mathbf{X}_\alpha \\ \mathbf{v}_\beta &= \mathbf{y} - \mathbf{A}\mathbf{X}_\beta \\ \min_{\mathbf{X}_\alpha} \varphi(\mathbf{X}_\alpha) &= \varphi(\hat{\mathbf{X}}_\alpha) \\ \min_{\mathbf{X}_\beta} \varphi(\mathbf{X}_\beta) &= \varphi(\hat{\mathbf{X}}_\beta) \end{aligned} \right\} \quad (8)$$

where

$$\left. \begin{aligned} \varphi(\mathbf{X}_\alpha) &= \sum_{i=1}^n \rho_\alpha(v_{i\alpha}) = \sum_{i=1}^n v_{i\alpha}^2 v_{i\beta}^2 = \sum_{i=1}^n v_{i\alpha}^2 w_\alpha(v_{i\beta}) = \mathbf{v}_\alpha^T \mathbf{w}_\alpha(\mathbf{v}_\beta) \mathbf{v}_\alpha \\ \varphi(\mathbf{X}_\beta) &= \sum_{i=1}^n \rho_\beta(v_{i\beta}) = \sum_{i=1}^n v_{i\beta}^2 v_{i\alpha}^2 = \sum_{i=1}^n v_{i\beta}^2 w_\beta(v_{i\alpha}) = \mathbf{v}_\beta^T \mathbf{w}_\beta(\mathbf{v}_\alpha) \mathbf{v}_\beta \end{aligned} \right\} \quad (9)$$

and

$$\mathbf{w}_\alpha(\mathbf{v}_\beta) = \text{Diag}(v_{1\beta}^2, v_{2\beta}^2, \dots, v_{n\beta}^2)$$

$$\mathbf{w}_\beta(\mathbf{v}_\alpha) = \text{Diag}(v_{1\alpha}^2, v_{2\alpha}^2, \dots, v_{n\alpha}^2)$$

The competitive estimators $\hat{\mathbf{X}}_\alpha$ and $\hat{\mathbf{X}}_\beta$ are solutions of the problem Eq. (8) when gradients \mathbf{g}_α and \mathbf{g}_β are zero vectors, i.e., when the following equation system is fulfilled (for $\mathbf{v}_\alpha = \hat{\mathbf{v}}_\alpha = \mathbf{y} - \mathbf{A}\hat{\mathbf{X}}_\alpha$ and $\mathbf{v}_\beta = \hat{\mathbf{v}}_\beta = \mathbf{y} - \mathbf{A}\hat{\mathbf{X}}_\beta$):

$$\left. \begin{aligned} \mathbf{g}_\alpha(\mathbf{X}_\alpha, \mathbf{X}_\beta) &= \frac{\partial \varphi(\mathbf{X}_\alpha)}{\partial \mathbf{X}_\alpha} = -2\mathbf{A}^T \mathbf{w}_\alpha(\mathbf{v}_\beta) \mathbf{v}_\alpha = \mathbf{0} \\ \mathbf{g}_\beta(\mathbf{X}_\alpha, \mathbf{X}_\beta) &= \frac{\partial \varphi(\mathbf{X}_\beta)}{\partial \mathbf{X}_\beta} = -2\mathbf{A}^T \mathbf{w}_\beta(\mathbf{v}_\alpha) \mathbf{v}_\beta = \mathbf{0} \end{aligned} \right\} \quad (10)$$

Because for the functions $\varphi(\mathbf{X}_\alpha)$ and $\varphi(\mathbf{X}_\beta)$ the following Hessians exist:

$$\left. \begin{aligned} \mathbf{H}_\alpha(\mathbf{X}_\beta) &= \frac{\partial^2 \varphi(\mathbf{X}_\alpha)}{\partial \mathbf{X}_\alpha \partial \mathbf{X}_\alpha^T} = -2\mathbf{A}^T \mathbf{w}_\alpha(\mathbf{v}_\beta) \frac{\partial \mathbf{v}_\alpha}{\partial \mathbf{X}_\alpha^T} = 2\mathbf{A}^T \mathbf{w}_\alpha(\mathbf{v}_\beta) \mathbf{A} \\ \mathbf{H}_\beta(\mathbf{X}_\alpha) &= \frac{\partial^2 \varphi(\mathbf{X}_\beta)}{\partial \mathbf{X}_\beta \partial \mathbf{X}_\beta^T} = -2\mathbf{A}^T \mathbf{w}_\beta(\mathbf{v}_\alpha) \frac{\partial \mathbf{v}_\beta}{\partial \mathbf{X}_\beta^T} = 2\mathbf{A}^T \mathbf{w}_\beta(\mathbf{v}_\alpha) \mathbf{A} \end{aligned} \right\} \quad (11)$$

then Newton's method can be applied to compute $\hat{\mathbf{X}}_\alpha$ and $\hat{\mathbf{X}}_\beta$ (e.g TEUNISSEN 1990). Let us consider necessary conditions Eq. (10) (gradients are referred to each other by shared variable \mathbf{X}_α and \mathbf{X}_β), the iterative formula can be written as ($j = 1, \dots, k$)

$$\left. \begin{aligned} \mathbf{X}_\alpha^j &= \mathbf{X}_\alpha^{j-1} + d\mathbf{X}_\alpha^{j-1}, & d\mathbf{X}_\alpha^j &= -\mathbf{H}_\alpha^{-1}(\mathbf{X}_\beta^{j-1})\mathbf{g}_\alpha(\mathbf{X}_\alpha^{j-1}, \mathbf{X}_\beta^{j-1}) \\ \mathbf{X}_\beta^j &= \mathbf{X}_\beta^{j-1} + d\mathbf{X}_\beta^{j-1}, & d\mathbf{X}_\beta^j &= -\mathbf{H}_\beta^{-1}(\mathbf{X}_\alpha^j)\mathbf{g}_\beta(\mathbf{X}_\alpha^j, \mathbf{X}_\beta^{j-1}) \end{aligned} \right\} \quad (12)$$

The iterative process Eq. (12) is ended for such $j = k$, where $\mathbf{g}_\alpha(\mathbf{X}_\alpha^{k-1}, \mathbf{X}_\beta^{k-1}) = \mathbf{0}$ and $\mathbf{g}_\beta(\mathbf{X}_\alpha^k, \mathbf{X}_\beta^{k-1}) = \mathbf{0}$. Thus $\hat{\mathbf{X}}_\alpha = \mathbf{X}_\alpha^k$, $\hat{\mathbf{X}}_\beta = \mathbf{X}_\beta^k$ and $\hat{\mathbf{v}}_\alpha = \mathbf{y} - \mathbf{A}\hat{\mathbf{X}}_\alpha$, $\hat{\mathbf{v}}_\beta = \mathbf{y} - \mathbf{A}\hat{\mathbf{X}}_\beta$. The estimates of the least squares method $\hat{\mathbf{X}}_{LS} = (\mathbf{A}^T\mathbf{A})^{-1}\mathbf{A}^T\mathbf{y}$ and $\hat{\mathbf{v}}_{LS} = \mathbf{y} - \mathbf{A}\hat{\mathbf{X}}_{LS}$ can be a starting point for such iterative process.

Examples

Let, as it was in the first part of the paper, \mathbf{y}^T be a vector of measurements of some quantity X and let $\mathbf{v} = \mathbf{y} - \mathbf{A}\mathbf{X}$ be the classical, functional model, where $\mathbf{A}^T = [1, 1, 1, 1, 1]$. Then the LS estimates are as follows: $\hat{\mathbf{X}}_{LS} = 4$ and $\hat{\mathbf{v}}_{LS}^T = [-3, -2, -1, 2, 4]$. Let now the optimisation problem Eq.(8) with split functional model

$$\mathbf{v}_\alpha = \mathbf{y} - \mathbf{A}\mathbf{X}_\alpha$$

$$\mathbf{v}_\beta = \mathbf{y} - \mathbf{A}\mathbf{X}_\beta$$

be considered. Then the following competitive estimator can be obtained (mostly in compliance with "intuitional" values from the first part of the paper):

$$\hat{X}_\alpha = 1.87, \quad \hat{\mathbf{v}}_\alpha^T = [-0.87, 0.13, 1.13, 4.13, 6.13]$$

$$\hat{X}_\beta = 7.19, \quad \hat{\mathbf{v}}_\beta^T = [-6.19, -5.19, -4.19, -1.19, 0.81]$$

The main results of the iterative estimation process Eq. (12), which lead to the final results presented above are listed in Table 1 (\mathbf{P} is the weight matrix in the LS method).

Table 1

Iterative process results

\mathbf{y}	$\hat{\mathbf{v}}_{LS}$	\mathbf{v}_β^1	\mathbf{v}_α^1	\mathbf{v}_β^2	\mathbf{v}_α^2	$\hat{\mathbf{v}}_\beta = \mathbf{v}_\beta^3$	$\hat{\mathbf{v}}_\alpha = \mathbf{v}_\alpha^3$
1.00	-3.00	-4.06	-1.03	-6.18	-0.87	-6.19	-0.87
2.00	-2.00	-3.06	-0.03	-5.18	0.13	-5.19	0.13
3.00	-1.00	-2.06	0.97	-4.18	1.13	-4.19	1.13
6.00	2.00	0.94	3.97	-1.18	4.13	-1.19	4.13
8.00	4.00	2.94	5.97	0.82	6.13	0.81	6.13
	$\hat{\mathbf{X}}_{LS}$	\mathbf{X}_β^1	\mathbf{X}_α^1	\mathbf{X}_β^2	\mathbf{X}_α^2	$\hat{\mathbf{X}}_\beta = \mathbf{X}_\beta^3$	$\hat{\mathbf{X}}_\alpha = \mathbf{X}_\alpha^3$
	4.00	5.06	2.03	7.18	1.87	7.19	1.87
	$[\mathbf{P}]_{ii}$	$[\mathbf{w}_\beta(\hat{\mathbf{v}}_{LS})]_{ii}$	$[\mathbf{w}_\alpha(\mathbf{v}_\beta^1)]_{ii}$	$[\mathbf{w}_\beta(\mathbf{v}_\alpha^1)]_{ii}$	$[\mathbf{w}_\alpha(\mathbf{v}_\beta^2)]_{ii}$	$[\mathbf{w}_\beta(\mathbf{v}_\alpha^2)]_{ii}$	$[\mathbf{w}_\alpha(\mathbf{v}_\beta^3)]_{ii}$
	1	9	16.5	1.1	38.2	0.7	38.3
	1	4	9.4	0.0	26.8	0.2	26.9
	1	1	4.2	0.9	17.4	1.3	17.5
	1	4	0.9	15.8	1.4	17.0	1.4
	1	16	8.6	35.6	0.7	37.6	0.7

B. Consider a levelling network with one unknown point, four fixed points and four height differences measured in two epochs. Measurement results were simulated under assumption that $\delta_H^t = H_\beta - H_\alpha = 0.100$ is a theoretical difference of the unknown point heights in two measurement epochs α and β . Figure 2 presents the network sketch together with the simulated results of measurements.

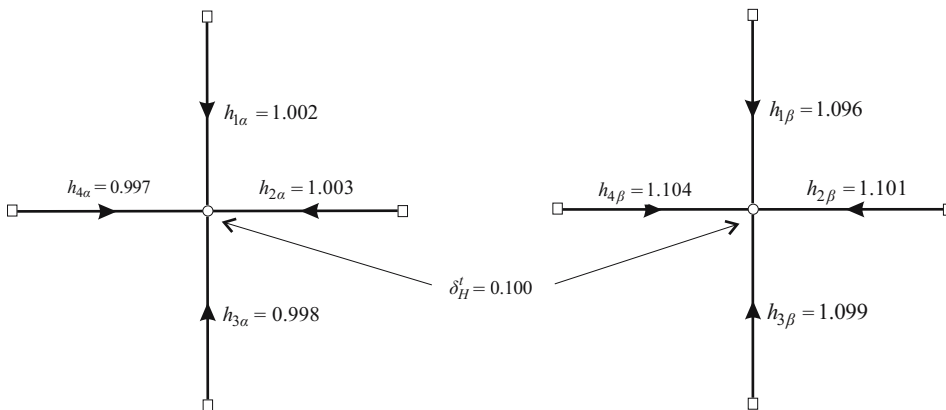


Fig. 2. Levelling network sketch

According to the principles of the proposed method all the observations can be written as one vector of measurement results (the observation order does not matter)

$$\begin{aligned}\mathbf{y}^T &= [h_{1\alpha}, h_{1\beta} : h_{2\alpha}, h_{2\beta} : h_{3\alpha}, h_{3\beta} : h_{4\alpha}, h_{4\beta}] = \\ &= [1.002, 1.096 : 1.003, 1.10 : 0.998, 1.099 : 0.997, 1.104]\end{aligned}$$

and two competitive, functional models can be formulated $X_\alpha = H_\alpha, X_\beta = H_\beta$)

$$\mathbf{v}_\alpha = \mathbf{y} - \mathbf{A}H_\alpha, \quad \mathbf{v}_\beta = \mathbf{y} - \mathbf{A}H_\beta$$

where $\mathbf{A}^T = [1_1, 1_2, \dots, 1_8]$. hus, the optimisation problem Eq. (8) can be solved in six steps iterative process Eq. (12), and results in

$$\hat{H}_\alpha = 1.000,$$

$$\hat{\mathbf{v}}_\alpha^T = [0.002, 0.096 : 0.003, 0.101 : -0.002, 0.099 : -0.003, 0.104]$$

$$\hat{H}_\beta = 1.100,$$

$$\hat{\mathbf{v}}_\beta^T = [-0.098, -0.004 : -0.097, 0.009 : -0.102, 0.001 : -0.103, 0.004]$$

It should be emphasised that $\hat{H}_\beta - \hat{H}_\alpha = \delta_H^t$ and also $\forall i: \hat{v}_{i\alpha} - \hat{v}_{i\beta} = \delta_H^t$.

Conclusions

The method proposed here is an extension of M -estimation class where measurement results can be realizations of either of two different, competitive, random variables. The algorithm presented in Eq. (12) can be applied to the robust estimation of the parameters (example A) as well as to estimation of geodetic points displacements (example B).

The cross-weighting principle, concerning the competitive residuals of the same observation, is theoretical foundation of the proposed estimation method. This paper assumed that the weight functions are convex, squared ones. However, other solutions are also possible if only other assumed weight function fulfil required theoretical conditions Eq. (6).

The solution of the optimisation problem Eq. (8) proposed here refers to Newton's method. Such algorithm is especially effective with the assumed weight functions (the examples show that satisfactory results can be obtained after few iterative steps).

Acknowledgments

The research is supported by the Polish Ministry of Science and Higher Education under the grant “New methods of estimation of parameters in a functional model of geodetic observations (M_{split} estimation)”, no. N N526 255 734.

This paper was presented on 13th FIG Symposium on Deformation Measurement and Analysis and 4th Symposium on Geodesy for Geotechnical and Structural Engineering (Lisbon, 2008 May 12-15).

References

- CASPARY W., HAEN W. 1990. *Simultaneous estimation of location and scale parameters in the context of robust M-estimation*. Manuscr. Geod., 15: 273-282
- GUI Q., ZHANG J. 1998. *Robust biased estimation and its applications in geodetic adjustment*. J. Geod., 72: 430-435.
- HAMPEL F.R., RONCHETTI E.M., ROUSSEUW P.J., STAHEL W.A. 1986. *Robust statistics. The approach based on influence functions*. John Wiley & Sons, New York.
- HUANG Y., MERTIKAS S.P. 1995. *On the design of robust regression estimators*. Manuscr. Geod., 20: 145-160.
- HUBER P.J. 1981. *Robust statistics*. John Wiley & Sons, New York.
- KOCH K.R. 1996. *Robuste Parameterschätzung*. Allg. Vermess. Nachr., 103(1): 1-18.
- KADAJ R. 1988. *Eine verallgemeinerte Klasse von Schätzverfahren mit praktischen Anwendungen*. ZfV, 113(4): 157-166.
- KOCH K.R. 1999. *Parameter estimation and hypothesis testing in linear model*, 2nd edn. Springer, Berlin, Heidelberg, New York.
- KRARUP T., KUBIK K. 1983. *The Danish Method; experience and philosophy*. Deutsche Geodätische Kommission bei der Bayerischen Akademie der Wissenschaften, München, Reihe A, 7: 131-134.
- TEUNISSEN P.J.G. 1990. *Nonlinear least squares*. Manuscr. Geod., 15: 137-150.
- WIŚNIEWSKI Z. 1996. *Estimation of third and fourth order central moments of measurement errors from sums of powers of least squares adjustment residuals*. J. Geod., 70: 256-262.
- WIŚNIEWSKI Z. 1999. *Concept of robust estimation of variance coefficient (VR-estimation)*. Bollettino di Geodesia e Scienze Affini, 3: 291-310.
- XU P. 1989. *On robust estimation with correlated observations*. Bull. Géod., 63: 237-252.
- YANG Y. 1994. *Robust estimation for dependent observations*. Manuscr. Geod., 19: 10-17.
- YANG Y., SONG L., XU T. 2002. *Robust estimation for correlated observations based on bifactor equivalent weights*. J. Geod., 76: 353-358.
- ZHU J. 1996. *Robustness and the robust estimate*. J. Geod., 70: 586-590.

Accepted for print 26.09.2008 r.

INITIAL RESULTS OF RTK/OTF POSITIONING USING THE NTRIP DATA TELETRANSMISSION TECHNOLOGY

***Mieczysław Bakuła, Renata Pelc-Mieczkowska,
Barbara Chodnicka, Małgorzata Rogala, Arkadiusz Tyszko***

Chair of Satellite Geodesy and Navigation
University of Warmia and Mazury in Olsztyn

Key words: NTRIP, GPS, RTK, OTF, GPRS.

Abstract

The paper presents the initial results of RTK/OTF satellite measurements made using NTRIP Internet data transmission. Two permanent reference stations belonging to the University of Warmia and Mazury in Olsztyn were used for test measurements. As a result of measurements taken at three measurement points situated 1,5 to 20 kilometers from the reference stations the accuracies of up to a few centimeters were obtained for points situated in the open terrain. The accuracies obtained at the point with numerous covers in the form of tree branches ranged from several centimeters to almost 3 meters, which is characteristic for GPS measurements taken under conditions of limited availability of satellites.

WSTĘPNE WYNIKI POZYCJONOWANIA RTK/OTF Z WYKORZYSTANIEM TECHNOLOGII TELETRANSMISJI DANYCH NTRIP

***Mieczysław Bakuła, Renata Pelc-Mieczkowska, Barbara Chodnicka, Małgorzata Rogala,
Arkadiusz Tyszko***

Katedra Geodezji Satelitarnej i Nawigacji
Uniwersytet Warmińsko-Mazurski w Olsztynie

Słowa kluczowe: NTRIP, GPS, RTK, OTF, GPRS.

Abstrakt

W artykule przedstawiono wstępne wyniki pomiarów satelitarnych RTK/OTF wykonanych z wykorzystaniem internetowego przesyłania danych NTRIP. Do pomiarów testowych wykorzystano dwie permanentne stacje referencyjne należące do Uniwersytetu Warmińsko-Mazurskiego w Ol-

sztytnie. W wyniku pomiarów przeprowadzonych na trzech punktach pomiarowych, oddalonych od 1,5 do 20 kilometrów od stacji referencyjnych, uzyskano kilkucentymetrowe dokładności dla punktów zlokalizowanych na otwartym terenie. Dokładności uzyskane na punkcie, nad którym znajdowały się liczne zaslony w postaci gałęzi drzew, wahały się od kilkunastu centymetrów do prawie 3 metrów, co jest charakterystyczne dla pomiarów GPS wykonywanych w warunkach ograniczonej dostępności satelitów.

Introduction

Currently the satellite positioning method RTK/OTF (Real Time Kinematic/ On The Fly) is the technologically most advanced kinematic method for determining coordinates of points in real time. That method allows obtaining precise coordinates in real time thanks to which it finds wide application in numerous areas, including: land, water and air navigation, hydrography, road safety and first of all land survey measurements (e.g. BAKUŁA et al. 1998, CIEĆKO et al. 2006, GRZEGORZEWSKI et al. 2001, POPIELARCZYK et al. 2006).

GPS RTK measurement method is based on determining the coordinates of a mobile receiver (or a number of mobile receivers) in relation to the reference station transmitting continuously corrections/satellite observations. The set for GPS RTK measurements consists of a reference station and mobile receiver. The reference station is a land survey GPS receiver with the antenna centered on a point with known coordinates and a device for transmission of corrections. The mobile station on the other hand consists of land survey receiver with a GPS antenna, device for reception of data from the reference station and handheld computer in which the results of GPS/RTK measurement are recorded (*Ashtech Z-family...* 1998, *GPS Fieldmate...* 1998). Traditionally in RTK/OTF measurements local reference stations fixed for the time of measurement on the reference point and using radio-modem for GPS data transmission are used. That model requires the use of at least two satellite receivers and the distance between the mobile receiver and the reference station is limited by the radio-modem range, which is important particularly in case of dense buildings or measurements taken in forest conditions (BAKUŁA et al. 2006).

Currently, the network of permanent reference stations assuring continuous access to observations from reference stations with high accuracy is developing dynamically worldwide thanks to which performance of GPS RTK measurements using only one GPS receiver is becoming possible.

In Poland, the Main Office of Geodesy and Cartography is implementing a multifunction system of precise satellite positioning ASG-EUPOS that will encompass GNSS reference stations evenly spread (at the distance of ca. 70 km) over Poland and the neighboring countries (PODLASEK 2007). Correc-

tions from the reference stations will be transmitted using the INTERNET/GPRS technology (OSZCZAK et al. 2004), which currently is the most advanced method of GPS data teletransmission. The NTRIP system is one of the solutions allowing long distance transmission of the corrections. Under the name of NTRIP (Networked Transport of RTCM via Internet Protocol) the protocol of making available and transmitting the DGNSS (Differential GNSS) corrections allowing increasing of positioning accuracy in real time has been made available (PETERZON, 2004, LENZ, *Networked Transport of RTCM...*). Scientists from the Federal Agency for Cartography and Geodesy (BKG) and, as partners, employees from the University of Dortmund and specialists of Trimble Terrasat GmbH worked on creating and development of that new technique. NTRIP is based on stateless protocol of documents transmission HTTP 1.1 (Hypertext Transfer Protocol). NTRIP consists of the following components (Fig. 1):

- NTRIP Source, station or stations generating streams of GNSS data. Sources have their allocated (by administrator) unique names (mountpoint)
- NTRIP Server, software based in a PC, transmitting data from the NTRIP Source to NTRIP Caster. The password and the above mentioned name are allocated by the administrator
- NTRIP Caster, HTTP server – the main system component. Its task is to receive, copy and split the data (HTTP Splitter Server), allowing simultaneous access to data from one source to multiple users
- NTRIP Client, the user who may select a NTRIP Source/mountpoint from the list of currently available ones. The Client may transmit the data received to a GNSS receiver, record the data on the hard drive or transmit data to another IP address.

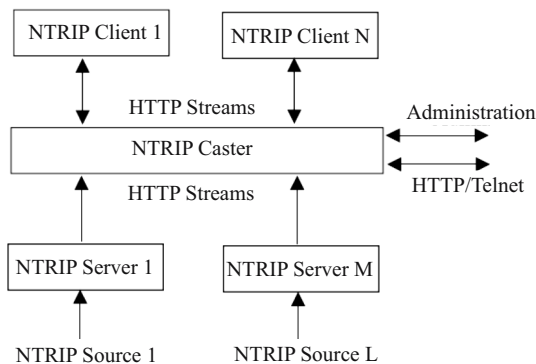


Fig. 1. Diagram of data distribution system operation using the NTRIP protocol (source BKG – Bundesamt für Kartographie und Geodäsie)

NTRIP protocol offers the possibility of making GNSS data available in two ways. The first way is transfer of data from a single reference station while the second one allows transmission of a stream of information from the reference stations (Fig. 2).

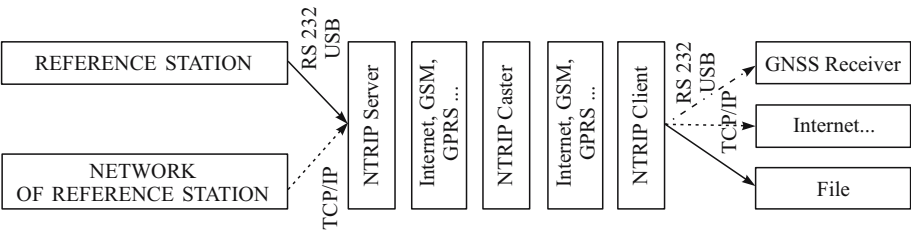


Fig. 2. Diagram of GNSS data presentation and transfer in NTRIP system

The paper presents the initial results of RTK measurements during which RTK corrections from reference stations were transmitted using the NTRIP technology.

Methodology of studies

Positioning of measurement points and reference stations

Three triangulation points (0474, 0409, 0016) situated in Olsztyn and vicinity and two reference stations: LAM6 belonging to the ASG-PL network, situated in Lamkówko at the geodesic satellite observatory of the University

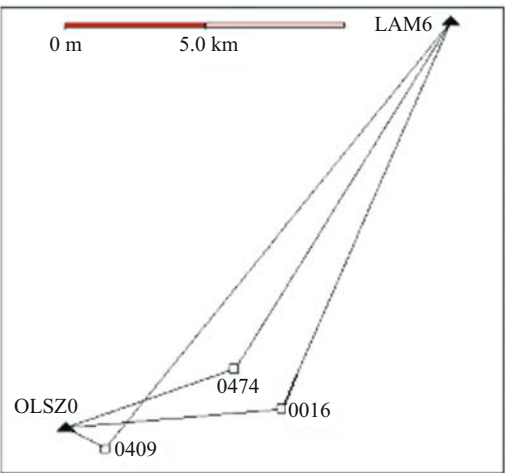


Fig. 3. Diagram of measurement points and reference station positions

of Warmia and Mazury in Olsztyn and OLSZ0, situated in the building of the Faculty of Geodesy and Land Management of the University of Warmia and Mazury in Olsztyn were selected for test measurements (Fig. 3).

Reference station OLSZ0 was included in the NTRIP system in September 2009. As of that moment satellite observations are both transmitted by NTRIP Server (Fig. 4) to NTRIP Caster and recorded on PC hard drive. Synchronized data with one-second interval are made available on current bases on a specially configured FTP server. In that reference station an Ashtech Z-XII receiver is working (Fig. 5). The GPS antenna is fixed on the roof

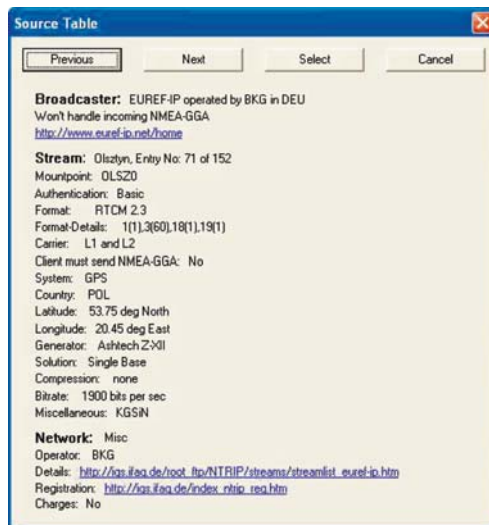


Fig. 4. NTRIP Server – information on OLSZ0 station



Fig. 5. Reference station OLSZ0

of a three-stores building. Differential adjustment data is transmitted using the RTCM-104 standard. The receiver was configured to transmit three types of messages. The first one is DGPS differential corrections broadcast at one-second interval. The second type of messages containing reference station coordinates is transmitted at one-minute interval. Carrier phase measurements and pseudorange measurements are broadcast once per second. The minimum topocentric height is set at 5 degrees.

LAM6 station is equipped with a ROGUE SNR-8000 receiver with an AOAD/M-T antenna. Adjustments from both stations can be transmitted via a radio-modem in GPRS technology and in NTRIP protocol while raw data is made available for post-processing.

Measurement points 0474 and 0016 were located in open terrain while point 0409 was overhang by terrain obstacles in the form of branches of deciduous trees (Fig. 6), which caused significant deterioration of measurement results in that point Measurement of the covered point allowed analysis of the cover influence on RTK measurements accuracy. All measurement points were permanently fixed with concrete blocks with a cross clearly marked at their upper face.



Fig. 6. Test points 0474, 0409, 0016

Distances of individual measurement points to the reference station OLSZO were a few kilometers (1,5 km, 6,4 km and 7,8 km respectively for points 0409, 0474 and 0016), while the distance to the LAM6 station several kilometers (19,6 km, 14,6 km and 15,1 km respectively for points 0409, 0474 and 0016).

Hardware and software

The mobile set used during the studies consisted of a land survey receiver Ashtech Z-Surveyor, GPS antenna by Ashtech mounted on two-meter pole, HUSKY controller and mobile telephone Motorola V547 with mobileNTRIP

v 1.0 software allowing reception of RTK corrections in NTRIP protocol (Fig. 7). The controller was configured so that the measurement results were recorded in the flat national system of coordinates “2000”, and height of points in the system of ellipsoid heights. Position recording interval was set at the level of 5 seconds but the actual interval ranged from 5 seconds to around 1 minute. That situation was caused by momentary loss of connection with the reference station and loss of ambiguity determination.



Fig. 7. Measurement set

RTK terrain measurements vs. post-processing

Test measurements were taken on 14-15 May 2007. The division into measurement sessions is presented in Table 1. Measurement time for individual points was planned so that the number of available satellites and their geometric distribution should guarantee achievement of high measurement accuracy and similar during all measurement sessions. The following GPS parameters were assumed for all measurement sessions: minimum height of satellites above the horizon 15° , measurement interval 1 s, and the assumed recording interval for RTK position was 5 s, the minimum number of satellites 5 and the value of PDOP < 6 .

As a result of measurements in consecutive sessions 26, 8, 29, 52, 52, 51, 52 positions were obtained respectively for which the ambiguity was solved. The results of measurements were recorded in a HUSKY controller in the text file containing such information as: consecutive position number, flat coordinates x,y for consecutive points in “2000” system, ellipsoid height and accuracy analysis.

Table 1

Schedule of division into measurement sessions

Session number	Measurement point number	Reference station	Date	Measurement performance time in UTC
1	409	OLSZ0	14.05.2007	11:08 – 11:23
2		LAM6		12:00 – 12:02
3		OLSZ0		12:46 – 13:02
4	474	LAM6	15.05.2007	8:20 – 9:00
5		OLSZ0		9:03 – 9:44
6	16	OLSZ0	15.05.2007	10:27 – 10:40
7		LAM6		10:48 – 11:28

On the basis of raw data from mobile receiver and data obtained from reference stations the coordinates of points 0409, 0474, 0016 were computed in post-processing. Data from station OLSZ0 had one-second interval while the interval of data from station LAM6 was 5 seconds. Ashtech Office Suit for Survey v 2.0. (*Ashtech Office Suit...* 1998) was used for computations. Coordinates of measurement points were computed by means of RTK/OTF kinematic post-processing method.

As a result of post-processing the total of 5958 positions were obtained including 4725 positions for which ambiguity was solved. During sessions 1-7 84, 0, 344, 475, 2500, 842, and 480 fixed type positions were obtained respectively. During the second measurement session no solution was obtained and because of that and because of a very low number of RTK positions computed the second session was excluded from further works.

Next, the coordinates computed were transformed into the flat system x,y “2000” using TRANSPOL software (Technical guidelines G-1.10... 2001). In that software the distance of geoid from the ellipsoid needed for reduction of ellipsoid heights to normal heights was also computed.

Analysis of results

Flat coordinates of measurement points obtained as a result of RTK/OTF measurements and post-processing were compared with the known coordinates of those points (in the system “2000”), that were considered the true ones (Fig. 8). On the basis of that comparison the accuracy of determination of coordinates for individual points during individual measurement sessions was made.

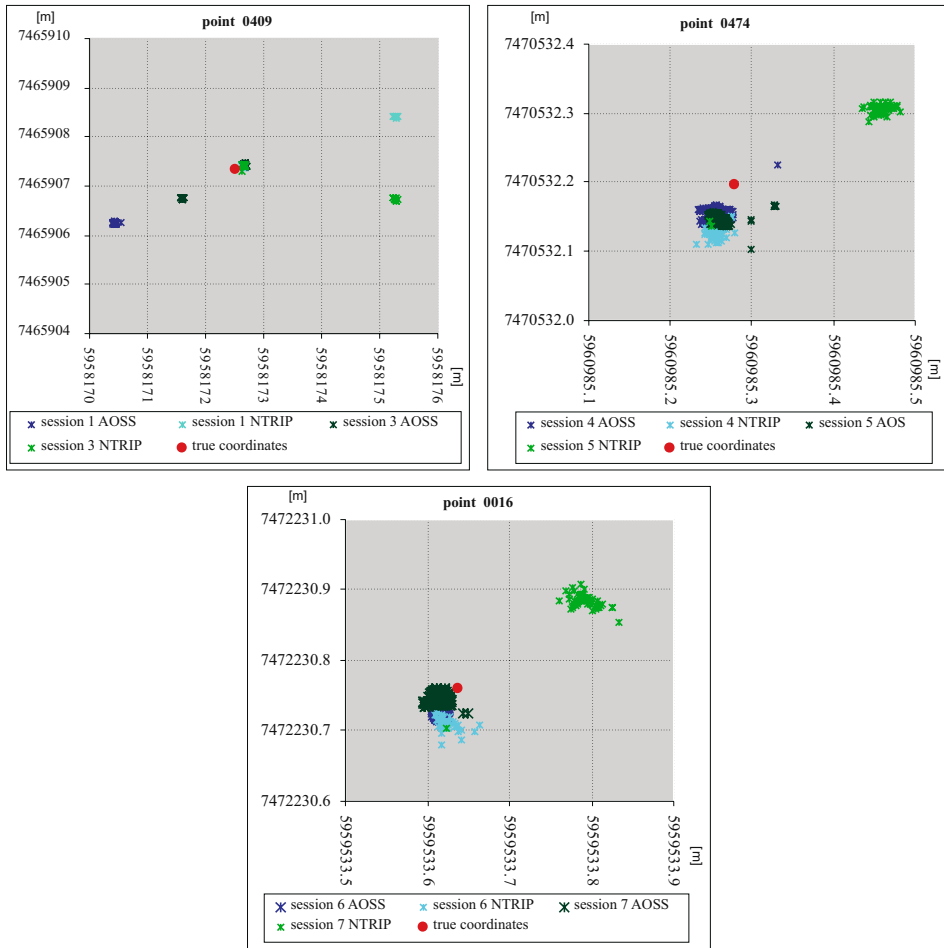


Fig. 8. Flat distribution of obtained coordinates in “2000” system

Accuracy of determination of point 0409 flat coordinates over which there were numerous obstructions in form of branches of deciduous trees ranged for RTK/OTF method from a few centimeters to almost 3 meters. In post-processing accuracy of from fifteen centimeters to almost 2,5 m was obtained (Fig. 9). Analyzing individual measurement sessions for point 0409 for both RTK method and post-processing groups of consecutive determinations of the position can be identified characterized by a relatively high precision. For RTK measurements in session 1 (reference station OLSZO) from the beginning of the session up to determination number twenty the determination accuracy was several centimeters and next it deteriorated rapidly to 3 meters and stayed

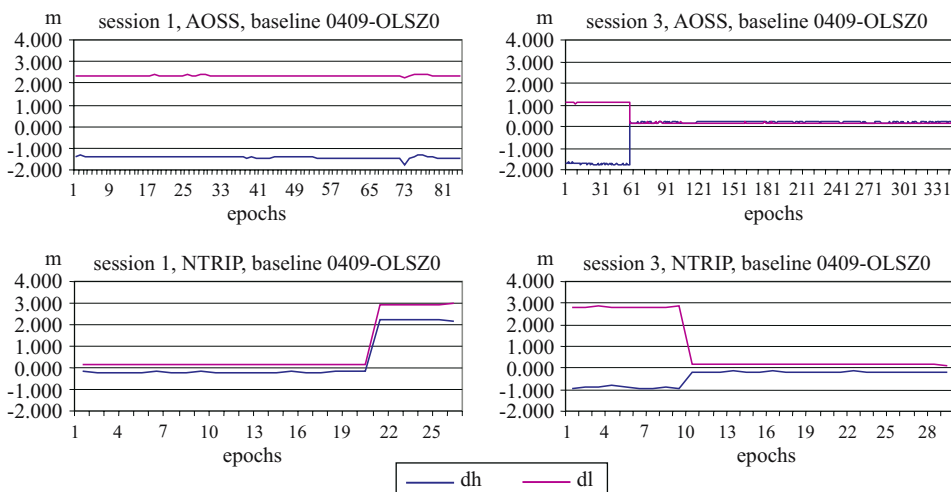


Fig. 9. Accuracies obtained for sessions 1 and 3

at that level until the end of the session. In post-processing on the other hand, during the entire first session the accuracy ranged from 2,26 m to 2,38 m. Obtaining the accuracy of almost 2,5 m in the first group of session one in post-processing while in direct RTK measurements accuracies of several centimeters were obtained for the same group may indicate that the computation algorithms of the receiver may allow obtaining better results under difficult observation conditions than the algorithms applied in computation software. During session 3 (reference station OLSZ0), from the session beginning up to a certain moment the accuracy was around 2,7 m for RTK method and over 1 m for post-processing and next it rapidly increased to 10-18 cm for RTK measurements and 15-25 cm for post-processing. It should be noticed that during session 3 increase in accuracy of coordinates determination is tightly linked with the increase of visible satellites and improved geometry of their distribution (Fig. 10.), while for session 1 the relation between accuracy and PDOP coefficient is not so obvious, which is characteristic for GPS measurements performed under conditions of limited access to the celestial sphere, particularly in case of covers in form of tree branches.

Flat coordinates of point 0474 were determined with accuracy better than 10 centimeters for both RTK method and post-processing in case of both OLSZ0 and LAM6 station with the exception of RTK/NTRIP results from session 5 (Fig. 11). Accuracy of determination of point 0474 coordinates by RTK method using corrections from OLSZ0 station was around 20 cm during the entire session and for LAM6 station it was several times better at 6

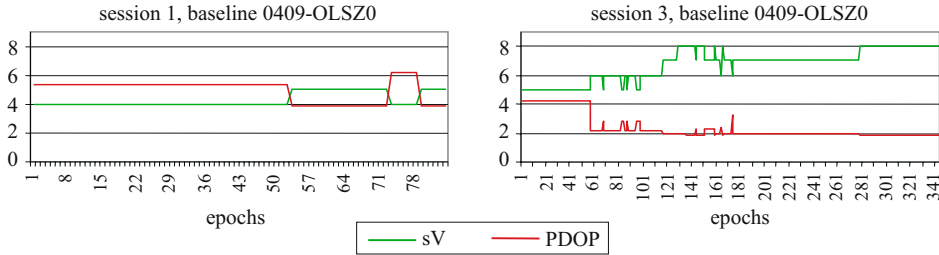


Fig. 10. PDOP coefficient value and number of satellites available during sessions 1 and 3

to 10 cm, which is surprising considering the fact that the distance of measurement point from LAM6 station was twice larger than the distance from OLSZ0 station and exceeded 14 km. Results obtained in post-processing were characterized by accuracy at the level of 3-7 cm for both reference stations, and the results obtained for OLSZ0 station were characterized by a slightly higher precision, which could be caused by changes in the PDOP coefficient value during the fourth measurement session (Fig. 12).

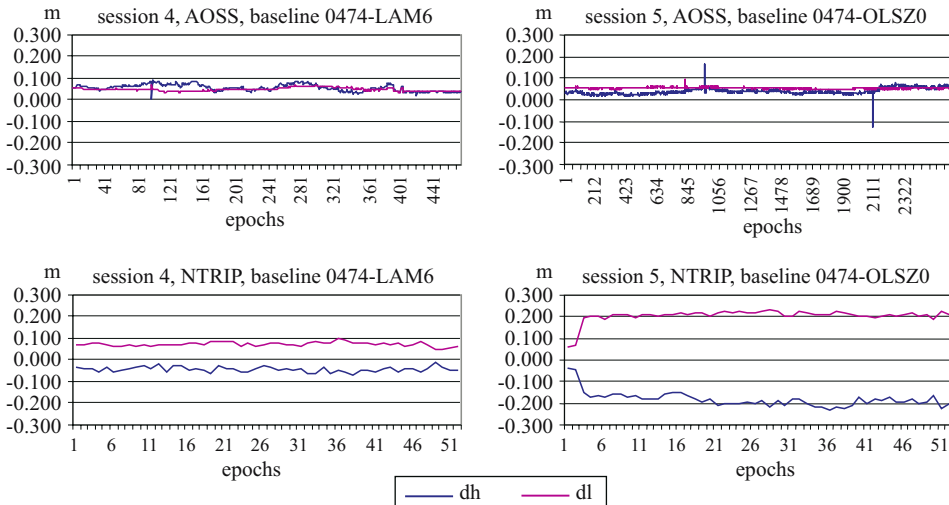


Fig. 11. Accuracy of measurement results for point 0474

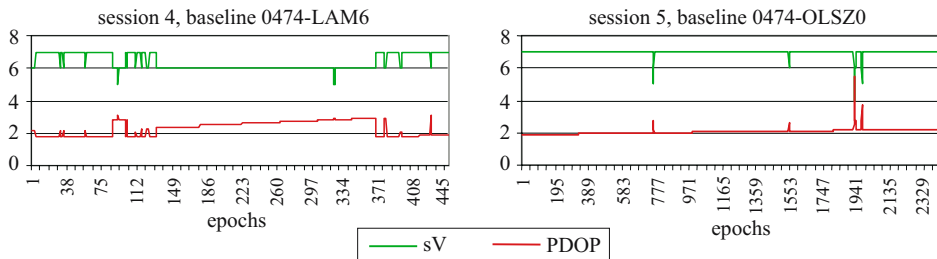


Fig. 12. PDOP coefficient value and number of satellites available during measurements at point 0474

During sessions 6 and 7, when coordinates of point 0016 were determined in RTK measurements accuracies of 4-8 cm and 6-22 cm respectively were obtained for flat coordinates, (Fig. 13), that is the opposite than in case of point 0474, better results were obtained using corrections from station OLSZ0 than from station LAM6, and the distance from points 0016 and 0474 to stations OLSZ0 and LAM6 were similar and they were for point 0016 7,8 km and 15,1 km respectively. In post-processing the accuracies of under 5 cm were obtained for both sessions and, similar to the case of point 0474 precision of the results obtained in post-processing was slightly higher for vector 0016-OLSZ0 than the vector 0016-LAM6. During the entire measurement from 6 to 9 satellites were available and the PDOP coefficient was 2-3, with the exception of rapid, short increase in its value during session 7 (Fig. 14).

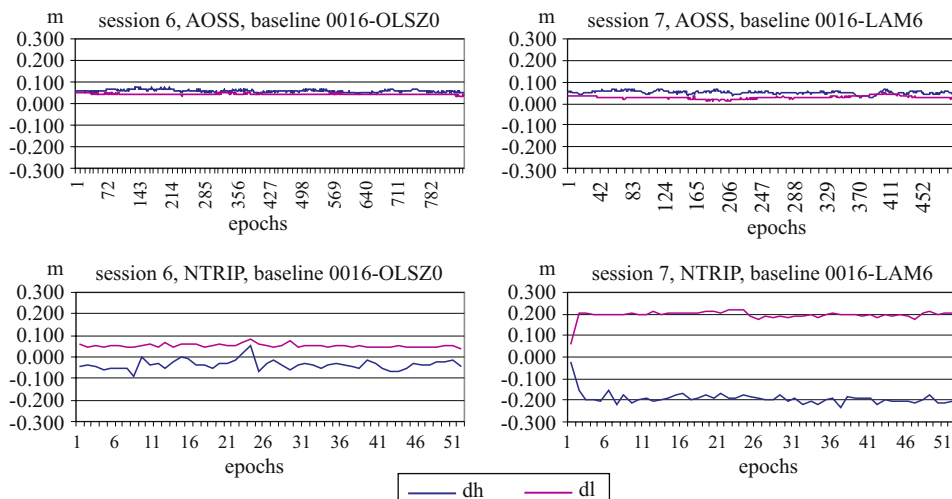


Fig. 13. Accuracy of measurement results for point 0016

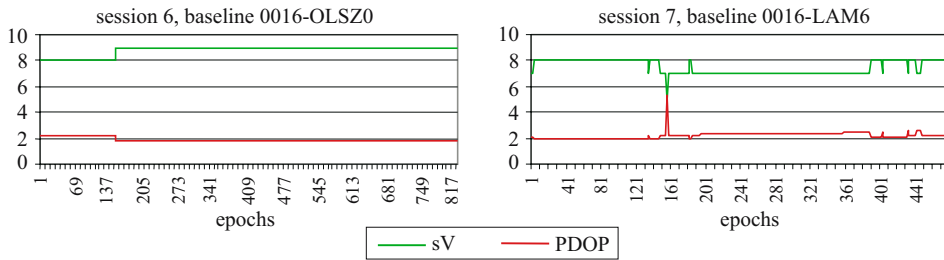


Fig. 14. PDOP coefficient value and number of satellites available during measurements at point 0016

Ellipsoid heights of measurement points obtained directly from RTK measurements results and computed in post-processing were reduced to normal heights (distance of geoid to ellipsoid was determined in TRANSPOL software) and next the results were compared to heights of those points considered true.

Accuracy of height determination for point 0409 ranged from several centimeters to over 1,7 m in post-processing and from 15 cm to over 2 m in RTK measurements. The heights determined, similar to flat coordinates for that point, were characterized by relatively high precision in individual groups. Height of points 0474 and 0016 were determined with the accuracy of below 10 cm with the exception of RTK measurements from sessions 5 and 7 for which the height determination accuracy was around 20 cm. Height determinations from sessions 4, 5, 6 and 7 were distributed in the same way as accuracies of flat coordinates although they were characterized by a slightly lower precision.

Summary and conclusions

Accuracy of results from measurements by RTK/OTF method using the NTRIP protocol for transmission of corrections, as indicated by the initial experiments, can be a few centimeters. Results of RTK measurements conducted under conditions of unlimited access to the celestial sphere actually match the results obtained in post-processing, although the results obtained directly from RTK/OTF measurements show a slightly lower precision than the results from post-processing.

On the other hand results of measurements conducted under conditions of access to the celestial sphere limited by numerous tree branches deserve attention. In this case characteristic decreases in accuracy of RTK/OTF measurements with the increase of PDOP coefficient occur although that dependence is not tight and as a consequence PDOP coefficient cannot be in

this case the reliable indicator of measurements accuracy. Inconsistency of RTK measurements results with the results obtained in post-processing is highly characteristic for GPS measurements conducted under forest conditions. On the basis of session 1 and referring to the experiments described in earlier literature it can be concluded that in certain situations it is possible to obtain much better accuracy in direct RTK measurements than in post-processing. This situation suggests that computation algorithms applied in the receivers are better and allow more accurate determination of coordinates under more difficult observation conditions than the algorithms of software applied.

RTK/OTF measurements with application of NTRIP technology may be applied with success in land survey measurements that require lesser than higher than one centimeter accuracy however particular care and limited confidence in measurement results should be applied under conditions of limited access to the celestial sphere. Measurements in difficult conditions should be made by experienced measurement teams and subjected to control (e.g. by multiple re-initialization on the point). It is also necessary to conduct comprehensive studies allowing assessment of accuracy as well as credibility and availability of RTK/NTRIP measurements under conditions of limited access to the celestial sphere.

References

- Ashtech Office Suite for Survey, User's Manual*. 1998. Ashtech and Spectra Precision Terrasat GmbH Germany, USA.
- Ashtech Z-family, Technical Reference Manual*. 1998. Ashtech, Magellan Corporation, USA.
- BAKUŁA M., KAPCIA J., OSZCZAK S. 1998. *Technika RTK GPS w pracach realizacyjnych na polach naftowych w Zjednoczonych Emiratach Arabskich*. Materiały konferencyjne z Seminarium Komisji Geodezji Satelitarnej PAN nt. „Zastosowanie technik kosmicznych w geodezji i geodynamice”, Wrocław.
- BAKUŁA M., OSZCZAK S. 2006. *Experiences of RTK Positioning in Hard Observational Conditions During Nysa Kłodzka River Project*. Reports on Geodesy, 1(76): 71-79, Vienna, Austria.
- CIECKO A., OSZCZAK B., OSZCZAK S. 2006. *Driver-By DTM – GPS and GSM Power Cost-Effective Terrain Modeling*. GPS Word, 17(4): 44-49.
- GPS Fieldmate, Operation and Reference Manual*. 1998. Ashtech, USA.
- GRZEGORZEWSKI M., OSZCZAK S., BAKUŁA M. 2001. *Badania nad precyzyjnym wyznaczeniem trasy lotu samolotu TS 11 ISKRA*. Zeszyty Naukowe WSOSP w Dęblinie, 2: 35-43.
- LENZ E., *Networked Transport of RTCM via Internet Protocol (NTRIP) – Application and Benefit in Modern Surveying Systems*. <http://www.fig.net>
- Networked Transport of RTCM via Internet Protocol (NTRIP)* ver. 1.0, <http://igs.bkg.bund.de/>
- OSZCZAK S., OSZCZAK B., GRYGORCZUK P. 2004. *Teletransmisja DGPS/RTK za pomocą GSM/GPRS z wykorzystaniem n-stacji referencyjnych i dedykowanych APN*. Seminarium nt. Satelitarne metody wyznaczania pozycji we współczesnej geodezji i nawigacji, Kraków.
- PETERSON M. 2004. *Distribution of GPS-data via Internet*. Information Technology Engineering at Uppsala University.
- PODLASEK S. 2007. *Trzy poziomy ASG-EUPOS*. Geodeta, 5(144): 24-26.

-
- POPIELARCZYK D., OSZCZAK S. 2006. *Application of Integrated Satellite DGPS/GPRS Navigation and Hydrographic Systems for Safe Sailing on Great Mazurian Lakes in Poland*. ION NTM 2006, Conference proceedings, pp. 188-194, Monterey, CA, USA.
- Wytyczne Techniczne G-1.10. Formuły odwzorowawcze i parametry układów współrzędnych. 2001. Główny Urząd Geodezji i Kartografii, Warszawa.

Accepted for print 6.10.2008 r.

TRIBOLOGIC PROPERTIES OF SELECTED MATERIALS

Marián Kučera, Ján Pršan

Department of Machine Design, Faculty of Engineering
Slovak University of Agriculture in Nitra

Key words: pin on disk test, adhesive wear, wear resistance.

Abstract

The contribution brings evaluation of selected materials regarding wear resistance in conditions of chosen experiment. Systemic approach to the task in question is emphasised. The results of basic material are compared to results of material of weld deposits. The results of tribologic experiment enable prediction of certain characteristics of friction pairs in conditions of particular friction node. The following materials had been chosen for the particular experiment:

- steel 12 050 (C45) in state after heat treat,
- steel 12 050 (C45) in state after hardening.

Selected materials are compared to weld deposits C 508 and C-64 after being welded on and heat treated. The tribologic experiment was carried out on device TE 97/A, which ranks in category of “pin – disk” test devices. The resistance of selected materials was evaluated regarding size of weight loss and regarding energy.

In the experiment conditions it was observed that combinations of material C 508 + C 64 indicated the best results for both categories of test samples. For this combination of material, not the state of heat treatment but good friction characteristics was determining

WŁAŚCIWOŚCI TRYBOLOGICZNE WYBRANYCH MATERIAŁÓW

Marián Kučera, Ján Pršan

Katedra Budowy Maszyn, Wydział Techniczny
Słowacki Uniwersytet Rolniczy w Nitrze

Słowa kluczowe: eksperyment: czop – tarcza, zużycie adhezyjne, odporność na zużycie.

Abstrakt

Przedstawiono ocenę wybranych materiałów w aspekcie ich odporności na zużycie w warunkach eksperymentu laboratoryjnego. Problem rozwiązywano systemowo. Wyniki dla materiału podstawowego porównano z wynikami uzyskanymi dla warstw napawanych. Uzyskane w eksperymencie trybologicznym wyniki pozwalają na predykcję właściwości par trących konkretnego wężla.

Do eksperymentu wybrano:

- stal 12 050 (C45) w stanie po uszlachetnieniu,
- stal 12 050 (C45) w stanie po hartowaniu.

Właściwości wybranych materiałów porównywano z właściwościami napoin utworzonych z materiałów C 505 i C 64 w stanie po napawaniu i obróbce cieplnej. Właściwy eksperyment trybologiczny realizowano, korzystając z urządzenia TE 97A, należącego do kategorii maszyn badawczych w układzie czop – tarcza. Odporność materiałów na zużycie oceniano na podstawie ubytków ich masy oraz zużycia energii.

Eksperyment wykazał, że w obydwu kategoriach próbek najlepsze wyniki osiąga się w kombinacji z materiałami C 509 + C 64, w których decydujący nie był ich stan obróbki cieplnej, lecz prawdopodobnie ich dobre właściwości cierne.

Introduction

Friction as an important physical effect required a lot of theoretic and experimental work to be understood. Many theories have evolved, explaining the effect in a more or less complex way. Systemic approach is necessary for the complex solution of friction and related attrition in both theoretic and experimental sphere. Regarding tribologic properties of materials, it is the right choice of material or material pair, geometric shape, roughness, etc. which is important. Regarding tribometry, it is a question of the test device, choosing own test methods as well as the right shape and size of the test samples. Choosing appropriate approach to solving the problem of adhesive friction and related wear is also very important.

Specific working conditions of agricultural machinery effect its working life. This is sometimes relatively short as a result of heterogenous forms of breaking the components and components' surface. Relative short working life of machinery's and devices' components in agricultural production is caused by (KUČERA 1991):

- excessive wear,
- variability of the work regime,
- aggressive environment.

For the purpose of handling durability it is necessary to recognize basic causalities and relations, which determine defects and decrease operating reliability.

For the specification of the reliability as a complex attribute of the system, analysis of operating conditions is the ultimate factor. Operating reliability of a machine is directly connected to problems arising in tribologic node of the machinery. It is place where functional parts of the node interact with each other with simultaneous affection of other factors.

Tribologic node:

- pin or shaft,
- sleeve bearing, shaft seal etc.,

- grease medium,
- environment,

ranks among frequent nodes in agricultural machinery and is very important for the transmission of the torque or power from engine to functional parts of adapters. The solution of a particular tribologic node requires systemic approach (BALLA 1979).

The problem is even more complicated in case of a need of supplying the worn surface. As it is tribologic node with weld deposit that is concerned, the knowledge of materials' properties, effect of alloying elements and effect of the welding technique on weld deposits' properties, is of the utmost importance (BLÁŠKOVÍČ, ČOMAJ 2006).

Adhesive wear is complicated process of damaging surface layers of friction pairs material during interaction of bearing surfaces undulations.

The pattern of the deformation depends on the penetration depth of irregularities into the other part's surface as well as on the radius of the particular penetrating irregularity. In case of elastic deformation, surface layers faults are of high-cycle contact fatigue pattern. In case of plastic deformation, the surface attrition is determined by low-cycle contact fatigue.

The contribution deals with possibility of prediction of friction pairs behaviour based on results of tribologic experiment. In this contribution we would like to mention several aspects of systemic approach to selection of material, preparation of samples and methods of testing in relation to agricultural machinery.

Within the experimental work, material used for production of components of "shaft, pin" type have undergone analysis. Selected materials were compared to each other as well as to weld deposits recommended by producers for refitting the worn surfaces.

Material and methods

We paid great attention to selection of appropriate material. We assessed components of shaft or pin – type of various agricultural devices (tractor, harvester, straw-cutter, mobile machines, etc.), with worn functional parts of cylindrical shape (KUČERA 1992).

We found out that 22 types of steel is used for production of group of 186 components:

3 types of steel class 11 (11 500, 11 523, 11 600)

4 types of steel class 12 (12 020, 12 050, 12 060, 12 061)

2 types of steel class 13 (13 240, 13 242)

8 types of steel class 14 (14 140, 14 220, 14 221, 14 223, 14 230, 14 231, 14 240, 14 331)

4 types of steel class 15 (15 130, 15 142, 15 230, 15 240)

1 type of steel class 16 (16 231)

More results arising from the observed group:

- 16.7% of components were manufactured from untreated steel
- 11.8% of components were treated, with exposition areas inductive hardened
- 38.2% of components were manufactured from treated steel
- 30.1% of components were cemented and hardened on exposition functional parts

Treatment itself or in combination with another type of heat processing was used for 52.7% of components.

From the group of materials mentioned above, the selected types of steel were chosen for purposes of the experimental wear resistance test:

- steel 11 500 (EN, E 295) as representative of steel type used in natural state
- steel 12 050 (EN, C45) as representative of steel type used after heat treated and inductive hardened
- steel 14 220 (EN, 16MnCr5) as representative of steel type used for components with cemented and hardened surfaces.

For the purpose of the particular experiment material C 45 was selected as representative of steel types used for manufacturing of components of “shaft-type” with treated and hardened surface.

This material was compared to weld deposits of additional material C 508, recommended by manufacturer for hard surfacing of worn surfaces of shafts without heat treatment. The samples were hard surfaced on material C 45 of tubular shape using welding technique in shielding gas MIG/MAG, by unifilar and two-wire process.

Selection of test methods and test devices

For the selection of test methods, test devices and evaluation of results, definition of wear according to STN 01 5050 was followed:

Wear (attrition, deterioration) is undesirable change in surface or size of solid entity, that is caused either by interaction of functional surfaces or interaction of functional surface and medium, which starts the wear. Wear is demonstrated as removing or transferring elements of surface by mechanical motivation.

Regarding this definition we decided for:

- adhesive wear test without greasing

Tests were executed on test device of type TE 97/A – Fig.1, which ranks among “pin-disk” devices with flat contact of friction nod elements. The test

device is suitable for comparison tests of selected materials. The fundamental of the test is that test samples of pin shape are imprinted to facing surfaces of rotating disk using hydraulic cylinder and constant force. Pins have been manufactured from material C 45 plus another weld deposits mentioned above. The counter part was made of material 12 020 (C 15 E).

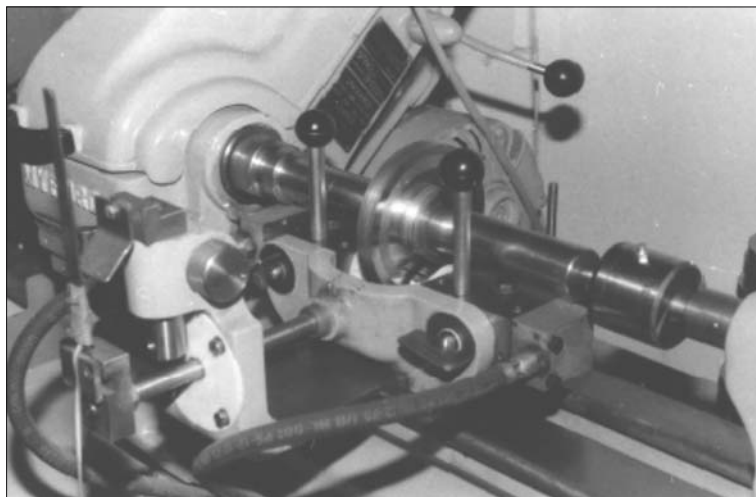


Fig. 1. View of active part of device TE 97/A

Test parameters

Test parameters were selected from test parameters of adhesive wear test without greasing used in tribologic laboratory in order to enable the best possible comparison of tribologic properties of supplied samples.

Parameters of the test are as follows:

– pressure in hydraulic circuit	1.47 MPa
– compressive force on the pin	74.3 N
– surface speed of the test radius	3.2 m.s ⁻¹
– exposition time	15, 30, 45, 75 s
– material of the counter part	steel 12 020
– dimensions of the sample	8 x 50 mm

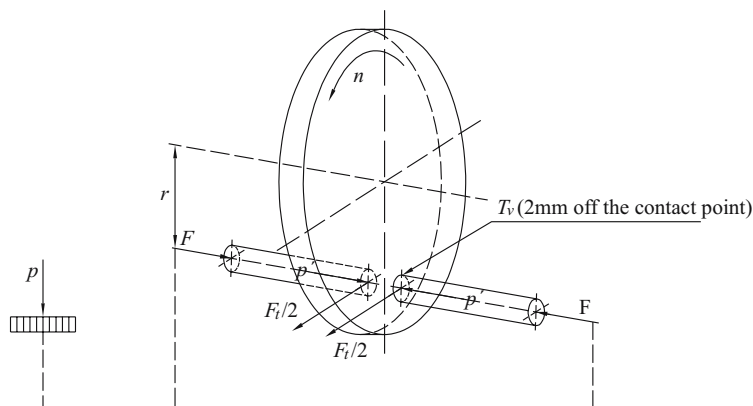


Fig. 2. Illustrates principled scheme of device TE 97/A

Preparation of samples

Hard surfacing was executed on experimental welding machine ENZ-100 in shielding gas CO_2 . The samples for adhesive wear resistance test were welded on bar of 105 mm in diameter made of material C 45 by rotating welding technique. For every sample 20 to 25 mm were welded on. The welding-on parameters are listed in Table 1. After cooling, the samples were lathed into ring shape, which was then divided in 15 parts. Another latheing prepared the active part of the sample (Fig. 3c), which was imbeded into counter part and pasted by aldurit. The thickness of the weld deposit on the facial surface after completion was 2 mm. Four pairs of test samples were prepared from each weld deposit. After heat treatment, the elements were modified according to (Fig. 3d) and lathed to final measure 8 mm in diameter.

Table 1
Parameters of hard surfacing of samples for wear test without greasing

Additive material			Speed of feeding [m min ⁻¹]		Intensity of hard surface flow [A]	Arc voltage [V]	Rotation speed of spindle [min ⁻¹]	Weld deposit gradient [mm min ⁻¹]	CO ₂ consumption [l min ⁻¹]
OD	SD	ØOD/ØSD [mm]	OD	SD					
C508	–	1.2 / 0	4.7	–	165	20	2.5	5	12
C508	C64	1.2 / 0.93	3.4	2.4	115	20	1.7	5	12
2xC508	–	2x 1.2 / 0	2.0	–	145	20	2.2	5	12

OD – arc wire, SD – cold wire

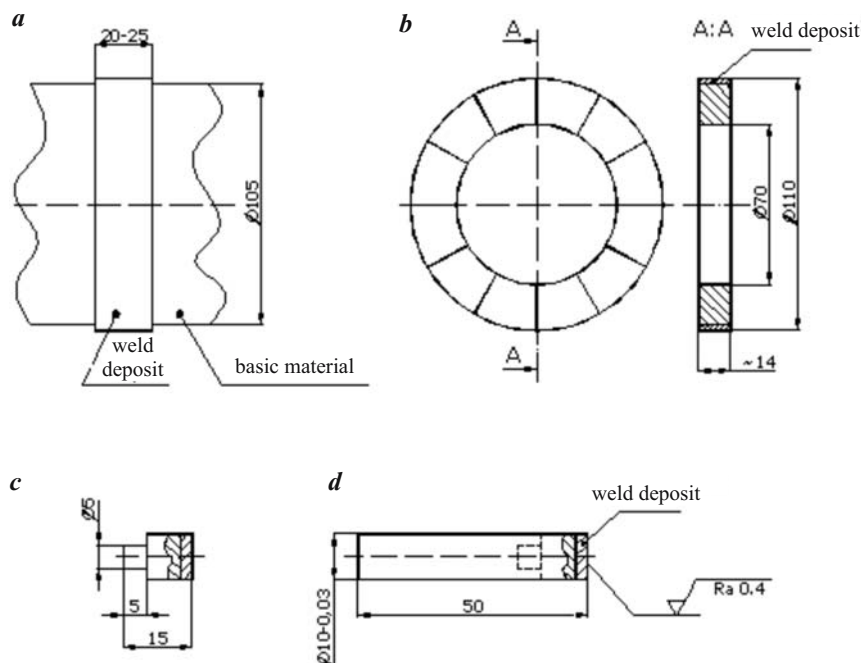


Fig. 3. Preparation of test element: a) weld deposit on basic material, b) partition of the ring into 12 parts, c) active part of the sample, d) test element before the final treatment

Despite being difficult, the way of samples preparation mentioned above guaranteed, that the active part of the samples, especially in case of weld deposits, will correspond with real surfaces as far as behaviour is concerned.

Figure 3 shows our approach to testing the wear of sliding nod using chosen material pairs in conditions which simulate part of real nod's surface. Cross comparison of different materials of samples was possible thanks to material of the counter part being the same in each sequence of the test. Conditions of the test followed the methodology elaborated by prestigious test stations. After consultations with workers from these stations we decided to evaluate the energy demandingness of the wear process. This method appeared convenient especially for comparison of wear resistance of basic material with properties of weld deposits (BLÁŠKOVÍČ 1990).

The same procedure was used for preparation of elements made of basic material C 45, as comparative material.

Characteristics of test elements, the status of their heat treat and temper is shown in table 2. Figure 4 illustrates shape and dimensions of the disk for adhesive wear test without greasing.

Table 2

Samples characteristics for wear test without greasing

Sample no.	Basic material	Additive material	Heat treatment	Surface hardness (HV)
1	12 050 (C 45)	C 508	Hardening 850°C/water,tempering 170°C/1h./air	554
2	12 050 (C 45)	C 508+C64	Hardening 850°C/water, tempering 170°C/1h./air	598
3	12 050 (C 45)	2 x C 508	Hardening 850°C/water, tempering 170°C/1h./air	527
4	12 050 (C 45)	–	Hardening 850°C/water, tempering 170°C/1h./air	606
5	12 050 (C 45)	C 508	–	368
6	12 050 (C 45)	C 508+C64	–	368
7	12 050 (C 45)	2 x C 508	–	q296
8	12 050 (C 45)	–	Hardening 850°C/water, tempering 650°C/1h./air	256

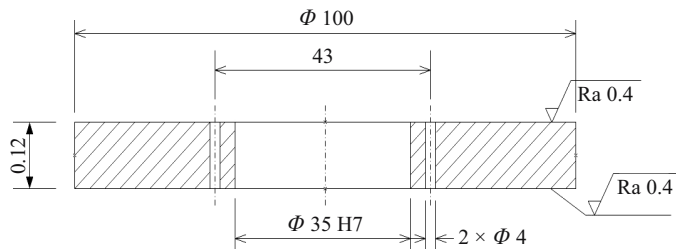


Fig. 4. Shape and dimensions of the disk for wear test without greasing

During the test, changes in friction force are scanned and recorded. The friction force was scanned and recorded by tensometric scanner. The record of the course of friction force enables evaluation of:

- Maximum friction force,
- Mean value of the friction force,
- Frictional labor,
- Friction factor.

The wear of the samples was detected by direct observation before and after the test. After proper degreasing and drying, samples were weighted on

analytic scales MEOPTA. The result of the wear test on device TE 97/A is diagram showing the relation between extent of wear and time of test.

We used coefficient of tribologic capacity K^* as criteria for evaluation of the result of the wear test without greasing on device TE 97/A. K^* expresses quantity of friction labor needed for detachment of unit quantity of material.

The hardness was measured on the front of the samples i.e. at the point of interaction of the sample with testing disk. Hardness tester MEOPTA – VICKERS with load of spire $F = 295,3$ N was used for measuring.

Evaluation of results

In case of tests without greasing, we detected the quantity of friction labor – from the course of friction force at given time – and its contribution to weight loss – coefficient K_{VZ} , (K^*).

Coefficient K^* is referred to as coefficient of tribologic capacity of weld deposits (materials).

Comparing the rate of wear and friction labor to material etalon we get K_N coefficient, which is referred to as coefficient of relative tribologic capacity of weld deposit (material). Besides these criteria, our test type enables defining:

- ratio of friction coefficient to weight loss,
- coefficient K^* to weight loss,
- coefficient K_N to weight loss.

Criteria K_N accepts physical nature of detachment of surface particles during friction.

Interpretation of results of adhesive wear test without greasing

The objective of adhesive wear test without greasing on device TE 97/A was to assess:

- weight loss of basic materials and weld deposits,
- coefficient of tribologic capacity of weld deposits,
- ratios of friction coefficient to values of weight loss,
- transfer of material for selected pairs, nature of transferred elements and its chemical composition.

We observed weight loss relating to time on device TE 97/A (Fig. 1).

Results were obtained by weighing the samples before and after the test.

$$\Delta m = m_o - m_1, \text{ g} \quad (1)$$

We detected the wear rate at exposition time of 15, 30, 45, 75 seconds. The results are listed in table 3.

Results of adhesive wear test without greasing on device TE97/A

Table 3

Sample no.	Material	Heat treatment	Wear W_0 , mg after test time [s]			
			15	30	45	75
1	C 508	Hardening	1.4	4.65	5.5	6.95
2	C 508 + C 64	Hardening	1.65	4.5	8.45	5.2
3	2 x C 508	Hardening	1.35	3.35	4.75	5.3
4	12 050	Hardening	1.25	1.85	1.85	8
5	C 508	–	2.3	2.85	5	7.3
6	C 508 + C 64	–	0.05	0.2	1.45	4.95
7	2 x C 508	–	1.1	5.45	2.8	8
8	12 050(C 45)	Heat treated	2	1.1	1.8	6.6

Graphic presentation of the results of the adhesive wear test without greasing on device TE 97/A is shown in Figure 5 and 6.

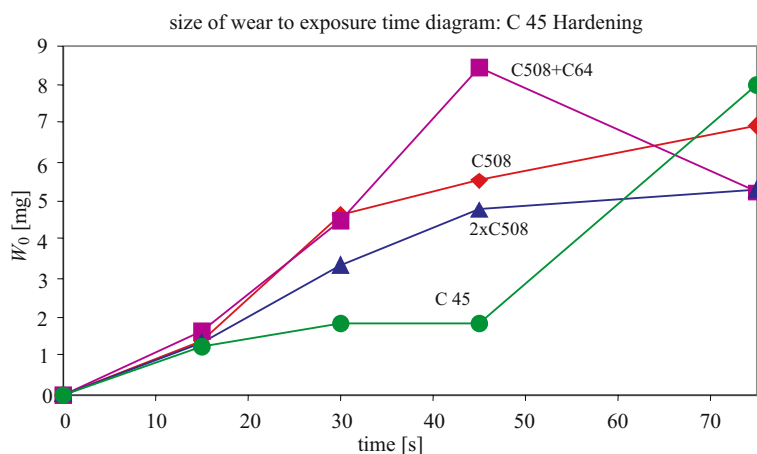


Fig. 5. Size (W_0 , mg) to exposure time diagram for selected group of test material C45 in state after hardening

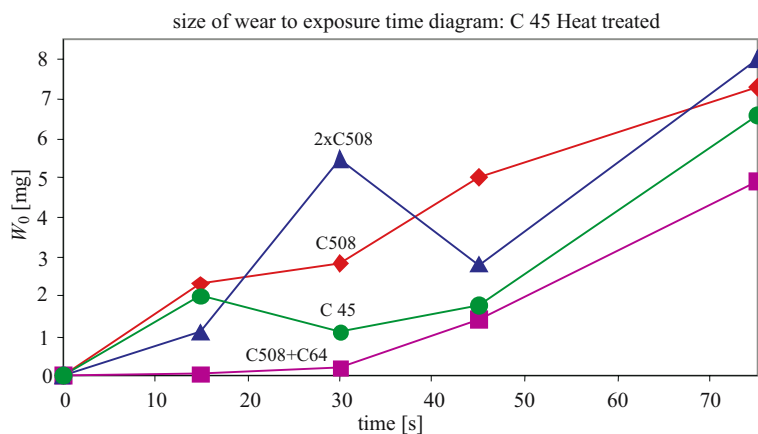


Fig. 6. Size (W_0 , mg) to exposure time diagram for selected group of test material C45 in state after heat treated

To simplify the evaluation of results, two groups of samples were formed. The first group involves hardened samples. That means, that basic material was hardened and weld deposits for this material were heat treated – inductive hardened – too. The second group involves treated material. Only basic material was treated. Weld deposits for this material were not heat treated after being made.

Based on results listed in table 3 and shown in Figure 5 and 6, we may point out, that sample no. 2 with weld deposit marked C508 + C64 indicated minimum wear from the first group of samples, i.e. for treated steel. Sample no. 3, i.e. 2xC508, indicated very similar values. Sample no. 4, i.e. basic material, indicated the highest value of wear rate.

In case of the second group of samples, treated samples, weld deposit labelled C508+C64 indicated minimum loss. But as contrasted to treated steel, the major weight loss was not indicated for basic material, but for weld deposit marked 2xC508.

We may state, that samples with weld deposits made with combination of additional materials C508+C64 are the best of the whole group, while it is not the hardness that plays the decisive role, but probably good frictional attributes of the combination of additional materials. It must be stressed out, that during surfacing with technology MAG the degree of mixing of weld metal with basic material is 20 to 30%. The degree of mixing declines as cold wire is added. That means, the weld deposit has approximately the same properties as additive material, therefore it shows satisfying results in the area of adhesive wear.

Evaluation of tribologic capacity

In laboratory conditions, weight loss of weld deposits W_0 was observed on devices, which enable observing the course of friction force F_T during loading by constant force F_N at given time t . Time t is proportional to friction path L .

Based on the fact introduced above we may describe friction labor A , N.m. as follows:

$$A = \int_0^t F_T \cdot t \cdot dt \quad (2)$$

When relating the friction labor to unit weight (volume) of worn weld metal, we get relation:

$$K^* = \frac{A}{W_0}, \text{ Nm kg}^{-1} \quad (3)$$

K^* value is referred to as coefficient of tribologic capacity of weld deposits and expresses the quantity of friction labor needed for detachment of unit quantity of weld material.

If we relate values of the wear W_0 and friction labor A to etalon material, then it may be stated:

$$K_N = \frac{K_s^*}{K_e^*} = \frac{\frac{A_s}{W_{0s}}}{\frac{A_e}{W_{0e}}} = \frac{A_s}{A_e} \cdot \frac{W_{0e}}{W_{0s}} \quad (4)$$

A_s – friction labor of the sample, J,

A_e – friction labor of etalon, J,

W_{0s} – wear of sample, g,

W_{0e} – wear of etalon, g,

K_N is referred to as coefficient of relative tribologic capacity of weld deposit.

Table 3 displays results of the hardness testing at body front of samples and as well calculated values of coefficient of tribologic capacity of weld deposits K^* and coefficient of relative tribologic capacity of weld deposits K_N .

Table 4

Chart of hardness as measured, K^* and K_N

Sample no.	Material	Heat treatment	Hardness HV	K^* (Nm kg ⁻¹)·10 ⁸	K_N –
1	C 508	Hardening	554 – 620	2.382	1.536
2	C 508 + C 64	Hardening	598 – 626	3.841	2.478
3	2 x C 508	Hardening	527 – 586	3.062	1.976
4	12 050	Hardening	606 – 644	2.446	1.578
5	C 508	–	368 – 400	2.348	1.514
6	C 508 + C 64	–	368 – 398	3.339	2.153
7	2 x C 508	–	269 – 297	1.754	1.131
8	12 050 (C 45)	Heat treated	256 – 262	3.141	2.026
etalon	12 020(C 15 E)	–	160 – 180	1.55	1

K_N criteria accepts physical basis of detachment of particles from the surface during friction process and enables assessment of weld deposits for tribologic use.

To assess the suitability of weld deposits using coefficients of tribologic capacity we operated with two material groups again.

The first group involves samples made of steel C 45 hardened (samples 1-4) and samples with weld deposits after hardening. Within evaluations according to coefficient of tribologic capacity of weld deposits K^* , the highest values were achieved for weld deposits made with combination of additive material C508+C64. Based on K^* value we point out, that weld deposits of the combination of materials mentioned above achieve the highest adhesive wear resistance in given conditions. Slightly lower values achieved sample no. 3 with additive material 2xC508. The lowest values achieved sample no. 1 with additive material C508. It is necessary to notice that single additive material marked C508 attains lower order values than C508 in combination. Practically, it is therefore much more convenient to use this additional material in combination, either with cold wire C64 or for welding with two-wire 2xC508.

In case of the second group of materials (samples 5-8) (only basic material was treated), within evaluations according to coefficient of tribologic capacity of weld deposits K^* , the highest values were achieved for weld deposits made by combination of additive material C508+C64. At this point it is possible to observe, that the basic material C 45 achieved very similar values. The order of other materials was: material C508 and 2xC508. Samples of weld deposit made with additive material marked 2xC508 attained low K^* values. Practically, this presents the lowest adhesive wear resistance in given conditions.

The evaluation of weld deposits using K_N coefficient, following the relation (4), accepts physical nature of detachment of particles related to etalon.

Conclusion

The objective of this contribution was not to present results of friction and wear test, but to mention possible solutions of the problem. Some results are presented “in alieno loco” and can be found in literature listed below. From the observation that was carried out during many experiments we find it necessary to mention the importance of systemic approach in each sequence of given experiment. This regards:

- selection of material,
- difficulty of experiment,
- availability of test devices,
- evaluation methods of results,
- application of results, etc.

Today, it is necessary to extend this problem to area of non-stationary processes and to utilize attainable methods for mathematic simulation of specific processes.

This article developed within the context of designing the research target:

- VEGA 148/03 110: Design of experimental testing methods and parameters simulation and characteristics of sliding nodes for agricultural machines.
- VEGA 1/0712/08: The analysis of random loading process on tribologic properties of selected materials.

References

- BALLA J. 1979. *Systémovo – analytické riešenie tribologických problémov poľnohospodárskych strojov*. Habilitačná práca, Nitra.
- BLÁŠKOVIC P. 1990. *Hodnotenie tribologickej únosnosti návarov*. Sympóziu Intertribo 1990, Vysoké Tatry.
- BLÁŠKOVIC P., ČOMAJ M. 2006. *Renovácia naváraním a žiarovým striekaním*. STU v Bratislave, ISBN 80-227-2482-3.
- KUČERA M. 1988. *Výskum možností mechanizovaného nanášania vrstiev pri renovácii súčiastok*. Nitra VÚPT, Záverečná správa.
- KUČERA M. 2006. *Analýza trecích dvojíc a skúšky opotrebenia materiálov. Analysis of friction pairs and test of wear of materials*. In: Zborník vedeckých prác „Nové trendy v konštruovaní a v tvorbe technickej dokumentácie 2006“, Nitra, Slovenská poľnohospodárska univerzita, s. 132-135. ISBN 80-8069-701-9.
- KUČERA M. 2006. *Tribologický experiment a analýza produktov opotrebenia. Tribological experiment and analysis of products of wear-out*. In: Zborník vedeckých prác „Nové trendy v konštruovaní a v tvorbe technickej dokumentácie 2006“, Nitra, Slovenská Poľnohospodárska Univerzita, s. 132-135. ISBN 80-8069-701-9.
- KUČERA M. 1991. *Vlastnosti vrstiev navarených v ochrane CO₂ určených pre renováciu v poľnohospodárstve*. KDP, SPU, Nitra.

ELECTROMAGNETIC FORCES IN POLARIZABLE, MAGNETIZABLE, CONDUCTING MEDIUM

Zofia T. Kurlandzka

Department of Technological and Computational Education
University of Warmia and Mazury in Olsztyn

Key words: electromagnetic field, polarization and magnetization currents, polarization and magnetization charges, electromagnetic force, electromagnetic stress.

A b s t r a c t

The aim of the paper is an extension of the Dixon-Eringen (DIXON, ERINGEN 1965) model of the polarizable and magnetizable deformable dielectric to the media with conductivity. The author starts with the microscopic model assuming that besides the electric dipoles, which are taken into considerations in the Dixon-Eringen model, the magnetic dipoles according to the Chu concept of magnetization and free charges are present (FANO, CHU, ADLER 1960). Hence the macroscopic polarization, magnetization, conductive and convective currents densities, polarization and magnetization charges and currents densities are derived. Basing on these results the Lorentz force is obtained. In result the electromagnetic volume force and the electromagnetic stresses are received. In a sense they are an extension of the Dixon-Eringen model of electromagnetic interactions in the deformable dielectric to the polarizable, conducting media.

SILY ELEKTROMAGNETYCZNE W OŚRODKU Z POLARYZACJĄ, MAGNETYZACJĄ I PRZEWODNOŚCIĄ

Zofia T. Kurlandzka

Zakład Edukacji Technicznej i Informatycznej
Uniwersytet Warmińsko-Mazurski w Olsztynie

Słowa kluczowe: pole elektromagnetyczne, ładunki polaryzacji i magnetyzacji, prądy polaryzacji i magnetyzacji, siły elektromagnetyczne, naprężenia elektromagnetyczne.

A b s t r a k t

Celem pracy jest uogólnienie modelu dielektryka odkształcalnego Dixona-Eringena (DIXON, ERINGEN 1965) na ośrodek z przewodnością. Przyjęto koncepcję mikroskopowej struktury ośrodka jako składającej się z dipoli elektrycznych, dipoli magnetycznych, które zgodnie z hipotezą Chu są

odpowiedzialne za magnetyzację (FANO, CHU, ADLER 1960), oraz ładunków swobodnych. Następnie na podstawie tego modelu określono makroskopowe wielkości, jak: polaryzacja, magnetyzacja, gęstości ładunków swobodnych, prądu przewodzenia i konwekcyjnego oraz gęstości ładunków i prądów polaryzacji i magnetyzacji. Na podstawie tych wielkości wyznaczono elektromagnetyczne siły objętościowe i naprężenia elektromagnetyczne. Uzyskane wyniki są uogólnieniem modelu dielektryka Dixona-Eringen, w którym nie występuje magnetyzacja na polaryzowalny ośrodek przewodzący.

Introduction

The aim of the paper is an extension of the Dixon-Eringen model of the ideal deformable dielectric to the model of the polarizable, magnetizable and conducting media.

R.C. Dixon and A.C. Eringen assumed a microscopic concept of the dielectric as the medium consisting of the electric dipoles and quadrupoles. Basing on the assumption, that on any charge of the dipole and of the quadrupole the Lorentz force acts, by means of an averaging procedure the electromagnetic force acting on the volume element of the medium was received. The assumption of the electric quadrupoles leads to the model of the polar dielectric. If the quadrupoles are neglected, the symmetric stress tensor is received.

The very same procedure, if it is assumed, that beside the electric dipoles there are free charges connected with the conductivity leads to the terms, which can not be expressed by means of the macroscopic electromagnetic quantities. However it turned out, that if the Chu concept (CHU, FANO, ADLER 1960) of polarization and magnetization charges and currents is applied, the microscopic approach after averaging procedures leads to the macroscopic electromagnetic quantities such as free charges and conductive and convective currents densities, polarization, magnetization, polarization and magnetization charge and currents densities. Basing on these quantities and the concept of the macroscopic Lorentz force the electromagnetic volume force and electromagnetic stresses are derived. The results are an extension of the Dixon-Eringen interactions in the polarizable deformable media to the interactions in polarizable deformable media with conductivity.

Charges and currents

Let us consider a volume dv of a medium. Let \mathbf{x} denotes a position of its mass center. It is assumed, that in the volume there are the electric dipoles consisting of the couple of electric positive and negative charges q_{α}^{+} , q_{α}^{-} , $q_{\alpha}^{-} = -q_{\alpha}^{+}$, the magnetic dipoles of positive and negative magnetic charges μ_{γ}^{+} ,

$\mu_\gamma^+, \mu_\gamma^- = -\mu_\gamma^+$, and the free electric charges q_β^f . In the absence of an external electromagnetic field the positive and the negative charges of the electric and of the magnetic dipoles occupies the same place given respectively by means of the position vectors $\mathbf{x} + \xi_\alpha, \mathbf{x} + \xi_\gamma$. Under influence of the external electromagnetic field the charges move. The positive and the negative charges of the electric dipoles change their position respectively to $\mathbf{x} + \xi_\alpha^+, \mathbf{x} + \xi_\alpha^-$ while the positive and negative magnetic charges to $\mathbf{x} + \xi_\gamma^+, \mathbf{x} + \xi_\gamma^-$.

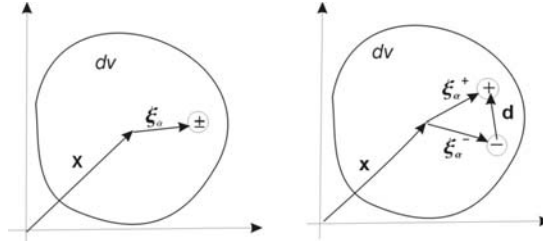


Fig. 1. The electric dipole before and after polarization

The electric and the magnetic moments of the dipoles are respectively

$$q_\alpha^+ (\xi_\alpha^+ - \xi_\alpha^-), \mu_\gamma^+ (\xi_\gamma^+ - \xi_\gamma^-) \quad (1)$$

The motion of the free charges under influence of the external electric field generates an electric current

$$q_\beta^f (\dot{\mathbf{x}} + \dot{\xi}_\beta) \quad (2)$$

where $q_\beta^f \dot{\mathbf{x}}$ is the convection current and $q_\beta^f \dot{\xi}_\beta$ is the conduction current (ERINGEN, MAUGIN 1989, FANO, CHU, ADLER 1960).

The electric and magnetic moments cause polarization and magnetization of media. The electric and magnetic charge densities q, μ , the electric current density \mathbf{j} , the polarization and magnetization densities \mathbf{p}, \mathbf{m} are defined by means of the formulas

$$\begin{aligned} q dv &= \sum_\beta q_\beta^f, \mathbf{j} dv = \sum_\beta q_\beta^f (\dot{\mathbf{x}} + \dot{\xi}_\beta) = q \mathbf{v} dv + \mathbf{j} dv \\ \mathbf{p} dv &= \sum_\alpha q_\alpha^+ (\xi_\alpha^+ - \xi_\alpha^-), \mathbf{m} dv = \sum_\gamma \mu_\gamma^+ (\xi_\gamma^+ - \xi_\gamma^-) \end{aligned} \quad (3)$$

The term $q\mathbf{v}$ denotes the density of the convective current, \mathbf{j} is the conduction current density, \mathbf{v} a velocity of the mass center of the volume element dv .

Under influence of the external electric field the positive charges of the electric dipoles move to the surface in the direction of the polarization vector \mathbf{p} , while the negative charges move in the direction opposite to the polarization vector. Thus on the surface da of the volume dv the external electric field generates the surface charge

$$\mathbf{p} \cdot \mathbf{n} da$$

where \mathbf{n} denotes the normal unit vector external to the surface da .

Let q^p denotes the volume density of the polarization charges. The total number of the positive and of the negative charges of the electric dipoles before polarization and in the polarized body remains the same. In the polarized body the total number of these charges consists of the surface charges on the surface S

$$Q^p = \oint_S \mathbf{p} \cdot \mathbf{n} da = \oint_S \sigma^p da$$

where σ^p is the surface density of the polarization charges and from the charges in the volume V of the body

$$\int_V q^p dv$$

Here q^p denotes the volume density of polarization charges. Thus

$$\oint_S \mathbf{p} \cdot \mathbf{n} da + \int_V q^p dv = 0$$

Hence by means of the Green theorem

$$\oint_S \mathbf{p} \cdot \mathbf{n} da = \int_V \text{div} \mathbf{p} dv = - \int_V q^p dv$$

the volume and surface densities of the polarization charges are respectively

$$q^p = -\operatorname{div} \mathbf{p}, \quad \sigma^p = \mathbf{p} \cdot \mathbf{n} \quad (4)$$

An analogous analysis of the magnetization leads to the conclusion, that the surface and the volume densities of the magnetic charges are

$$\sigma^m = \mu_0 \mathbf{m} \cdot \mathbf{n}, \quad q^m = -\mu_0 \operatorname{div} \mathbf{m} \quad (5)$$

where μ_0 is the permeability of free space.

The electric and magnetic charges densities change in time. The changes are due to the dependence of the electromagnetic field on time and due to the deformation of the body. Taking into account the charge conservation

$$\oint_S \mathbf{j} \cdot \mathbf{n} da + \frac{d}{dt} \int_V q dv = 0$$

and (4), (5)

$$\int_V q^p dv = - \int_V \operatorname{div} \mathbf{p} dv = - \oint_S \mathbf{p} \cdot \mathbf{n} da$$

$$\int_V q^m dv = - \int_V \mu_0 \operatorname{div} \mathbf{m} dv = - \oint_S \mu_0 \mathbf{m} \cdot \mathbf{n} da$$

it results

$$\oint_S \mathbf{j}^p \cdot \mathbf{n} da + \frac{d}{dt} \oint_S \mathbf{p} \cdot \mathbf{n} da, \quad \oint_S \mathbf{j}^m \cdot \mathbf{n} da + \frac{d}{dt} \oint_S \mu_0 \mathbf{m} \cdot \mathbf{n} da \quad (6)$$

where $\mathbf{j}^p, \mathbf{j}^m$ are the densities of the polarization and magnetization currents.

Let us remind, that the deformable body is considered, then

$$x^k = x^k(X^K, t), \quad p^l(x^k, t) = p^l[x^k(X^K, t), t], \quad n_l da = da_l$$

$$\dot{x}^k = \left. \frac{dx^k}{dt} \right|_{\mathbf{x} \text{ fixed}} = \frac{\partial x^k}{\partial t}, \quad \frac{dp^l}{dt} = \frac{\partial p^l}{\partial t} + p^l_{;k} v^k$$

where \mathbf{X} denotes the material coordinates, \mathbf{x} the spatial coordinates of the material points of the body, $p^l_{;k}$ is the covariant derivative of p^l . For the time derivative of an integral of a field $\phi[x^k(X^K, t), t]$ over the material surface S the following dependence holds (ERINGEN 1962)

$$\frac{d}{dt} \int_S \phi da_k = \int_S \left[\left(\frac{\partial \phi}{\partial t} + \phi_{;m} v^m \right) da_k + \phi (-v^m_{;k} da_m + v^m_{;m} da_k) \right]$$

Hence the polarization and magnetization currents densities are

$$\begin{aligned} \mathbf{j}^p &= \frac{\partial \mathbf{p}}{\partial t} + \mathbf{v} \operatorname{div} \mathbf{p} + \operatorname{rot}(\mathbf{p} \times \mathbf{v}) = \dot{\mathbf{p}} \\ \mathbf{j}^m &= \frac{\partial(\mu_0 \mathbf{m})}{\partial t} + \mathbf{v} \operatorname{div}(\mu_0 \mathbf{m}) + \operatorname{rot}(\mu_0 \mathbf{m} \times \mathbf{v}) = \mu_0 \dot{\mathbf{m}} \end{aligned} \quad (7)$$

The stars denote the convective derivatives (ERINGEN, MAUGIN 1989).

Electromagnetic forces

The electric free charges and currents, polarization and magnetic charges and currents defined in the previous section contribute to the forces acting in the body. The volume charge densities and the current densities contribute to the volume force acting on the volume element of the body

$$\begin{aligned} \mathbf{f} &= \mathbf{f}^e + \mathbf{f}^m \\ \mathbf{f}^e &= (q^f + q^p)(\mathbf{e} + \mathbf{v} \times \mathbf{b}) + (\dot{\mathbf{j}} + \mathbf{j}^p) \times \mathbf{b} \\ \mathbf{f}^m &= q^m(\mathbf{h} - \mathbf{v} \times \mathbf{d}) - \mathbf{j}^m \times \mathbf{d} \end{aligned} \quad (8)$$

The density of the electric free charge, polarization charge density, conduction current, and polarization current contribute to the electric part of the volume force \mathbf{f}^e . The magnetic charges and the magnetic current contribute to the magnetic part \mathbf{f}^m of the volume force. In the above formulas \mathbf{e} , \mathbf{h} denote the electric and magnetic field intensity, \mathbf{d} , \mathbf{b} are the electric displacement and the magnetic induction. The last quantities can be expressed by means of the electric and magnetic intensities and polarization and magnetization (FANO, CHU, ADLER 1960, SUFFCZYŃSKI 1969).

$$\mathbf{d} = \epsilon_0 \mathbf{e} + \mathbf{p}, \quad \mathbf{b} = \mu_0 (\mathbf{h} + \mathbf{m}) \quad (9)$$

Inserting the last dependences and the formulas (4), (5), (7) into (8) one obtains the electric and magnetic parts of the volume force in the form

$$\begin{aligned} \mathbf{f}^e &= (q - \text{div} \mathbf{p}) \mathbf{e} + [\hat{\mathbf{j}} + (q - \text{div} \mathbf{p}) \mathbf{v} + \mathbf{p}^*] \times \mathbf{b} \\ \mathbf{f}^m &= -\mathbf{h} \text{div} \mathbf{m} - (\mathbf{m}^* - \mathbf{v} \text{div} \mathbf{m}) \times (\epsilon_0 \mathbf{e} + \mathbf{p}) \end{aligned} \quad (10)$$

On the surface $\mathbf{n} da$ polarization and magnetic charges $\mathbf{p} \cdot \mathbf{n} da$, $\mathbf{m} \cdot \mathbf{n} da$ appear. Hence on the surface S of the body the electromagnetic force appears

$$\oint \mathbf{t} da = \oint \{ \sigma^p (\mathbf{e} + \mathbf{v} \times \mathbf{b}) + \sigma^m (\mathbf{h} - \mathbf{v} \times \mathbf{d}) \} da$$

Hence, it results

$$\begin{aligned} \oint_S t^k n_k da &= \oint_S [p^k (e_l + \epsilon_{lmn} v^m b^n) + \mu_0 m^k (h_l - \epsilon_{lmn} v^m d^n)] n_k da \\ &= \int_V [p^k (e_l + \epsilon_{lmn} v^m b^n) + \mu_0 m^k (h_l - \epsilon_{lmn} v^m d^n)]_{,k} dv \\ &= \int_V \tau^k_{l;k} dv \end{aligned}$$

Here τ^k_l denotes the electromagnetic stress tensor

$$\tau^{kl} = p^k e^l + \mu_0 m^k h^l + \epsilon^{lmn} v_m (p^k b_n - m^k d_n) \quad (11)$$

Electromagnetic and mechanical field equations

To determine the electromagnetic field in the deformable medium let us start with the electromagnetic integral laws. For moving media it should be taken into considerations, that the effective electric and magnetic intensities are respectively

$$\mathbf{e} + \mathbf{v} \times \mathbf{b}, \quad \mathbf{h} - \mathbf{v} \times \mathbf{d}$$

Thus the integral laws can be written in the form:

The Faraday's law

$$\oint_C (e_k + \varepsilon_{klm} v^l b^m) dx^k = - \frac{d}{dt} \int_S b_k n^k da \quad (12)$$

The Ampère's law

$$\oint_C (h_k + \varepsilon_{klm} v^l d^m) dx^k = - \frac{d}{dt} \int_S d_k n^k da + \int_S (\hat{j}_k + v_k q) n^k da \quad (12)$$

The Gauss laws

$$\oint d_k n^k da = \int q dv, \quad \oint b_k n^k da = 0 \quad (14)$$

The time derivatives of the integrals over the material surfaces, Green and Stokes theorems lead to the local Maxwell equations in the form

$$\begin{aligned} \text{rot}(\mathbf{e} + \mathbf{v} \times \mathbf{b}) &= - \dot{\mathbf{b}} \\ \text{rot}(\mathbf{h} - \mathbf{v} \times \mathbf{d}) &= \dot{\mathbf{d}} + \hat{\mathbf{j}} + q\mathbf{v} \\ \text{div} \mathbf{d} &= q, \quad \text{div} \mathbf{b} = 0 \end{aligned} \quad (15)$$

If (9), the polarization charge and current densities and the magnetization charge and current densities are inserted into the local equations (14), they can be written in the form

$$\begin{aligned} \text{rot}(\mathbf{e} + \mathbf{v} \times \mathbf{b}) &= - \mu_0 \dot{\mathbf{h}} - \mathbf{j}^m \\ \text{rot}(\mathbf{h} - \mathbf{v} \times \mathbf{d}) &= e_0 \dot{\mathbf{e}} + \mathbf{j}^p + \hat{\mathbf{j}} + q\mathbf{v} \\ e_0 \text{div} \mathbf{e} &= q^p + q, \quad \mu_0 \text{div} \mathbf{h} = q^m \end{aligned} \quad (16)$$

Under assumption that the electromagnetic fields and the velocities of the points of media are finite, the boundary conditions on the surface S of the body resulting from (12)-(14) are of the form

$$[(\mathbf{e} + \mathbf{v} \times \mathbf{b}) - \mathbf{e}^v] \times \mathbf{n} = 0, \quad [(\mathbf{h} - \mathbf{v} \times \mathbf{d}) - \mathbf{h}^v] \times \mathbf{n} = 0$$

$$(\mathbf{d} - e_0 \mathbf{e}^v) \cdot \mathbf{n} = 0, \quad (\mathbf{b} - \mu_0 \mathbf{h}^v) \cdot \mathbf{n} = 0$$

where \mathbf{e}^ν , \mathbf{h}^ν denote the electric and the magnetic intensities in free space. The form corresponding to (16) is

$$(\mathbf{e} - \mathbf{e}^\nu) \times \mathbf{n} + \mathbf{b} (\mathbf{v} \cdot \mathbf{n}) = 0, \quad (\mathbf{h} - \mathbf{h}^\nu) \times \mathbf{n} + \mathbf{d} (\mathbf{v} \cdot \mathbf{n}) = 0 \quad (17)$$

$$e_0(\mathbf{e} - \mathbf{e}^\nu) \cdot \mathbf{n} = -\sigma^p, \quad \mu_0(\mathbf{h} - \mathbf{h}^\nu) \cdot \mathbf{n} = -\sigma^m$$

Taking into considerations the electromagnetic force acting on the material volume dv of the body and the electromagnetic stress acting on its surface da the local form of the equations of motion are obtained in the form

$$(\sigma^{ij} + \tau^{ij})_{;i} + f^j + \rho F^i = \rho \frac{\partial^2 u^j}{\partial t^2}$$

where σ^{ij} is the mechanical part of the stress dependent on strains, $\rho \mathbf{F}$ is the mechanical body force, \mathbf{u} the displacement vector.

If the stress tensor $\sigma + \tau$ is not symmetric, then the couple stress tensor appear

$$m^i_j = \varepsilon_{jlm} \mu^{ilm}$$

The couple stress satisfies the equation

$$\sigma^{[jk]} + \tau^{[jk]} + \mu^{ijk}_{;i} = 0$$

Here the square brackets denote the antisymmetric parts of the tensors σ , τ . The corresponding boundary conditions on the surface S are

$$(\sigma_{ij} + \tau_{ij})n^i = \tau^\nu_{ij}n^i + t_j$$

$$\mu_{ijk}n^i = 0$$

In the above formulas τ^ν denotes the Maxwell stress tensor in free space

$$\tau^\nu_{ijk} = e_0 e^\nu_i e^\nu_j + \mu_0 h^\nu_i - \frac{1}{2} \delta_{ij} (e_0 e^\nu_k e^\nu_k + \mu_0 h^\nu_k h^\nu_k)$$

The equations of the electromagnetic field and the equations of motion are coupled. The above model should be completed with the thermodynamic

considerations leading to the constitutive equations for the polarization, magnetization, conductive current and mechanical parts of the stress tensor and the couple stress tensor. Such investigations will be the matter of further considerations.

Conclusions

In result of the investigations presented here the electromagnetic forces and stresses acting in the polarized and magnetized body with conductivity are derived. The approach is between (DIXON, ERINGEN 1965) and Chu formulation (FANO, CHU, ADLER 1960). The results differ from those derived by the authors referred. Determination of the polarization and magnetization charge and current densities is a merit of the Chu approach. Owing to this the macroscopic Lorentz force can be derived. Because a deformable body is considered here, the polarization and magnetization currents density contain the additional terms if compared with the Chu results. The polarization and magnetization currents densities derived by Chu are (PENFIELD, HERMANN, HAUS 1967)

$$\mathbf{j}^p = \frac{\partial \mathbf{p}}{\partial t} + \text{rot}(\mathbf{p} \times \mathbf{v}), \quad \mathbf{j}^m = \frac{\partial \mathbf{m}}{\partial t} + \text{rot}(\mathbf{m} \times \mathbf{v})$$

and do not contain the terms

$$\mathbf{v} \text{div} \mathbf{p}, \quad \mu_0 \mathbf{v} \text{div} \mathbf{m}$$

present in (7). However the presented approach, differs from the Dixon-Eringen approach the electromagnetic volume force obtained by the author is the same as the electromagnetic volume force in (DIXON, ERINGEN 1965), if it is assumed that the media is not conducting and not magnetizable.

Moreover in Chu approach it was not taken into account, that the surface densities of polarization and magnetization charges generate the electromagnetic stresses. The electromagnetic stresses in Chu approach result from thermodynamic considerations and differs from these obtained by the author. Here again the electrical stresses in the Dixon-Eringen model are the same as derived by the author, if it is assumed, that the media is not magnetizable and the quadrupole effects are neglected. It should be noticed, that in the Dixon-Eringen approach the electromagnetic stresses are derived on a formal way as a term appearing in the form of divergence in the volume force resulting from the model. In the approach presented here the electromagnetic stress tensor result directly from the physical model.

In conclusion it should be emphasised, that the electromagnetic interactions derived by the author are an extension of the Dixon-Eringen interaction for the polarizable media to the polarizable and conducting media. It does not concerns magnetization as the still controversial Chu approach is completely different than commonly accepted.

References

- DIXON R.C., ERINGEN A.C. 1965. *A dynamical theory of polar elastic dielectric*. Int. J. Engn. Sci., 3: 359-398.
- ERINGEN A.C. 1962. *Nonlinear theory of continuous media*. Mc Graw Hill, New York.
- ERINGEN A.C., MAUGIN G.A. 1989. *Electrodynamics of Continua*. Vol. I, II. Springer.
- FANO R.M., CHU L.J., ADLER R.B. 1960. *Electromagnetic fields, Energy and Forces*. Wiley & Sons, New York.
- PENFIELD P., HERMANN A. HAUS. 1967. *Electrodynamics of Moving Media*. MIT Press.
- SUFFCZYŃSKI M. 1969. *Elektrodynamika*. PWN.

Accepted for print 11.04.2008 r.

SELECTED PROBLEMS OF MEASUREMENT UNCERTAINTY – PART 1

Sylwester Kłysz^{1,2}, Janusz Lisiecki¹

¹ Division for Reliability & Safety of Aeronautical Systems
Air Force Institute of Technology in Warsaw

² Faculty of Technical Sciences
University of Warmia and Mazury in Olsztyn

Key words: measurement uncertainty, A-type and B-type uncertainty evaluation, normal (Gaussian) and rectangular distribution, uncertainty budget.

Abstract

The rules for evaluation of measurement uncertainty are presented in this paper. It includes the list of definitions for basic terms that are associated with the issue and explains how to evaluate the measurement uncertainty for well-defined physical parameters that are considered as the measurands (part 1). Next, the methods for evaluation of measurement uncertainty are exhibited on the examples when measurement uncertainty is estimated for verification of a micrometer as well as evaluated for basic reliability parameters (part 2).

WYBRANE ZAGADNIENIA NIEPEWNOŚCI POMIARU – CZ. 1

Sylwester Kłysz^{1,2}, Janusz Lisiecki¹

¹ Zakład Niezawodności i Bezpieczeństwa Techniki Lotniczej
Instytut Techniczny Wojsk Lotniczych w Warszawie

² Katedra Materiałów Funkcjonalnych i Nanotechnologii
Uniwersytet Warmińsko-Mazurski w Olsztynie

Słowa kluczowe: niepewność pomiaru, niepewność typu A i typu B, błąd pomiaru, rozkład normalny i prostokątny, budżet niepewności.

Abstrakt

W pracy podano zasady postępowania podczas wyznaczania niepewności pomiaru. Przedstawiono podstawowe pojęcia dotyczące tego zagadnienia oraz sposób wyznaczania niepewności pomiaru dobrze określonej wielkości fizycznej stanowiącej wielkość mierzoną (cz.1). Przedstawiono sposób szacowania niepewności pomiaru na przykładzie szacowania niepewności podczas sprawdzania mikrometru i szacowania niepewności podstawowych parametrów wytrzymałościowych (cz. 2).

Introduction

Every measurement is aimed at determination of the measured value, i.e. value of the specific parameter that is the objective of measurements.

Yet measurements results are only approximated or evaluated (estimated) value of the measured parameter and therefore the results is complete only when it is provided with the estimated uncertainty.

Following the Manual Expression of Measurement Uncertainties (*Wyrażanie niepewności pomiaru*. 1999):

“Uncertainty (of measurement) is the parameter that is associated with measurement results and exhibits dispersion of values that can be assigned to the measured value in justified manner”.

Expression of uncertainty in measurement refers to a well-defined physical parameter that is considered as the measured value and can be characterized by z single value obtained from measurements. The term “value” (measurable quantity) stands for the property of the phenomenon, material or substance that can be qualitatively described and quantitatively evaluated. Uncertainty of measurements is a result of random errors that can occur during measurements. It is important to distinguish the term “error” and the term “uncertainty of measurements”. Every error represents a random variable, while uncertainty of measurements is a parameter for distribution of error probabilities.

In accordance to requirements of the standard PN-EN ISO 10012 (PN-EN ISO 10012:2004):

- evaluation of the uncertainty should take account for not only uncertainty of the measurement equipment calibration, but also for all the other components of uncertainty that are essential for the specific measurement process. Relevant methods for the analysis should be applied,
- if any uncertainty components are so insignificant as compared to other components that evaluation of such insignificant components is unjustified in technical and economical aspects, calculation thereof should be given up and the decision should be recorded,
- measurement uncertainty should be evaluated for every measurement process that is covered by any measurement management system,
- measurement uncertainty should be recorded and all the known reasons for measurement variations must be documented,
- efforts devoted to evaluation and recording of measurement uncertainty should be commensurable to the significance of the measurement results to the product quality.

In accordance to requirements of the standard PN-EN ISO/IEC 17025, the accredited laboratory:

- it should have in place the working procedure on evaluation of measurement uncertainty,

- when it performs its own calibration and verification procedures it should have in place the working procedure (instruction) for evaluation of measurement uncertainty for every calibration or verification,
- when the character of the applied research method disables strict, metrological and statistically justifiable calculations of measurement uncertainty the efforts should be made to identify all the uncertainty components and estimate them in reasonable manner based on available knowledge on capabilities of the method and gathered past experience, such a way of uncertainty evaluation should be described,
- in case when examinations are carried out by means of a well-known method where boundary limits for main sources of measurement uncertainty and the methods for result reporting are truthfully defined, such results should be reported in accordance with the relevant statements of the research procedure or instruction,
- sources of uncertainties include the applied patterns and reference materials, used methods and equipment, environmental conditions, properties and status of the objects that are subject to examination or calibration as well as the performing staff.

Measurement equation

The dependence of measurement results, considered as the random variable Y , on a number of random variables X_1, \dots, X_n , associated with the measurement process, i.e. directly measurable parameters, correction factors, physical constants and deviations and errors thereof is described by the formula:

$$Y = f(X_1, X_2, X_3, \dots, X_{n-1}, X_n) \quad (1)$$

The function f of the above equation may express no physical law and merely describe the measurement process. It should cover all the parameters that can affect the modelling of the measurement result. Initial parameters (arguments for the function f) should be defined as accurately as practically feasible in order to determine values thereof in unambiguous manner.

The estimation of the initial parameter Y , that is adopted as the measurement result, shall be the value of y that is determined by the same equation as above, but with the X_1, \dots, X_n values substituted with their estimators x_1, \dots, x_n , namely:

$$y = f(x_1, x_2, x_3, \dots, x_{n-1}, x_n) \quad (2)$$

Determining of standard uncertainties for all the components

At the outset, it is necessary to estimate standard uncertainties $u(x_i)$ for all the initial parameters that influent the research process (Dokument EA-4/02 1999, PIOTROWSKI, KOSTYRKO 2000, PN-EN ISO/IEC 17025 2005). For the research (measurements) where series of observations are carried out the **method** of statistical analysis of the **A-type** is applicable to the series of observations. If uncertainty of the input value cannot be determined on the basis of a series of measurements, the **B-type method** is applied, where the standard uncertainty is evaluated on the basis of information about possible range of variations for the measured parameter in question.

The A-type method (for the measured value or errors of its measurements described by Gaussian distribution of measurement results) achieves the best evaluation (estimator) for the mathematical expectation μ associated with the random variable x as the arithmetical mean \bar{x} provided that n independent observations were made under repeatable measurement conditions.

$$\bar{x} = \frac{1}{n} \sum_{i=1}^n x_i \quad (3)$$

The standard uncertainty of the A-type is equivalent to standard deviation of the mean value over a series of experiments. The standard deviation is calculated by the following formula:

$$u_A(\bar{x}) = \frac{u(x)}{\sqrt{n}} \quad (4)$$

where:

$$u(x) = \sqrt{\frac{1}{n-1} \sum_{i=1}^n (x_i - \bar{x})^2} \quad (5)$$

The foregoing formulas are true only for sufficiently long series of observations ($n > 30$ is usually assumed), when the mean value is a trustworthy estimation for the mathematical expectation.

The correction factor $\frac{1}{\sqrt{n}}$ for the experimental standard uncertainty drops rapidly nearby the beginning of the coordinate system (for $n = 4$ it is halved) but for large n (above a dozen) tends to decrease rather slowly. It is

why excessive expanding of measurement series seems to be unjustified. Needless to say that it is really difficult to make sure that measurement conditions shall be repeatable for long series of measurements. However, number of measurements should be high enough to guarantee that the arithmetical mean is a trustworthy estimation for the mathematical expectation.

Long series of measurements ($n > 30$) should be launched when the combined standard uncertainty $u_p(x)$ is to be found out. Such a type of uncertainty is used later on when similar measurements are taken under the same conditions. Then, after completion of the series of n_1 new measurements, the variation of measurement (observation) distribution becomes known and the uncertainty can be determined by the following formula:

$$u_A(\bar{x}) = \frac{u_p(x)}{\sqrt{n_1}} \quad (6)$$

If variation of measurement (observation) distribution remains unknown, the required number of measurements in a series depends on the desired confidence interval for the expanded uncertainty.

In case of the B-type method, where we have to deal with a single measurement result or with figures acquired from documents or literature references, the boundary limits a_+ and a_- can be evaluated for the input variable X_i and then the standard uncertainty is calculated by the formula:

$$u_B(x_i) = \frac{a}{\sqrt{k}} \quad (7)$$

where:

$$a = \frac{a_+ + a_-}{2}$$

The value $u_B(x_i)$ as calculated in the foregoing manner is referred to as the standard uncertainty of B-type. It is the method for analysis of conditions where underlying reasons for errors may occur and is recommended for analysis and estimation of instrumental (equipment) errors.

The following features attributable to any source of errors should be taken into account:

- availability of information on the probability distribution applicable to the specific parameter (e.g. Gaussian, rectangular, triangular),
- information on possible boundaries of the variability interval for the specific parameter value, x_i belongs to (a_-, a_+) ,

– probability of the fact that the specific value of the x_i parameter falls into the predefined interval.

Calculation results, obtained in the above manner do not have to be worse than those that are based on repeatable observations. Table 1 presents the values of “uncertainties of uncertainties” that origin in the statistic way, depending on the number of observations. The data in the table exhibit that even for $n = 10$ observations the “uncertainty of uncertainties” is still as high as 24%. This allows to conclude that calculation of standard uncertainty with use of the A-type method do not have to be more dependable than in case when the standard uncertainty is calculated with use of the B-type method and in many cases of experiments when number of measurements must be limited, the components obtained from calculations with use of the B-type method may be even better defined than respective components that are obtained from calculations with the A-type method.

Table 1

Ratios of experimental standard deviations for the arithmetical means for n independent observation with Gaussian distribution over standard deviation of the mean value

Number of observations n	$\sigma[s(\bar{q})] / \sigma(\bar{q})$ %
2	76
3	52
4	42
5	36
10	24
20	16
30	13
50	10

Source: Dokument EA-4/02 (1999)

Determining of the composed standard uncertainty

For the values of parameters that are measured in direct way, when the standard uncertainties of both A and B types are taken into account, the composed standard uncertainty u_C is the square root of the sum of squares for the both uncertainty values.

$$u_C = \sqrt{u_A^2 + u_B^2} \quad (8)$$

In most cases the parameter value y is not measured in direct way but determined on the basis of measurements for other parameters x_i that remain in strict relations with the desired parameter that are defined by a specific function (see measurement equation (6)).

Based on the total differential the *law for propagation of uncertainties* is formulated in the following way:

$$u_C(y) = \sqrt{\sum_1^n \left(\frac{\partial f}{\partial x_i} \right)^2 u^2(x_i)} \quad (9)$$

$$u(y_i) = |c_i| \cdot u(x_i) \quad (10)$$

where:

$u(x_i)$ – standard uncertainties for measurements of input parameters, calculated with use of either A or B method; the composed standard uncertainty $u_C(y)$ is then the estimation of the standard deviation σ_y and characterizes dispersion of values that by justified reasons can be associated with the measured value y ,

$\frac{\partial f}{\partial x_i} = c_i$ – partial derivatives that are referred to as sensitivity coefficients.

The law for propagation of uncertainties is true in the input parameters are uncorrelated, which is the most common practice.

However, if the provision on mutual independence of input values is not met, the formula with account for covariances must be applied:

$$u_C^2(y) = \sum_{i=1}^m \left(\frac{\partial f}{\partial x_i} \right)^2 u^2(x_i) + 2 \sum_{i=1}^{m-1} \sum_{j=i+1}^m \left(\frac{\partial f}{\partial x_i} \right) \left(\frac{\partial f}{\partial x_j} \right) u(x_i, x_j) \quad (11)$$

The final result for measurements of the parameter Y is calculated on the basis of the defined function (measurement equation) where arithmetical means of directly measurable parameters are substituted:

$$\bar{y} = f(\bar{x}_1, \bar{x}_2, \dots, \bar{x}_n) \quad (12)$$

Uncertainty budget

If individual input parameters are mutually independent, the information that is essential for analysis of the measurement uncertainty can be brought together into a table (see Table 2). Such a table assures clarity of the analysis and is referred to as the uncertainty budget.

Table 2

Uncertainty budget for calculation of a composed uncertainty for uncorrelated input parameters

Parameter symbol X_i	Parameter estimation x_i	Standard uncertainty $u(x_i)$	Probability distribution	Sensitivity coefficient c_i	Contribution to the composed uncertainty $u_i(y)$
X_1	x_1	$u_A(x_1) = \frac{U}{2}$	Gaussian	c_1	$u_1(y) = c_1 \cdot u_A(x_1)$
X_2	x_2	$u_B(x_2) = \frac{x_2}{2\sqrt{3}}$	rectangular	c_2	$u_2(y) = c_2 \cdot u_B(x_2)$
X_N	x_N	$u_B(x_N) = \frac{x_N}{2\sqrt{6}}$	triangular	c_N	$u_N(y) = c_N \cdot u_B(x_N)$
Y	y	–	–	–	$u_c(y)$

Source: PN-EN ISO 9000 (2001)

Determining of the expanded uncertainty

In case of direct measurements the expanded uncertainty U is the product of the expansion coefficient and the composed standard uncertainty:

$$U(y) = k_\alpha \cdot u_C(y) \quad (13)$$

where $u_C(y)$ is calculated with use of the formula for direct measurements.

The expansion coefficient for the guaranteed confidence level p_α should be calculated on the basis of the distribution for a standardized random value, where the distribution is a convolution of both the Gaussian and uniform (rectangular) distributions, when the set of samples is large. Otherwise, when the set of sample size is small, the t -Student distribution should be applied.

For indirect measurements, the expanded uncertainty, denoted as U , is obtained by multiplication of the standard composed uncertainty $u_C(y)$ by the expansion coefficient k_α :

$$U(y) = k_\alpha \cdot u_C(y) \quad (14)$$

where $u_C(y)$ is calculated with use of the formula for indirect measurements and the result in the following form:

$$y = y \pm U(y) \quad (15)$$

is recorded for the confidence level of p_α .

Exact calculation of expansion coefficients for the desired confidence levels is a sophisticated job for indirect measurements as it needs to know the function of the probability density distribution for the random value that is used for modelling of measurement results y . Such a function is a convolution of component distribution for random variables that are used for modelling of input parameters. Calculation of such convolutions is difficult, except for some specific cases that include convolution of any number of Gaussian distributions, which is the Gaussian distribution itself and its parameters can be easily calculated.

It is why approximated methods are practically used for calculation of the expansion coefficient.

Approximated methods for calculation of the expanded uncertainty (*Analiza błędów...* 2007)

Method I – with use of predefined values for expansion coefficients

It consists in application of the coefficient $k_\alpha = 2$ for the confidence level $p_\alpha \approx 95\%$ and $k_\alpha = 3$ for the confidence level $p_\alpha \approx 99\%$.

It is the method that is used for measurement experiments that involve independent input parameters X_i and:

- distributions for all the components of the standard composed uncertainty $u_C(y)$ are of Gaussian type,
- distributions for the components of the standard composed uncertainty $u_C(y)$ are of rectangular type, but with the same width and not less than 3 distributions are available,
- there is quite many input parameters X_i (practically not less than 4), the composed standard uncertainty $u_C(y)$ is free of domination by the component of the standard uncertainty that is calculated by means of the A-type method for the series of only few observations or by the component of the standard uncertainty that is calculated by means of the B-type method from the presumed rectangular distribution (i.e. the uncertainties $c_i u(x_i)$ and $c_i u_B(x_i)$ contribute to the $u_C(y)$ i $u_C(y)$ in comparable degree) and is much higher than a single component $c_i u_B(x_i)$.

Method II – geometrical superposition

It consists in calculation of the expanded uncertainty U for every single input parameter (for every component of the error) and then the expanded

uncertainty for the output value U_y is calculated as the square root of the sum of squares for all the component uncertainties, in accordance with the formula:

$$U_y = \sqrt{U_{x_1}^2 + U_{x_2}^2 + \dots + U_{x_n}^2} \quad (16)$$

Expansion coefficients for component uncertainties must be calculated for the same confidence level.

Method III – ordinary (algebraic) sum

Adding in the uncertainty domain:

$$U = U_A + U_B \quad \text{or} \quad U_y = U_{x_1} + U_{x_2} + \dots + U_{x_n} \quad (17)$$

The method assumes the worst case for accumulation of errors, i.e. the situation when all the component errors are of the maximum value and are of the same sign. It is very little probably, which means that the method exaggerates uncertainty of measurements and is the most pessimistic one.

However, the method is used for workshop measurements due to easy calculation as well as for specific cases or, for instance, when tolerances are to be found out or when components of machinery must be manufactured with defined play.

Method IV – dominating component

It is recommended for the cases when one of the component uncertainties of either A or B types is the dominating factor.

If $u_A \geq u_B$, the substitutions $k_\alpha = k_A$ must be made in the formula (13), Similarly, if $u_B \geq u_A$ the substitution in the formula (13) should be $k_\alpha = k_B$.

For the Gaussian probability distribution and for the confidence level of 95.45% the expansion factor should be $k_\alpha = 2$, whereas for the confidence level of 99.73% – $k_\alpha = 3$.

For the rectangular probability distribution and for the confidence level of 95% the expansion factor should be $k_\alpha = 1.65$, whereas for the confidence level of 99% – $k_\alpha = 1.71$.

Method V – effective degrees of freedom

For this method the expanded uncertainty is denoted as U_p and calculated by the following formula:

$$U_p = k_p \cdot u_C(y) = t_p(v_{\text{eff}}) \cdot u_C(y) \quad (18)$$

where t_p stands for the t coefficient attributable to the t -Student distribution that can be read from relevant reference tables in accordance with the selected confidence level p_α and for the effective number of the degrees of freedom v_{eff} . The figure v_{eff} is to be calculated by the Welch-Satterthwaite formula

$$v_{\text{eff}} = \frac{u_C^4(y)}{\sum_{i=1}^N \left(\frac{\partial f}{\partial x_i} \right)^4 \frac{u_i^4(x_i)}{v_i}} \quad (18)$$

where:

$u_C(y)$ – composed standard uncertainty for the output value,

$u(x_i)$ – standard uncertainties for the input parameters, $i = 1, 2, \dots, N$,

v_i – number of the degrees of freedom for $u(x_i)$.

Practical calculation of the number of degrees of freedom for $u(x_i)$:

– if distribution for the $u(x_i)$ is of the Gaussian type, then

$$v_i = n - 1$$

– if distribution for the $u(x_i)$ is of the rectangular type with the presumed width of a , then $u(x_i) = \frac{a}{2\sqrt{3}}$ is adopted with no uncertainty as the limits for

such decomposition are known and then $v_i \rightarrow \infty$, hence $1/v_i \rightarrow 0$,

– if the source of errors is rated to the B group and available information of that error source indicate that the standard uncertainty $u(x_i)$ can be merely estimated with the specific relative error $\delta_{ui} = \frac{\Delta u(x_i)}{u(x_i)}$, then $v_i \approx \frac{1}{2} \cdot \frac{1}{\delta_{ui}^2}$.

For instance, under the assumption that $u(x_i)$ is estimated with the error of 25%, number of the degrees of freedom shall amount to: $v_i \approx 1/2 \cdot (1/0.25^2) \approx 8$.

References

- Analiza błędów i niepewności pomiarów*. 2007. www.eti.pg.gda.pl/katedry/kose/dydaktyka.
- PIOTROWSKI J., KOSTYRKO K. 2000. *Wzorcowanie aparatury pomiarowej*. Wydawnictwo Naukowe PWN, Warszawa.
- PN-EN ISO 9000. 2001. *Systemy zarządzania jakością. Podstawy i terminologia*.
- PN-EN ISO/IEC 17025. 2005. *Ogólne wymagania dotyczące kompetencji laboratoriów badawczych i wzorcujących*.
- Wyrażanie niepewności pomiaru przy wzorcowaniu*. 1999. Dokument EA-4/02.
- Wyrażanie niepewności pomiaru*. 1999. Przewodnik GUM.
- PN-EN ISO 10012:2004. *Systemy zarządzania pomiarami. Wymagania dotyczące procesów pomiarowych i wyposażenia pomiarowego*.

Accepted for print 27.06.2008 r.

SELECTED PROBLEMS OF MEASUREMENT UNCERTAINTY – PART 2

Sylwester Kłysz^{1,2}, Janusz Lisiecki¹

¹ Division for Reliability & Safety of Aeronautical Systems
Air Force Institute of Technology in Warsaw

² Faculty of Technical Sciences
University of Warmia and Mazury in Olsztyn

Key words: measurement uncertainty, A-type and B-type uncertainty evaluation, normal (Gaussian) and rectangular distribution, uncertainty budget.

Abstract

The rules for evaluation of measurement uncertainty are presented in this paper. It includes the list of definitions for basic terms that are associated with the issue and explains how to evaluate the measurement uncertainty for well-defined physical parameters that are considered as the measurands (part 1). Next, the methods for evaluation of measurement uncertainty are exhibited on the examples when measurement uncertainty is estimated for verification of a micrometer as well as evaluated for basic reliability parameters (part 2).

WYBRANE ZAGADNIENIA NIEPEWNOŚCI POMIARU – CZ. 2

Sylwester Kłysz^{1,2}, Janusz Lisiecki¹

¹ Zakład Niezawodności i Bezpieczeństwa Techniki Lotniczej
Instytut Techniczny Wojsk Lotniczych w Warszawie

² Katedra Materiałów Funkcjonalnych i Nanotechnologii
Uniwersytet Warmińsko-Mazurski w Olsztynie

Słowa kluczowe: niepewność pomiaru, niepewność typu A i typu B, błąd pomiaru, rozkład normalny i prostokątny, budżet niepewności.

Abstract

W pracy podano zasady postępowania podczas wyznaczania niepewności pomiaru. Przedstawiono podstawowe pojęcia dotyczące tego zagadnienia oraz sposób wyznaczania niepewności pomiaru dobrze określonej wielkości fizycznej stanowiącej wielkość mierzoną (cz. 1). Przedstawiono sposób szacowania niepewności pomiaru na przykładzie szacowania niepewności podczas sprawdzania mikrometru i szacowania niepewności podstawowych parametrów wytrzymałościowych (cz. 2).

Estimation of uncertainty for verification of a micrometer

The error of micrometer readout can be calculated with use of the formula (ARENDALSKI 2003):

$$E_x = (L - W + P_t) \pm U(E_x) \quad (1)$$

where:

- L – the maximum readout from the micrometer for three measurements of dimensions,
- W – rated length of the standardized plate (W_n) with account for the correction factor – deviations of the plate length,
- P_t – correction factor for temperature conditions,
- $U(E_x)$ – the expanded uncertainty at the confidence level of $1_\alpha = 0.95$.

The value of the temperature correction factor is neglected.

Uncertainty equation

Due to the fact that input parameters are uncorrelated, the standard uncertainty connected with the already determined absolute deviation for the micrometer readout can be expressed by the formula:

$$u_c(E_x) = \sqrt{\sum (c_i \cdot u_i)^2} \quad (2)$$

where:

- c_i – sensitivity coefficients, i.e. the partial derivatives of the measurement function for the function components.

In this case $c_i = 1$ or $c_i = -1$. The standard uncertainty for the limit error can be then expressed in the following form:

$$u_c(E_x) = \sqrt{u^2(L) + u^2(W) + u^2(P_t)} \quad (3)$$

Determining of component standard uncertainties

The standard uncertainty for the micrometer readout is determined on the basis of the instrument resolution r , that for this case is 0.002 (readout with use a magnifying glass), by means of the B-type method and with the assumption of the rectangular distribution of the uncertainty:

$$u(L) = \frac{r}{2\sqrt{3}} = 0.00058 \text{ mm} \quad (4)$$

The standard uncertainty for the standardized plate length is determined on the basis of the expanded uncertainty U for determining of the deviation of the plate length from its rated length as provided by the calibration certificate. The B-type method is applied with assumption of the Gaussian distribution.

$$u(W) = \frac{U}{2} \quad (5)$$

The standard uncertainty for the temperature correction factor $u(P_t)$ is determined under the assumption that coefficients of thermal expansion for the standardized plate and for the micrometer are the same: $\alpha_W = \alpha_L = \alpha_t = 11,5 \cdot 10^{-6} \text{ }^\circ\text{C}^{-1}$ and $\Delta t = t_W - t_L$ (where: $t_W = 20^\circ\text{C}$, t_L – ambient temperature in the laboratory room $T_l = 20 \pm 10^\circ\text{C}$). The uncertainty $u(\Delta t)$, as determined with use of the B-type method (rectangular distribution) amounts to $\frac{\Delta t}{2\sqrt{3}}$. Thus:

$$u(P_t) = W \cdot \alpha_t \cdot \frac{\Delta t}{2\sqrt{3}} \quad (6)$$

Expanded uncertainty

If all values of component uncertainties $u(E_x)$ are comparable, the expanded uncertainty at the confidence level of $1 - \alpha = 0.95$ can be calculated with the formula:

$$U(E_x) = 2 \cdot u_c(E_x) \quad (7)$$

If the uncertainty $u_c(E_x)$ has one dominating component (e.g. $u(L)$) and the rectangular distribution is assumed, then the distribution can be considered as the distribution for readout errors and then the expanded uncertainty at the level of confidence of $1 - \alpha = 0.95$ can be calculated with the formula:

$$U(E_x) = 1.65 \cdot u_c(E_x) \quad (8)$$

If the uncertainty $u_c(E_x)$ has two dominating components (e.g. $u(L)$ and $u(W)$) and the rectangular distribution is assumed for the both components with the respective spans $R_1 = 2a_1$ and $R_2 = 2a_2$, the components can be

superposed to make up the trapezoidal evenarmed distribution with the span of $R = 2a = 2(a_1 + a_2)$ and upper base of $b = 2a\beta$, where $\beta = (a_2 - a_1)/(a_2 + a_1)$.

Then the composed uncertainty amounts to

$$u_c(E_x) = \sqrt{u^2(x_1) + u^2(x_2)} = \frac{\sqrt{a_1^2 + a_2^2}}{\sqrt{3}} \quad (9)$$

The expanded uncertainty at the confidence level of $P = 1 - \alpha = 0.95$ can be calculated by the formula:

$$U(E_x) = \frac{1 - \sqrt{(1 - P)(1 - \beta^2)}}{\sqrt{\frac{1 + \beta^2}{6}}} \cdot u_c(E_x) \quad (10)$$

Finally, the indication error value shall be:

$$E_x = \max \{d - U(E_x), d + U(E_x)\} \quad (11)$$

where:

d – the maximum deviation from the W dimension, $d = L - W$.

Note: uncertainty components $u_c(E_x)$ can be considered as insignificant and then neglected if

$$u_c(E_x) - u_c^*(E_x) \leq 0,05 u_c(E_x)$$

(where $u_c^*(E_x)$ – the composed uncertainty with one or two components ignored), i.e. when omission of one or two components in the formula for the uncertainty calculation results in alteration of such uncertainty by not more than 5%.

Uncertainty budget

All the informations for analysis of uncertainty are brought together in the table 1.

Table 1

Uncertainty budget for calculation of the composed uncertainty for verification of a micrometer

Parameter symbol X_i	Parameter estimation x_i	Standard uncertainty $u(x_i)$	Contribution of $u(x_i)$ into the standard uncertainty for each individual standardized plate (of n)			
L	–	Eq. (4)	$c_i u_1(L_1)$	$c_i u_2(L_2)$	$c_i u_3(L_3)$	$c_i u_n(L_n)$
W	–	Eq. (5)	$c_i u_1(W_1)$	$c_i u_2(W_2)$	$c_i u_3(W_3)$	$c_i u_n(W_{3n})$
P_i	0	Eq. (6)	$c_i u_1(P_{i1})$	$c_i u_2(P_{i2})$	$c_i u_3(P_{i3})$	$c_i u_n(P_{in})$
E_x	$L - W$	–	Eq. (3)	Eq. (3)	Eq. (3)	Eq. (3)

Estimation of uncertainty for determination of the tensile strength

Tensile strength (CWA 15261-2. 2005)

$$R_m = f(F_m, \bar{d}_0) = \frac{F_m}{S_0} = \frac{4F_m}{\pi \bar{d}_0^2} \quad (12)$$

where:

 F_m – maximum force recorded during the tensile test, S_0 – initial cross-section of the specimen, \bar{d}_0 – initial average diameter of the specimen.

Uncertainty equation

Due to the fact that input parameters are uncorrelated, the standard uncertainty connected with the determined tensile strength of the specimen is defined by the following formula:

$$u(R_m) = \sqrt{\sum (c_i \cdot u_i)^2} \quad (13)$$

where:

 c_i – sensitivity coefficients, i.e. the partial derivatives of the measurement function for the i^{th} function components, u_i – standard uncertainties for individual components.

In this case $c_{Fm} = \frac{4}{\pi \bar{d}_0^2}$ and $c_{d0} = -\frac{8F_m}{\pi \bar{d}_0^3}$, thus:

$$u(R_m) = \sqrt{\left(\frac{4}{\pi \bar{d}_0^2}\right)^2 u^2(F_m) + \left(-\frac{8F_m}{\pi \bar{d}_0^3}\right) u^2(\bar{d}_0)} \quad (14)$$

Determination of component standard uncertainties

The uncertainty for measurement of the specimen diameter is calculated by means of:

- a) on the basic of the arithmetical means for the series of six measurements (the A-type method), with the t -Student distribution assigned (for $p_\alpha = 68.27\%$):

$$u(\bar{d}_{0s}) = 1.11 \cdot \sqrt{\frac{\sum_{k=1}^n (d_{0k} - \bar{d}_0)^2}{n(n-1)}} \quad (15)$$

where:

n – number of measurements, or

- b) on the basic of the micrometer resolution, with use of the formula:

$$u(d_{0m}) = \frac{0.01}{2\sqrt{3}} \quad (16)$$

where:

$u(d_{0m})$ amounts to 0.00289 mm.

The value which is higher is adopted for further calculations.

Major factors that affect total uncertainty of measurement of the F force include:

- uncertainty of the measurement of the force

$$u_w(F_m) = \frac{U_{Fm} \cdot F_m}{200} \quad (17)$$

where:

U_{Fm} – the uncertainty of measurement (in percents), attributable to the dynamometer of the machine, as read from the calibration certificate for the force that is the closest to the force value F_m measured during the tensile test and for the selected range of the applied measuring head,

- zero adjustment in the forcemeasuring path,
- possible misalignment of the force applied,
- ambient temperature during test and rate of the load application.

The error that results from the aforementioned factors was evaluated to $\pm 1\%$. Therefore, the uncertainty for measurement of the maximum force shall be calculated with the formula:

$$u(F_m) = \frac{0.01 \cdot F_m}{\sqrt{3}} \quad (18)$$

Uncertainty budget

The information for further analysis of uncertainty is presented in the Table 2.

Table 2
Uncertainty budget for composed uncertainty for tensile strength

Parameter symbol X_i	Parameter estimation x_i	Standard uncertainty $u(x_i)$	Sensitivity coefficient c_i	Contribution into the composed standard uncertainty $u(x_i)$
F_m	–	Eq. (18)	$\frac{4}{\pi \bar{d}_0^2}$	$c_i \cdot u(F_m)$
\bar{d}_0	–	Eq. (15) or (16)	$-\frac{8F_m}{\pi \bar{d}_0^3}$	$c_i \cdot u(\bar{d}_0)$
R_m	$\frac{4F_m}{\pi \bar{d}_0^2}$	–	–	Eq. (14)

Determination of the expanded uncertainty

The relative expanded uncertainty with the expansion coefficient $k_\alpha = 2$ at the confidence level of $1 - \alpha = 0.95$ is calculated as:

$$U(R_m) = \frac{2 \cdot u(R_m)}{R_m} \cdot 100\% \quad (19)$$

Estimation of the uncertainty for determination of the proof stress

Proof stress (at non proportional elongation)

$$R_{p0.2} = f(F_{0.2}, \bar{d}_0) = \frac{F_{0.2}}{S_0} = \frac{4F_{0.2}}{\pi \bar{d}_0^2} \quad (20)$$

where:

$F_{0.2}$ – tension force that is applied during the test and then brings to permanent elongation of the specimen equal to 0.2% of the measurement length that corresponds to the extensometer base,

S_0 – initial cross-section of the specimen,

\bar{d}_0 – initial average diameter of the specimen.

Uncertainty equation

Due to the fact that input parameters are uncorrelated, the standard uncertainty connected with the determined proof stress is defined as:

$$u(R_{p0.2}) = \sqrt{\sum (c_i \cdot u_i)^2} \quad (21)$$

where:

c_i – sensitivity coefficients, i.e. the partial derivatives of the measurement function for the i^{th} function component,

u_i – standard uncertainties for individual components.

In this case $c_{F0.2} = \frac{4}{\pi \bar{d}_0^2}$ and $c_{d0} = -\frac{8f_{0.2}}{\pi \bar{d}_0^3}$, thus:

$$u(R_{p0.2}) = \sqrt{\left(\frac{4}{\pi \bar{d}_0^2}\right)^2 u^2(F_{0.2}) + \left(-\frac{8F_{0.2}}{\pi \bar{d}_0^3}\right)^2 u^2(\bar{d}_0)} \quad (22)$$

Determination of component standard uncertainties

The uncertainty for measurement of the specimen diameter – equations (15 ÷ 17).

Overall uncertainty for measurement of the force $F_{0.2}$:

$$u_c(F_{0.2}) = \sqrt{u^2(F_{0.2}) + u^2(\Delta F_{0.2}) + u^2(F_{0.2E})} \quad (23)$$

where subsequent components result from:

– uncertainty of the force measurement [see formula (18)]

$$u(F_{0.2}) = \frac{0.01 \cdot F_{0.2}}{\sqrt{3}}$$

– recording frequency during automatic measurement

$$u(\Delta F_{0.2}) = \frac{F_{0.2(1)} - F_{0.2(2)}}{2\sqrt{3}}$$

where:

$F_{0.2(1)}$ – the closest value of force that was higher than $F_{0.2}$,

$F_{0.2(2)}$ – the closest value of force that was lower than $F_{0.2}$;

– inclination of the straight line that is parallel to the linear section of the σ - ε curve that is described by the formulas: $\sigma_{0.2E} = E(\varepsilon - 0.002)$ or

$$F_{0.2E} = \frac{\Delta F}{\Delta \varepsilon} (\varepsilon - 0.002)$$

$$u(F_{0.2E}) = \sqrt{\left(\frac{\varepsilon - 0.002}{\Delta \varepsilon}\right)^2 \cdot u^2(\Delta F) + \left(-\frac{\Delta F(\varepsilon - 0.002)}{(\Delta \varepsilon)^2}\right)^2 \cdot u^2(\Delta \varepsilon) + \left(\frac{\Delta F}{\Delta \varepsilon}\right)^2}$$

where:

$$u(\Delta F) = \sqrt{u^2(F_{\max}) + u^2(F_{\min})}$$

where:

$$u(F_{\max}) = \frac{0.01 \cdot F_{\max}}{\sqrt{3}} \quad \text{and} \quad u(F_{\min}) = \frac{0.01 \cdot F_{\min}}{\sqrt{3}}$$

$$u(\Delta \varepsilon) = \sqrt{u^2(\varepsilon_{\max}) + u^2(\varepsilon_{\min})}$$

where:

$$u(\varepsilon_{\max}) = \frac{K_\varepsilon \cdot \varepsilon_{\max}}{\sqrt{3}} \quad \text{and} \quad u(\varepsilon_{\min}) = \frac{K_\varepsilon \cdot \varepsilon_{\min}}{\sqrt{3}}$$

$$U(\varepsilon) = \frac{K_\varepsilon \cdot \varepsilon}{\sqrt{3}}$$

where:

K_ε – accuracy class of the applied extensometer.

Uncertainty budget

The informations for further analysis of uncertainty are presented in the Table 3.

Uncertainty budget for composed uncertainty for proof stress

Table 3

Parameter symbol X_i	Parameter estimation x_i	Standard uncertainty $u(x_i)$	Sensitivity coefficient c_i	Contribution into the composed standard uncertainty $u(x_i)$
$F_{0.2}$	–	Eq. (23)	$\frac{4}{\pi \bar{d}_0^2}$	$c_i \cdot u_c(F_{0.2})$
\bar{d}_0	–	Eq. (15) or (16)	$-\frac{8F_{0.2}}{\pi \bar{d}_0^3}$	$c_i \cdot u(\bar{d}_0)$
$R_{p0.2}$	$\frac{4F_{0.2}}{\pi \bar{d}_0^2}$	–	–	Eq. (22)

Determination of the expanded uncertainty

The relative expanded uncertainty with the expansion coefficient $k_\alpha = 2$ at the confidence level of $1 - \alpha = 0.95$ is calculated with the following formula:

$$U(R_{p0.2}) = \frac{2 \cdot u(R_{p0.2})}{R_{p0.2}} \cdot 100\% \quad (24)$$

Recapitulation

On the basic of presented above methods for determination of measurement error and uncertainties the analysis of micrometer verification results and test proficiency results (in with accredited testing laboratory of Air Force Institute of Technology have been participated) were done.

The research covered verification of the analogue micrometer with its measurement range $0 \div 25$ mm, serial No 102-217-9157246, manufactured by MITUTOYO company. For reference the set of gauge plates was used, No 714390, with its calibration certificate No M11-419-578.3/2004.

The verification procedure was carried out at the ambient temperature of $20 \pm 0.2^\circ\text{C}$, in accordance with the instruction from the metrological surveillance IW-31-11-L5, for the full measurement range of the micrometer when the gauge plates with rated sizes of $W_n = 1; 1.05; 1.5; 2; 5; 8; 10; 15; 20; 25$ mm were subsequently used. Verification results are collected in Table 6.

Table 6
Results of the micrometer verification, (mm)

Length of the standardized plate W_n	Readout / established value					Indication error	
	readout I L_1	readout II L_2	readout III L_3	maximum deviation from the W dimension d	measurement uncertainty $U(E_x)$	$d+U(E_x)$	$d-U(E_x)$
1	1.000	1.000	1.001	0.001054	0.0009	2.0	0.1
1.05	1.051	1.050	1.051	0.000921	0.0009	1.9	0.0
1.5	1.500	1.500	1.500	0.000008	0.0009	0.9	-0.9
2	2.000	2.001	2.000	0.001060	0.0009	2.0	0.1
5	5.000	5.001	5.001	0.001048	0.0009	2.0	0.1
8	8.000	8.001	8.001	0.001006	0.0009	1.9	0.1
10	10.0011	0.0011	0.001	0.000948	0.0009	1.9	0.1
15	15.0011	5.0011	5.001	0.000920	0.0009	1.8	0.0
20	20.002	20.001	20.001	0.001911	0.0009	2.8	1.0
25	25.002	25.002	25.001	0.001798	0.0009	2.7	0.9

Verification result was accepted as passing one, because the indication error equal $2.8 \mu\text{m}$ was less than the permissible limit error for micrometric instruments $E_g = \pm 4 \mu\text{m}$ (PN-82/M-53200).

In 2005 the Laboratory for Material Strength Testing (LMST) participated in the survey of competence – the proficiency test (PT) (scope of strength tests for round steel bars under room temperature). The survey was organized by the Institut für Eignungsprüfung (Germany). The survey brought together research laboratories from 29 countries and 78 of the participants had the accreditation in accordance with the standard EN ISO/IEC 17025.

The examination results along with uncertainties values, calculated in accordance with the foregoing formulas, are presented in Table 5.

Based on comparison of data covered by the report (*Proficiency Test...* 1999) submitted to the Institut für Eignungsprüfung with the information presented in Table 5 the conclusions about general matching of the results can be made. The LMST laboratory has fulfilled the requirements related to the competence survey and was granted with the certificate.

Table 5
Measurement results obtained by the LMST laboratory during the competence survey in 2005

No of specimens	$R_{p0.2}$ (MPa)	$U(R_{p0.2})$ (%)	R_m (MPa)	$U(R_m)$ (%)	A (%)	$U(A)$ (%)	E (MPa)	$U(E)$ (%)
1	719	± 3.06	796	± 1.24	13.9	± 1.18	185 000	± 2.13
2	721	± 3.01	795	± 1.21	14.3	± 1.17	186 400	± 2.13
3	718	± 3.03	792	± 1.28	13.5	± 1.17	187 200	± 2.14
4	714	± 3.01	784	± 1.18	16.1	± 1.17	185 300	± 2.11
5	704	± 3.12	781	± 1.24	14.8	± 1.17	186 200	± 2.18
6	712	± 3.01	792	± 1.20	14.1	± 1.18	188 700	± 2.11
Average LMST	715	± 3.04	790	± 1.23	14.6	± 1.17	186 500	± 2.13
Participants	712	± 2.00	790	± 1.30	16.2	± 2.00	186 500	± 4.00
Organizers	691	± 2.30	786	± 1.36	15.7	± 1.20	n/a	n/a

References

- ARENDALSKI J. 2003. *Niepewność pomiarów*. Oficyna Wydawnicza Politechniki Warszawskiej, Warszawa
- CWA 15261-2. 2005. *Measurement uncertainties in mechanical tests on metallic materials – Part 2. The evaluation of uncertainties in tensile testing*.
- Proficiency Test-Tensile Test Steel-Round bar at room temperature (TTSRR 2005) – Final Report*. 2006. Institut für Eignungsprüfung.

Accepted for print 27.06.2008 r.

POWER OUTPUT OF A WIND TURBINE IN TUBULAR HOUSING EQUIPPED WITH A DIFFUSER

Leszek Romański

Institute of Agricultural Engineering
Wrocław University of Environmental and Life Sciences

Key words: wind turbine, tubular housing, diffuser, power output of a wind turbine.

A b s t r a c t

This paper presents the results of a study conducted on a model wind turbine in tubular housing equipped with a diffuser. The impact of the diffuser's diameter and length on the wind turbine's power output was tested. The highest output was reported when the ratio of the diffuser's inlet and outlet diameter was 1.7 and relative diffuser length reached approximately 0.6.

MOC SIŁOWNI WIATROWEJ PRACUJĄCEJ W OBUDOWIE RUROWEJ WYPOSAŻONEJ W DYFUZOR

Leszek Romański

Instytut Inżynierii Rolniczej
Uniwersytet Przyrodniczy we Wrocławiu

Słowa kluczowe: siłownia wiatrowa, obudowa rurowa, dyfuzor, moc siłowni wiatrowej.

A b s t r a k t

W artykule przedstawiono wyniki badań modelu siłowni wiatrowej pracującej w obudowie rurowej z zainstalowanym dyfuzorem. Testowano wpływ średnicy i długości dyfuzora na generowaną przez tę siłownię moc. Najwyższe wartości mocy uzyskano wówczas, gdy stosunek średnicy wlotowej do wylotowej dyfuzora wynosił 1,7, a względna długość dyfuzora około 0,6.

Introduction

There is a growing demand for the supply of electric power with low wattage of 0.5 – 2 kW to sites which remain outside the reach of power transmission lines. Such sites include stations for monitoring forests and freeways, power supply units of hydrological and meteorological stations, agricultural driers, fish pond aeration units, etc. The construction of transmission lines connecting remote and isolated power receivers is not financially justified. The same applies to photovoltaic fuel cells due to their low efficiency and high production costs (FILIPOWICZ 2002, AKHAMOV 2006). The construction of mini wind farms in the vicinity of such sites seems to offer a reasonable solution to the problem (LEE 2000). Mini wind farms have already been introduced in highly industrialised countries, in particular in Germany. Standard rotor diameter does not exceed 2 m. A wind turbine's low output of 0.2 – 1 kW does not always meet user needs. With constant wind force, a turbine's output can be maximised by increasing the rotor diameter as in theory, it raises the device's output to a second power.

A new solution was proposed to ensure that the increase in power output does not require resizing of the wind turbine. The blade and turbine set were placed in tubular housing connected to a diffuser. Owing to this solution, the resulting power output will be several dozen percent higher than that of conventional wind turbines.

Objective

The objective of this study was to determine the impact of the diffuser's geometric parameters on the power output of a wind turbine in tubular housing.

Methodology and investigated site

The investigated site was a three-blade model wind turbine in tubular housing with a diffuser (Fig. 1). Rotor diameter was 338 mm and the diameter of the tubular housing was 340 mm. Diffusers with the diameter of 340, 374, 408, 440 and 510 mm were built to investigate the impact of the diffuser's outlet diameter on the wind turbine's power output. Three diffuser lengths were applied in this study: 70, 140 and 210 mm, respectively (Fig. 2).

Since a universal mathematical model describing the operation of a wind turbine will be developed at subsequent stages of the study, relative dimen-

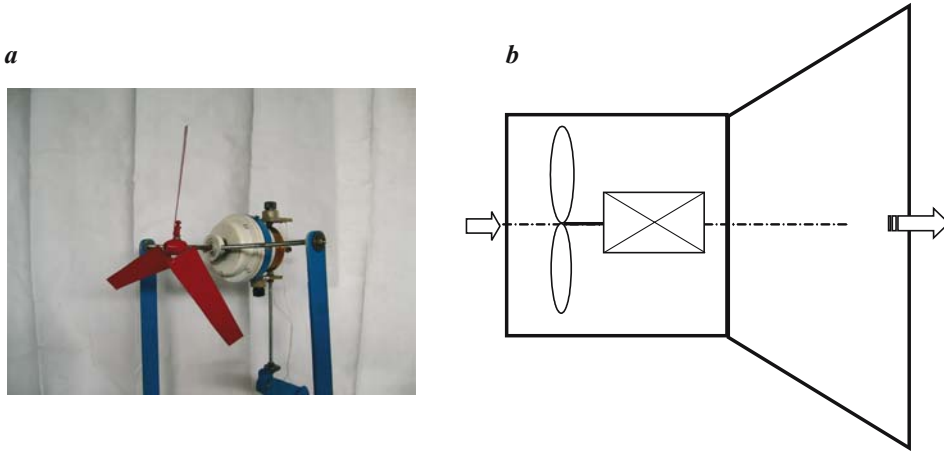


Fig. 1. Wind turbine model (a) and a diagram of tubular housing with a diffuser (b)

sions were applied to process the results obtained in the investigated site, i.e. the diffuser's relative diameter and relative length. This solution will support the application of the geometric probability law during the construction of larger structures in the future.

The diffuser's relative diameter i_d was defined as the ratio of its outlet diameter to the diameter of the wind turbine's tubular housing. The relative diameter was 1, 1.1, 1.3, 1.5 and 1.7, respectively. The diffuser's relative length j_d was the ratio of diffuser length to housing diameter. The relative length was 0.2, 0.4 and 0.6, respectively. Higher values were not applied in line with DZIERŻANOWSKI'S (1983) claim that they do not contribute to a further increase in the turbine's output.

In addition to the previously applied lengths, diffuser length of 0.8 was also introduced to determine the impact of the diffuser's relative length on the wind turbine's power output.

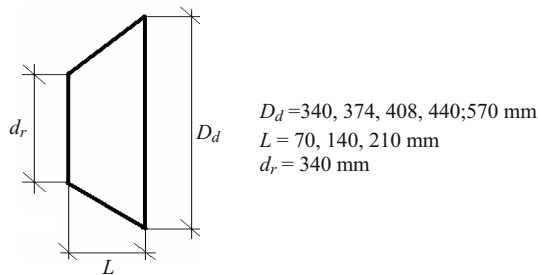


Fig. 2. Diffuser geometry

A single phase, self-excited AC turbine applied in Jarecki centrifuges was used.

The study was conducted in an aerodynamic tunnel with the diameter of 0.7 m and length of 4 m (Fig. 3). The velocity of the air stream flowing through the tunnel was in the range of 0-4.5 m s⁻¹ (WIERCIŃSKI 2005). The measurement methodology and the method of determining the wind turbine's power output are described in a paper by CHARKIEWICZ and ROMAŃSKI (2007).

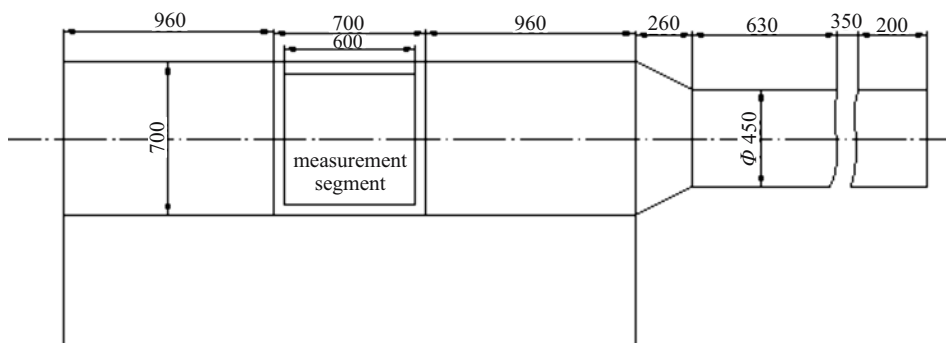


Fig. 3. Diagram of the aerodynamic tunnel

Results and analysis

The impact of the diffuser's geometry parameters on the power output of the model wind turbine in tubular housing is presented in Figure 4 and in Figure 5. Tests were performed at air stream velocity of 4.5 m s⁻¹. The analysis of the above relationship indicates that the power output of the model wind turbine in tubular housing is largely determined by the diffuser's diameter. The dependencies for three diffuser lengths were described with second degree polynomials with very high coefficients of determination of more than 0.95.

A steep increase in power output was observed from small values of the diffuser's relative diameter up to 1.5. A power output decrease was reported in respect of diameters larger than 1.65, which is why the relative output diameter of a diffuser should be kept under 1.65.

The measurements to determine the dependence between the power output of a wind turbine with a diffuser and diffuser length were performed for relative diffuser diameters of 1.1, 1.3, 1.5 and 1.7. The investigated relationships show a characteristic pattern as the wind turbine's power output increased proportionally to an increase in the diffuser's relative length in the

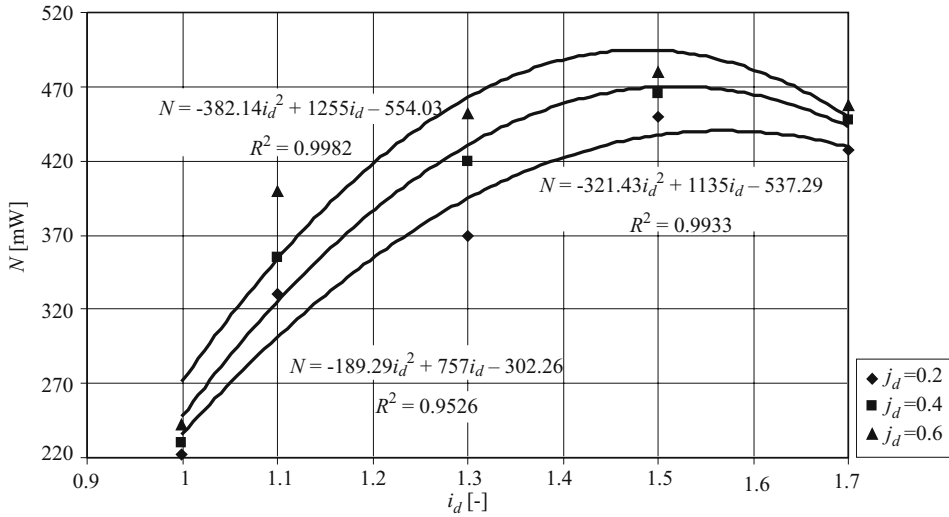


Fig. 4. Relationship between the power output of a wind turbine with a diffuser and the diffuser's relative output diameter

range of 0.2 – 0.6. A minor drop in output was reported when the diffuser's relative length exceeded 0.6. These results confirm the findings of other authors who observed that the ratio between the diffuser's length and its diameter should not exceed 0.6 (DZIERŻANOWSKI 1983).

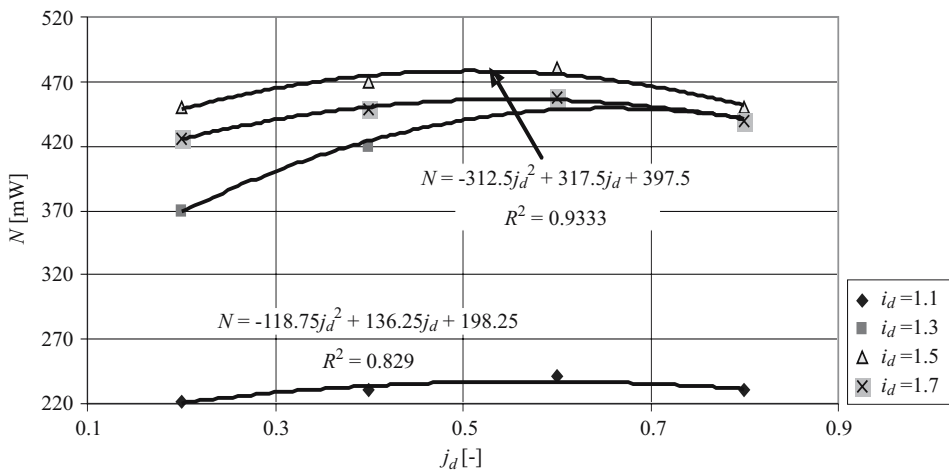


Fig. 5. Relationship between a wind turbine's power output and the relative length of the diffuser

Conclusions

1. A wind turbine's power output increases rapidly with an increase in the diffuser's relative diameter. The highest output is reported at a relative diameter of 1.5.

2. An increase in diffuser length leads to an increase in a wind turbine's power output. The highest output is reported at a relative diffuser length of around 0.6.

References

- AKHMATOV V. 2006. *Induction turbines for wind power*. Vorg Inc.
- CHARKIEWICZ M., ROMAŃSKI L. 2007. *Praca siłowni wiatrowej w obudowie rurowej*. IX Międzynarodowa Konferencja Naukowa pt. „Teoretyczne i aplikacyjne problemy inżynierii rolniczej”, s. 50-51.
- DZIERŻANOWSKI P. 1983. *Turbinowe silniki odrzutowe*. Wydawnictwo Komunikacji i Łączności. Warszawa.
- FILIPOWICZ M. 2004. *Małe turbiny wiatrowe*. Nafta & Gaz Biznes, 4: 62-64.
- LEE E. 2000. *Optimization of Turbomachinery Airfoil Shapes in Viscous Unsteady Compressible Flows*. Pennsylvania State University.
- POPRAWSKI R., SALEJA W. 1999. *Zasady opracowania wyników pomiarów*. Oficyna wydawnicza PW, Wrocław.
- WIERCIŃSKI Z. 2005. *On capability of using four point sphere probe to flow velocity measurement*. Tech. Sc., 8: 1-25.

Accepted for print 14.08.2008 r.

OPERATING EFFICIENCY OF A NON-MEMBRANE GROUND HEAT AND MASS EXCHANGER AFTER 15 YEARS OF OPERATION

Leszek Romański

Institute of Agricultural Engineering
Wrocław University of Environmental and Life Sciences

Key words: ground exchanger, rock bed, operation, air temperature and humidity.

A b s t r a c t

This paper presents the results of a study conducted in 1991 and 2006 on a non-membrane ground heat and mass exchanger. The obtained results indicate that under similar operating conditions, the increase in air temperature at the exchanger outlet in the winter fell by approximately 16.5% after 15 years of operation. Relative humidity remained at a similar level within the range of 74-80% which corresponds to standard requirements. In the summer, air cooling efficiency was lower by 17% and air humidity was lower by 5%.

EFEKTY PRACY BEZPRZEPONOWEGO GRUNTOWEGO WYMIENNIKA CIEPŁA I MASY PO 15 LATACH EKSPLOATACJI

Leszek Romański

Instytut Inżynierii Rolniczej
Uniwersytet Przyrodniczy we Wrocławiu

Słowa kluczowe: wymiennik gruntowy, złożo kamienne, eksploatacja, temperatura i wilgotność powietrza.

A b s t r a k t

W artykule przedstawiono wyniki badań przeprowadzonych w latach 1991 i 2006 na gruntowym bezprzeponowym wymienniku ciepła i masy. Stwierdzono, że w porównywalnych warunkach pracy urządzenia, zimą, przyrost temperatury powietrza na wyjściu z wymiennika był o około 16,5% mniejszy niż przed 15 laty. Wilgotność względna utrzymywała się na podobnym poziomie i wynosiła 74-80%, co odpowiada wymogom normatywnym. Latem schłodzenie powietrza było mniej efektywne o 17%, a nawilżanie powietrza niższe o 5%.

Introduction and Objective of the Study

Non-membrane ground heat and mass exchangers with horizontal air flow have been used in Poland for 30 years. The first exchangers with a granite rock bed were built at the Wrocław University of Technology (BESLER, SPRYSZYŃSKI 1980, BESLER 1985), and exchangers with a basalt bed were built 10 years later at the Institute of Agricultural Engineering in today's Wrocław University of Environmental and Life Sciences (ROMAŃSKI 1995). The main element of the exchanger system, a rock bed, is usually set underground at the depth of more than 2 m. Since at the depth of 3-4 m, ground temperature is roughly constant and it corresponds to the mean annual temperature of ambient air, which reaches around 10°C in Poland's climatic zone, it has been assumed that the parameters of ventilation air can be modified by passing it through a rock bed. In the summer, air is cooled and humidified and in the winter, it is heated and dried before it enters the ventilation system. The structure and the operation of exchangers has been described in detail in the above quoted publications.

Many practitioners presently believe that the efficiency of these types of heat exchangers drops after more than 10 years of operation (PIEŃKOWSKA 2005). Silting decreases the rock bed's porosity and, consequently, impairs its efficiency. The operating parameters of air (temperature, humidity) exiting the heat exchanger are also lower in newly built deposits.

The objective of this study was to confirm or rule out the assumption that operating time affects the parameters of treated ventilation air.

Methodology

The structure of a ground heat and mass heat exchanger has been described in detail by ROMAŃSKI (1995). The diagram of a test stand indicating the location of measurement sensors is presented in Figure 1.

Thermocouples were placed in the rock bed with a 0.7 m scale to measure the temperature of air passing through the deposit. A set of MM1 microclimate meter sensors was used to measure the outlet air temperature, relative humidity and stream velocity. The air stream flowing through the exchanger was measured based on air velocity determined with the use of the continuity equation. The temperature of ambient air at the inlet was measured with a mercurial thermometer (with the precision of 0.5°C), and humidity was determined with an Assman psychrometer which was also used to calibrate the microclimate meter.

The study was performed in 1991 and 2006, in the winter and summer. The air stream flowing through the deposit was similar in all measurements, reaching 1300 m³ s⁻¹.

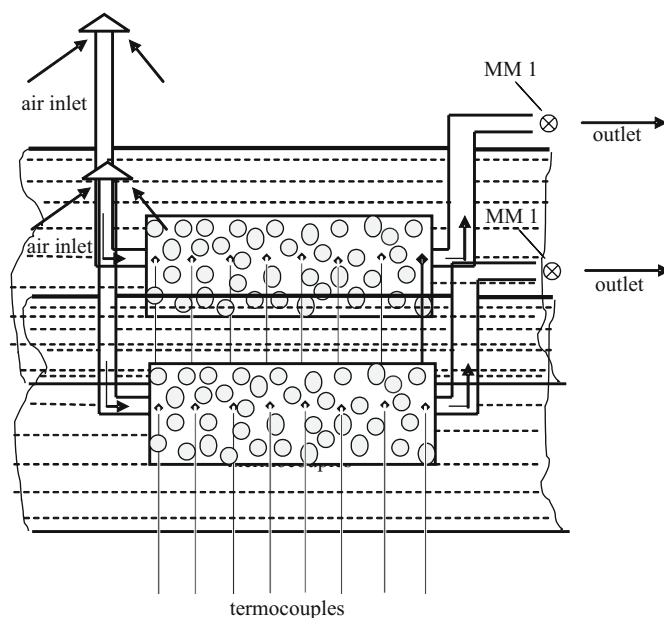


Fig. 1. Diagram of a test stand

Results

In a period marked by low ambient air temperatures, the study was conducted under similar conditions in January and November. The course of air temperature and relative humidity at the inlet and outlet of the exchanger is presented in Figure 2.

Despite similar inlet air parameters, the average increment in temperature at the exchanger outlet was 4.8°C in 1991 (Fig. 2a) and 4.0°C in 2006 (Fig. 2b), indicating a drop of 16%. Since the air stream passing through the exchanger had similar parameters in both investigated years, the only logical cause of the decrease in the average temperature increment at the exchanger outlet in 2006 is the lower porosity of the rock bed. The definition and the method of determining rock bed porosity are presented in a study by ROMAŃSKI (2001).

The drop in air volume between rocks probably resulted from a high water table in some years and the silting up of the deposit. The deposit was opened a year ago to reveal that some rocks had been covered with a layer of soil both at the bottom and in the wall area of the deposit. The above has led to a decrease in the exchanger's cross-section which, in line with the continuity equation, speeded up the flow of the air stream through the exchanger.

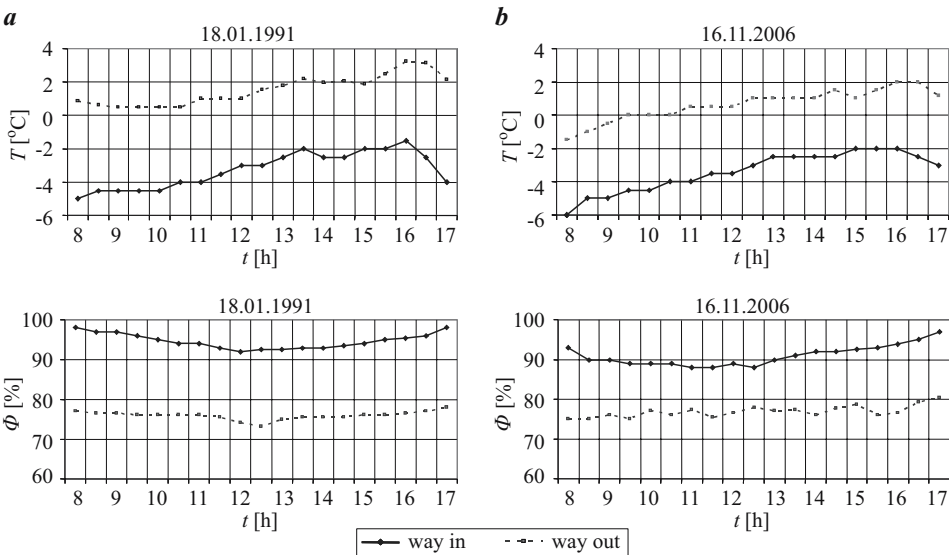


Fig. 2. Changes in the temperature and relative humidity of air at the inlet and outlet of the exchanger in the winter: a) 1991, b) 2006

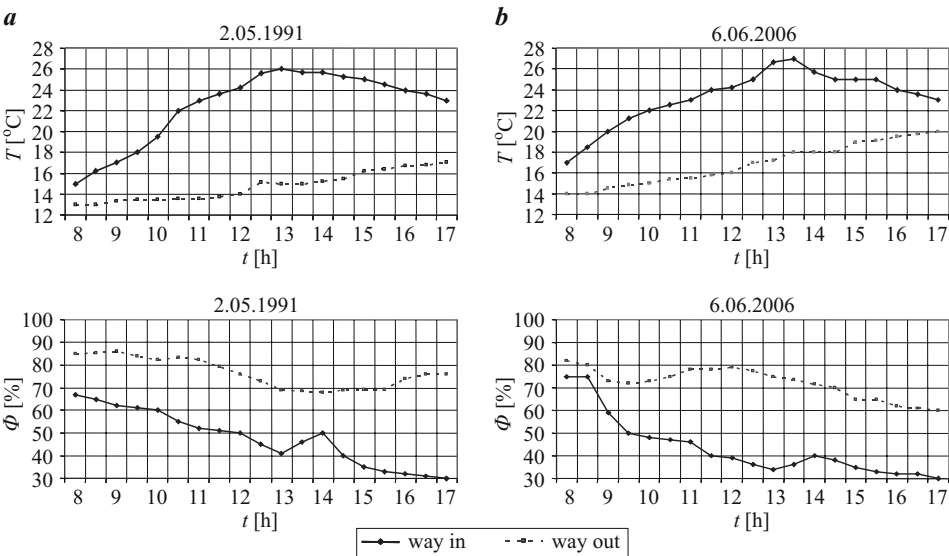


Fig. 3. Changes in the temperature and relative humidity of air at the inlet and outlet of the exchanger in the summer: a) 1991, b) 2006

Consequently, air was less heated due to a shorter time of passage through the exchanger.

Changes in relative air humidity at the exchanger outlet indicate that in both measurement years, this parameter remained in the range of 74-80% (Fig. 2) which meets standard requirements.

An analysis of temperature changes at the outlet of the ground exchanger in the summer (Fig. 3) shows that the maximum temperature drop (13:00 PM) in a new device (Fig. 3a) was 13°C. Following 15 years of operation of the same device (Fig. 3b), temperature dropped by only 10°C. Therefore, the average drop in the temperature of the air stream after passage through the rock deposit was 17% lower in the summer. Similarly to the drop in air heating efficiency in the winter, the reduced efficiency of air cooling was also caused by lower porosity of the rock bed. Even when the relative humidity of ambient air fell below 40% in the summer, air humidity at the outlet of the exchanger was never lower than 60%.

Thermocouples were placed in the axis of the exchanger rock bed to register changes in the temperature of the air stream subject to the distance travelled in the exchanger (Fig. 4). As expected, air temperature decreased with an increase in the length of the rock bed.

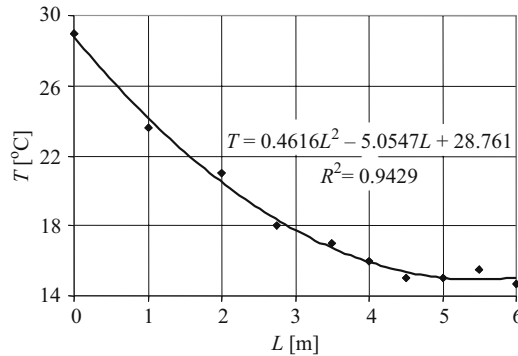


Fig. 4. Relationship between the temperature of air passing through the ground exchanger and the length of the rock bed

Further changes in temperature were not noted when air travelled a distance greater than 4.5 m. This is a very important observation for practitioners as it implies that these types of non-membrane exchangers do not require the installation of rock beds longer than 4.5-5 m.

Conclusions

1. Following 15 years of operation of a ground heat and mass exchanger, the increase in air temperature at the exchanger outlet fell by 15% in the winter. Air cooling efficiency decreased by 17% in the summer.

2. Following the same period of operation, the relative humidity of air at the exchanger outlet remained constant in the winter, while a 5% drop was noted in the summer.

3. The optimal length of the rock bed in a non-membrane ground exchanger with a basalt rock bed is 4.5-5 m.

References

- BESLER G., SPRYSZYŃSKI Z. 1980. *Możliwości wykorzystania naturalnej energii gruntu do termowentylacji i klimatyzacji pomieszczeń*. COW, s. 11-12.
- BESLER G. 1985. *Podstawy projektowania bezprzeponowych gruntowych wymienników ciepła i masy dla klimatyzacji i termowentylacji*. Raport SPR-13 85. Instytut Inżynierii Chemicznej i Urządzeń Ciepłych Politechniki Wrocławskiej.
- BESLER G., BESLER M., KWIECIEŃ D. 1996. *Grunt – ekologiczne źródło energii cieplnej*. COW, 6: 268-272.
- PIEŃKOWSKA H. 2005. *Radon exhalation from building materials and soil*. Techn. Sc., 8: 27-39.
- ROMAŃSKI L. 1995. *Odzysk ciepła zmagazynowanego w ziemi dla celów wentylacji*. Zesz. Nauk. AR Wrocław, 258: 35-43.
- ROMAŃSKI L. 2001. *Badania modelowe bezprzeponowego wymiennika ciepła w aspekcie oporów przepływu powietrza*. Inż. Rol., 13: 403-409.

Accepted for print 14.08.2008 r.

METHODS OF DIAGNOSING AN ACWW 1000 SUGAR CENTRIFUGE WITH THE USE OF VIBRATION PROCESSES*

Krzysztof Ligier

Chair of the Building, Exploitation of Vehicles and Machines
University of Warmia and Mazury in Olsztyn

Key words: sugar centrifuge, diagnosing, diagnostic algorithms.

A b s t r a c t

This paper presents a method of diagnosing a sugar centrifuge ACWW 1000, which employs vibration processes. The condition assessment was based on the RMS value for vibration speed amplitude. Shewhart's control charts were used to determine the warning and critical values. Campaign and inter-campaign period diagnosis algorithms were developed.

METODA DIAGNOZOWANIA WIRÓWKI CUKROWNICZEJ ACWW 1000 Z WYKORZYSTANIEM PROCESÓW DRGANIOWYCH

Krzysztof Ligier

Katedra Budowy, Eksploatacji Pojazdów i Maszyn
Uniwersytet Warmińsko-Mazurski w Olsztynie

Słowa kluczowe: wirówka cukrownicza, diagnozowanie, algorytmy diagnozowania.

A b s t r a k t

W pracy przedstawiono metodę diagnozowania wirówki cukrowniczej ACWW 1000 z wykorzystaniem procesów drganiowych. Jako podstawę oceny stanu przyjęto wartość RMS amplitudy prędkości drgań. Do określenia wartości ostrzegawczych i krytycznych wykorzystano metodę kart kontrolnych Shewhardta. Opracowano algorytmy diagnozowania kampanijnego i międzykampanijnego.

*Aim of the study: developing a diagnostic method for an ACWW 1000 sugar centrifuge to be employed by maintenance services.

Introduction

In terms of effectiveness, a dynamic strategy (according to the technical condition) is the most beneficial of maintenance strategies. However, it requires appropriate diagnostic methods to assess the facility momentary condition and foresee its changes in future. The requirements concern machines in continuous operation, whose role is critical to the technological process. One of such machines is a sugar centrifuge ACWW 1000.

Study object

A group of 12 ACWW1000-type sugar centrifuges was examined. An ACWW 1000 sugar centrifuge is a continuous centrifuge used in sugar production. The working speed of the centrifuge basket is 1800 rpm. Torque is transferred from the engine to the basket shaft directly through a permanent flexible coupling.

A centrifuge diagram is shown in Figure 1. Masecuite is fed through a feeding pipe (4) into the basket (3) and spread evenly on sieve surfaces by centrifugal force. In the course of centrifuging, powdered sugar is separated on sieves from the so-called “run-off” syrup. The products are carried off from the centrifuge by draining pipes (5).

The ACWW 1000 centrifuge power transmission system is shown in Figure 2. It consists of an electric engine (1) connected through a flexible coupling (2) with a shaft (3), on which a basket (4) with sieves is placed. The shaft with

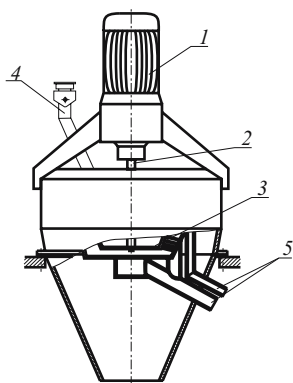


Fig. 1. A diagram of an ACWW1000 centrifuge: 1 – engine, 2 – drive shaft, 3 – basket with sieves, 4 – feeding pipe, 5 – draining pipes

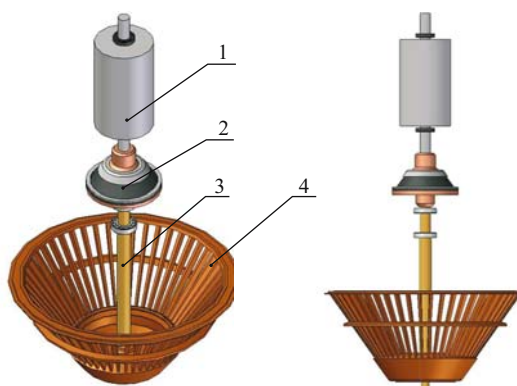


Fig. 2. View of the power transmission system of an ACWW1000 sugar centrifuge: 1 – engine, 2 – flexible coupling, 3 – shaft, 4 – basket

a basket is bearing supported on one side with two rolling bearings, placed in a gyro-socket cradle. A detailed structure of the rotating system of an ACWW 1000 centrifuge and its mathematical model were presented in another paper (WOROSZYŁ et al. 2005).

Selecting the diagnostic signals

The best way to identify most faults of the rotating system elements (rolling bearings, coupling) is spectral analysis, owing to its universality and the abundant literature which describes it (CEMPEL 1989, ŻÓLTOWSKI 1996). A specification of faults identified with spectral analysis and the corresponding frequencies are presented in Table 1.

Table 1
Fault states identified by spectral analysis of centrifuges

Fault state	Typical (dominant) frequency and measuring points	Notes
Lack of balance of the rotating system	First harmonic (30 Hz) – measurement on the bearing support	If the values of vibration amplitude for the harmonic frequency change during a measurement, it indicates a technological lack of balance – interference caused by a working medium.
Loss of elasticity by the flexible coupling	Second harmonic (60 Hz) – measurement on the coupling casing	Increased amplitudes of vibrations are possible for the 1, 3, 4 harmonic frequency.
Lack of balance of the engine cooling fan or the engine rotor	First harmonic (30 Hz) – measurement on the engine	The vibration speed amplitude for the 1 st harmonic frequency at point 1 is higher than at points 2 and 3.
Defect of the centrifuge shaft bearings	Frequencies above 100Hz usually yield an image of grouped peaks – measurement on bearing support	It has been noted that in order to identify defects of a centrifuge shaft bearings it is enough to conduct a spectral analysis of the vibration speed of up to 1200 Hz.
Defect of the engine bearings	Frequencies above 100Hz usually yield an image of grouped peaks – measurement on the engine	

Selection of the measuring points

The measuring point selection was based on the diagram of interactions between centrifuge elements, shown in Figure 3 (LIGIER 2005).

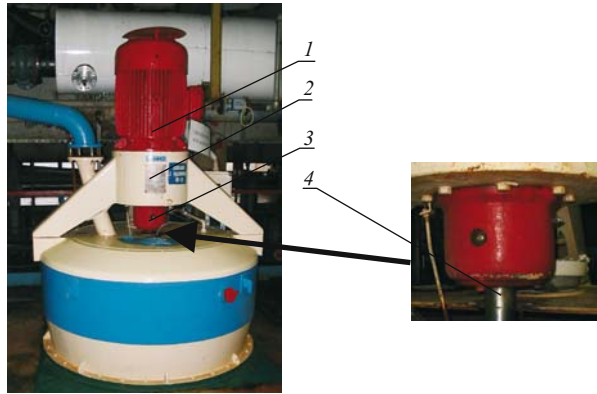


Fig. 4. The position of the measuring points 1, 2, 3 and 4 on an AWW 1000 centrifuge 1 – engine, 2 – coupling cover, 3 – bearing support case, 4 – centrifuge shaft

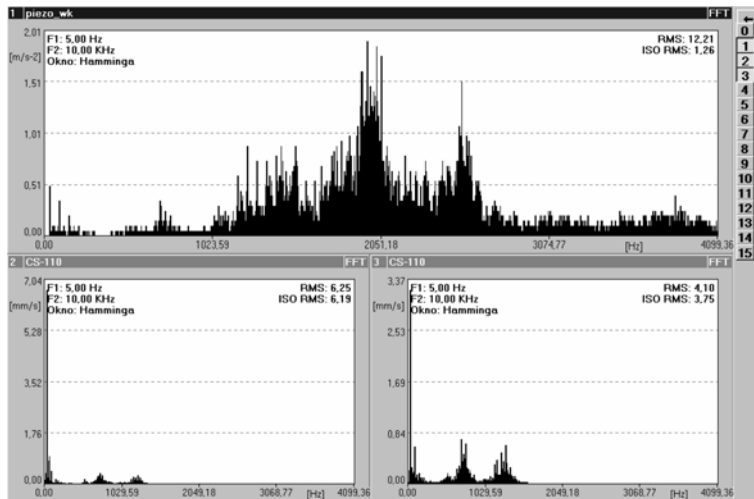


Fig. 5. A spectrum of centrifuge vibrations, measuring point 3

The spectrum shown in Figure 6 shows a considerable increase in the vibration speed amplitude (20 mm/s) for the first harmonic frequency of the centrifuge shaft (30 Hz). This indicates a lack of balance of the rotating system of the sugar centrifuge.

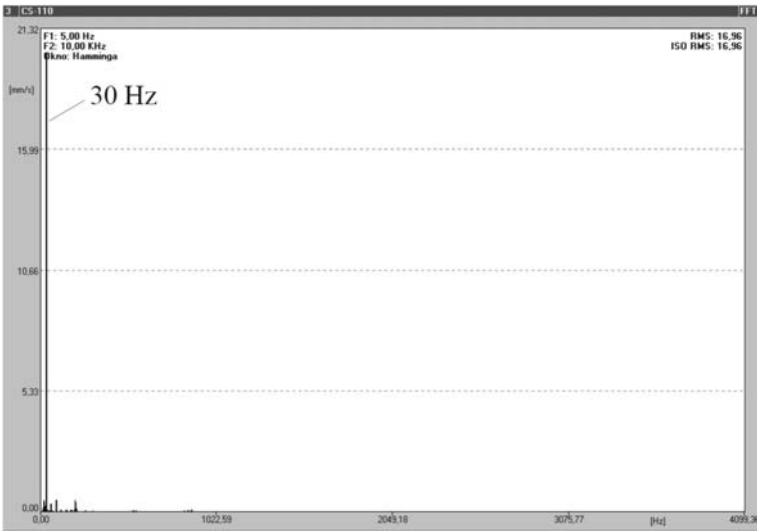


Fig. 6. A vibration speed spectrum for a centrifuge no. 1, measuring point no. 3

Figure 7 shows a spectrum of vibrations of a centrifuge with the defective flexible coupling. This is indicated by an increase in the vibration speed amplitude for the second harmonic frequency, which is higher than that for the first harmonic.

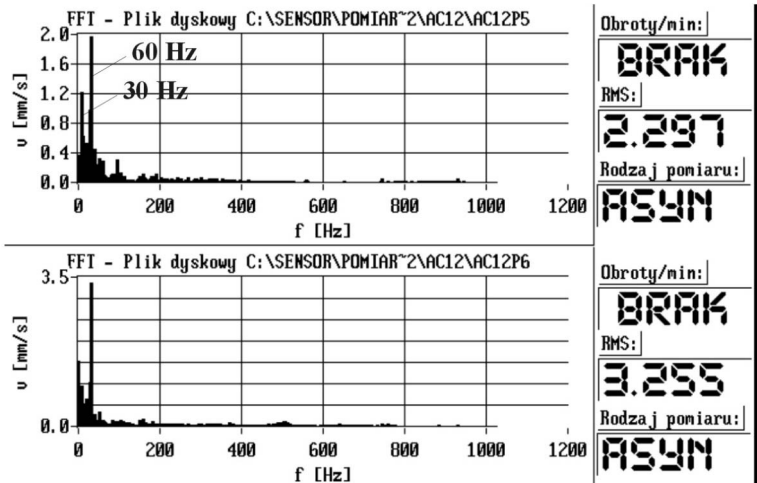


Fig. 7. Vibration spectrum for a centrifuge no. 12, measuring point no. 3 – defective coupling

Figure 8 shows a vibration speed spectrum for measurement point 1 (on the engine) and no. 3 (on the bearing support). A comparison of the registered spectra reveals that the vibration amplitude for the first harmonic frequency is higher than for point 3. This provides grounds for the conclusion that the source of vibrations is situated closer to point no. 1, which indicates that the lack of balance of the engine fan is the cause.

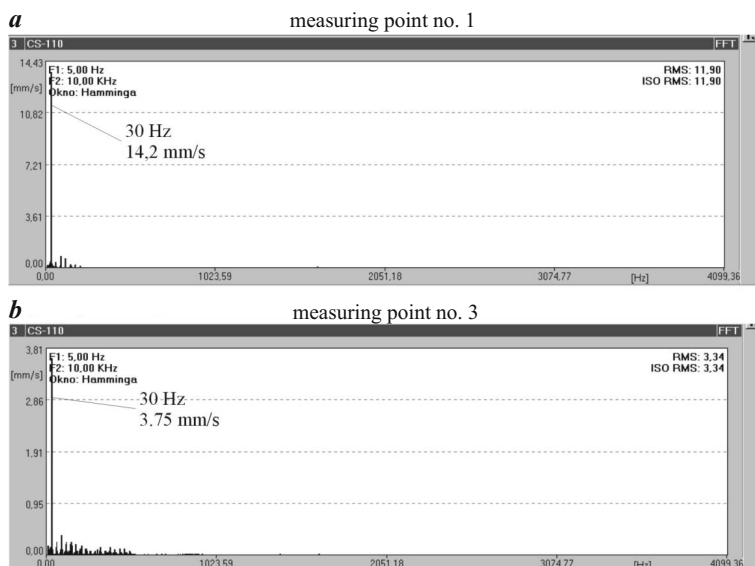


Fig. 8. Vibration spectra for centrifuge no. 2 – lack of balance of the engine rotor

Determination of the limiting values

According to PN-90/N-01358 (Methods of measurement and assessment of machine vibrations), for an assessment of a general condition of a machine, based on vibration analysis, application of vibration speed amplitude RMS values is recommended. According to the standard, ACWW 1000 centrifuges are classed as group II machines. It should be assumed that the acceptable value of vibrations for the machines is 7.1 mm/s, and the warning value – 4.5 mm/s. Due to the interfering effect of the centrifuged medium, the values can only be applied in the inter-campaign centrifuge diagnostics. They had to be corrected for the diagnostics in the campaign period. To this end, Shewhart's control charts were used (MIKOŁAJCZAK et al. 2002).

The warning and critical values were determined, defined in the following manner:

- the upper warning line – $UWL = \bar{X} + 2\sigma$,
- the upper control (limiting) line – $UCL = \bar{X} + 3\sigma$.

where:

\bar{X} – signal mean value;

σ – standard deviation.

In order to determine the value of the examined diagnostic signal, which is registered in the operational conditions, a passive and active-passive diagnostic experiment was conducted. Table 2 shows a specification of the UWL and UCL values calculated for V_{RMS} , based on the data collected during the sugar production campaigns of 2001-2002.

Table 2

Specification of results of calculation of UWL and UCL values for V_{RMS} , for three measuring points (to be applied during the campaign period)

Statistical parameter	V_{RMS} at measuring point no. 3 [mm/s]	V_{RMS} at measuring point no. 2 [mm/s]	V_{RMS} at measuring point no. 1 [mm/s]
UWL	12.36	7.60	7.69
UCL	15.55	9.41	9.58

It is noteworthy that the warning and control values are different for measuring point 3 than for measuring points 1 and 2. This is associated with the considerable effect of the load of the centrifuged mass on the vibrations of the lower bearing.

Shewhart's control charts can be related only to a selected machine, by marking the values of the measured signal for consecutive measurements (values of V_{RMS} vs. time). An example of such a chart is given in Figure 9; it indicates the possibility of using such charts to analyse changes of the value of the examined signal and taking corrective actions at an appropriate time.

The frequency of diagnosis is determined based on the practical knowledge of the defect development rate and on the observation of changes of the analysed signal.

During an inter-campaign period, it is beneficial to measure vibrations vs. rotation for the centrifuge start run. This makes it possible to estimate the rotation speeds which trigger resonance. An example vibration speed amplitude vs. rotation for a centrifuge start run is shown in Figure 10.

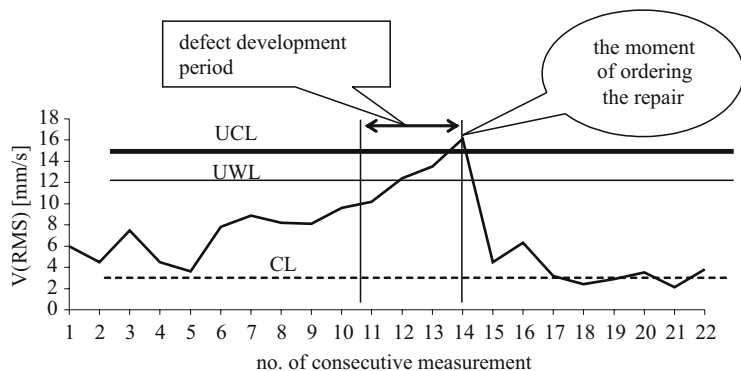


Fig. 9. Vibration speed amplitude RMS values for 22 consecutive measurements of centrifuge no. 6 – measuring point no. 3

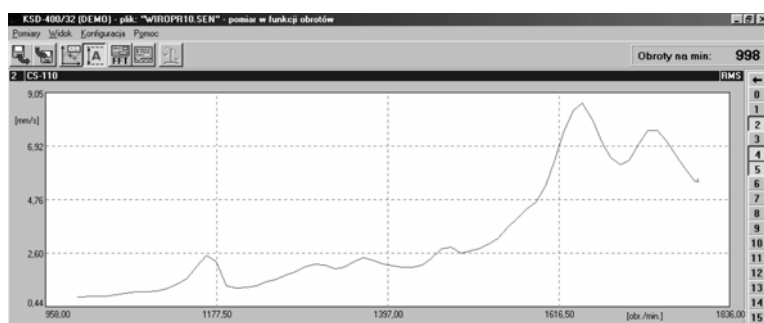


Fig. 10. Vibration speed amplitude vs. rotation for a centrifuge start run

An analysis of diagrams shows that a vibration amplitude increases for the rotational speeds of 1163, 1644 and 1735 rpm, which corresponds to the frequencies of 13, 27 and 29 Hz. This can be employed in determination of the maximum speed of a centrifuge which does not cause the resonance and applying the speed during the campaign period as the working speed.

Diagnostic algorithms

Due to the use of centrifuges in campaigns, different diagnostic algorithms have been proposed for the campaign and inter-campaign periods; they are shown in Figure 11 and 12.

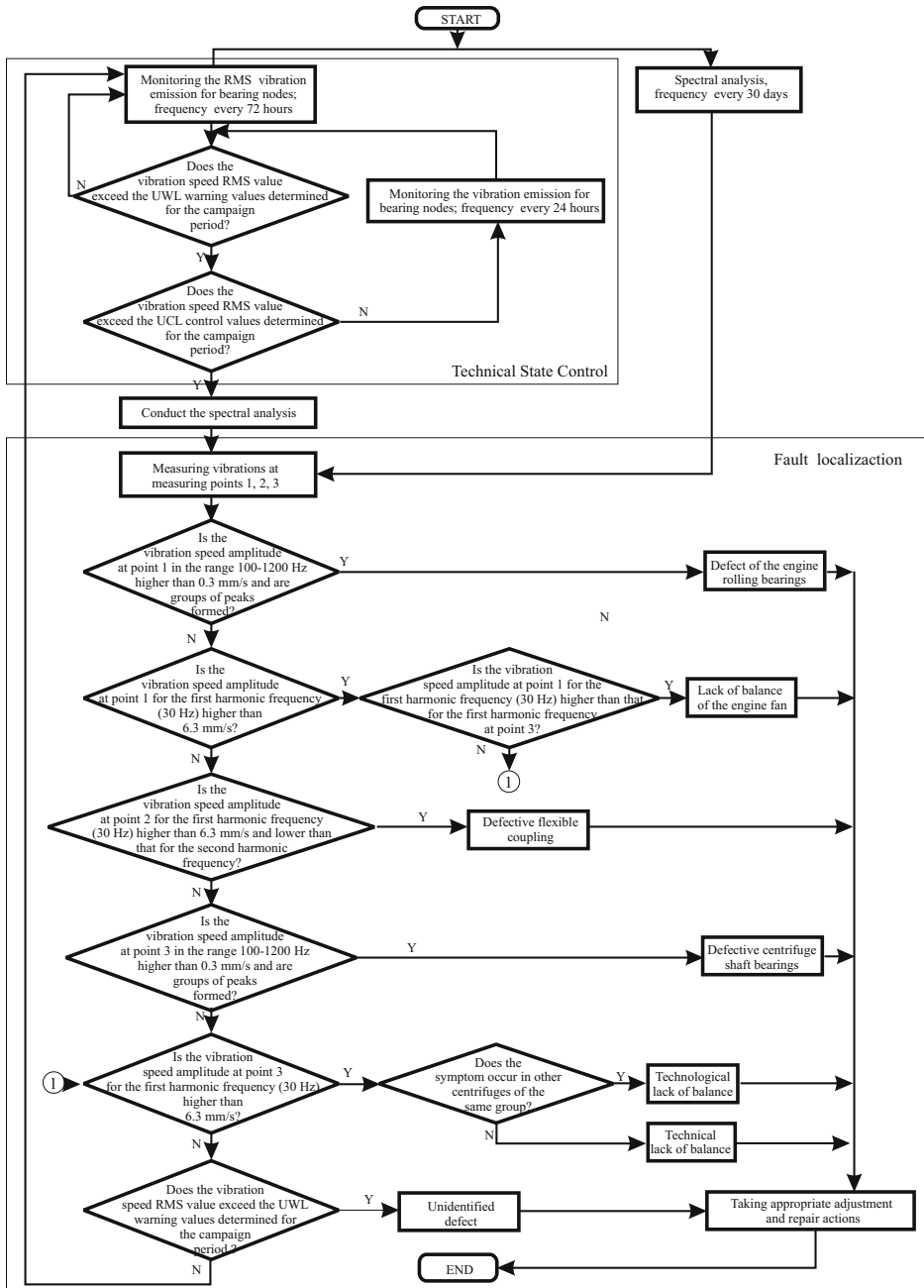


Fig. 11. Diagnostic algorithm for a campaign period for an ACWW 1000 sugar centrifuge

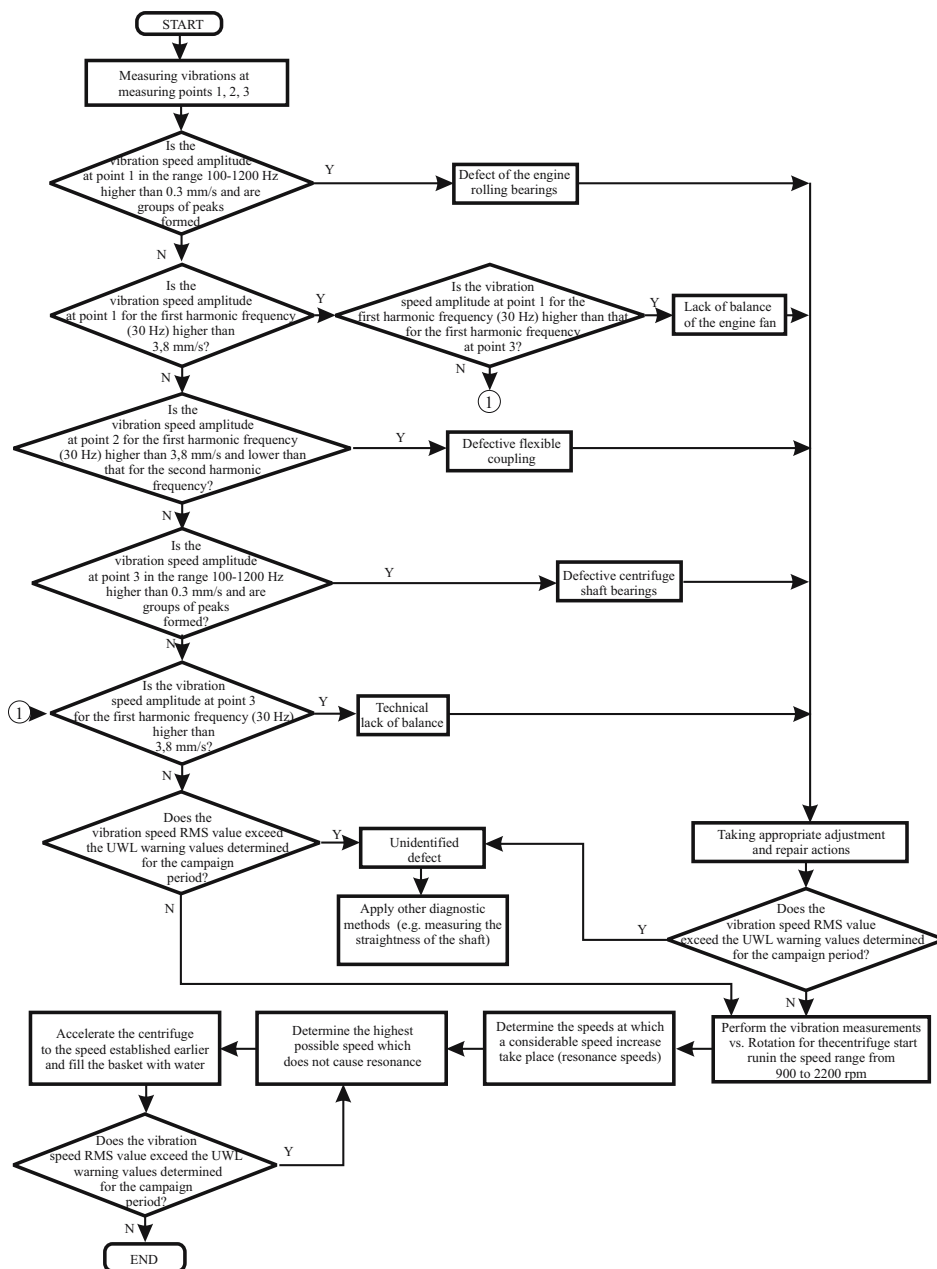


Fig. 12. Diagnostic algorithm for an inter-campaign period for an ACWW 1000 sugar centrifuge

Summary

Vibration processes generated during a centrifuge operation provide information which helps diagnose the device technical condition and identify most faults which occur in the course of its operation, without switching it off.

The diagnostic algorithms proposed in this paper help to make assessment of the machine condition and preparation for a sugar production campaign as well as of its condition during the campaign.

The condition assessment in the algorithms is based on the vibration speed amplitude RMS value for which the warning and critical values for the campaign and inter-campaign periods have been determined. Spectral analysis has been applied to identify the device faults resulting from technical and technological defects. The measurement of vibrations vs. rotational speed for the centrifuge start run allows for easy identification of resonance speeds for particular centrifuges, which in turn helps determine the maximum safe operation speed for each device.

Reference

- CEMPEL C. 1989. *Wibroakustyka stosowana*. PWN, Warszawa.
- LIGIER K. 2005. *Metoda diagnozowania wirówki cukrowniczej ACWW 1000 z wykorzystaniem procesów drganiowych*. Rozprawa doktorska, ATR, Bydgoszcz.
- MIKOŁAJCZAK P., RYCHLIK A. 2002. *Metoda wyznaczania wartości ostrzegawczych i kontrolnych sygnału diagnostycznego z wykorzystaniem kart kontrolnych Shewharta*. Diagnostyka, 28.
- WOROSZYŁ S., LIGIER K., MIKOŁAJCZAK P. 2005. *Mathematical model of the rotor system of a sugar centrifuge ACWW1000*. Technical Sciences, 8: 211-219.
- PN-90/N-01358, *Metody pomiarów i oceny drgań maszyn*.
- ŻÓŁTOWSKI B. 1996. *Podstawy diagnostyki maszyn*. Wydawnictwo Uczelniane ATR, Bydgoszcz.

Accepted for print 25.09.2008 r.

EFFECT OF ENVIRONMENT-FRIENDLY MODIFICATION OF Al-12%Si ALLOY ON ITS STRUCTURE

***Tomasz Lipiński¹, Anna Góral², Paweł Mikołajczyk¹,
Marcin Cudakiewicz³, Anna Wach¹***

¹ Chair of Materials and Machinery Technology
University of Warmia and Mazury in Olsztyn

² Institute of Metallurgy and Material Sciences
Polish Academy of Sciences in Kraków

³ BUJALSKI Sp z o.o. in Dywity

Key words: al alloys, silumin, crystallization, modification, structure.

Abstract

The paper presents the results of a study on the modification of Al-12%Si alloy with a homogeneous modifier produced by fast cooling at a rate of 100 and 200 K/s. The homogeneous modifier had the chemical composition of the modified alloy, and it contained 0, 7, 12 and 20% Si. The modifier was mixed with liquid Al-Si alloy in the crucible for one minute. The effect of cooling rate and the modifier content of alloy mass on alloy structure was determined in the study. An analysis of the modification of eutectic Al-Si alloy with a homogeneous modifier obtained by fast cooling of the treated alloy showed that the modifier affected the structure of Al-12%Si alloy.

EKOLOGICZNA MODYFIKACJA STOPU Al-12%Si A JEGO STRUKTURA

Tomasz Lipiński¹, Anna Góral², Paweł Mikołajczyk¹, Marcin Cudakiewicz³, Anna Wach¹

¹ Katedra Technologii Materiałów i Maszyn
Uniwersytet Warmińsko-Mazurski w Olsztynie

² Instytut Metalurgii i Inżynierii Materiałowej PAN w Krakowie

³ BUJALSKI Sp z o.o. w Dywitach

Słowa kluczowe: stopy Al, krystalizacja, modyfikacja, struktura.

Abstract

W pracy przedstawiono wyniki badań nad modyfikacją stopu Al-12%Si modyfikatorem homogenicznym, wytworzonym przez szybkie studzenie modyfikatora z prędkością 100 i 200 K/s. Modyfikator homogeniczny ma skład chemiczny stopu modyfikowanego i zawiera 0, 7, 12 i 20% Si. Modyfikator

dodawano do tygla wraz z ciekłym stopem Al-Si i przetrzymywano przez jedną minutę. W pracy przedstawiono wpływ prędkości studzenia i zawartości modyfikatora w odniesieniu do masy obrabianego stopu na jego strukturę. Analiza procesu modyfikacji eutektycznego stopu Al-Si modyfikatorem homogenicznym otrzymanym z obrabianego stopu przez szybkie studzenie wykazała oddziaływanie modyfikujące na strukturę stopu Al-12%Si.

Introduction

Among the numerous characteristics that allow to differentiate between particular types of aluminum casting alloys, the most significant role is played by their mechanical properties (hardness, tensile strength, elongation), physical properties (specific gravity, electrical conductivity, thermal conductivity) and chemical properties (resistance to corrosion). In most cases, construction materials are selected so as to attain the optimal technological properties at the lowest possible weight and cost. These criteria are often met by silumin – a series of popular alloys of non-ferrous metals. Studies on the improvement of the properties of casting alloys have been continuously conducted over the recent years. Both the microstructure and properties of alloys may be altered via modification with chemical components, optimization of the crystallization process, heat treatment or a combination of these methods (ATASOY 1984, BORKOWSKI 1999, NOVA 2004, SZAJNAR 2008).

The initial structure of Al-12%Si alloy is composed of granular and acicular β phase, with α phase as matrix. The hard, irregular, often pointed β phase is responsible for the poor mechanical properties of said alloy. Therefore, the analyzed alloy can be used for practical purposes following the disintegration of its structure, in particular of the eutectic β phase.

One of the methods applied to enhance the properties of AlSi alloys is chemical modification. Particular chemical elements exert different types of influence on the structure of alloys and the related mechanical properties. Silumin modified with sodium has desirable mechanical properties and can be used for casting in different branches of industry, but certain problems are encountered during alloy recycling. Chemical elements (modifiers) added to the mixture at the stage of alloy production may enter into interactions, thus limiting the recycling capacity of alloy, even if they occur in small amounts (KRUPIŃSKI 2008, LIPIŃSKI 2000, 2008, LJUTOVA 2008, OLEJNIK 2007, PEZDA 2007, PTACEK 1999, ROMANKIEWICZ 2006, VALENCIK 2008, WOŁCZYŃSKI 1980, 1990, ZYSKA 2007).

While searching for alternative methods of improving the engineering properties of Al-12%Si alloy, an attempt was made to modify its structure with the use of a constituent with the chemical composition of the treated alloy. The tested homogenous modifier (with the chemical composition of the treated

alloy, obtained by fast cooling) was expected to have a significant effect on the modification process, resulting in changes in the microstructure of eutectic silumin.

Aim of the study, methods and results

The objective of the present study was to determine whether eutectic alloy Al-12%Si can be modified by means of Al-12%Si alloy cooled at various rates, used as a modifier.

Homogenous modifiers are additions designed for modification of the same alloys from which they were obtained. To obtain a homogenous modifier, Al-12%Si alloy was melted and then cooled on a metal plate at three different rates, i.e. $v_1 = 100$ K/s, and $v_2 = 200$ K/s. This enabled to produce three different components (cooled at v_1 , and v_2), which were refined immediately before adding to the alloy. The components were put into a crucible containing liquid Al-12%Si alloy, and kept there for one minute. The alloy temperature was 750°C. The modifier content of the alloy is given as weight in weight concentration (mass fraction). For comparative purposes, two castings were produced (without additions), at the beginning and at the end of the study.

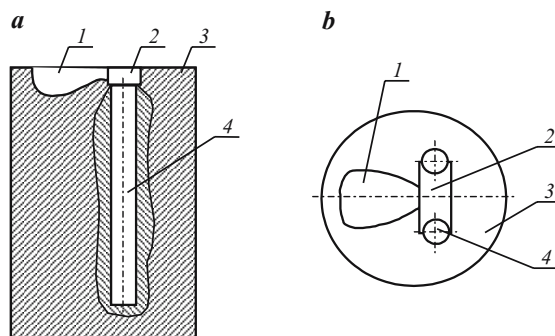


Fig. 1. Mould sections *a*) section, *b*) top view of the casting mold: 1 – reservoir, 2 – cross-gate, 3 – mold, 4 – sample for strength testing

Two samples, 16x140 mm, were obtained in each experiment. A 10 mm strip was cut off at the bottom of each sample. The face of cut served as metallographic specimen for microstructure analysis. Samples for mechanical tests were obtained from the upper part of the casting. A structural analysis was performed using an OLYMPUS IX70 microscope (magnification 2.5-1000x), and OLYMPUS DP-SOFT and MultiScan software. Samples for metal-

lographic tests were taken from the lower part of the samples designed for mechanical tests. Hardness tests were performed on the upper parts of strength test samples (six measurements per sample). Prior to measurements, side surfaces of samples, 5 mm wide, were grinded. All measurements were carried out according to the standard EN 10003-1 Metallic materials-Brinell test-Part1: Test method, using a Brinell/Vickers hardness tester, model HPO-250, with a standard ball, 2.5 mm in diameter, at a load of 612.9 N. A tensile strength test was performed according to the Polish Standard PN-EN 10002-1+AC1: 1998 Metals-Tensile test-Test method, at ambient temperature, using a universal strength testing machine (W.P.M. Germany), determining tensile strength R_m and percentage elongation A .

Results and Discussion

An analysis of the structural composition of Al-12%Si alloy treated with Al-12%Si modifier cooled at different rates revealed that cooling at $v_1 = 100$ K/s resulted, within the analyzed range, in a gradual improvement in the structure and mechanical properties of the alloy along with an increase in the content of the above modifier. Alloy treatment with Al-12%Si modifier cooled at $v_2 = 200$ K/s allowed to improve alloy structure within a relatively short period of time. A noticeable effect was reported following the addition of 0.2% modifier, but an increase in the amount of this constituent to 0.8% caused no considerable changes. An approximately 0.8% content of the modifier in the mixture resulted in reduced eutectic dispersion and worsened the mechanical properties of alloy, which are directly related to its structural composition. The modifier produced at a cooling rate of $v_2 = 200$ K/s was found to have the most beneficial influence. An increase in its content did not cause rapid changes in the mechanical properties of alloy, which remained at an optimal level following the addition of said modifier. Of particular note is also the high activity of this constituent.

Figure 2 presents the structure of Al-12%Si alloy cast without prior treatment with alloying constituents, while Figure 3 shows the structure of this alloy after such treatment. The microstructure of Al-12%Si alloy not treated with alloy-forming elements comprises primary silicon crystals dispersed in a solid solution of silicon in aluminum – α and a solid solution of aluminum in silicon – β as a eutectic mixture ($\alpha + \beta$) – Figure 2. The eutectic is composed of irregular-shaped grains of β phase. As a result, the mechanical properties of the alloy are relatively poor.

Alloy treatment with a constituent produced from Al-12%Si alloy by cooling at $v_1 = 100$ K/s contributed to the refinement of alloy structure, proportional

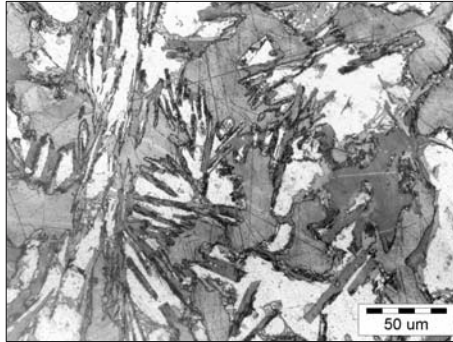


Fig. 2. Microstructure of Al-12%Si alloy cast without prior treatment with alloying constituents

to the increasing content of the modifier in the mixture. Following the addition of 0.2% modifier to Al-12%Si alloy, primary silicon crystals became oval and regular (Fig. 3), and they gradually passed into the eutectic mixture whose proportion is much higher in modified alloys than in non-modified ones.

After the treatment of Al-12%Si alloy with 0.4% modifier cooled at $v_1 = 100$ K/s, silicon crystals became much smaller and the formation of acicular structure began (Fig. 4). Visible are grains of α phase surrounded by acicular eutectic. Changes in the structural composition of alloy are reflected in changes in its mechanical properties, primarily in tensile strength (ATASOY 1984).

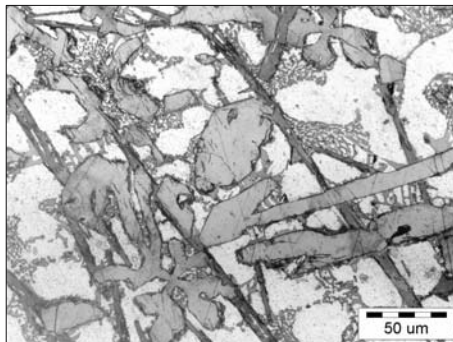


Fig. 3. Effect of 0.2% homogenous modifier produced at a cooling rate of $v_1 = 100$ K/s on the microstructure of Al-12%Si alloy

Further modification was observed as the amount of modifier was increased to 0.6% (Fig. 5). Branched crystals of AlSiFeMn phase became visible. The grain size of β phase decreased, and silicon crystals passed into the eutectic

mixture. The structure comprised typical acicular eutectic ($\alpha + \beta$) and small amounts of fine grains of β phase.

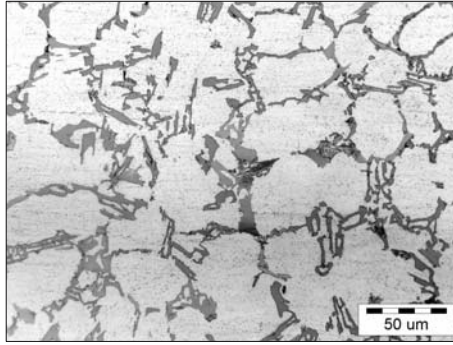


Fig. 4. Effect of 0.4% homogenous modifier produced at a cooling rate of $v_1 = 100$ K/s on the microstructure of Al-12%Si alloy

The treatment of Al-12%Si alloy with 0.8% modifier resulted in further refinement of the structure (Fig. 6). Visible are primary dendritic crystals of α phase, irregular eutectic cells in the inter-dendrite spaces and the branching of β phase. An improvement was noted in the mechanical properties of alloy, including an increase in percentage elongation. Primary silicon crystals disappeared as Al-12%Si alloy was modified with 1.0% homogeneous modifier cooled at $v_1 = 100$ K/s. Structure refinement was observed (Fig. 7), and eutectic cells became regular in shape.

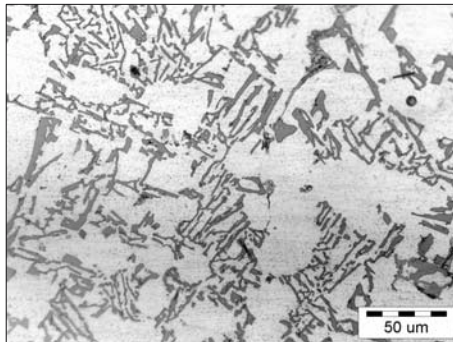


Fig. 5. Effect of 0.6% homogenous modifier produced at a cooling rate of $v_1 = 100$ K/s on the microstructure of Al-12%Si alloy

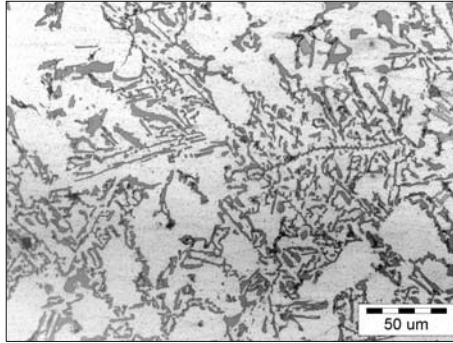


Fig. 6. Effect of 0.8% homogenous modifier produced at a cooling rate of $v_1 = 100$ K/s on the microstructure of Al-12%Si alloy

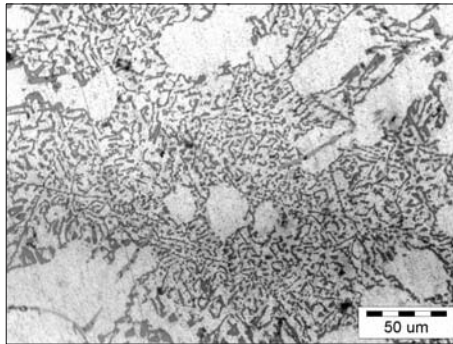


Fig. 7. Effect of 1.0% homogenous modifier produced at a cooling rate of $v_1 = 100$ K/s on the microstructure of Al-12%Si alloy

As the amount of modifier was increased to 0.4%, fine, regular-shaped eutectic ($\alpha + \beta$) cells could be observed in the inter-dendrite spaces of α phase (Fig. 8). This was supposed to greatly improve the mechanical properties of alloy (ATASOY 1984).

Alloy treatment with a constituent produced from Al-12%Si alloy by cooling at $v_2 = 200$ K/s permits structure refinement, proportional to the modifier content of the mixture. As illustrated in Figure 9, the treatment of Al-12%Si alloy with 0.2% modifier resulted in almost complete disappearance of grains of primary β phase. Visible is the branching of β phase.

An increase in the amount of homogeneous modifier to 0.6% resulted in the size reduction of eutectic cells, but larger precipitates of β phase were also noted (Fig. 10).

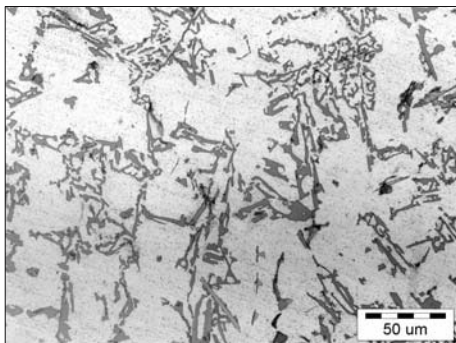


Fig. 8. Effect of 0.4% homogenous modifier produced at a cooling rate of $v_2 = 200$ K/s on the microstructure of Al-12%Si alloy

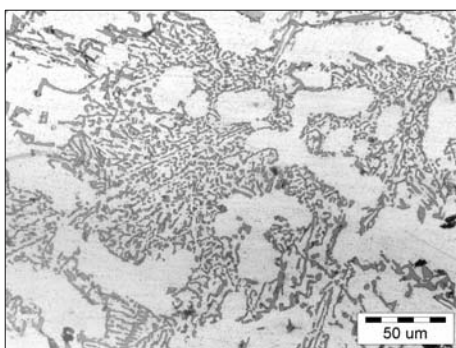


Fig. 9. Effect of 0.2% homogenous modifier produced at a cooling rate of $v_2 = 200$ K/s on the microstructure of Al-12%Si alloy

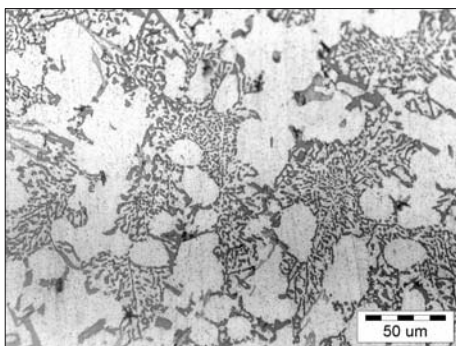


Fig. 10. Effect of 0.6% homogenous modifier produced at a cooling rate of $v_2 = 200$ K/s on the microstructure of Al-12%Si alloy

After the treatment of Al-12%Si alloy with 0.8% modifier, the primary α phase expanded and the dispersion of eutectic ($\alpha + \beta$) decreased (Fig. 11). The treatment of Al-12%Si silumin with 1.0% homogeneous modifier caused a further increase in the size of eutectic cells, particularly of β phase (Fig. 12).

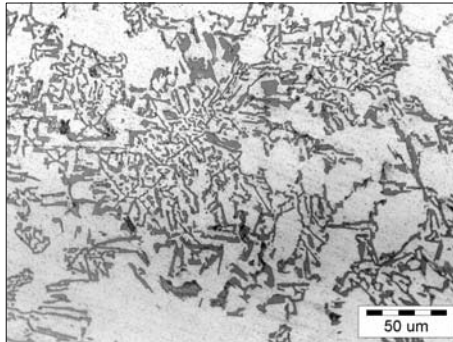


Fig. 11. Effect of 0.8% homogenous modifier produced at a cooling rate of $v_2 = 200$ K/s on the microstructure of Al-12%Si alloy

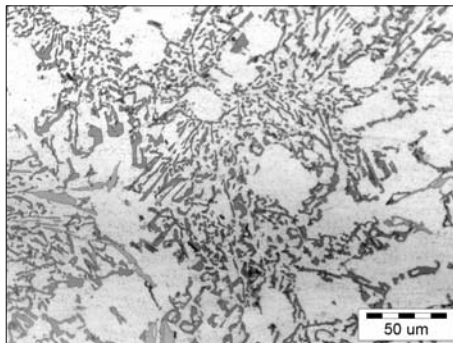


Fig. 12. Effect of 1.0% homogenous modifier produced at a cooling rate of $v_2 = 200$ K/s on the microstructure of Al-12%Si alloy

Conclusions

An analysis of the microstructure of hypereutectic and hypoeutectic silumin treated with a homogeneous modifier revealed lamellar structure. Interplanar distances were constant and comparable for all variants of treatment, which is indicative of stationary crystallization.

The effect of the grain size of homogeneous modifiers produced at various cooling rates on the modification process is analogous to the effect of the critical nucleus size on homogeneous nucleation.

A faster rate of cooling of homogeneous modifiers results in a shift in temperature and character of crystallization in accordance with the distribution of the cooperative growth zone. Structure dispersion also increases proportionally to cooling rate. An increase in the cooling rate of homogeneous modifiers is followed by a decrease in Si content and structure refinement of Al-Si alloys. Thus, the properties of such modifiers are determined by cooling rate.

The modification of hypereutectic and hypoeutectic silumin with a homogeneous modifier enabled to obtain an alloy with a desirable structure comprising fine eutectic cells ($\alpha + \beta$) and α phase dendrites. Fibrous eutectic was not observed in any of the analyzed cases, but its character may be indicative of a low temperature gradient.

The introduction of modifiers, in the form of chemical elements and compounds, to alloys may lead to certain problems with recycling (according to literature data, some of the constituents exert antagonistic effects). Therefore, environment-friendly modification may be a viable alternative for products whose physical and mechanical properties do not deteriorate during this process.

References

- ATASOY O.A., YILMAZ F., ELLIOTT R. 1984. *Growth structures in aluminium-silicon alloys. I. The coupled zone.* Journal of Crystal Growth, 66.
- BORKOWSKI S. 1999. *Quality controll of cast constructional materiale for example cast iron.* WNT, Warszawa.
- KRUPIŃSKI M., DOBRZYŃSKI L.A., SOKOŁOWSKI J.H. 2008. *Microstructure analysis of the automotive Al-Si-Cu casting.* Archives of Foundry Engineering, 8.
- LIPIŃSKI T. 2008. *Improvement of mechanical properties of AlSi7Mg alloy with fast cooling homogenous modifier.* Archives of Foundry Engineering, 8.
- LIPIŃSKI T. 2000. *Influence multicomponents mixtures for increase properties of cast alloys Al-Si.* Balttechmasz-2000. Kaliningrad.
- LIU J., ELLIOTT R. 1996. *Lamellar fault formation during eutectic growth.* Journal of Crystal Growth, 162.
- LJUTOVA O.V., VOLCHOK I.P. 2008. *Increase of foundry properties of secondary silumins.* Archives of Foundry Engineering, 8.
- NOVA I., EXNER J., HOSEK Z., NOVAKOVA I. 2004. *Crystallization of Al-Si alloys in the course of high pressure die-casting.* Archives of Foundry, 4(14).
- OLEJNIK E., FRAŚ E. 2007. *A visualization of the eutectic solidification process.* Archives of Foundry Engineering, 7.
- PEZDA J. 2007. *Continous modification of AK11 silumin with multicomponent salt on base of NaCl.* Archives of Foundry Engineering, 7.
- PTACEK L. 1999. *Slitiny hliniku na odlitku.* Slavarenstvi, 1.
- ROMANKIEWICZ F., ROMANKIEWICZ R. 2006. *Wpływ modyfikacji na strukturę i morfologię przelotów siluminu AK132.* Archives of Foundry, 6(22).
- SZAJNAR J., WRÓBEL T. 2008. *Inoculation of pure aluminium aided by electromagnetic field.* Archives of Foundry Engineering, 8.
- VALENCIK S., TRESA D. 2008. *Proposal of recycling system for waste aluminium.* Archives of Foundry Engineering, 8.

-
- WOŁCZYŃSKI W., CIACH R. 1980. *Growth of unidirectional eutectic binary alloys*. Solidifications Technology in the foundry and cast house. The Metals Society.
- WOŁCZYŃSKI W. 1990. *Application of the Chemical Potential Gradient in the Description of Eutectic Steady Growth*. Metalurgy and Foundry, 2.
- ZYSKA A., KONOPKA Z., ŁĄGIEWKA M. 2007. *The solidification of squeeze cast AlCu4Ti alloy*. Archives of Foundry Engineering, 7.

Accepted for print 16.10.2008 r.

TRUSS ANALYSIS IN VIEW OF THE REPLACEMENT OF DEGRADED STRUCTURAL COMPONENTS

Waldemar Dudda

Department of Mechanical Engineering and Fundamentals of Machine Design
University of Warmia and Mazury in Olsztyn

Key words: numerical analysis, cyclic loading, corrosion degradation, energy-based criterion.

A b s t r a c t

The study involved a numerical analysis of trusses under cyclic loading. Particular components of such structures are exposed to plastic deformation and corrosion damage and they dissipate energy, including the contributions of irreversible phenomena such as the work of non-elastic strains. The lifetime of individual structural components may be estimated applying the energy-based criterion. During numerical simulation, the most degraded component was replaced after the set number of load cycles. The aim of the analysis was to determine the optimal cycle during which a given component should be replaced with a new one. The paper presents the results of calculations regarding a sample truss construction. An analysis of those results provided a basis for determining the optimal cycle during which the most degraded component should be replaced.

ANALIZA KONSTRUKCJI W ASPEKTCIE WYMIANY DEGRADUJĄCYCH SIĘ ELEMENTÓW

Waldemar Dudda

Katedra Mechaniki i Podstaw Konstrukcji Maszyn
Uniwersytet Warmińsko-Mazurski w Olsztynie

S ł o w a k l u c z o w e: analiza numeryczna, obciążenie cykliczne, degradacja korozyjna, kryterium energetyczne.

A b s t r a k t

Artykuł dotyczy numerycznej analizy konstrukcji kratowych obciążonych cyklicznie. Poszczególne elementy konstrukcji ulegają plastycznej i korozyjnej degradacji oraz dysypują energię, na którą składają się wkłady od nieodwracalnych zjawisk typu praca na odkształceniach niesprężystych. Trwałość poszczególnych elementów konstrukcji jest oceniana według kryterium energetycznego.

W trakcie symulacji numerycznej po zadanej liczbie cykli obciążenia jest wymieniany najbardziej degradujący się element. Analiza ma na celu określenie optymalnego cyklu, w którym powinna nastąpić wymiana elementu na nowy. W pracy przedstawiono wyniki obliczeń przykładowej konstrukcji kratowej. W wyniku analizy otrzymanych wyników określono optymalny cykl wymiany najbardziej degradującego się elementu.

Introduction

The paper presents an analysis of truss behavior, performed using numerical modeling of load cycles. During cyclic loading of a sample truss construction, its structural components are exposed to plastic deformation and corrosion damage, leading to a decrease in the cross-sectional area of truss members. This results in stress increment, particularly in components which are at the greatest risk of attaining the elastic limit, and in material strengthening. At the moment plastic strains occur in successive load cycles, the material dissipates energy corresponding to the work of non-elastic strains. Each type of material is characterized by a certain value of irreversibly dissipated energy. When this value is exceeded, the material undergoes permanent damage. The level of this energy is referred to as critical energy (JAKUBOWSKI 2000). It follows that “numerical damage” of a given truss member takes place when energy dissipation exceeds the critical level during cyclic loading, while the number of the load cycle during which this level is exceeded determines the critical number of load cycles for a given truss construction. During numerical simulation with the use of the finite element method, after the set number of cycles, the most degraded truss member is “regenerated”, i.e. reconstituted to fitness for use by restoring its initial parameters including cross-sectional area, mechanical properties and the zero level of dissipated energy. Simulation is continued to determine the critical number of load cycles and the optimal number of cycles after which a given component should be replaced with a new one. Studies of that kind contribute to the development of a new branch of science known as “combined shakedown” which investigates, among others, the modes of material degradation including stress corrosion, electrochemical corrosion, low-cycle corrosion fatigue and failure (DUDDA, BADUR 2001).

Numerical applications

D-KRAT program was used for numerical simulation. The main part of the program is *Mini-Mod* library which contains Finite Element Method solver procedures and enables a non-linear analysis of structures. The solution of

a non-linear system of equations is obtained via an incremental-iteration process. Load increments are determined by parameter λ whose increments $\Delta\lambda$ are selected so as to form a closed cycle of loads (DUDDA, BADUR 2000, 2001). Non-linear load paths are tracked using the numerical technique developed by CHRÓSCIELEWSKI (1996). Another part of the program is *Mini-Kor* module enabling to estimate the degree of degradation of particular structural components. At present this module contains models describing such phenomena as stress corrosion, electrochemical corrosion, high-temperature corrosion and low-cycle corrosion fatigue. It was assumed that the above three types of corrosion take place on the surface of a structural component, and that they lead to a decrease in the bearing surface of a truss member. The rate \dot{d} of thickness decrement of the external layer of material exposed to corrosion can be described by the following formulas (DUDDA 2005):

– stress corrosion

$$\dot{d}_{SC} = C_{SC} |\sigma - \sigma_{gr}|^n e^{(T-T_0)/B} \quad (1)$$

– electrochemical corrosion and high-temperature corrosion

$$\dot{d}_{HC} = C_{HC} (T/T_0)^\kappa |\nabla T|^m \quad (2)$$

– low-cycle corrosion fatigue

$$\dot{d}_{LC} = C_{LC} N^\mu (\Delta\varepsilon)^b e^{(T-T_0)/B} \quad (3)$$

where:

d – thickness decrement [mm], T – temperature, N – number of cycles, σ – stress, σ_{gr} – stress limit below which stress corrosion is not observed, $\Delta\varepsilon$ – strain range, C_{SC} , n , B , C_{HC} , κ , m , C_{LC} , μ , b – model constants that are to be calibrated in one-dimensional experiments (JAKUBOWSKI 2000).

A single load cycle was divided into computational steps with very small load increments ($\Delta\lambda \leq 0.05$). After every load increment, thickness decrement was calculated as the following sum: $d^j = d_{SC}^j + d_{HC}^j + d_{LC}^j$ (where j is the number of a truss member), and the cross-sectional area of the j -th member was updated. The updated values of the cross-sectional areas of all truss members provided a basis for updating the stiffness matrix used for calculations at successive increment steps. If plastic strain occurred in a given structural component during numerical simulation, the unit dissipation energy corresponding to this component was calculated as the work of stress on its plastic strains. This energy was compared with critical energy whose value

was computed based on the empirical dependence proposed by (JAKUBOWSKI 2000):

$$U_{kr} = 0.0025 (3R_m + R_e) A_{10} \quad (4)$$

where:

R_m – tensile strength [Mpa], R_e – yield point [Mpa], A_{10} – percentage unit elongation after the tensile failure of a tenfold specimen.

If the value of dissipated energy exceeds the level of critical energy, the program stops calculations, enabling the user to introduce changes (e.g. restore the initial values of cross-sectional areas and properties of the material – regeneration of a truss member) and to continue analysis on the effect of these changes on truss behavior.

Additionally, the subprograms developed for the visualization of computation results (DUDDA 2005) permit to track the equilibrium path, structure deformation, degradation of the cross-sectional areas and energy dissipation of particular truss members.

Numerical analysis of a truss

A truss construction consisting of 21 members was analyzed in the study (Fig. 1). The initial cross-sectional areas of all members were adopted at 5 cm^2 . It was assumed that all components were made of the same material, i.e. constructional steel St2.

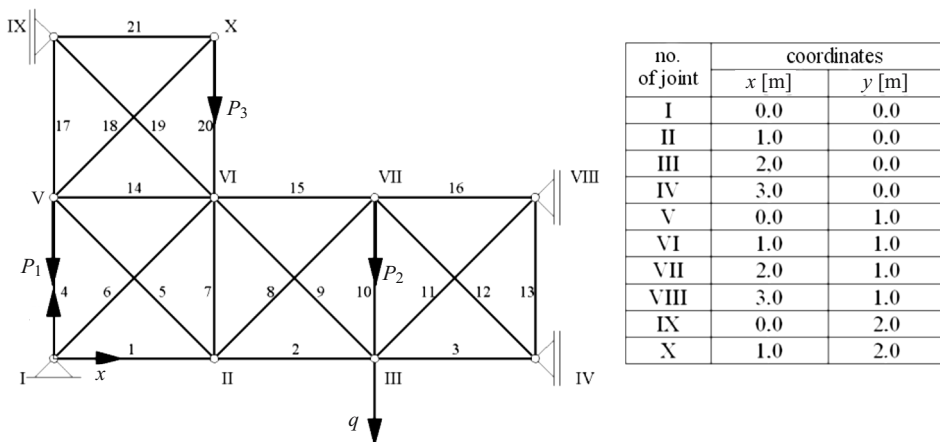


Fig. 1. Structure geometry

Material constants were as follows: Young's modulus $E = 2.1 \cdot 10^5$ MPa, modulus of strain hardening $E_T = 1 \cdot 10^4$ MPa, yield point $R_e = 200$ MPa, tensile strength $R_m = 420$ MPa ultimate elongation $A10 = 29\%$.

It follows from the above values that critical energy determined by dependence (4) was $U_{kr} = 106$ Mpa.

The truss was exposed to cyclic loading: $P_1 = \lambda \cdot 40$ kN, $P_2 = \lambda \cdot 120$ kN and $P_3 = \lambda \cdot 70$ kN (Fig. 1). Load control parameter λ was modified with the increment of $\Delta\lambda = 0.05$, as shown in Figure 2. Each cycle corresponded to 100 working hours.



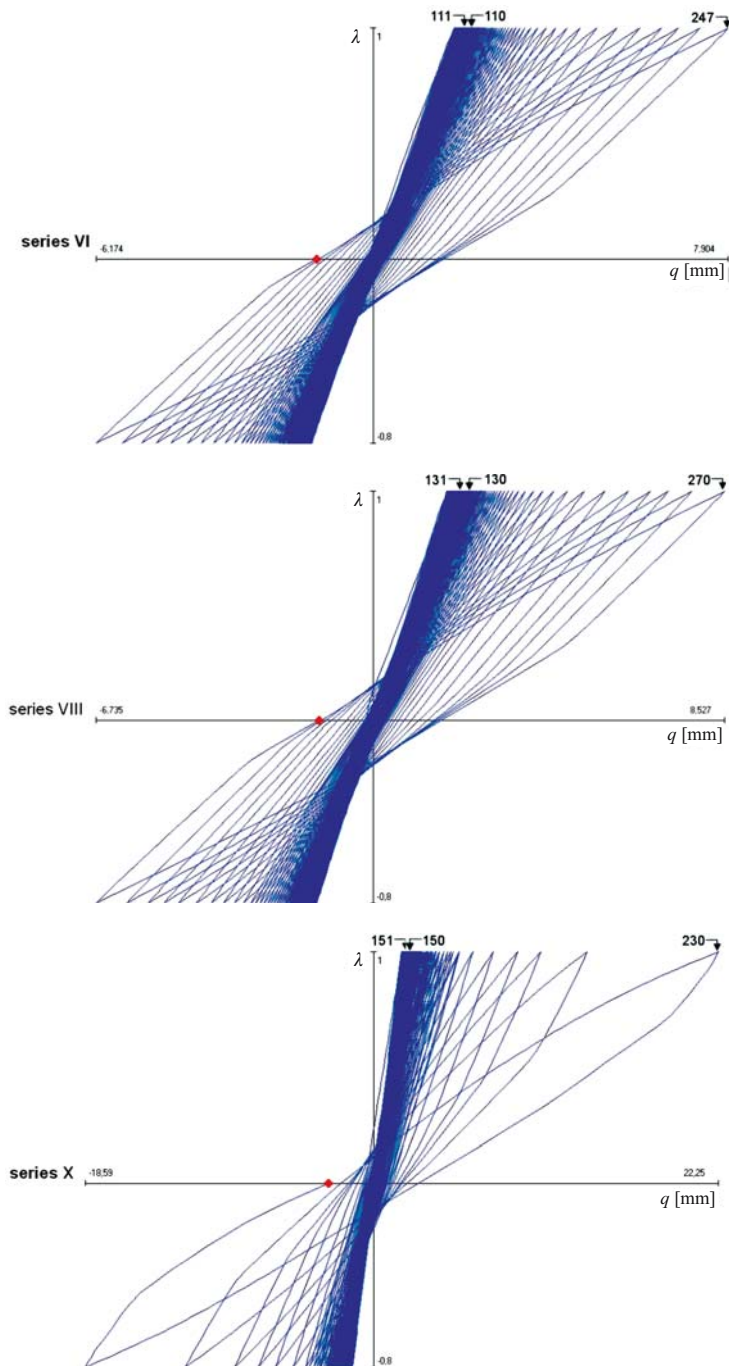
Fig. 2. Sequence of changes in load parameter λ

The parameters of corrosion models were as follows: $C_{SC} = 2 \cdot 10^{-5}$, $C_{HC} = 4.6 \cdot 10^{-6}$, $C_{LC} = 3.5 \cdot 10^{-6}$, $n = 1$, $\sigma_{gr} = 150$ MPa, $\kappa = 1$, $\vartheta = 1$, $\mu = 1.6$ and $b = 1$. Each cycle lasted for 360 hours, and it increased proportionally to $\Delta\lambda$, whereas temperature remained constant during the cycles, at 20°C. Based on the values of the above constants, the rates of corrosion of particular types were as follows: $\dot{d}_{SC} = 10^{-3}$ mm/h, $\dot{d}_{HC} = 0.4$ mm/year and $\dot{d}_{LC} = 1.5 \cdot 10^{-4}$ mm/cycle (DUDDA 2005).

Ten series of numerical computations were performed for the discussed truss. In successive series, truss member no. 4 was regenerated at a later stage. The number of load cycles after which truss member no. 4 was regenerated is shown in Table 1.

Table 1
Computational series and the number of cycles during which truss member no. 4 was replaced

Series number	I	II	III	IV	V	VI	VII	VIII	IX	X
Number of cycles N_w until truss member no. 4 was replaced	60	70	80	90	100	110	120	130	140	150

Fig. 3. Equilibrium path of control displacement $q = f(\lambda)$

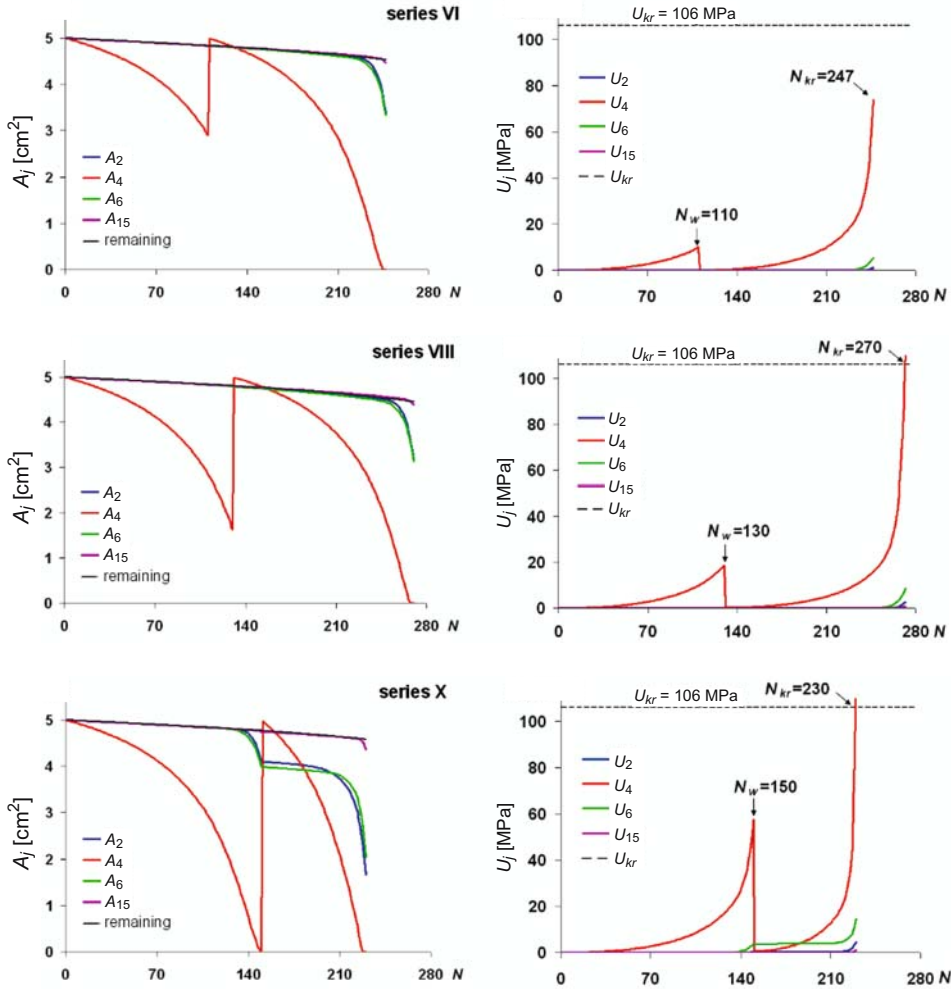


Fig. 4. Degradation of the cross-sectional areas of truss members A_j and energy dissipation U_j as dependent on the number of cycles N

In each series, after the replacement of truss member no. 4 for a new one, the computations were continued until energy dissipated by any member exceeded the critical level or until the cross-sectional area of any member underwent total corrosive degradation.

The relationship between control displacement q (Fig. 1.) and load parameter λ , as well as the increments of dissipated energy E_i and changes in the cross-sectional areas of truss members A_i , were monitored during numerical simulation. The results of computations for series VI, VIII and X are presented in Figures 3 and 4.

Results and discussion

In order to determine the effect of the moment of component regeneration on the behavior of truss construction during successive load cycles, the results of all computational series were presented in two figures, 5 and 6. Figure 5 shows the distribution of the critical number of load cycles until the moment of total degradation as dependent on the number of cycles after which a given component was regenerated. Figure 6 shows the distribution of the highest values of control displacement q for cycles immediately before and after the replacement of the degraded component, and for the critical number of cycles.

An analysis of Figure 5 indicates that when truss member no. 4 was regenerated after 130 cycles, the construction could be subjected to further loading until cycle 270. The replacement of this component during the remaining series resulted in lower values of the critical number of cycles.

The distribution of the maximal values of control displacement (Fig. 6) shows that if truss member 4 was replaced between cycle 60 and 140, the maximal control displacements corresponding to the critical number of cycles remained within the range of 6 to 9 mm. The regeneration of truss member no. 4 after 150 cycles led to a rapid increment in control displacement, which reached the value of 22.25 mm. Figure 6 also shows that the moment of component regeneration had no effect on the values of control displacement in the cycles following component replacement.

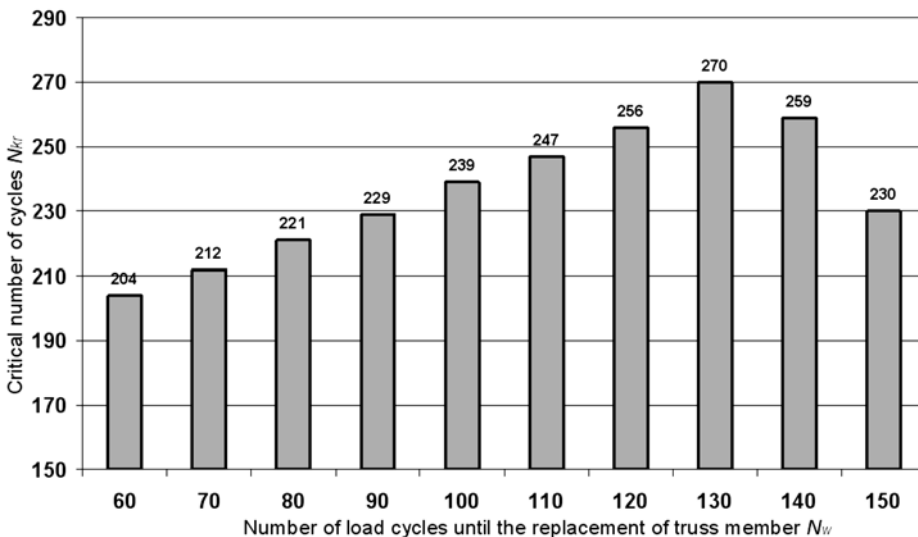


Fig. 5. Critical number of cycles N_{cr} in successive computational series

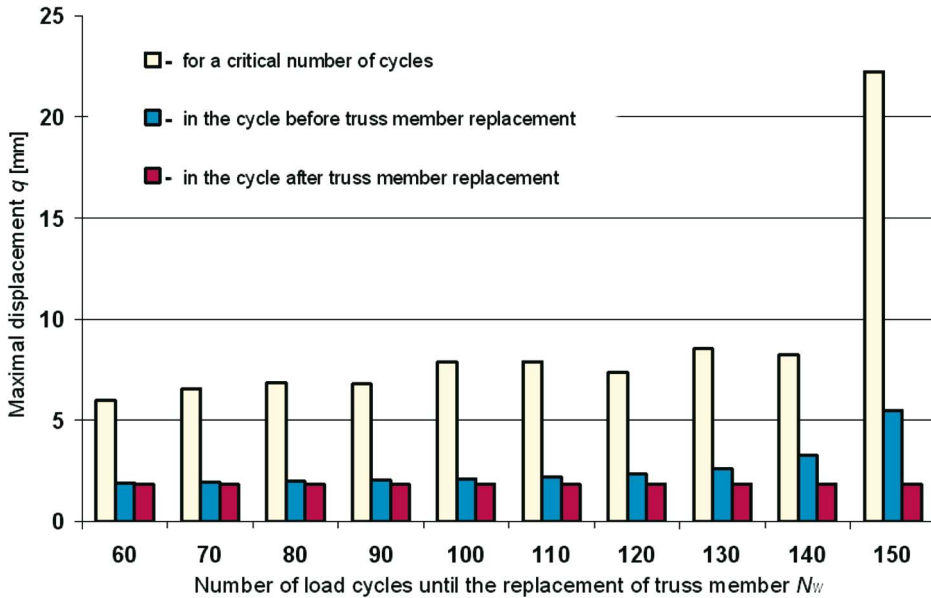


Fig. 6. Distribution of the maximal values of control displacement q

As illustrated in Figure 6, the replacement of truss member no. 4 until cycle 130 was not followed by significant changes in the value of maximal displacement. Considerable changes occurred if said component was replaced after cycle 130. Therefore, the optimal moment for truss member replacement was cycle 130, as confirmed by the energy-based criterion which was adopted as the main criterion for estimating construction durability. Another appropriate moment for the replacement could be cycle 140. However, it should be noted that in subsequent cycles the truss construction comes closer to the moment of stability loss and damage. A rapid increment in displacement observed when said component was replaced after 140 cycles could increase the risk of stability loss during the process. The stability of the analyzed truss gradually decreased starting from that cycle.

Conclusions

The calculations carried out in this study and an analysis of the obtained results indicate that the tools applied in the area of structural mechanics can be used to develop numerical models that enable to simulate the process of structure degradation under cyclic loading. The results of computations pro-

vide information about the behavior of a given structure as a whole and about the degradation of particular components, which in turn allows to determine the durability of truss constructions and express it as the number of load cycles until the replacement of degraded components.

References

- CHRÓŚCIELEWSKI J. 1996. *Rodzina elementów skończonych klasy C^∞ w nieliniowej sześcioparametrowej teorii powłok*. Zeszyty naukowe Politechniki Gdańskiej, 540, praca hab., Gdańsk.
- DUDDA W., BADUR J., CHRÓŚCIELEWSKI J. 2000. *Weryfikacja metody obliczeń konstrukcji kratowej obciążonej w zakresie sprężysto-plastycznym*. Archiwum IMPPAN, 151, Gdańsk.
- DUDDA W., BADUR J. 2001. *Ocena żywotności konstrukcji przy użyciu numerycznych metod mechaniki*. Wydawnictwo UWM, Olsztyn, ss. 109-119.
- DUDDA W. 2005. *Numerical modelling of a structure corrosive degradation during work cycles*. Letters of Institute of Fluid-Flow Machinery, Polish Academy of Sciences, 1456: 1-144, Gdansk.
- JAKUBOWSKI M. 2000. *Mechanizm propagacji pęknięć korozyjno-zmęczeniowych w stali austenitycznej zbliżonej do AISI 316LN*. Materiały XVIII Sympozjum Zmęczenia Materiałów i Konstrukcji, Bydgoszcz-Pieczyska, pp. 179-186.
- KOCAŃDA S., SZALA J. 1997. *Podstawy obliczeń zmęczeniowych*. WNT, Warszawa.

Accepted for print 16.10.2008 r.

Reviewers

Andrzej Ambrozik, Janusz Badur, Tadeusz Biliński,
Stanisław Borkowski, Romana Cielątkowska, Zbigniew Gnutek,
Zdzisław Hajducki, Ryszard Hołownicki, Roman Kadaj,
Elżbieta Kusińska, Oleh Klyus, Paweł Lindsted,
Stanisław Maciejewski, Rudolf Michałek, Janusz Piechocki,
Andrzej Radowicz, Tadeusz Rawa, Leonard Runkiewicz,
Cezary Specht, Marek Szmytkiewicz, Małgorzata Trojanowska